Preface

The knowledge and skills required for scientists to prepare efficacious advanced polymer based devices can be acquired through an experimental process that begins with a ***design****. The slowest step in this learning process is often found to be the* ***synthesis*** *of new polymers that are hypothesized to be effective agents. After a synthesis has been completed,* ***evaluation*** *of the new material must be carefully carried out in order to determine the success of the work and to allow accurate comparison with past results. Poly(p-phenylene vinylene) PPV and its derivatives are known far and wide in the research field of conjugated polymers as promising materials. Hence, it is not surprising that this dissertation focuses on this class of polymers. The existing backbone structure is used in the design of novel materials by applying strategies towards tailored functionalization. In this way, the chemical and physical properties of the conjugated material are adapted to specification and new opportunities are created for PPV derivatives in 'plastic electronic' applications. The polymer preparation and characterization is done at our laboratory. The evaluation of the new materials in advanced polymer based devices is in process in co-operation with other research groups. The endeavours described in this work certainly have lead to significant new knowledge. This knowledge may well lead some day to new technologies.*

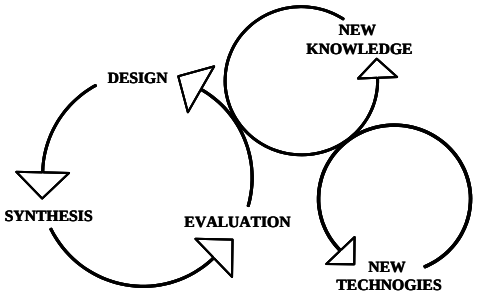

Table of contents

Chapter 1

General Introduction

Chapter one includes a general introduction to this work. In a first section a concise description of conjugated polymers is given. Since the scope of this work is restricted to the conjugated polymer poly(para-phenylene vinylene) (PPV) and some of its derivatives, this class is dealt with into somewhat more detail. Functionalization of PPV leads to materials with unique properties that expand the application range of their non-functional counterparts. As will be presented in the aim and outline of this thesis, we show a special interest in the synthesis and characterization of non-ionic polar functionalized PPV-type polymers.

1.1 Conjugated polymers

- **Polymers take charge**

Most people think of polymers in terms of plastic boxes, mouldings, grocery bags, and a host of other common structural uses where the mechanical properties of plastics are tuned for the purpose of support. Another very common use of polymers is in insulation of electrical wires, to protect them – and us – from short-circuits. Generally, we are used to polymers – that is, plastics – being somehow the opposite of metals. They insulate and do not conduct electricity. Yet Alan J. Heeger, Alan G. MacDiarmid and Hideki Shirakawa were rewarded with the year 2000 Nobel Prize in Chemistry for 'the discovery and development of electrically conductive polymers'. In 1977 this trio of scientists observed high conductivities by oxidizing polyacetylene (PA) with chlorine, bromine or iodine vapour.[1] The 'doped' form of PA had a conductivity of 10^5 Siemens per meter (S m^{-1}), this was 10^9 times more than the original PA films and higher than that of any previously known polymer. As a

comparison, teflon has an electrical conductivity of 10^{-16} S m^{-1}, while the conductivity of silver or copper equals 10^{8} S m^{-1}.

▪ Electronic properties of conjugated polymers

The discovery of Heeger, MacDiarmid and Shirakawa clearly opened up the field of 'plastic electronics' and since then, various conductive polymers have been devised (Figure 1-1). An extended survey of the literature on the polymerization chemistry towards the different classes of polymers is presented in several review articles and specialized books.[2]

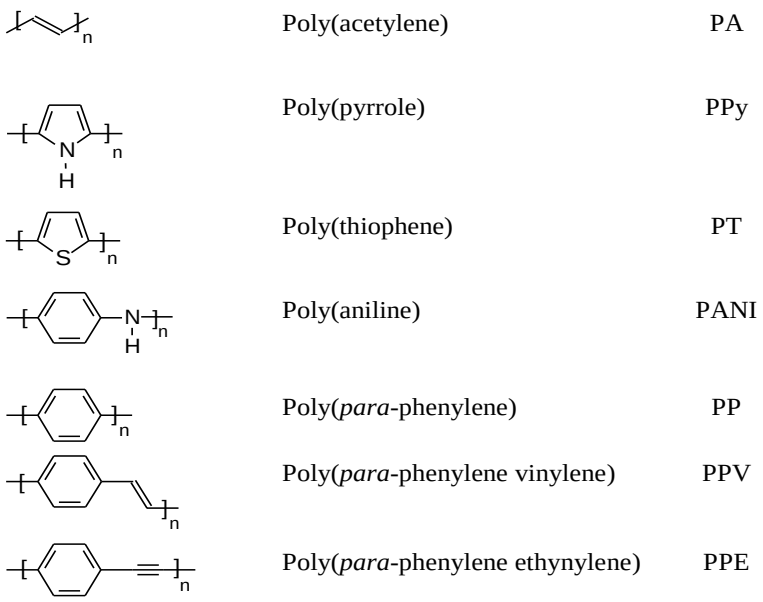

Figure 1-1 Several common conjugated polymers

A key property of all conjugated polymers is the extended π-conjugated system, a sequence of alternating single and double bonds along the polymer backbone. However, conjugation is not the only condition that has to be fulfilled to make a polymer material conductive. In addition, the plastic needs to be modified by injecting charge carriers *i.e.* electrons and holes, into the polymer. Charge carriers can be generated by several processes like electrical

stimulation, photo-excitation or chemical doping. The charge transport is based on a "hopping" mechanism. The conjugated system allows the charges to move along the chain (intrachain hopping). Besides, interchain hopping between conjugated parts of different chains is possible. The latter is limiting the mobility of the charge carriers.

The electronic properties of a polymer material are mainly determined by its electronic structure, which can be described by the molecular orbital theory[3]. According to this theory, overlap of adjacent atomic p_z-orbitals yields lower energy bonding (π) and higher energy anti-bonding (π^*) molecular orbitals. When many molecular orbitals are spaced together, the π-orbitals generate an apparently continuous, occupied valence band (VB), while the π^*-orbitals produce the conduction band (CB). The energy spacing between the highest occupied molecular orbital (HOMO) and the lowest unoccupied molecular orbital (LUMO) is called the band gap (E_g). The size of this band gap determines the electronic and optical properties of the material. In metals this band gap is zero, where for conjugated polymers it varies from 0.5 to 4 eV. By synthesizing the appropriate chemical structures, the band gap of conjugated polymers is tuned.

- **Optical properties of conjugated polymers**

Electroluminescence (EL) - the conversion of electrical energy into light - and the closely related phenomenon of photoluminescence (PL) - the conversion of (UV-)light into visible light - are seen in a wide range of conjugated polymers.[4] The process of EL is depicted in Figure 1-2. Electrons and holes are injected into a polymer *i.e.* negative polarons are formed in the LUMO by injection of electrons at the cathode and positive polarons are formed by 'injection of holes' in the HOMO. The resulting charges migrate in the polymer under influence of an applied electric field and recombine by formation of an exciton. Decay of this exciton to the ground state, can lead to the emission of light. The process of PL is depicted in Figure 1-3. When an incident photon has sufficient energy to excite an electron from the valence

band into the conduction band of a fluorescent polymer, an electron can be promoted from the HOMO to the LUMO. Two new energy states are filled with one electron of opposite spin (singlet excited state). The exciton can decay to the ground state radiatively (*i.e.* PL) or non- radiatively.

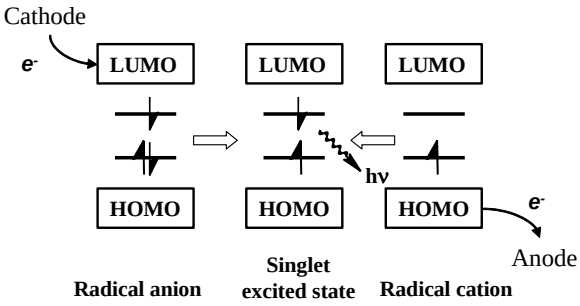

Figure 1-2 Electroluminescence

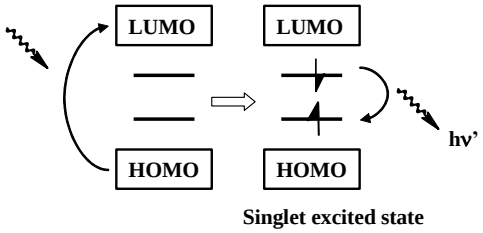

Figure 1-3 Photoluminescence

EL was first reported for anthracene single crystals in the 1960s.[5] The early studies on these organic semi-conductors established that the process responsible for EL requires injection of electrons from one electrode and holes from the other, the capture of oppositely charged carriers (*i.e.* recombination) and the radiative decay of the excited electron-hole state (exciton) produced by this recombination process. EL from conjugated polymers was first reported in 1990[6], using poly(*para*-phenylene vinylene) (PPV) as the single semi-conducting layer between two electrodes. Since then, the development in this field was rapid, leading to prototype devices who meet now realistic specifications for industrial applications.

▪ Applications of conjugated polymers

The combination of electronic (*e.g.* the band gap E_g) and optical properties (EL and PL efficiency) of semi-conductors with the mechanical properties and processability of polymers, makes conjugated polymers unique and potentially useful for a wide range of applications. Organic materials have the advantage of being light, low-cost and easy to process. Moreover, they can be deposited on flexible substrates, bending where their inorganic competitors would crack. In addition, the diversity of possible synthetic methods can lead to an infinite variability of organic compounds, which in principle allows scientists to tailor the properties of the conjugated polymers to all needs. These advantages opened up important new vistas for chemistry and physics, and for technology in general. At first, the poor processability and environmental stability of the conductive polymers hampered commercial success, but during the 1980s, the material properties were enhanced significantly due to improved synthesis methods and processing technology. This led to improved purity and solubility of conjugated polymers, which enabled their exploitation as the active materials in a wide range of devices. Among the numerous applications of conjugated polymers are polymer light emitting diodes[4,7] (PLEDs), field effect transistors[8] (FETs), sensors[9] and solar cells[10], all being pushed towards commercialization by academic and industrial research teams. Although totally organic solar cells are still considerably less efficient than single-crystal gallium arsenide, silicon, or Grätzel cells, progress has been impressive in the past few years. In particular, Carroll *et al.* reported power conversion efficiencies approaching 5 % for bulk heterojunction photovoltaics based on 1-(3-methoxycarbonyl)-propyl-1-phenyl-(6,6) C61 (PCBM) and poly(3-hexylthiophene) (P3HT).[11] According to the latest press release of the same scientists, recently 6 % efficiency is reached, moving organic conjugated polymers closer to practical use in photovoltaic systems. Amorphous silicon cells achieve 12%, so if developments in organic synthesis and device fabrication technology continue to raise the power conversion efficiencies, flexible polymer based solar cells might even replace the inorganic counterparts completely.

1.2 Poly(*para*-phenylene vinylene)

Within the wide range of different classes of conjugated polymers (Figure 1-1), this work will only focus on the conjugated polymer poly(*para*-phenylene vinylene) (PPV) and its derivatives. PPV shows a single-double bond alternation through phenylene rings that are connected in *para* by vinylene bonds. The parent PPV has an energy gap between π and π^* states of about 2.5 eV and produces yellow-green luminescence.[4]

1.2.1 What's on the PPV tonight?

As previously stated, the real breakthrough of this type of conjugated polymer came in 1990 when Jeremy Burroughes, Richard Friend and Donal Bradley discovered that if they put a small voltage through the plastic, a yellow-green light was emitted.[6] Realizing the commercial significance of their discovery they patented it and set up the company 'Cambridge Display Technology (CDT)' in order to develop their product for commercial use.[12] Since 1990 many different polymers have been shown to emit light under the application of an electric field but PPV and its derivatives are still important candidates as active layers in LED devices based on organic compounds. The emission colour of the polymer strongly depends on the chemical composition. By chemical modification of the polymer structure, a range of soluble light-emitting polymers emitting in the range from 400 nm to 800 nm is made available. This means that any colour in the visible spectrum can be obtained. The introduction of PLEDs would bring a whole new dimension to the craze for flat screen plasma television and flat screen monitors, being thinner, lighter, more robust, flexible and having a wider viewing angle (180^o). Also a wide variety of other opto-electronic applications for this family of conjugated polymers is envisaged, which are in various stages of development. Examples include field effect transistors (FETs), (bio)sensors and photovoltaic cells.[8-10] In addition, PPV and its derivatives showed recently possible application in light-emitting electrochemical cells (LECs).[13]

1.2.2 Synthesis of poly(*para*-phenylene vinylene)

PPV itself is a polymer with a very low solubility in commonly used organic solvents and therefore very difficult to process. In the earliest stages, PPV-type polymer chemistry was limited to the production of low molecular weight and sparingly soluble polymers. Owing to the poor solubility of these conjugated polymers, detailed structural and molecular weight information was not available from common techniques such as high-resolution NMR or gel permeation chromatography (GPC). Polymer chemists have long sought to prepare soluble conjugated PPV-type polymers, so that solution polymerization, processing and characterization could be optimized. The addition of solubilizing side chains onto the conjugated backbone proved very effective in improving the solubility and processability of conjugated polymers. This breakthrough triggered a massive research effort focused on the synthesis, physicochemical properties and application of structurally diverse PPV-type polymers.

The range of approaches towards the preparation of PPV and its derivatives appear unlimited and in many cases the reader tends to get lost. However, from synthetic point of view, two major different approaches for obtaining PPV derivatives can be distinguished: the step polymerizations and the so-called precursor routes. The step polymerizations deliver double bonds between the aromatic rings immediately after synthesis. This approach towards PPV occurs mostly through step-growth polycondensation reactions, such as the well-known Wittig[14], McMurray[15] and Knoevenagel[16] condensation reactions. Transition-metal catalyzed coupling reactions of suitable halogen compounds with olefins (Heck reaction)[17], unsaturated organostannanes (Stille reaction)[18], and organoboranes (Suzuki reaction)[19] have been employed less frequently for both PPV oligomers and polymers. PPV-type polymers can also be prepared in a direct way by electrochemically polymerization of different types of monomer compounds.[20] Essentially, all these routes lead to insoluble and infusible materials, [21] unless polymers are formed decorated with long solubilizing side chains.

Solubilizing spacers are often long alkyl or alkoxy chains. Poly(2-methoxy-5,2'-ethylhexyloxy-1,4-phenylene vinylene) (MEH-PPV) [7a,22] and poly(2-methoxy-5-(3,7-dimethyloctyloxy)-1,4-phenylene vinylene) (MDMO-PPV)[23] are examples of PPV derivatives that are still soluble in the conjugated form, which opens the possibility to efficient processing (Figure 1-4). These 2,5-substituted dialkoxy-PPV materials have emerged as a bench-mark in the field of conjugated polymers and nowadays they are commercially available.

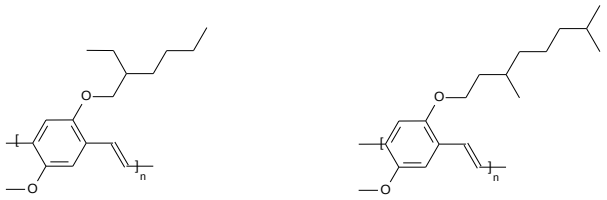

Figure 1-4 Chemical structures of MEH- and MDMO-PPV

Although very often processability can be achieved by the introduction of these solubilizing side chains, unfortunately this is not always possible, especially not for complex functionalized materials which are required for applications such as biosensors.

A second way to come to processable polymers is the precursor approach, which relies on the design and synthesis of an intermediate, soluble precursor polymer that can be cast into thin films, before solid-state conversion to the final conjugated polymer. The use of such precursor routes may be an excellent method to introduce sufficient processability. As said before, this processability is essential for the successful incorporation of the conjugated polymer into a variety of devices. The precursor routes towards PPV-type polymers are all based on the same kind of chemistry, which can be described by a general scheme depicted in Figure 1-5.

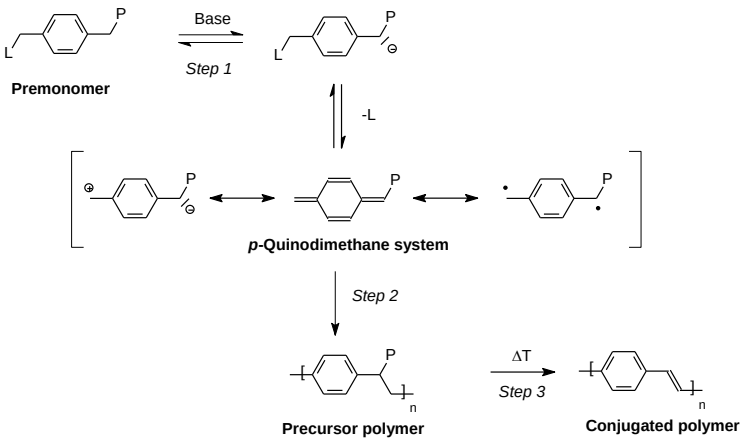

Figure 1-5 General reaction scheme of the precursor routes towards PPV

The first step is a base induced 1,6-elimination from the premonomer, *i.e.* a *p*-xylene derivative, leading to the *in situ* formation of the actual monomer, the *p*-xylylene or *p*-quinodimethane (*p*-QM) system. This reaction is assumed to proceed *via* the monomer anion, which expels a leaving group to yield the actual monomer in the polymerization. The intermediate *p*-QM system can be represented both under its diamagnetic and paramagnetic resonance form. The three structures contribute differently to the character of the molecule.[24] The polymerization of the highly reactive *p*-quinodimethane intermediate to the precursor polymer occurs spontaneously. This is a chain polymerization evidenced by the presence of high molecular weights at low monomer conversion.[25] Arguments about the mechanism (either anionic or radical) are still ongoing and beyond the scope of this work, however a radical mechanism seems to be more favourable. It is believed that the anionic polymerization mechanism rather results in low molecular weight material.[26] In the third step the conjugated structure is obtained either directly or by a thermal treatment depending on the specific chemical structure of the starting monomer and the polymerization conditions.

The different precursor routes towards PPV-type polymers differ in the substituents on the *p*-xylene derivative, *i.e.* the leaving group (L) and polarizer

group (P) and the polymerization conditions (base, solvent, reaction temperature and time). An overview of the specific polarizer and leaving groups for the most common precursor routes towards PPV is presented in Table 1-1.

Precursor route	**Leaving group (L)**	**Polariser (P)**
Gilch	Cl	Cl
Wessling-Zimmerman	$^{+}SR_2X^{-}$	$^{+}SR_2X^{-}$
Xanthate	SC(S)OR	SC(S)OR
Dithiocarbamate	$SC(S)NR_2$	$SC(S)NR_2$
Sulfinyl	Cl, Br	S(O)R

Table 1-1 Overview of the specific polarizer and leaving group for various precursor routes

The most used precursor approach in industry to obtain PPV-type polymers is the dehydrohalogenation route or the Gilch route.[25,27] This route gives an easy entry to a wide range of substituted high molecular weight organic PPV derivatives. Another well-established representative of the class of precursor routes is the sulfonium or Wessling-Zimmerman precursor route.[28] However, this route shows some severe drawbacks, limiting its use in a commercially successful chemistry, such as the poor solubility of the ionic precursor polymer in good spin casting solvents like chlorobenzene and toluene. Further, the precursor polyelectrolyte is relative instable and therefore may show side reactions during polymerization and storage of the precursor polymer.[29] The xanthate precursor route was developed by Son *et al.* as a modification of the sulfonium precursor route in an attempt to circumvent the drawbacks.[30] The non-ionic xantate precursor polymer is stable and soluble in organic solvents. Until recently, this precursor route was the most eligible candidate for the synthesis of poly(2,5-thienylene vinylenes) (PTVs).[31] Drawbacks however, in the use of this route towards PTV are the rather low yield and the high polydispersities of the obtained polymers. In 2003 Henckens *et al.* discovered the dithiocarbamate route which allowed for the synthesis of PTV in good

yields with lower polydispersities and defect content compared to polymers obtained *via* the xanthate route.[32] Recently, it was shown that this route can also be used for the synthesis of PPV-type polymers.[33] Notice that the Gilch, the Wessling-Zimmerman, the xanthate and the dithiocarbamate precursor route all have in common that they use a symmetrically substituted *p*-xylene derivative, where the same functional group both acts as leaving group to yield a *p*-quinodimethane system and as a polarizer that is expelled during thermal treatment resulting in the conjugated structure. This symmetry can cause unwanted side reactions such as solvent substitution, branching, cross linking, gelation or preliminary elimination.[34] Hence the use of symmetrical monomers can have a negative influence on device preparation and performance. To avoid many of these drawbacks, the sulfinyl route was developed in our laboratory.[35] This alternative and promising synthetic route is distinguished from the other routes by a chemical differentiation between the leaving group (halogen atom) and the polarizer (sulfinyl group). The chemical differentiation in the asymmetric monomer allows full control over both the stability of the precursor polymers and the polymerization reaction.

1.3 Functionalized PPV-type polymers

▪ Functionalized polymers

Functionalized polymers attract considerable attention due to their significantly expanded property and application range as compared to their non-functional counterparts.[36] Examples are numerous, including attachment of charged functionalities to polymers to assemble by the layer-by-layer technique[37], which finds among other things applications such as superior LEDs.[38] Other examples include the use of functionalities capable of molecular recognition to create novel composite materials[39] and molecularly imprinted matrices for sensor applications,[40] side-chain functionalities for the creation of reactive membranes[41] and reactive side group functionalized on block copolymers that can be used for surface modification.[42]

▪ Functionalized conjugated polymers

Functionalized conjugated polymers have properties that are not only derived from their macromolecular conjugated structure, but also depend to a significant extent on their functional group substituents, which usually introduce a difference in polarity or reactivity as compared to the polymer backbone. Introducing chemical functionality to PPV polymers provides access to a wide variety of material properties that stem from the functional groups used. Chemical heterogeneity on the polymer chains can lead to enhanced reactivity, phase separation or association. Therefore, the functionalization of conjugated organic polymer based materials is a powerful method for tuning the properties of these materials. A major intent in the preparation of PPV-like compounds is to improve the performance in device operation. One direction to achieve this aim is the adjustment of the polymer electron affinity by substitution with electron withdrawing groups[43] or by introduction of electron deficient aromatic rings containing nitrogen in the polymer backbone[44]. Another research goal is to tune the emission spectra of the PPV derivatives by tailoring the optical band gap by means of substitution with electron withdrawing or donating groups.[45]

Functionalization is mostly based on substitution at the aromatic nucleus but occasionally the vinylic carbons are substituted.[43c,46] Use of alternative aromatic moieties instead of phenyl units also leads to compounds analogous to PPV.[21h,47] Within the scope of this work, we will only focus on PPV derivatives which are functionalized by incorporation of functional side chains onto the phenyl units of the polymer backbone. More specifically, we are interested in the development of polar functionalized PPV-type polymers.

▪ Polar functionalized PPV-type polymers

Currently, PPV derivatives featuring ionic side groups which render the materials soluble in water and other polar solvents trigger considerable research effort.[48,49] The report on the synthesis of a water soluble PPV derivative by Shi

and Wudl using the Wessling route was probably one of the most important initial contributions to this area.[50] In the decades since this early report appeared, several synthetic methods have been developed, leading to many new PPV-type polyelectrolyte structures decorated with functional groups such as sulphonate[51] (SO_3^-) and carboxylate[52] (CO_2^-). These anionic water soluble PPV derivatives are good candidates as basic structures for building biological and chemical sensors, exhibiting rapid and collective response to relatively small perturbations in local environments, *e.g.* amplified fluorescence quenching. This amplified fluorescence quenching is achieved by electron or energy transfer due to facile energy migration along the conjugated backbone and the relatively strong electrostatic binding of the oppositely charged quenchers with ionic conjugated polymers. Although anionic PPVs exhibit remarkable opto-electronic properties and have been reported on detecting proteins as biological target by electron transfer, these polymers suffer from their intrinsic shortcomings such as relatively low PL quantum efficiency and their anionic charges that cannot be used to detect anionic biomolecules by electrostatic attraction. Most recently, cationic fluorescent conjugated polymers containing ammonium (NR_3^+) functionalities were successfully developed for obtaining optimized sensory materials.[53]

Next to the polar functionalized PPV-type polymers bearing ionic side groups, another direction of research has been towards the preparation of PPV derivatives bearing non-ionic polar side chains. The low reactivity of the non-ionic polar side chains mostly excludes interference with other functionalities and makes these materials a worthwhile tool to develop the skills in handling this class of materials. Since an easily accessible group of PPV analogues are those originating from 1,4-dialkoxybenzene,[54] most reports build on the successful polymerization of non-ionic dialkoxy-phenyl monomers. Considerable research has focused on the synthesis of PPV derivatives bearing oligo(ethylene oxide) side chains. These polymers show interesting properties for use as active layer in light emitting electrochemical cell devices[55] and sensor systems[56]. The number of articles devoted to these materials is still increasing. Less common are the reports on functionalized polar PPV-type

polymers which are tailored with amine groups[57] (NH_2), bromine atoms[58] or hydroxy moieties[59] (OH).

- **Synthesis of functionalized PPV derivates**

Generally, there are two ways to introduce functionality into a PPV-type material. In a first approach, the desired functionalized side chain is incorporated into the reactive monomer, which is subsequently polymerized *via* a precursor route or otherwise. This approach is used for the wide majority of functionalized conjugated polymers described in literature. However, the functionalized monomers may unfavourably intervene in the polymerization reaction, which may result in insufficiently high molecular weights or may even hamper polymerization altogether. Another common problem of the direct polymerization of functionalized monomers is the decomposition or transformation of the substituents towards other functionalities during the polymerization reaction.

A second possible approach towards tailored structures and tunable properties is based on the attachment of functionality to a preformed polymer scaffold *via* post-polymerization functionalization. Here, the reactions are performed on the conjugated polymers themselves, rather than going *via* a sometimes cumbersome monomer synthesis approach. The post-polymerization functionalization approach is applicable to a wide variety of functionalities and considerably simplifies the procedures for acquiring complex structures. In addition, this approach offers the versatility of using the exact same polymer backbone for the attachment of very different molecular entities. This allows isolation and comparison of the functionality contribution to the polymer behaviour and therefore provides a general framework for the study of structure-property relationship in polymers.

The approach of functionalization after polymerization has been applied extensively and successfully to conventional non-conjugated polymers.[37-42, 60] The post-polymerization functionalization method employed on the conjugated

polymers polyacetylene,[61] polyaniline,[62] polypyrrole[63] and poly(thiophene)[64] was electrochemical, which limits its applicability. Thus far, most reported post-polymerization functionalization reactions on conjugated PPV-type polymers have been limited to the deprotection of functional groups after polymerization,[65] a method which only allows for the introduction of a limited number of functionalities. More ambitious functionalization reactions were reported for conjugated polythiophene polymers. For instance, one report describes the synthesis of polythiophenes bearing N-hydroxysuccinimide ester side groups, which allows for a generation of plethora of functionalized polythiophenes *via* post- polymerization functionalization through a reaction between the NHS groups and different amine-bearing molecules.[66] In another report, a bromo-alkyl functionalized polythiophene is readily transformed into functionalized polymers bearing carboxylic acids, amines and thiols.[67]

1.4 Aim and outline

- **Aim**

The aim of the research presented in this work is the synthesis and the characterization of novel functionalized PPV derivatives. Functionalities are built in as side chains onto the phenyl groups of the PPV backbone with a variety of objectives in mind. A first major objective for the functionalization of the PPV backbone is to find PPV-type polymers which are compatible with processing from environmentally friendly solvent systems. Hitherto, chlorobenzene is often used for processing the conjugated material in electronic applications. However, this carcinogenic solvent is unacceptable from environmental and economical point of view. By attaching polar functional groups onto the conjugated backbone, the polarity of the material is increased and it is expected that in this way also the solubility in environmentally friendly solvent systems, *e.g.* alcohols and water, will be enhanced. The polar functionalized PPV-type polymers soluble in water or alcohol systems known in literature, all bear ionic side groups, which make them less suitable for certain applications. We set ourselves a target to prepare water and/or alcohol soluble PPV derivatives bearing non-ionic polar side chains.

A second reason which makes polar functionalized PPV derivatives worthwhile to develop is that these materials may have interesting properties to act as active layer in plastic photovoltaic (PV) cells. After all, blends of conjugated polymers and fullerene derivatives are promising candidates for PV applications. The conjugated polymers currently used in the blends are characterized by low dielectric constants. As a result, strongly bound excitons are created after absorption of light. These electron-hole pairs need to be dissociated into free charge carriers in order to be collected at the electrodes before recombination takes place. It is anticipated that an increased polarity leads to higher dielectric constants and therefore to an enhanced charge dissociation efficiency.[68] In addition, tailored functionalization might lead to a better morphology and thus to an enhanced photovoltaic performance.

Besides the possible improvement in efficiency of organic solar cells by increasing the polarity of the conjugated materials, efforts are made in this work to develop PPV-type material systems fitted with complex and specific functionalities for PV applications. Also the application of functionalized PPV-type polymers in advanced polymer based devices such as biosensors is within the objectives of our work.

The functionalized PPV-type polymers have been prepared with either the Gilch route or the sulfinyl precursor route. The Gilch route is relevant since it is the classical method industry employs to prepare PPV-type polymers. The use of the more elaborate sulfinyl route is significant since it results in polymers with enhanced properties. If applicable, a comparative study is made between the results of functionalized PPV derivatives prepared *via* the Gilch route with the results of the same material prepared *via* the sulfinyl precursor route. Some highly tailored and complex functionalized PPV-type polymers are prepared *via* a versatile synthetic strategy involving post-polymerization functionalization.

▪ Outline

Chapter two focuses on a series of polar functionalized 2,5-substituted PPV derivatives bearing oligo(ethylene glycol) and/or alkyl substituents. The impact of the variation of the polarity of the side chains on the optical, electronic and solubility characteristics is investigated with spectroscopic and electrical measurements. In **Chapter three**, two strategies are developed to further increase the polarity of PPV and fine-tune the solubility properties. In the first strategy, two branched oligo(ethylene glycol) side chains are introduced at every repeating unit of a PPV backbone. In the second strategy a PPV derivative with four polar oligo(ethylene oxide) chains is prepared. The solubility and UV-Vis absorption characteristics are studied in various solvents with different polarities. **Chapter four** deals with the synthesis of *para*-crown ether-functionalized PPV derivatives. The ability to form host–guest complexes with Na^+, K^+ and Rb^+ ions is investigated by ^1H NMR titration. **Chapter five** presents the synthesis of an alcohol-functionalized PPV derivative. Emphasis is put on the study of the copolymerization behaviour. **Chapter six** presents the synthesis of a polar carboxylic acid containing PPV derivative. This polymer is used as a platform for further functionalization in **Chapter 7**, where different post-polymerization functionalization methods are put to the test in order to obtain complex functionalized PPV derivatives. Finally, in **Chapter 8** some of the functionalized PPV-type polymers described throughout this work are tested in a prototype impedimetric biosensor. This dissertation is completed with general conclusions, perspectives and summaries in English and in Dutch. At the very end, some words of thanks and personal appreciation are extended to a number of people who have directly and indirectly contributed to this dissertation.

1.5 References

[1] a) Shirakawa, J.; Louis E. J.; MacDiarmed, A. G.; Chiang, C. K.; Heeger A. J. *J. Chem. Soc. Chem. Comm.* **1977**, 579. b) Chiang, C. K.; Fincher, C. R.; Park, Y. W.; Heeger, A. J.; Shirakawa, H.; Louis, E. J.; Gau, S. C.; MacDiarmid, A. G.; *J. Chem. Soc., Chem. Commun*. **1977**, *39 (17)*, 1098-1101.

[2] a) Feast, W. J., Tsibouklis, J.; Pouwer, K. L.; Groendaal, L.; Meijer, E. W. *Polymer* **1996**, *37 (22)*, 5017-5047. b) Chien, J. C. W. *Polyacetylene: chemistry, physics and materials science*, Academic Press, Orlando, **1984**. c) Curran, S.; Stark-Hauser, A.; Roth, S. *Organic conductive molecules and polymers*, John Wiley & Sons, New York **1997**, vol 2.2. d) Rodriguez, J.; Grande, H. J., Othero, T. F. *Handbook of organic conductive molecules and polymers*, John Wiley & Sons, New York **1997**, vol 2, 505. e) Mc Cullough, R. D. *Adv. Mat.* **1998,** *10*, 93-116. f) Kovacic, P.; Jones, M. B. *Chem. Rev.* **1987,** *87*, 357-359. g) Roncali, J. *Chem. Rev.* **1992,** *92*, 711. h) Roncali, J. *Chem. Rev.* **1997,** *97*, 173. i) Kiebooms, R. ; Menon, R.; Lee, K. *Handbook of advanced electronic and photonic materials and devices*, Academic Press **2001** vol. 8, 1.

[3] Shriver, D. F.; Atkins, P. W.; Langford, C. H. *Inorganic Chemistry - second edition*, Oxford University Press, **1994**, 91.

[4] Friend, R. H.; Gymer, R. W.; Holmes, A. B.; Burroughes, J. H.; Marks, R. N.; Taliani, C.; Bradley, D. C.; Dos Santos, D. A.; Brédas, J. L.; Lögdlund, M.; Salaneck, W. R. *Nature* **1999**, *397*, 121-128.

[5] a) Pope, M.; Kallman, H.; Magnante, P. *J. Chem. Phys.* **1963**, *38*, 2042-2043. b) Helfrich, W.; Schneider, W. G. *Phys. Rev. Lett. B* **1965**, *14*, 229.

[6] Burroughes, J. H.; Bradley, D. D. C.; Brown, A. R.; Marks, R. N.; Mackay, K.; Friend, R. H.; Burn, P. L. *Nature* **1990**, *347*, 539.

[7] a) Braun, D.; Heeger, A. J.; *Appl. Phys. Lett.* **1991**, *58*, 1982. b) Burn, P. L.; Holmes, A. B.; Kraft, A.; Bradley, D. D. C.; Brown, A. R.; Friend, R. H.; Gymer, R. W. *Nature,* **1992,** *356*, 47. c) Bradley, D. D. C. *Synthetic Metals* **1993**, *54*, 401-415. d) May, P. *Physics World* **1995**, *8(3)*, 52. e) Salbeck, J.

Ber. Bunsenges. Phys. Chem. **1996**, *100*, 1666. f) Kraft, A.; Grimsdale, A. C.; Holmes, A. B. *Angew. Chem. Int. Ed.*, **1998,** *37*, 402.

[8] a) Roth, S., *One-dimensional metals* **1995**, Weinheim VCH, 209-231. b) Sirringhaus, H.; Tessler, N.; Friend, R. H. *Science* **1998**, *280*, 1741. c) Horowitz, G. *Adv. Mat.* **1998**, *10(5)*, 365. d) Bao, Z.; *Adv. Mat.* **2000**, *12*, 227. e) Dimitrakopoulos, C. D.; Malenfant, R.L. *Adv. Mat.* **2002**, *14(2)*, 99. f) Scheinert, S.; Paasch, G. *Phys. Stat. Sol.* **2004**, *201 (6)*, 1263-1301.

[9] a) Mac Diarmid, A. G.; Zhang, W. J.; Huang, Z.; Wang, P.-C.; Huang, F.; Xie, S. *Polymer Prepr.* **1997**, *11 (5)*, 333. b) Heeger, P. S.; Heeger, A. J. *Proc. Natl. Acad. Sci* **1999**, *96 (22)*, 12219-12221. c) Chen, L.; McBranch, W.; Wang, H.; Helgeson, R.; Wudl, F.; Whitten, D. G. *Proc. Natl. Acad. Sci* **1999**, *96 (22)*, 12219 - 12221. d) Chen, L.; McBranch, D. W.; Wang, H.-L.; Helgeson, R.; Wudl, F.; Whitten, D. G. *Proc. Natl. Acad. Sci* **1999**, *96 (22)*, 12287-12292. e) Tyler McQuade, D.; Pullen, A. E.; Swager, T. M. *Chem. Rev.* **2000**, *100*, 2537-2574. f) Gerard M.; Chaubey, A.; Malhotra, B. D. *Biosensors and Bioelectronics* **2002**, *17*, 345-359.

[10] a) Rostalski, J.; Meissner, D. *Solar Energy Materials & Solar Cells* **2000,** *61*, 87-95. b) Brabec, J. C.; Sariciftci, N. S.; Hummelen, J. C. *Adv. Funct. Mater.* **2001**, *11*, 15-48. c) Hoppe, H.; Sariciftci, N. S. *J. Mater. Res.* **2004**, *19 (7)*, 1924-1945. d) Hoppe, H.; Niggeman, M.; Winder, C.; Kraut, J.; Heisgen, R.; Hinsch, A. Meissner, D.; Sariciftci, N. S. *Adv. Funct. Mater.* **2004**, *14 (10)*, 1005-1011.

[11] Reyes-Reyes, M.; Kim, K.; Carroll, D. L. *Appl. Phys. Lett.* **2005**, *87*, 083506.

[12] http://www.cdtltd.co.uk

[13] a) Pei, Q.; Yu, G.; Zhang, C.; Yang, Y.; Heeger, A. J. *Science* **1995**, *269*, 1086. b) Pei, Q.; Yang, Y.; Yu, G.; Zhang, C.; Heeger, A. J. *J. Am. Chem. Soc.* **1996**, *118*, 3922. c) Holzer, L.; Wenzl, F. P.; Tasch, S.; Leising, G. *Appl. Phys. Lett.* **1999**, 2014-2016. d) Yang, C.; He, G.; Sun, Q.; Li, Y. *Synth. Met.* **2001**, *124*, 449-453. e) Yang, C.; He, G.; Sun, Q.; Li, Y. *Synth. Met.* **2001**, *124*, 449-453. f) Leger, J. M.; Carter, S. A.; Ruhstaller, B. *J. Appl. Phys.* **2005**, *98*, 124907. g) Gu, Z.; Shen, Q-D.; Zhang, J.; Yang, C.-Z.; Bao, Y.-J. *J. Appl. Polym. Sci.* **2006**, *100 (4)*, 2930 – 2936.

[14] a) McDonald, R. N.; Campbell, T. W.; *J. Am. Chem. Soc.* **1960,** *82,* 4669. b) Hörhold, H.-H.; Opfermann. J. *Makromol. Chem.* **1970**, 131, 105.

[15] a) Rehahn, M.; Schlüter, A.-D. *Macromol. Chem., Rapid Commun.* **1990,** *11*, 375-379. b) Stalmach, V.; Kolsharm, H.; Brehm, I.; Meier, M. *Liebigs Ann.* **1996**, 1449-1456. c) Rehahn, M.; Schlüter, A. D. *Makromol. Chem. Rapid Commun.* **1990**, *11*, 375.

[16] a) Lenz, R. W.; Handlovits, C. E. *J. Org. Chem.* **1960**, *25*, 813. b) Staring, E. G. J.; Demandt, R. C. J. E.; Braun, D.; Rikken, G. L. J.; Kessener, Y. A. R. R. ; Venhuizen, A. H. J.; Knippenberg, M. M. F.; Bouwmans, M. *Synth. Met*. **1995,** *71*, 2179. c) Moratti, S. C.; Bradley, D. D. C.; Friend, R. H.; Greenham, N. C.; Holmes, A. B. *Polym. Prepr*. **1994**, *35*, 214.

[17] a) Heck, R.F. *Org. React.* **1982,** *27*, 345. b) Greiner, A.; Heitz, W. *Makromol. Chem., Rapid Commun.* **1988**, *9*, 581-588.

[18] a) Babudri, F.; Cieco, S. R.; Farinola, G. M.; Naso, F.; Bolognesi, A.; Porzio, W. *Macromol. Rapid Commun.* **1996,** *17*, 905-911. b) Bao, Z.; Chan, W. K.; Yu, L. *J. Am. Chem. Soc.* **1995**, *117*, 12426.

[19] Koch, F.; Heitz, W. *Macromol. Chem. Phys.* **1997**, *198*, 1531-1544.

[20] a) Chang, W.P.; Whang, W.T.; Lin, P.W. *Polymer* **1996**, *37*, 1513. b) Nishihara, H.; Tateishi, M.; Aramaki, K.; Ohsawa, T.; Kimura, O. *Chem. Lett.* **1987,** 539. c) Chang, W.-P.; Whang, W.-T.; Lin, P. W. *Polymer* **1996**, *37*, 1513-1518.

[21] a) Heitz, W.; Brügging, W., Freund, L.; Gailberger, M.; Greiner, A.; Jung, H.; Kampschulte, U.; Niesser, N.; Osan, F.; Schmidt H. W.; Wicker, M. *Makromol. Chem.* **1988,** *189*, 119-127. b) Martelock, H.; Greiner, A.; Heitz, W. *Makromol. Chem.* **1991,** *192*, 967-979. c) Greiner, A.; Martelock, H.; Noll, A.; Siegfried, N.; Heitz, W. *Polymer* **1991,** *32 (10), 1857-1861*. d) Remmers, M.; Schulze, M.; Wegner, G. *Macromol. Rapid Commun.* **1996,** *17*, 239-252. e) Cooke, A. W.; Wagener, K. B. *Macromolecules* **1990**, *24*, 1404. f) Rehahn, M.; Schlüter, A.-D. *Chem. Lett.* **1987,** *11*, 375. g) Hanack, M.; Segura, J. L.; Spreitzer, H. S. *Adv. Mater*. **1996**, *8*, 663.

[22] Wudl, F.; Sardanov, G. *US Patent* 5, 189, 136, **1993**.

[23] Becker, H.; Spreitzer, H.; Kreuder, W.; Kluge, E.; Schenk, H.; Parker, I.; Cao Y. *Adv. Mater.* **2000,** *12(1)*, 42.

[24] a) Hiberty, P.C.; Karafiloglou, P. *Theoret. Chim. Acta (Berl.)* **1982**, *61*, 171-177. b) Döhnert, D.; Koutecky, J. *J. Am. Chem. Soc.* **1980**, *102 (6)*, 1789. c) Flynn, C. R.; Michl, J. *J. Am. Chem. Soc.* **1974**, *96 (10)*, 3280.

[25] a) Gilch, H. G.; Wheelwright, W. L. *J. Polym. Sci.: A* **1966**, *4*, 1337-1349. b) Louwet, F. *Ph.D Dissertation* **1993** Limburgs Universitair Centrum Diepenbeek, Belgium.

[26] Vanderzande, D. J. M.; Hontis, L.; Palmaerts, A.; Van Den Berghe, D.; Wouters, J.; Lutsen, L.; Cleij, T. *Proc. of SPIE* **2005**, *5937* 116-125.

[27] Becker, H.; Spreitzer, H.; Ibrom, K.; Kreuder, W. *Macromolecules* **1999**, *32*, 4925.

[28] a) Wessling, R.A.; Zimmerman, R.G. U.S. Pat. **1968** 3 401 152; 3 404 132; **1970** 3 532 643; **1972** 3 706 677 b) Wessling, R.A. *J. Polym. Sci., Polym. Symp.* **1985**, *72*, 55. c) Garay, R. G.; Myrian, N. S.; Montani, R. S. Hernandez, S. A. *Designed Monomers and Polymers.* **2000**, *3 (2)*, 231-244.

[29] a) Shah, H. V.; McGhie, A. R.; Arbuckle, G.A. *Thermochimica acta* **1996**, *287*, 319. b) Hsieh, B. R.; Antoniadis, H.; Abkowitz, M. A.; Stolka, H. *Polym. Prep.* **1992**, *33*, 414. c) Lahti, P. M.; Sarker, A.; Garay, R. O.; Lenz, R. W. Karasz, F. E. *Polymer* **1994**, *35*, 1312.

[30] a) Son, S.; Dodabalapur, A.; Lovinger, A. J.; Galvin, M. E. *Science* **1995**, *269*, 376. b) Son, S.; Lovinger, A. J.; Galvin, M. E. *Polym. Mater. Sci. and Engin.* **1995**, *72*, 567.

[31] a) Henckens, A. *Ph.D Dissertation* **2003** Limburgs Universitair Centrum, Diepenbeek, Belgium. b) Mitchell, W. J.; Pena, C.; Burn, P. L. *J. Mater. Chem.* **2002**, *12*, 200-205.

[32] Henckens, A.; Lutsen, L.; Vanderzande, D.; Knipper, M.; Manca, J.; Aernouts, T.; Poortmans, J. *Proc. Spie – Int. Soc. Opt. Eng.* **2004**, *5464*, 52-59. Henckens, A.; Duyssens, I.; Lutsen, L.; Vanderzande, D.; Cleij, T. J. *Polymer* **2006**, *47*, 123-131.

[33] Henckens, A.; Duyssens, I.; Lutsen, L.; Vanderzande, D.; Cleij, T. J. *Polymer* **2006**, *47*, 123-131.

[34] a) Garay, R. G.; Lenz, R. W. *Makromol. Chem. Suppl.* **1989**, *15*, 1. b) Yamada, S.; Tokito, S.; Tsutsui, T.; Saito, S. *J. Chem. Soc. Chem. Commun.* **1987**, 1448.

[35] a) Louwet, F.; Vanderzande, D. J. M.; Gelan, J. M. J. V.; Mullens, J. *Macromolecules* **1995**, *28*, 1330. b) van Breemen, A. J. J. M.; Issaris, A. C. J.; de Kok, M. M.; Van Der Borght, M. J. A. N.; Adriaensens, P. J.; Gelan, J. M. J. V.; Vanderzande, D. J. M. *Macromolecules* **1999**, *32(18)*, 5728-5735. c) Lutsen, L.; Adriaensens, P.; Becker, H.; van Breemen, A. J.; Vanderzande, D. J. M.; Gelan, J. *Macromolecules* **1999**, *32(20)*, 6517-6525.

[36] Patil, A.O.; Schulz, D.N.; Novak, B.N. *ACS Symposium series 704: Functional polymers: modern synthetic methods and novel structures* **1998,** Washington D.C., 1.

[37] Decher, G. *Science* **1997**, *277*, 1232.

[38] Onitsuka, O.; Fou, A. C.; Feireira, M.; Hsieh, B. R.; Rubner, M. F. *J. Appl. Phys.* **1996**, *80*, 4067.

[39] Boal A. K.; Ilhan, F.; DeRouchey, J. E.; Thurn-Albrecht, T.; Russell, T. P.; Rotello, V. M. *Nature* **2000**, *404*, 2202.

[40] a) Duffy, D. J.; Das, K.; Hsu, S. L.; Penelle, J.; Rotello, V. M.; Stidham, H.D. *J. Am. Chem. Soc* **2002**, *124*, 8290 b) Das, K.; Penelle, J.; Rotello, V. M. *Langmuir* **2003**, *19*, 3921.

[41] Tripp. J. A.; Stein, J. A.; Svec, F.; Frechet, J. M. J. *Org. Lett.* **2000,** *2*, 195.

[42] Wang, J.; Kara, S.; Long, T. E.; Ward, T. C. *J. Polym. Sci., Polym. Chem.* **2000**, *38*, 3742.

[43] a) Grimsdale, A. C.; Cacialli, F.; Grüner, J.; Li, X.-C.; Holmes, A. B.; Moratti, S. C.; Friend, R. H. *Synth. Met.*, **1996,** *76*, 165-167. b) Gurge, R. M.; Sarker, A.; Lahti, P. M.; Hu, B.; Karasz, F. E. *Macromolecules* **1996**, *29*, 4287-4292. c) Greenham, N. C.; Moratti, S. C.; Bradley, D. D. C.; Friend, R.C.; Holmes, A. B. *Nature*, **1993**, *365*, 628-630.

[44] a) Epstein, A. J.; Blatchford, J. W.; Wang, J. Z.; Jessen, S. W.; Gebler, D. D.; Lin, L. B.; Gustafon, T. L.. Wang, H.-L.; Park, Y. W.; Swger, T. M.; MacDiarmid, A. G. *Synth. Met.*, **1996,** *78*, 235-261. b) Yamamoto, T.; Sugiyama, K.; Kushida, T.; Inoue, T.; Kanbara, T. *J. Am. Chem. Soc.* **1996**,

118, 3930-3937. c) O'Brien, D.; Bleyer, A.; Bradley, D. D. C; Meng, S. *Synth. Met.*, **1996,** *76*, 235-261.

[45] Klärner, G.; Former, C.; yan, X.; Richert, R.; Müllen, K. *Adv. Mater*. **1996**, *8 (11*), 932.

[46] Kaul, S. N.; Fernande, J. E. *Macromolecules* **1990**, *23*, 2875-2879.

[47] Garay, R. O.; Naarmann, H.; Müllen, K. *Macromolecules* **1994**, *27*, 1922-1927.

[48] Pinto, M. R.; Schanze, K. S. *Synthesis* **2002**, *9*, 105-108.

[49] a) McGehee, M. D.; Miller, E. K.; Moses, D.; Heeger, A. J. *Advances in Synthetic Metals. Twenty Years of Progress in Science and Technology;* Bernier, P.; Lefrant, S.; Bidan, G. Eds.; Elsevier: Amsterdam, **1999**, 98. b) Chen, L.; Xu, S.; McBranch, D.; Whitten, D. *J. Am. Chem. Soc*. **2000**, *122*, 9302-9303.

[50] Shi, S.; Wudl, F. *Macromolecules* **1999**, *23*, 2119-2124.

[51] a) Wang, J.; Wang, D.; Miller, E. K.; Moses, D.; Bazan, G. C.; Heeger, A. J. *Macromolecules* **2000**, *33*, 5153-5158. b) Gaylord, B. S.; Wang, S.; Heeger, A. J.; Bazan, G. C. *J. Am. Chem. Soc*. **2002**, *124*, 5942-5643. c) Fan, C.; Plaxco, K. W.; Heeger, A. J. *J. Am. Chem. Soc*. **2001**, *123(26)*, 6417-6418. d) Ramachandran, G.; Smith, T. A.; Gómez, D.; Ghiggino, K. P. *Synth. Met.* **2005**, *152*, 17-20.

[52] a) Peng, Z.; Xu, B.; Zhang, J.; Pan, Y. *Chem. Commun.* **1999**, 1855. b) Fujii, A.. Sonoda, T.; Yoshino, K. *Jpn. J. Appl. Phys.* **2000**, *39*, L249. c) Fujii, A.. Sonoda, T.; Fujisawa, T.; Ootaka, R.; Yoshino, K. *Synth. Met.* **2001**, *119*, 189. d) Gin, D.; Yonezawa, K. *Synth. Met.* **2001**, *121*, 1291-1294. e) Wagaman, M. W.; Grubbs, R. H. *Macromolecules* **1997**, *30*, 3978-3985.

[53] a) Li, H.; Xiang, C.; Li, Y.; Xiao, S.; Fang, H.; Zhu, D. *Synth. Met.* **2003**, *135-136*, 483-484. b) Chen, X.; Wudl, F. *Polym. Prepr.* **2002**, *43 (1)*, 19. c) Li, H.; Li, Y.; Zhai, J.; Cui, G.; Liu, H.; Xiao, S.; Liu, Y.; Lu, F.; Jiang, L.; Zhu, D. *Chem. Eur. J.* **2003**, *9*, 6031-6038. d) Fan, Q.-L.; Zhang, G.-W.; Lu, X.-M.; Chen, Y.; Huang, Y.-Q.; Zhou, Y.; Chan, H. S. O.; Lai, Y.-H.; Xu, G.-Q.; Huang, W. *Polymer* **2005**, *46 (24)*, 11165-11173.

[54] a) Momii, T.; Tokito, S.; Tsutsui, T.; Saito, S. *Chem. Lett.* **1988**, 1201-1204. b) Delmotte, A.; Biesemans, M.; Raier, H.; Gielen, M.; Meijer, E. W. *Synth. Met.* **1993**, *58*, 325-334. c) Jin, J.; Park, C. K.; Shim, H. K. *Polymer* **1994**, *35*, 480.

[55] a) Garay, R. O.; Mayer, B.; Karasz, F. E.; Lenz, R. W. *J. Polym. Sci. Part. A Polym. Chem.* **1995**, *33*, 525. b) Carvalho, L. M.; Santos, L. F.; Guimaraes, F. E. G.; Gonçalves, D.; Gomes, A. S.; Faria, R. M. *Synth. Met.* **2001**, *119*, 361-362. c) Huang, C.; Huang, G.; Guo, J.; Huang, W.; Kang, E. T.; Yang, C.-Z. *Polym. Prepr*. **2002**, *43 (2)*, 574. d) Tasch, S.; Holzer, L.; Wenzl, F. P.; Gao, J.; Winkler, B.; Dai, L.; Mau, A. W. H.; Sotgiu, R.; Sampietro, M.; Scherf, U.; Müllen, K.; Heeger, A. J.; Leising, G. *Synth. Met.* **1999**, *102*, 1046-1049. e) Hwang, D.-H.; Chuah, B. S.; Li, X.-C.; Kim, S. T.; Moratti, S. C.; Holmes, A. B. *Macromol. Symp.* **1997**, *125*, 111-120. f) Morgado, J.; Friend, R. H.; Cacialli, F.; Chuah, B. S.; Rost, H.; Moratti, S. C.; Holmes, A. B. *Synth. Met.* **2001**, *122*, 111-113. g) He, G.; Yang, C.; Wang, R.; Li, Y. *Displays* **2000**, *21*, 69-72. h) Huang, C.; Huang, W.; Guo, J.; yang, C.-Z.; Kang, E.-T. *Polym.* **2001**, *42*, 3929-3938. i) Xiang, D.; Shen, Q.; Zhang, S.; Jiang, X. *J. Appl. Polym. Sci.* **2003**, *88*, 1350-1356. j) Morgado, J.; Cacialli, F.; Friend, R. H.; Chuah, B. S.; Rost, H.; Holmes, A. B. *Macromolecules* **2001**, *34*, 3094-3099.

[56] Holzer, L.; Winkler, B.; Wenzl, F. P.; tasch, S.; Dai, L.; Mau, A. W. H.; Leising, G. *Synth. Met.* **1999**, *100*, 71-77.

[57] a) Liang, Z.; Mindaugas, R.; Li, K.; Manias, E.; Wang, Q. *Chem. Mater*. **2003**, *15*, 2699-2701. b) Liang, Z.; Wang, Q. *Langmuir* **2004**, *20*, 9600-9606.

[58] Benvenho, A. R. V.; Lessmann, R.; Hümmelgen, I. A.; Mello, R. M. Q.; Li, R. W. C.; Bazito, F. F. C.; Gruber, J. *Mater. Chem. Phys*. **2006**, *95*, 176-182.

[59] Benjamin, I.; Hong, H.; Avny, Y.; Davidov, D.; Neumann, R. *J. Mater. Chem.* **1998**, *8 (4)*, 919-924.

[60] Shenhar, R.; Sanyal,A.; Uzun, O.; Rotello, V. M. *Macromolecules* **2004**, *37*, 92-98.

[61] Guiseppi-Elie, A.; Wnek, G. E. J. *Polym. Sci., Part A: Polym. Chem. 1985, 23*, 2601.

[62] a) Yue, J.; Epstein, A. J. *J. Am. Chem. Soc*. **1990**, *112*, 2800. b) Yue, J.; Wang, Z. H.; Cromack, K. R.; Epstein, A. J.; MacDiarmid, A. G. *J. Am. Chem. Soc.* **1991**, *113*, 2665.

[63] a) Vork, F. T. A.; Ubbink, M. T.; Janssen, L. J. J.; Barendrecht, E. *Recl. Trav.*
Chim. Pays-Bas **1985**, *104*, 215. b) Qi, Z.; Rees, N. G.; Pickup, P. *Chem. Mater*. **1996**, *8*, 701-707.

[64] Pud, A. A. *Synth. Met.* **1994**, *66*, 1 and references therein.

[65] a) Liang, Z.; Cabarcos, O. M.; Allara, D.L.; Wang, Q. *Adv. Mater*. **2004**, *16*, 823-827. b) Chan, E. W. L.; Lee, D. C.; Ng, M. K.; Wu, G. H.; Lee, K. Y. C.; Yu, L. P. *J. Am. Chem. Soc*. **2002**, *124*, 12238-12243.

[66] Bernier, S.; Garreau, S.; Béra-Abérem, M.; Gravel, C.; Leclerc, M. *J. Am. Chem. Soc*. **2002**, *124*, 12463-12468.

[67] Zhai, L. Z.; Pilston, R. L.; Zaiger, K. L.; Stokes, K. K.; McCullough, R. D. *Macromolecules* **2003**, *36*, 61-64.

[68] a) Mihailetchi, V. D.; Koster, L. J. A.; Blom, P. W. M.; Melzer, C.; de Boer, B.; van Duren, J. K. J.; Janssen, R. A. J. *Adv. Funct. Mat.* **2005**, *15*, 795. b) Mihailetchi, V. D.; Koster, L. J. A.; Hummelen, J. C.; Blom, P. W. M. *Physical Review Letters.* **2004**, *93 (12)*, 216601-1.

Chapter 2

2,5-Substituted PPV Derivatives with Different Polarities: The Effect of Side Chain Polarity on Solubility, Optical and Electronic Properties[a]

In Chapter 2 three 2,5-substituted polar PPV derivatives i.e. poly(2-methoxy-5-(triethoxymethoxy)-1,4-phenylene vinylene) (MTEM-PPV), poly(2,5-bis(triethoxymethoxy)-1,4-phenylene vinylene) (BTEM-PPV) and poly(2-(n-nonyloxy)-5-(triethoxymethoxy)-1,4-phenylene vinylene) (NTEM-PPV) are prepared and compared to the apolar poly(2-methoxy-5-(3,7-dimethyloctyloxy)-1,4-phenylene vinylene) (MDMO-PPV). It is demonstrated that the sulfinyl precursor route is suitable to obtain these polymers in excellent yield and with improved purity as compared to the Gilch route. Furthermore, the influence of the variation of the polarity of the side chains, i.e. oligo(oxyethylene) and alkyl substituents, on the optical and electronic properties is investigated with spectroscopic and electrical measurements. Also their solubility and solution properties are studied.

2.1 Introduction

As already mentioned in Chapter 1, poly(*p*-phenylene vinylene) (PPV) and related polymers are interesting electroactive polymers for a wide variety of opto-electronic applications.[1,2] For the successful application of PPV-type polymers in advanced opto-electronic applications, two issues are of particular interest, *i.e.* the purity of the conjugated system and the ability to adapt the chemical and physical properties to specification. This chapter focuses on both

[a] Part of this chapter is published in *Thin Solid Films* **2006**, *511-512*, 328-332.

issues, presenting PPV derivatives with a significantly improved purity as well as demonstrating the adjustment of the conjugated polymer properties by a careful choice of substituents.

A series of functionalized conjugated polymers with a 2,5-substituted PPV base structure are synthesized: poly(2-methoxy-5-(triethoxymethoxy)-1,4-phenylene vinylene) (MTEM-PPV), poly(2,5-bis(triethoxymethoxy)-1,4-phenylene vinylene) (BTEM-PPV) and poly(2-(*n*-nonyloxy)-5-(triethoxymethoxy)-1,4-phenylene vinylene) (NTEM-PPV). These polymers are compared to poly(2-methoxy-5-(3,7-dimethyloctyloxy)-1,4-phenylene vinylene) (MDMO-PPV) (Figure 2-1). MDMO-PPV - often also referred as OC_1C_{10}-PPV- is a typical representative of the class of PPV-type materials and used as a standard material in conjugated polymer research and development. This conjugated polymer has been the subject of investigation by workers at Philips and Covion[3] and also subject of extensive research towards photovoltaic (PV) devices.[4] Although MDMO-PPV will never be the ultimate conjugate polymer in fully commercial applications, it is clear that it plays the role of 'workhorse' already for many years in this field. Therefore it can be very interesting to compare new 2,5-substituted PPV derivatives with this 'workhorse'.

Furthermore, the effect of side chain polarity on the optical and electronic properties is investigated. Also the impact of altering the side chain on the observed solubility properties is studied. The capability to fine-tune the solubility properties is important to find environmentally friendly processing solvents for this type of polymers.

As already described in Chapter 1, PPV-type polymers are most commonly synthesized *via* precursor methods, in which soluble precursor polymers are converted to the conjugated structure *in situ* or with an additional elimination step. Due to the excellent solubility properties of the conjugated 2,5-substituted dialkoxy-PPVs, the use of a precursor route is not essential anymore to process these materials. However, in order to achieve a low defect level, a reproducible

and well-defined polymerization procedure is essential and precursor routes yield good results. All three polar functionalized 2,5-substituted conjugated polymers are prepared *via* the sulfinyl precursor route. The purity of the PPV-type polymers, here defined as the defect level in the conjugated system, is compared to previously reported polymers with comparable structures prepared by the dehydrohalogenation or Gilch route. The typical choice to work with both procedures can be justified by the use of the Gilch route as a standard procedure in industry and the promising results obtained for the sulfinyl route developed at the University Hasselt. In section 2.2, a comprehensive overview of the typical synthesis *via* the two mentioned processes is presented.

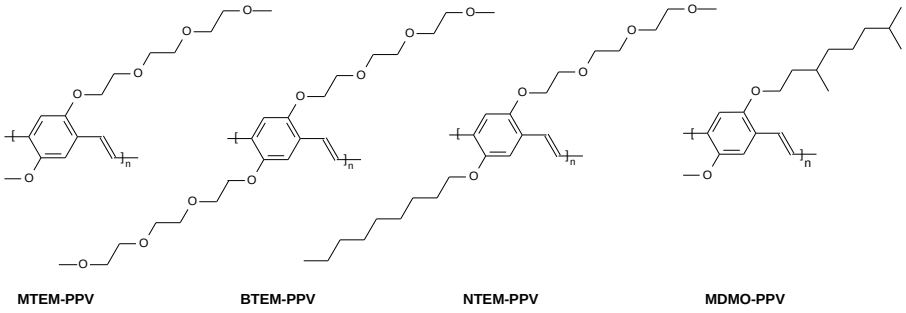

Figure 2-1 Overview of the three 2,5-substituted polar PPV derivatives which are compared with MDMO-PPV

2.2 Sulfinyl *versus* Gilch precursor route

▪ The dehydrohalogenation or Gilch route

The dehydrohalogenation route was first reported by Gilch and Wheelwright[5] and involves the basic treatment of a α,α'-dihalogen *p*-xylene derivative **1** with an excess of potassium *tert*-butoxide (K*t*BuO) in organic solvents. Due to premature basic elimination, precipitation occurred during the polymerization which led to insoluble PPV fragments. To prevent premature precipitation Swatos *et al.* presented a modification of the Gilch route that uses

one equivalent of K*t*BuO instead of an excess of base, to yield a soluble precursor polymer that can be converted to the conjugated form[6] Since the precursor polymer can no longer be isolated and processed if more than one equivalent is used, the Gilch route can only be called a 'precursor' route in the real sense of the word if no more than one equivalent of base is used during the polymerization. In literature no real distinction is made between the two routes - it is always referred to as the Gilch route and this appellation is kept throughout this work.

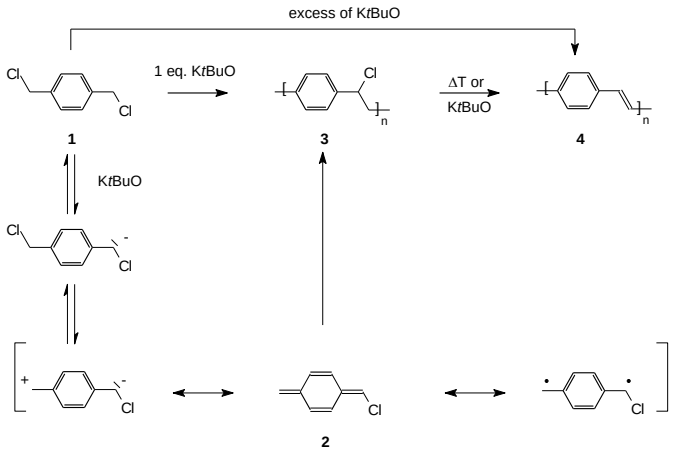

Scheme 2-1 The Gilch route

The mechanism of the Gilch route is depicted in Scheme 2-1. The first step is the base-induced elimination of HCl, leading to the 'real' monomer **2**, a quinodimethane (QM) derivative. The mechanism for the second step, the polymerization itself - either anionic or radical- is still under discussion. A broad community active in research of Gilch polymerization is convinced that an anionic polymerization process takes place. This hypothesis is most strongly advocated by Hsieh *et al.* [7] and more recently by Ferraris *et al.*[8] Recent work of Rehahn *et al.*[9] and of our group[10], substantiate that radical processes occur and are responsible for the formation of high molecular weight polymer. This discussion is beyond the scope of this work. The third and last step is the conversion of chlorine PPV precursor **3** to the conjugated material **4** by heat treatment (300°C, 1 hour) or by basic elimination with excess of base in case of

soluble PPV derivatives. Hydrogen chloride is produced during the elimination process, which may hamper efficient device performance. At present, the Gilch route is the most widely used route in industry, because it allows easy access to a large range of substituted PPV derivatives soluble in organic solvents, such as MDMO-PPV.[11]

- **The sulfinyl route**

To obtain highly reproducible materials in very high purity and with extremely low intrinsic defect levels, a new precursor route towards PPV-based polymers was designed in our laboratory, the so-called sulfinyl route.[12,13] A schematic representation of the typical steps occurring during the polymerization of a PPV derivative *via* the sulfinyl route is depicted in Scheme 2-2. Similar to the Gilch route, radical chain polymerization as well as anionic chain polymerization are possible and probably compete with each other. It is believed that high molecular weight materials are associated with a self-initiated radical chain polymerization and low molecular weight materials are obtained *via* an anionic mechanism.[14]

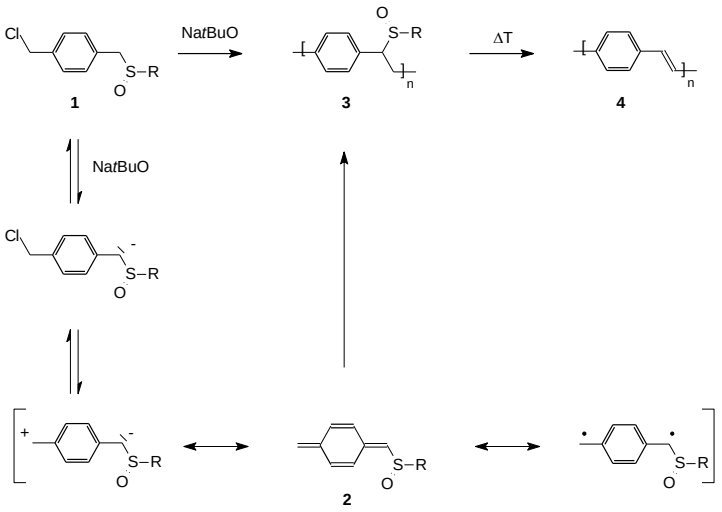

Scheme 2-2 The sulfinyl precursor route

The sulfinyl precursor route differs from the Gilch route and most other routes known in literature by the chemical differentiation in the monomer. The asymmetrical substituted sulfinyl monomer **1** shows a differentiation between on one hand the leaving group (*i.e.* halide) and on the other hand the polarizer (*i.e.* sulfinyl group) (Scheme 2-2). As polarizer and leaving group show contradictorily demands, the major advantage of this approach in comparison with precursor routes starting from symmetrically substituted monomers, is a fine-tuning of both functionalities. Halides (mostly chlorides) are chosen as leaving group, because of their high leaving group capacity, so the actual monomer in the polymerization – the *p*-QM **2**– is formed very efficiently upon elimination of this moiety. Furthermore halides are bad polarizers. Sulfinyl groups with solubilizing side chains (*e.g.* octyl side chain) introduce the opposite behaviour and fulfill the function of polarizer. When the sulfinyl monomer **1** is allowed to react with a base (usually Na*t*BuO), deprotonation occurs selectively *alpha* to the sulfinyl group as this position bears the most acid proton. By subsequent 1,6-elimination of the leaving group the *p*-QM system **2** is generated in such a way that propagation occurs *via* consecutive 'head-to-tail' additions and the undesired 'head-to-head' and 'tail-to-tail' additions are kept to an absolute minimum. In addition, the sulfinyl groups generate solubility on the precursor stage in solvents that are well suited for processing techniques. Another key feature of these groups is that they are stable at ambient temperature and easily expelled at elevated temperatures to realize complete elimination and yield a fully conjugated structure. Conversion to the final conjugated polymer can be accomplished by a thermal treatment at a temperature as low as 100 °C, which is relatively low compared to the temperatures used in the other precursor routes.[15] The elimination process leads to the expulsion of sulfenic acids, which are unstable and immediately dimerize to give thiosulfinates with concomitant loss of water. The thiosulfinates disproportionate with formation of thiosulfonates and disulfides.[15] Furthermore, the sulfinyl precursor route allows the straightforward introduction of various substituents along the conjugated backbone, which offers the possibility to tailor the properties of the material to suite a given application.[16, 17]

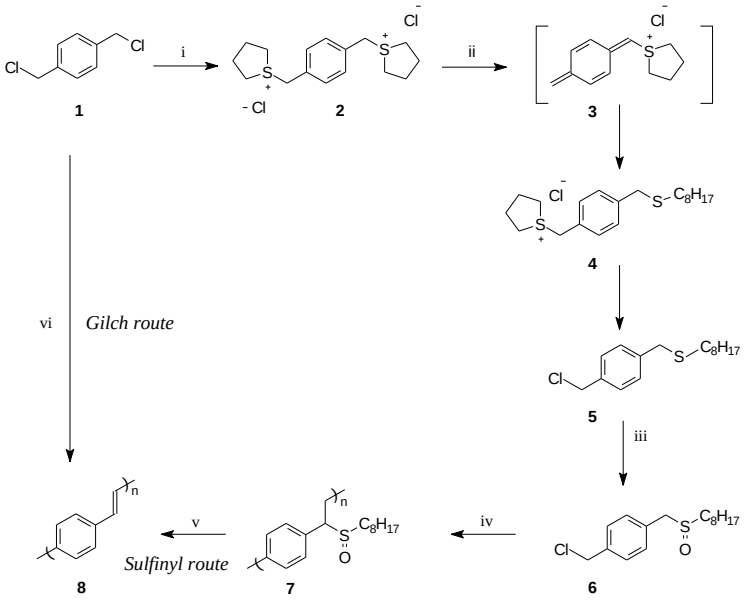

Scheme 2-3 Synthesis of PPV *via* the Gilch and the sulfinyl precursor routes (i: THT, MeOH; ii: RSH, Na*t*BuO, MeOH; iii: H_2O_2, TeO_2, HCl_{cat}, 1,4-dioxane; iv: Na*t*BuO, 2-BuOH; v: toluene; vi: K*t*BuO, 1,4-dioxane (dry))

A highly selective route to introduce the asymmetry of the sulfinyl monomers was developed within our group[18] as schematically depicted in Scheme 2-3. Simple nucleophilic substitution of an α,α'-dichloro-*p*-xylene derivative **1** with a thiolate anion yields a statistical 2/1/1 mixture of mono-thioether, di-thioether and the starting product, the α,α'-dichloro-*p*-xylene derivative. This mixture is hard to separate. To obtain selectively the mono-substituted thioether **5** in a high yield, a very smooth synthetic procedure was worked out as outlined in Scheme 2-3. Therefore a α,α'-bissulfonium-*p*-xylene **2** is reacted with an equimolar amount of a thiolate anion. This anion acts as a base with abstraction of a benzylic proton. Subsequent 1,6-elimination of a tetrahydrothiophene (THT) group affords a *p*-QM system **3** that undergoes thiolate attack and an α-sulfonium-α'-thioether p-xylene **4** is obtained. Azeotropic removal of the THT results in the corresponding chloro-compound **5** in a high yield. Selective oxidation of the thioethers is required to avoid

overoxidation. A simple and efficient method is the tellurium-catalyzed oxidation by means of H_2O_2 to afford the sulfinyl monomer **6**.

Although the chemical differentiation complicates to some extend the monomer synthesis, it allows an increased control over the polymerization and a controllable elimination of the obtained precursor polymer, leading to materials with dramatically improved opto-electronic characteristics as compared to the same materials prepared *via* other methods (section 2.7). Hence, the sulfinyl route is a particularly suitable method to demonstrate the reproducible adjustment of the physical properties of PPV-type polymers by changing the substituents.

2.3 Synthesis of three 2,5-substituted PPV derivatives with different polarities: NTEM-PPV, MTEM-PPV and BTEM-PPV

2.3.1 Synthesis of the sulfinyl monomers towards NTEM-PPV, MTEM-PPV and BTEM-PPV

The starting compounds 1-(n-nonyloxy)-4-(2-(2-(2-methoxy-ethoxy)-ethoxy)-ethoxy)benzene **3a**, methoxy-4-(2-(2-(2-methoxy-ethoxy)-ethoxy)-ethoxy)-benzene **3b** and 1,4-bis(2-(2-(2-methoxy-ethoxy)-ethoxy)-ethoxy)-benzene **3c** for the sulfinyl monomers are synthesized using a Williamson etherification with 4-methoxyphenol or dihydroquinone as the nucleophile towards toluene-4-sulfonic acid 2-(2-(2-methoxy-ethoxy)-ethoxy)-ethyl ester **1**. This tosylate ester is prepared in almost quantitative yield starting from the corresponding alcohol according to a literature procedure.[19] For **3a** an additional Williamson ether synthesis is required to obtain intermediate 4-(n-nonyloxy)phenol **2** first (Scheme 2-4).

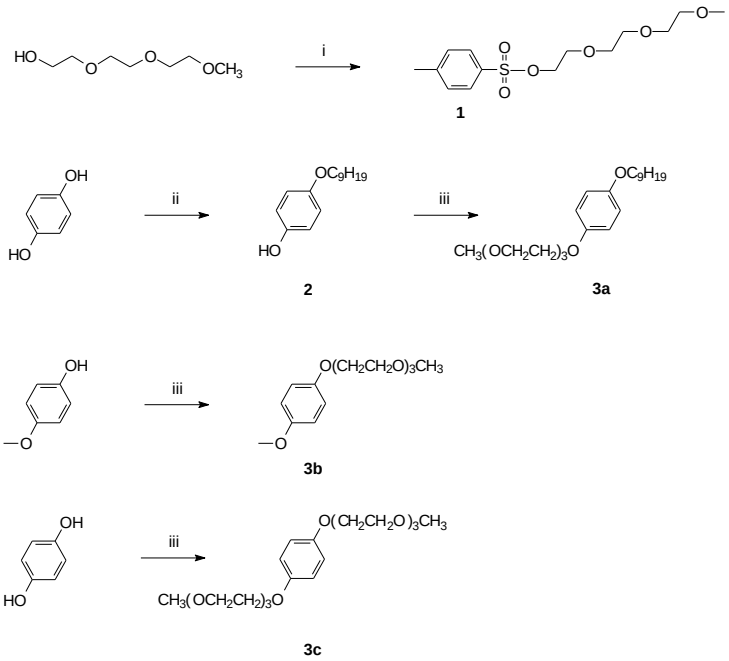

Scheme 2-4 Synthesis of the starting compounds **3** (i: TosCl, KOH, CH_2Cl_2, 0°C; ii: n-BrC_9H_{19}, NaI_{cat}, NaOH, EtOH; iii: **1**, KOH, EtOH, reflux)

The various steps towards the 2,5-substituted PPV derivatives poly(2-(n-nonyloxy)-5-(triethoxymethoxy)-1,4-phenylene vinylene) (NTEM-PPV) **9a**, poly(2-methoxy-5-(triethoxymethoxy)-1,4-phenylene vinylene) (MTEM-PPV) **9b** and poly(2,5-bis(triethoxymethoxy)-1,4-phenylene vinylene) (BTEM-PPV) **9c** starting from the corresponding functionalized benzenes **3a-c** are outlined in Scheme 2-5. In a first step the functionalized benzenes **3a-c** are chloromethylated according to an adapted literature procedure[11,17] using concentrated HCl and formaldehyde in acetic anhydride to give the corresponding chloromethylated compounds **4a-c**. To synthesize the asymmetrically substituted monomers **7a-c**, a selective route is employed, which was previously described.[18] The first step involves the synthesis of the α,α'-bissulfonium-*p*-xylylenes **5a-c**. Starting from **4a-c**, reaction with THT gives the corresponding bissulfonium salts **5a-c** in high yield. The symmetrical salts are then treated with an equimolar amount of an alkylthiolate anion, to obtain mono-substituted thioethers **6a-c** with a very high selectivity (90%). The thioethers can be oxidized to the asymmetric sulfinyl monomers **7a-c** using the

H_2O_2 as the oxidant (>70% after purification by column chromatography). It should be noted that **6a-b** and **7a-b** are present in a 1/1 mixture of regio-isomers, which is used without further separation.

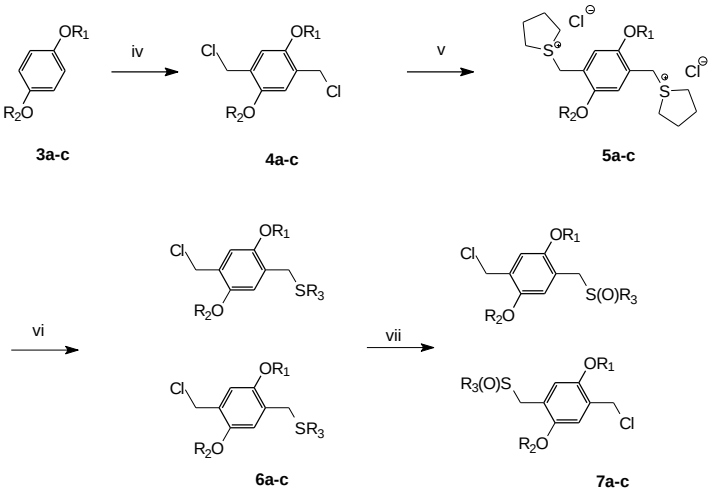

a (R_1= C_9H_{19}; R_2= $(CH_2CH_2O)_3CH_3$; R_3= C_8H_{17})
b (R_1= CH_3; R_2= $(CH_2CH_2O)_3CH_3$; R_3= C_8H_{17})
c (R_1= R_2= $(CH_2CH_2O)_3CH_3$; R_3= C_8H_{17})

Scheme 2-5 Synthesis of the sulfinyl monomers **7** (iv: *p*-CH_2O, Ac_2O, HCl, 70°C; v: THT, MeOH; vi: RSH, NatBuO, MeOH; vii: H_2O_2, TeO_2, HCl_{cat}, 1,4-dioxane)

2.3.2 Synthesis of sulfinyl precursor polymers towards NTEM-PPV, MTEM-PPV and BTEM-PPV

The sulfinyl monomers **7a-c** are polymerized in *sec*-BuOH according to a standard procedure developed in our group (Scheme 2-6).[13] The monomer and the base solution are brought in a set-up as depicted in Figure 2-2. The concentration of the monomer is 0.1 M when the total amount of solvent (base and monomer solution) is taken into account. Both base and monomer solutions are purged with a flow of nitrogen and the reaction temperature is maintained at 30 °C. After addition of the base solution to the monomer, the reaction is stirred for one hour at 30 °C. Subsequently, the mixture is poured into water and extracted with dichloromethane. After evaporation of the organic layer, the

precursor polymers **8a-c** are precipitated in a non-solvent, collected and dried in vacuum.

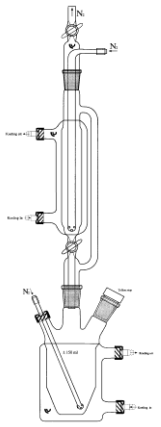

Figure 2-2 Set-up for the sulfinyl polymerization

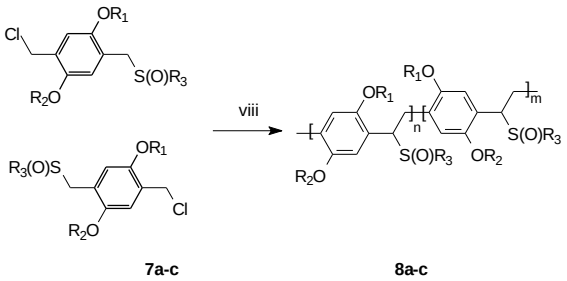

7a-c **8a-c**

a (R_1= C_9H_{19}; R_2= $(CH_2CH_2O)_3CH_3$; R_3= C $_8H_{17}$)
b (R_1= CH_3; R_2= $(CH_2CH_2O)_3CH_3$; R_3= C $_8H_{17}$)
c (R_1= R_2= $(CH_2CH_2O)_3CH_3$; R_3= C $_8H_{17}$)

Scheme 2-6 Synthesis of the sulfinyl precursor polymers **8** (viii: Na*t*BuO, 2-BuOH)

The precursor polymers **8a-c** are prepared in excellent yields (Table 2-1). Analytical SEC measurements of **8a-c** are performed *versus* polystyrene standards. The observed molecular weights M_w, which range from 6×10^4 to 28×10^4 g/mol, confirm that in all cases high molecular weight polymers are obtained (Table 2-1). Previously for MDMO-PPV a molecular weight of 31×10^4 g/mol is reported.[13] The introduction of the more polar oligo(oxyethylene) side chains results in a small decrease in the apparent molecular weight as compared to MDMO-PPV. However, it is not clear if this is a proper reflection of the actual molecular weight or the result of differences in the hydrodynamic volume, which induce different interactions with the GPC column.

Polymer	Yield (%)	M_w (g/mol)	PD
8a	69	60000	2.0
8b	82	210000	3.7
8c	92	280000	2.8
9a	63	60000	3.8
9b	91	90000	4.8
9c	87	260000	5.8

Table 2-1 Polymerization results for precursor polymers **8a-c** and conjugated polymers **9a-c**

2.3.3 Thermal elimination of the sulfinyl precursor polymers towards NTEM-PPV, MTEM-PPV and BTEM-PPV

The final step in the sulfinyl precursor route is the thermal elimination of the sulfinyl group as a result of which the precursor polymer converts into the conjugated structure (Scheme 2-7). The elimination process is well documented in literature and proceeds through a *syn*-elimination in which the transition state is believed to have a planar structure. Due to steric hindrance trans-vinylene bonds are obtained[15].

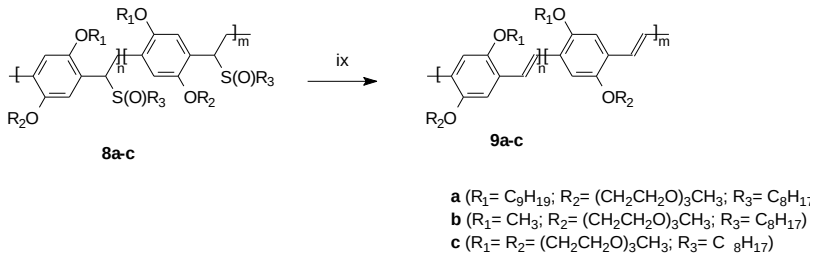

a (R_1= C_9H_{19}; R_2= $(CH_2CH_2O)_3CH_3$; R_3= C_8H_1;
b (R_1= CH_3; R_2= $(CH_2CH_2O)_3CH_3$; R_3= C_8H_{17})
c (R_1= R_2= $(CH_2CH_2O)_3CH_3$; R_3= $C_{8}H_{17}$)

Scheme 2-7 Elimination of the sulfinyl precursor polymers **9** (ix: toluene, reflux)

The elimination is performed in toluene solution. After the first elimination step, performed during a 3 h reaction time, the polymer is precipitated, collected and refluxed in fresh toluene for another 3 h (second elimination). After all, Roex *et al*. observed that this so-called two-step elimination procedure resulted in less that 0.5 % of non-eliminated groups for MDMO-

PPV.[20] Therefore, this procedure is applied for all polymers prepared in this work *via* the sulfinyl route. After purification in boiling toluene, the conjugated polymers NTEM-PPV **9a**, MTEM-PPV **9b** and BTEM-PPV **9c** are obtained in excellent yield (Table 2-1). The observed molecular weights M_w of **9a-c**, which range from 6×10^4 to 26×10^4 g/mol, are roughly in the same order of magnitude as those found for the corresponding sulfinyl precursor polymers **8a-c**, indicating that no significant degradation occurs during the elimination process (Table 2-1). The increase in the polydispersity values reflects the different hydrodynamic volumes of the more rigid conjugated backbones, as compared to the precursor polymers. The same effect has also been observed for MDMO-PPV.[13]

The elimination process of the sulfinyl groups of the precursor polymers **8a-c** can be monitored by *in situ* UV-Vis spectroscopy. For this purpose a specially designed oven containing the precursor polymer spin coated on a quartz window is placed in the beam of the spectrometer. A dynamic heating program of 2 °C/min from ambient temperature up to 250 °C, under a continuous flow of nitrogen is used.

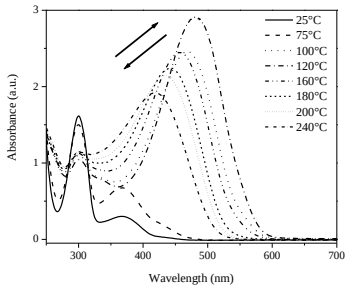

Figure 2-3 Thin film UV-Vis absorption spectra of the gradual formation of the conjugated polymer NTEM-PPV at selected temperatures

At room temperature, thin films of the precursor polymer of NTEM-PPV exhibit a strong absorbance with a maximum at λ_{max} = 300 nm (Figure 2-3). Upon heating from room temperature to 250 °C, a new absorption band appears which is associated with the conjugated system. During the elimination process, this band exhibits a gradual red shift (λ_{max} = 480 nm at 120 °C) with increasing temperature due to an increase of the average conjugation length

(Figure 2-3). When the absorbance at this maximum wavelength (λ_{max} = 480 nm) is monitored *versus* temperature, it becomes evident that the conjugated structure starts to develop around 70 °C. At temperatures above 120 °C, the absorption at 480 nm starts to decrease as a result of a thermochromic effect.[21] Whereas at room temperature the absorption maximum of **9a** in a thin film is positioned around λ_{max} = 510 nm, upon increase of temperature a reversible shift of this absorption maximum is observed to lower wavelength (*i.e.* λ_{max} = 480 nm at 120 °C). The same phenomenon is observed with FT-IR spectroscopy where the double bond signal at 970 cm^{-1} decreases upon heating and increases to its initial value when the sample is cooled to room temperature, further corroborating the reversible character of the observations. Similar observations are made for the precursor polymers of MTEM-PPV and BTEM-PPV.

2.4 UV-Vis thin film characterization

All reported polymers are fully characterized using different analytical techniques such as ^{1}H and ^{13}C NMR spectroscopy, elemental analysis and FT-IR spectroscopy as well as UV-Vis absorption spectroscopy (see experimental section). NTEM-PPV **9a**, MTEM-PPV **9b** and BTEM-PPV **9c** exhibit in the UV-Vis absorption spectrum a distinct absorption associated with the π–π^* transition, both in a thin film (Figure 2-4) and in solution (Table 2-2). The exact position of this absorption maximum is amongst others dependent on temperature and polymerization batch. Furthermore, in the case of thin films the morphology and in the case of solutions the solvent plays an important role. Keeping the above considerations in mind, for polymer NTEM-PPV **9a** at ambient temperatures an absorption maximum is found in the range λ_{max} = 508 - 524 nm in a thin film. For polymers MTEM-PPV **9b** and BTEM-PPV **9c** under the same conditions thin film absorption maxima are found in the range λ_{max} = 508 - 509 nm and λ_{max} = 509 - 518 nm, respectively. For comparison, a typical absorption maximum of MDMO-PPV obtained from a sulfinyl precursor polymer is located at λ_{max} = 517 nm.[15] This indicates that the

introduction of polar substituents in **9a-9c** does not have a substantial impact on the optical properties of the polymers, as compared to MDMO-PPV.

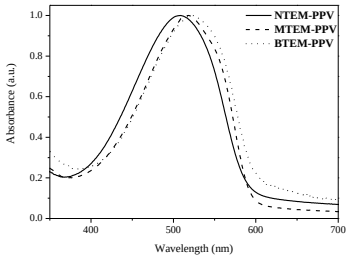

Figure 2-4 Thin film UV-Vis absorption spectra of NTEM-PPV **9a**, MTEM-PPV **9b** and BTEM-PPV **9c**

Solvent	**λ_{max} (nm) 9a**	**λ_{max} (nm) 9b**	**λ_{max} (nm) 9c**	**λ_{max} (nm) MDMO-PPV**
Toluene	505	492	496	509
Dioxane	512	486	494	512
Chlorobenzene	502	493	498	512
Tetrahydrofuran	500	487	498	506
Chloroform	495	483	489	505

Table 2-2 Overview of solution UV-Vis absorption maxima λ_{max} for NTEM-PPV **9a**, MTEM-PPV **9b** and BTEM-PPV **9c** as well as for MDMO-PPV in selected solvents

2.5 Comparison of the results of NTEM-PPV, MTEM-PPV and BTEM-PPV prepared *via* the Gilch and the sulfinyl precursor route

The three 2,5-substituted PPV derivatives **9a-c** described in this chapter, are prepared *via* the sulfinyl precursor route to achieve sufficiently low defect levels. An indication of the purity and defect levels of PPV-type polymers is most readily obtained from the position of the π–π^* absorption maxima. The PPV derivatives NTEM-PPV, MTEM-PPV and BTEM-PPV as well as MDMO-PPV obtained *via* the sulfinyl route display well-defined transitions in thin film UV-Vis spectroscopy in the range λ_{max} = 508-524 nm (Figure 2-4). To justify our choice that the sulfinyl precursor route is essential for obtaining

high purity polymers, we have compared these results with previous reports using the Gilch precursor route. This comparison has already been done for MDMO-PPV for which it has been demonstrated that the amount of structural irregularities is drastically reduced when using the sulfinyl precursor route and that improved polymer solubility, viscosity characteristics, microstructure and device performance are observed.[9, 22] Although to our best knowledge NTEM-PPV has not yet been described in literature, a similar polymer, *i.e.* poly(2-(undecoxy)-5-(diethoxymethoxy)-1,4-phenylene vinylene) prepared *via* the Gilch route has been prepared.[23] This polymer also has an amphiphilic character with both an alkyl and an oligo(oxyethylene) side chain. The reported λ_{max} of organized LB films of poly(2-(undecoxy)-5-(diethoxymethoxy)-1,4-phenylene vinylene) is 489 nm, compared to 508 - 524 nm for NTEM-PPV prepared *via* the sulfinyl precursor route. This indicates that NTEM-PPV has a dramatically improved purity as compared to this previously reported PPV derivative. A comparison for MTEM also displays a improvement in the optical properties, *i.e.* thin films of MTEM-PPV prepared by the Gilch route[24] absorb at λ_{max} = 494 nm, whereas the UV-Vis absorption spectrum of MTEM-PPV prepared by the sulfinyl route exhibits a distinct transition at λ_{max} = 508 - 509 nm. Finally, also for polymer BTEM-PPV a similar observation can be made. It has been reported that BTEM-PPV prepared *via* the Gilch route has an absorption maximum at λ_{max} = 498 nm,[24] as compared to λ_{max} = 509 - 518 nm for BTEM-PPV prepared by the sulfinyl route. Hence, we can conclude that for **9a-c** and for MDMO-PPV, the extra steps in the sulfinyl monomer synthesis are worthwhile since higher purity levels are achieved so that these conjugated polymers can now be used for opto-electronic applications.

2.6 UV-Vis solution characterization

Whereas the optical properties of NTEM-PPV, MTEM-PPV and BTEM-PPV and MDMO-PPV in thin films are very similar, these properties are different in solution. This is the result of the expected markedly different polarities of the individual polymers. For a typical solvent used in the manufacturing of organic PV devices[22] in which polymers **9a-c** as well as

MDMO-PPV readily dissolve, *i.e.* chlorobenzene, the solution absorption maximum ranges from λ_{max} = 493 nm for MTEM-PPV to 512 nm for MDMO-PPV (Table 2-2). Since the solution λ_{max} is generally less sensitive to external factors, as compared to the thin film λ_{max}, this large difference apparently is a result of solvatochromic effects of the PPV-type polymers. To further assess these effects, the solubility and UV-Vis absorption characteristics of NTEM-PPV, MTEM-PPV and BTEM-PPV as well as MDMO-PPV in various solvents with different polarities, *i.e.* E_TN values,[25] are studied. For this study a polymer concentration of approximately 0.1 mM (based on the repeating unit) is employed.

Solvent	**Polarity[24] (E_T^N)**	**9a**	**9b**	**9c**	**MDMO-PPV**
n-Hexane	0.009	--	--	--	--
Toluene	0.099	±	±	±	±
Dioxane	0.164	±	+	+	±
Chlorobenzene	0.188	+	+	+	+
Tetrahydrofuran	0.207	±	+	+	+
Chloroform	0.259	+	+	+	+
Acetone	0.355	--	-	±	--
Acetonitrile	0.460	-	-	±	--
Ethanol	0.654	--	-	-	--

Table 2-3 Overview of solubility's of polymers **9a-c** as well as of MDMO-PPV in selected solvents (+ completely soluble, no aggregation; ± completely soluble, aggregation observed by UV-Vis spectroscopy; - partially insoluble; -- fully insoluble)

It appears that none of the polymers are soluble in hexane, the most apolar solvent tested (Table 2-3). By using somewhat more polar solvents such as toluene and chlorobenzene, an orange or orange-red solution is obtained. At the other side of the polarity scale, all polymers are soluble in $CHCl_3$, but only BTEM-PPV is soluble in, for example, acetonitrile (Table 2-3). The solubility studies confirm that the introduction of polar substituents can lead to a better solubility of the PPV-type polymers in more polar solvents.

A more careful analysis of the UV-Vis absorption characteristics of the solutions, which is done in co-operation with Dra. Sofie Fourier, reveals a more complex behaviour than the one outlined above. In chlorobenzene, for all polymers a distinct transition is found in the UV-Vis absorption spectrum, as can be expected for this type of polymers (Table 2-2). However, at the respective edges of the polarity scale a more complex behaviour is observed. Although the polymers fully dissolve, an additional absorption is observed in the UV-Vis absorption spectrum as a shoulder around λ_{max} = 560 nm. This shoulder develops either instantaneously or over the course of a night, dependent on the particular solvent/polymer combination. This is exemplified for BTEM-PPV in Figure 2-5. For this polymer, the shoulder is present in toluene (at the apolar side of the polarity scale) and in acetone and acetonitrile (at the polar side of the polarity scale), whereas in solvents of intermediate polarity only the π–π* transition is observed. The shoulder appears as a result of π–π stacking interactions caused by aggregation of the conjugated systems.[26] This is in contrast to the situation in good solvents, in which no aggregation takes place.

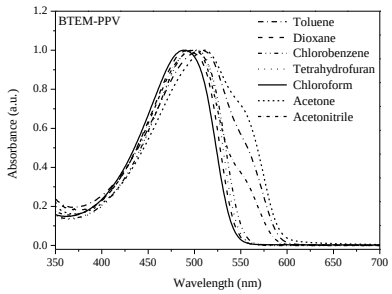

Figure 2-5 Solution UV-Vis absorption spectra of BTEM-PPV in various solvents, taken after 24 h. A polymer concentration of approximately 0.1 mM (based on the repeating unit) is employed

For solutions of the other polymers, similar observations can be made (Figure 2-6). Aggregation is most pronounced for NTEM-PPV, which displays this behaviour in most solvents. This is presumably the result of its amphiphilic character, resulting in a high affinity to form aggregates such as micellar like

structures. However, it should be noted that the exact nature and structure of the aggregates remains under investigation.

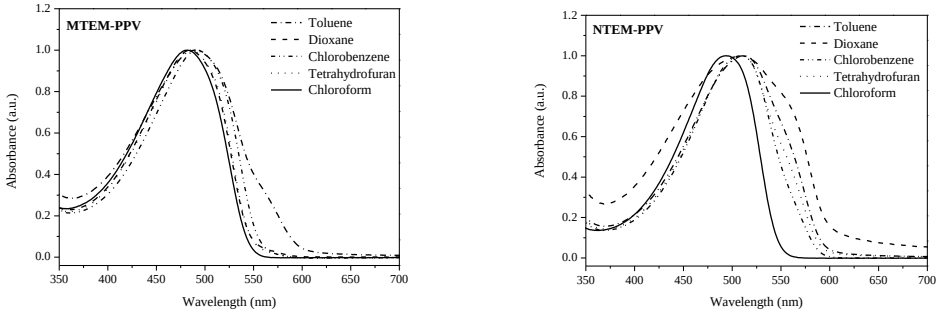

Figure 2-6 Solution UV-Vis absorption spectra of MTEM-PPV and NTEM-PPV in various solvents taken after 24 h. A polymer concentration of approximately 0.1 mM (based on the repeating unit) is employed

By studying the λ_{max} in various solvents, the solvatochromic effects become clear (Table 2-2). Apparently, the conformation of the π-conjugated backbone in solution is dependent on the specific side chain/solvent combination. The hypsochromic shifts of λ_{max} represent increasing deviations from a fully planar structure. Similar solvatochromic effects have been previously observed for other, more flexible, conjugated polymers, such as polysilanes.[27]

From the above studies on NTEM-PPV, MTEM-PPV and BTEM-PPV and MDMO-PPV it is evident that the nature of the side chains has a substantial influence on the solution properties. This will affect processing techniques in which solutions play an important role, such as various coating methods. By a careful choice of substituents, PPV derivatives can be prepared which are soluble in a wider range of solvents. Further research on the UV-Vis absorption characteristics of these 2,5-substituted PPV derivatives can be found in the dissertation of Sofie Fourier, who also studies the λ_{max} in various solvents at various temperatures.

2.7 Fluorescence spectroscopy

The polymers are also studied using fluorescence spectroscopy. In a thin film, NTEM-PPV, MTEM-PPV and BTEM-PPV exhibit a distinct fluorescence emission at λ_{em} = 587 nm (excitation wavelength λ_{exc} = 504 nm). For MDMO-PPV a similar λ_{em} = 590 nm has been reported in the literature.[13] This further confirms that the change in substituents has no significant influence on the thin film optical properties.

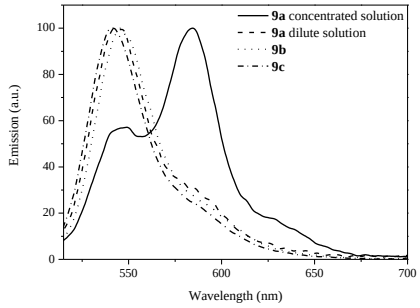

Figure 2-7 Fluorescence emission spectra of NTEM-PPV **9a**, MTEM-PPV **9b** and BTEM-PPV **9c** in $CHCl_3$ solutions

In $CHCl_3$ solution, for polymers MTEM-PPV and BTEM-PPV, a distinct emission is found at λ_{em} = 546 nm and 543 nm, respectively (Figure 2-7), which is blue-shifted with respect to the thin films as a result of the absence of π–π interactions (excitation wavelength λ_{exc} = 485 nm). For NTEM-PPV **9a** in dilute solution, a similar λ_{em} = 543 nm is found. However, at increasing concentrations, the intensity of this emission decreases and a new red-shifted emission at λ_{em} = 583 nm becomes dominant (Figure 2-7). This is the same wavelength as observed in thin films. Apparently, even in $CHCl_3$ solution, aggregation phenomena occur at higher concentrations.

2.8 Electrical characterization

In addition to the optical characterization, electrical measurements[b] are performed on NTEM-PPV, MTEM-PPV and BTEM-PPV as well as MDMO-PPV to further assess the impact of the side chains on the electronic properties. This study is done in co-operation with Drs. Martin Breselge of the Materials Physics research group at the Institute for Materials Research (IMO). It is found that the effect of side chain substitution is most pronounced in the relative permittivity (Table 2-4, Figure 2-8).

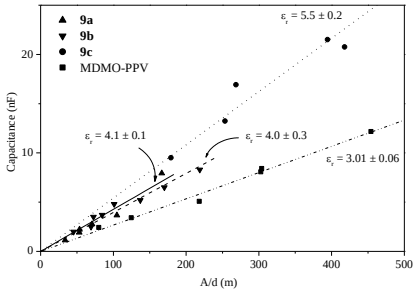

Figure 2-8 Capacitances of NTEM-PPV **9a**, MTEM-PPV **9b** and BTEM-PPV **9c** and MDMO-PPV as determined from the susceptance as a function of the capacitor's geometry A/d (intersection area/film thickness).

Polymer	**ε_r**	**μ (10^{-4} cm^2/Vs)**	**σ (10^{-4} S/m)**
MDMO-PPV	3.0	2 - 3	0.1 – 0.4
NTEM-PPV	4.1	3 - 6	2 – 7
MTEM-PPV	4.0	1 - 5	2 – 5
BTEM-PPV	5.5	1 - 4	3 – 7

Table 2-4 Overview of the obtained results for relative permittivity ε_r, the FET-mobility μ and the conductivity σ for NTEM-PPV, MTEM-PPV and BTEM-PPV and MDMO-PPV

[b] The experimental details for the electrical characterization can be found in the experimental part at the end of this section

For MDMO-PPV a relative permittivity of 3.0 is found. Replacement of the alkyl side chain of (MDMO-PPV) by an oligo(oxyethylene) side chain in MTEM-PPV, increases the permittivity by 1 to 4.0. Substituting the OCH_3-side chain by an OC_9H_{19}-side chain, *i.e.* NTEM-PPV, further increases the permittivity slightly by 0.1 to 4.1. Finally, by introducing a second oligo(oxyethylene) side chain, *i.e.* BTEM-PPV, a permittivity as high as 5.5 is obtained. So, the increased polarity of the side chains gives rise to an increase in relative permittivity of the PPV derivatives. This is corroborated by the fact that for triethyleneglycol dimethylether a relative permittivity of 7.5 has been reported.[25]

The observed increase in the relative permittivity is of interest for the application of these PPV-type polymers in PV devices. After all, the relative permittivity has a direct impact on the dissociation characteristics of the electron-hole pairs in an organic bulk heterojunction solar cell. Therefore, the increase in the permittivity may lead to an enhanced solar cell performance.[28] The conjugated polymers currently used in the blends are characterized by low dielectric constants. As a result, strongly bound excitons are created after absorption of light. These electron-hole pairs need to be dissociated into free charge carriers in order to be collected at the electrodes before recombination takes place.[29] Typically, the dissociation efficiency in MDMO-PPV and [6,6]-phenyl C_{61}-butyric acid methyl ester (PCBM) bulk heterojunction solar cells is only 60 % at short circuit conditions, representing a major loss mechanism in these devices.[28] Currently, BTEM-PPV is tested in a polymer:fullerene bulk heterojunction solar cell. This study is done in collaboration with Prof. dr. Paul Blom of the research group Molecular Electronics-Physics of Organic Semiconductors at the University of Groningen (The Netherlands). Preliminary results show that the increase of the dielectric constant in these polymer:fullerene blends leads to an enhanced charge dissociation of 72 % for this novel polymer:fullerene system.

In contrast to the effect of side chain polarity on the relative permittivity, the mobility values of all four PPVs are of the same order of magnitude and in

the range of 10^{-4} cm^2/Vs (Table 2-4). This is not surprising, since the PPV backbone is responsible for the hole-transport and is not substantially affected by the change in substituents. It should be noted that the obtained mobility values depend on the geometry of the channels, *i.e.* their lengths, and more general also on the applied electric field.[30] This is reflected by the range given for the mobility values in Table 2-4: Higher values were obtained for longer channels, which are less influenced by the contact resistance as compared to shorter channels.

The final electrical parameter of interest is the conductivity. Surprisingly, the conductivity values increased by one order of magnitude upon introduction of oligo(oxyethylene) side chains (Table 2-4). Whereas the conductivity of MDMO-PPV is in the range of 1-4 × 10^{-5} S/m, the conductivity values of NTEM-PPV **9a**, MTEM-PPV **9b** and BTEM-PPV **9c** exceed 10^{-4} S/m. This can partly be attributed to the capacitive nature of the structures. The higher permittivity of NTEM-PPV, MTEM-PPV and BTEM-PPV in comparison to MDMO-PPV increases the number of charge carriers in the channel for a given voltage, thus increasing the conductivity. However, the remarkable increase of one order of magnitude gives rise to assume that additional factors play a role. These factors are the subject of further investigations.

2.9 Conclusions

This chapter focused on the synthesis and extensive characterization of three 2,5-substituted polar PPV derivatives, NTEM-PPV, MTEM-PPV and BTEM-PPV. Their properties have been compared to the apolar MDMO-PPV, which is frequently employed in applications. All polymers were obtained *via* the sulfinyl precursor route and it was demonstrated that by using this route these polymers can be obtained in excellent yield and with improved purity as compared to the Gilch route. Having access to previously inaccessible high purity materials, the effect of the polarity of the side chains on the optical and electronic properties has been investigated. It was shown that the variation of the polarity of the side chains, *i.e.* various combinations of oligo(oxyethylene)

and alkyl substituents, does not significantly alter the thin film optical properties of these polymers. Furthermore, the FET-mobility remained unchanged. However, the solubility as well as solution properties were significantly affected by the polarity of the substituents. This resulted in a considerably expanded accessible solvent range. Solubility in polar solvents, such as acetonitrile, has been achieved. In addition, solvatochromism and aggregation phenomena have been observed. The effect of side chain polarity was also observed in the electrical properties, as a significant increase in relative permittivity and conductivity. Hence, this chapter successfully demonstrated both the preparation of high purity functionalized polar PPV-type polymers and the reproducible adjustment of their physical properties by changing the substituents, two major issues in the area of conjugated polymers. Finally, based on the presented work, further adjustments of the polarity can be accomplished as desired in a straightforward manner, as will be shown in Chapter 3.

2.10 Experimental Section

Chemical and optical characterization.

NMR spectra were recorded with a Varian Inova Spectrometer at 300 MHz using a 5 mm probe for ^{1}H NMR and at 75 MHz using a 5 mm broadband probe for ^{13}C NMR. Analytical Size Exclusion Chromatography (SEC) was performed using a Spectra series P100 (Spectra Physics) pump equipped with a pre-column and two mixed-B columns (Polymer Labs) and a Refractive Index (RI) detector (Shodex) at 40°C. THF was used as the eluent at a flow rate of 1.0 mL/min. Molecular weight distributions are given relative to polystyrene standards. GC-MS data were obtained with a Varian TSQ 3400 Gas Chromatograph and a TSQ 700 Finnigan Mat mass spectrometer. Elemental analysis was performed with a Flash EA 1112 Series CHNS-O analyzer. Differential Scanning Calorimetry measurements were performed on a TA instruments DSC 2920. The samples (10 mg) were heated from -100 °C to 150 °C at a heating rate of 10 °C/min under N_2 atmosphere. The *in situ* elimination

reactions were performed in a Harrick High Temperature Oven, which is positioned in the beam of a Perkin Elmer spectrum one FT-IR spectrometer (nominal resolution 4 cm^{-1}, summation of 16 scans). The temperature of the sample is controlled by a Watlow temperature controller (serial number 999, dual channel). The precursor polymers **7** were spin coated from a $CHCl_3$ solution (6 mg/mL) on a KBr pellet at 500 rpm. The spin coated KBr pellet (diameter 25 mm, thickness 1 mm) is in direct contact with the heating element. All experiments were performed at 2°C/min under a continuous flow of nitrogen. "Timebase software" supplied by Perkin Elmer is used to investigate regions of interest. *In situ* UV-Vis measurements were performed on a Cary 500 UV-Vis-NIR spectrophotometer, specially adopted to contain the Harrick high temperature cell (scan rate 600 nm/min, continuous run from 200 to 800 nm). The precursor polymer was spin coated from a $CHCl_3$ solution (6 mg/mL) on a quartz glass (diameter 25 mm, thickness 3mm) at 700 rpm. The quartz glass was heated in the same Harrick oven high temperature cell as was used in the FT-IR measurements. The cell was positioned in the beam of the UV-Vis-NIR-spectrophotometer and spectra were taken continuously. The heating rate was 2°C/min up to 250 °C. All measurements were performed under a continuous flow of nitrogen. "Scanning Kinetics software" supplied by Varian is used to investigate regions of interest. UV-Vis measurements were performed on a Cary 500 UV-Vis-NIR spectrophotometer (scan rate 600 nm/min, continuous run from 200 to 800 nm). FT-IR spectra were collected with a Perkin Elmer Spectrum One FT-IR spectrometer (nominal resolution 4 cm^{-1}, summation of 16 scans). Fluorescence spectra were obtained with a Perkin Elmer LS-5B luminescence spectrometer.

Electrical characterization.

The samples for thin film electrical characterization were prepared and measured in a glove box system under an inert N_2 atmosphere with less than 1 ppm O_2 and H_2O. The polymers were dissolved in chlorobenzene at 50 °C on a hotplate until completely dissolved. Thin films of different thickness were prepared by spin coating. In case of the sandwich structures used for

impedance spectroscopy, an aluminum contact was evaporated. The relative permittivity was obtained from spectral impedance measurements of ITO/polymer/aluminum sandwich structures. The samples consisted of a glass substrate with two indium tin oxide (ITO) strips acting as electrodes, a spin coated polymer layer acting as dielectric and four evaporated aluminum contacts acting as counter-electrodes (Figure 2-9).

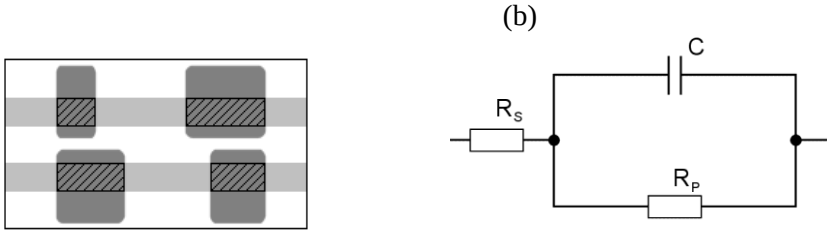

Figure 2-9 (a) Layout of the patterned ITO-glass substrates. The intersections (dashed area) of the ITO-strips (light gray) and the aluminum electrodes (dark gray) define capacitors of different size. (b) Equivalent circuit to fit the measurement data, with capacitance C, parallel resistance R_p and serial resistance R_s

The intersections of the metal electrodes and the ITO-strips defined capacitors of different sizes. The polymers were spin coated with varying film thickness to extend the number of different capacitor geometries. The complex impedance of the samples was measured with a HP4284 LCR-meter by applying a bias voltage of 0.8 V superposed by an oscillating voltage of 25 mV. Assuming the equivalent circuit in Figure 2-9, with a capacitance C, a parallel resistance R_p and a serial resistance R_s, the capacitance can be determined from the constant region of the susceptance. By plotting the capacitances C against the geometric factor A/d, the relative permittivity ε_r can be extracted from the slope of the graph, following the equation:

$$C = \varepsilon_0 \cdot \varepsilon_r \cdot \frac{A}{d}$$

where A is the size of the capacitor defined by the intersection of an ITO-strip and an aluminum electrode, d is the distance of the two electrodes determined by the thickness of the polymer film and ε_0 is the permittivity of free space. The field effect mobility μ and the conductivity σ, were measured in a field effect

transistor (FET) arrangement. The FET-chips employed in the electrical measurements were based on a doped Si-wafer with an aluminum gate electrode at one side and a Si-oxide layer with Au source and drain contacts at the side on which the conjugated polymer was deposited. Different geometries were employed, *i.e.* simple (two electrode) as well as interdigitated channels. The obtained channels were filled with the polymer under investigation by spin coating. Finally the FET substrates were glued with carbon paste on ceramic substrates to contact the gate electrode. To determine the mobility, the source-drain voltage as well as the gate voltage were swept from 0 V to -70 V. The mobility was extracted from the saturation regime by fitting the corresponding transfer characteristic in accordance with the parabolic approximation[31]:

$$I_{sd} = \frac{1}{2} \cdot \frac{W}{L} \cdot \mu \cdot C_{ox} \cdot \left(V_g - V_t\right)^2$$

In this equation, I_{sd} represents the source-drain current, W and L the channel width and length, μ the mobility, C_{ox} the specific capacitance of the insulating oxide (~17 nF/cm²), V_g the gate voltage and V_t the threshold voltage. The mobility is obtained independently from the threshold voltage from the coefficient of the quadratic V_g term.For determining the conductivity the gate electrode was disconnected and the measured I-V-characteristic was retrieved from the linear regime by using the equation:

$\sigma = \frac{L}{t \cdot W} \frac{\partial I_{sd}}{\partial V_{sd}}$ where t is the thickness of the polymer film measured by a micro-profiler; $\frac{\partial I_{sd}}{\partial V_{sd}}$ is the slope of the linear region determined from fitting a straight line through the measurement points.

Chemicals

All chemicals were purchased from Aldrich or Acros and used without further purification unless otherwise stated. Tetrahydrofuran (THF) and dioxane were distilled from sodium/benzophenone. MDMO-PPV monomers were synthesized and polymerized as described elsewhere.[13, 32]

Synthesis

Toluene-4-sulfonic acid 2-(2-(2-methoxy-ethoxy)-ethoxy)-ethyl ester 1. A three-necked flask equipped with mechanical stirrer, thermometer and N_2 inlet, is charged with 2-(2-(2-methoxy ethoxy)ethoxy)ethylalcohol (60.0 g, 0.37 mol), *p*-toluenesulfonyl chloride (71.5 g, 0.38 mol) and CH_2Cl_2 (250 mL). The homogeneous mixture is cooled to 0 °C with a $CO_{2(s)}$-acetone bath. Freshly powdered KOH (83.1 g, 1.47 mol) is added in small amounts under vigorous stirring while maintaining the reaction mixture below 5 °C (exothermic reaction). The mixture is stirred for 3 h at 0 °C after which CH_2Cl_2 (250 mL) and ice-water (300 mL) are added. The organic phase is separated and the aqueous phase is extracted with CH_2Cl_2 (2 x 150 mL). The combined organic layer is washed with water (150 mL), dried ($MgSO_4$) and concentrated under reduced pressure. The pure product was obtained in 98% yield as a colourless oil. ^{1}H NMR ($CDCl_3$): δ= 7.60 (d, 2H), 7.17 (d, 2H), 3.96 (t, 2H), 3.49 (t, 2H), 3.42-3.38 (m, 8H), 3.17 (s, 3H), 2.25 (s, 3H); MS (EI, m/z): 318 [M^+], 273, 259, 243, 229, 199, 172, 155, 91, 59, 45.

4-(*n*-Nonyloxy)phenol 2. A mixture of 4-methoxyphenol (25.0 g, 0.23 mol), NaOH (7.0 g, 0.17 mol) in EtOH (175 mL) was stirred for 2 h at ambient temperature under Ar atmosphere, after which a mixture of 1-bromononane (36.2 g, 175 mmol) and sodium iodide (0.6 g, 0.004 mol) in EtOH (75 mL) was added drop wise over a period of 1 h. The reaction mixture was stirred for 6 h at reflux temperature and overnight at 50 °C. After the total volume was reduced to 50 mL by evaporation and the solution was cooled down to ambient temperature, the product was extracted with CH_2Cl_2 (3 x 75 mL). The organic extracts were dried over anhydrous $MgSO_4$ and the solvent was evaporated to give the crude product as brown crystals. The pure product was obtained by column chromatography (SiO_2, eluent CH_2Cl_2) (22.7 g, 55 % yield). ^{1}H NMR ($CDCl_3$): δ = 6.75 + 6.74 (d, 4H), 3.87 (t, 2H), 1.73 (m, 2H), 1.39 (m, 12H), 0.86 (t, 3H); MS (EI, m/z): 236 [M^+].

1-(n-Nonyloxy)-4-(2-(2-(2-methoxy-ethoxy)-ethoxy)-ethoxy) benzene 3a. To a stirred solution of 2 (20.0 g, 0.085 mol) and KOH (5.2 g, 0.093 mol) in EtOH (150 mL) was added **1** (26.9 g, 0.085 mol) under N_2 atmosphere. The

reaction mixture was stirred at reflux temperature. As soon as the starting products are consumed (TLC monitoring), the total volume was reduced by evaporation and the solution were cooled down to ambient temperature. The product was extracted with CH_2Cl_2 (3 x 100 mL) and the organic extracts were dried over anhydrous $MgSO_4$. Removal of solvent gave the crude product. The pure product was obtained by column chromatography (SiO_2, eluent diethylether) to yield 3a as white crystals (20.5 g, 63 % yield). ^{1}H NMR ($CDCl_3$): δ = 6.81 + 6.80 (d, 4H), 4.07 (t, 2H), 3.86 (t, 2H), 3.80 (t, 2H), 3.66 (m, 6H), 3.52 (t, 2H), 3.36 (s, 3H), 1.72 (m, 2H), 1.25 (m, 12H), 0.86 (t, 3H); MS (EI, m/z): 382 [M^+].

Methoxy-4-(2-(2-(2-methoxy-ethoxy)-ethoxy)-ethoxy)-benzene 3b. Compound **3b** was prepared following the procedure described for **3a** using 4-hydroxy anisol (2.0 g, 0.016 mol) as the alcohol functionalized molecule in the reaction. A *Kugelrohr* distillation gave **3b** as a light yellow liquid (4.3 g, 99% yield). ^{1}H NMR ($CDCl_3$): δ = 6.69+6.70 (d, 4H), 3.92 (t, 2H), 3.69 (t, 2H), 3.60 (m, 5H), 3.51 (m, 4H), 3.43 (m, 2H), 3.24 (s, 3H); MS (EI, m/z): 270 [M^+], 151, 147, 136, 124, 109, 92, 77, 59.

1,4-Bis(2-(2-(2-methoxy-ethoxy)-ethoxy)-ethoxy)-benzene 3c. Compound **3c** was prepared following the procedure described for **3a** using hydroquinone (9.4 g, 0.08 mol) as the alcohol functionalized molecule and 2.2 equivalent **1**. The pure product was obtained by *Kugelrohr* distillation as a light yellow liquid (32.05 g, 93 % yield). ^{1}H NMR ($CDCl_3$): δ = 6.70 (s, 4H), 3.93 (t, 4H), 3.69 (t, 4H), 3.70- 3.51 (m, 12H), 3.41 (t, 4H), 3.24 (s, 6H); MS (EI, m/z): 402 [M+], 175, 151, 147, 136,110, 103.

1,4-Bis(chloromethyl)-2-(n-nonyloxy)-5-(2-(2-(2-methoxy-ethoxy)-ethoxy)-ethoxy)benzene 4a. To a stirred mixture of **3a** (14.7 g, 0.044 mol) and p-formaldehyde (3.6 g, 0.12 mmol), concentrated HCl (21 mL) was added drop wise under N_2 atmosphere. Subsequently, acetic anhydride (44 mL, 0.47 mol) was added at such a rate that the temperature did not exceed 70 °C. After addition was complete, the resulting solution was stirred at 70 °C for 3 h after which it was cooled down to room temperature and poured into water (100 mL). The reaction mixture was extracted with CH_2Cl_2 (3 x 100 mL) and dried over anhydrous $MgSO_4$. Evaporation of the solvent under reduced pressure

gave a white solid (20.3 g, 96 % yield). ^{1}H NMR ($CDCl_3$): δ = 6.93 + 6.88 (2s, 2H), 4.62 + 4.60 (2s, 4H), 4.14 (t, 2H), 3.95 (t, 2H), 3.84 (t, 2H), 3.72 (t, 2H), 3.64(m, 4H), 3.53 (t, 2H), 3.36 (s, 3H), 1.25 (m, 14H), 0.86 (t, 3H); MS (EI, m/z): 480 [M^+], 445, 410.

1,4-Bis(chloromethyl)-2-methoxy-5-(2-(2-(2-methoxy-ethoxy)-ethoxy)-ethoxy)-benzene 4b. With **3b** as reagent (8.8 g, 0.032 mol) and using the same procedure as for **4a**, **4b** was obtained after column chromatography (SiO_2, eluent diethylether) as an oil (7 g, 60% yield). ^{1}H NMR ($CDCl_3$): δ = 6.91+6.88 (d, 2H), 4.61+4.57 (2s, 4H), 4.12 (t, 2H), 3.81 (t, 2H), 3.70-3.54 (m, 11H), 3.33 (s, 3H); MS (EI, m/z): 366 [M^+], 332, 266, 231, 149, 103, 89, 69, 59.

1,4-Bis(chloromethyl)-2-methoxy-5-(2-(2-(2-methoxy-ethoxy)-ethoxy)-ethoxy)-benzene 4c. With **3c** as reagent (18.0 g, 0.045 mol) and using the same procedure as for **4a**, **4c** was obtained as an oil and used without further purification (20.8 g, 93% yield). ^{1}H NMR ($CDCl_3$): δ = 6.92 (s, 2H), 4.61 (s, 4H), 4.13 (t, 4H), 3.83 (t, 4H), 3.74-3.59 (m, 12H), 3.52 (t, 4H), 3.35 (s, 6H); MS (EI, m/z): 498 [M^+], 462, 426.

Bis-tetrahydrothiopheniumsalt of 1,4-bis(chloromethyl)-2-(n-nonyloxy)-5-(2-(2-(2-methoxy-ethoxy)-ethoxy)-ethoxy)benzene 5a. To a solution of **4a** (25.0 g, 0.038 mol) in MeOH (150 mL), tetrahydrothiophene (17 mL, 0.190 mol) was added, after which the white solution turned bright yellow. The mixture was allowed to react for 4 h at 50 °C, after which the total volume was reduced to 50 mL by evaporation. Subsequently the product was precipitated in cold diethylether (500 mL) after which the bissulfonium salt was filtered off, washed with diethylether (3 x 100 mL) and dried under vacuum. A white solid was obtained (15.7 g, 63% yield). ^{1}H NMR (D_2O): δ= 7.13+7.12 (2s, 2H), 4.44 + 4.41 (2s, 4H), 4.16 (t, 2H), 4.01 (t, 2H), 3.83 (t, 2H), 3.65 (t, 2H), 3.58(m, 6H), 3.38 (m, 8H), 3.24 (s, 3H), 2.23 (m, 8H), 1.72 (t, 2H), 1.13 (m, 12H), 0.71 (t, 3H).

Bis-tetrahydrothiopheniumsalt of 1,4-bis(chloromethyl)-2-methoxy-5-(2-(2-(2-methoxy-ethoxy)-ethoxy)-ethoxy)-benzene 5b. Following the procedure described for **5a** using **4b** (23.0 g, 0.063 mol) as reagent and 72 h reaction time at ambient temperature, **5b** was obtained as a white solid (27.0 g, 77% yield). ^{1}H NMR (D_2O): δ = 7.10 (s, 2H), 4.40-4.45 (2s, 4H), 4.18 (m, 2H),

3.83 (m, 2H), 3.80 (s, 3H), 3.45-3.64 (m, 8H), 3.36 (m, 8H), 3.24 (s, 3H), 2.21 (m, 8H).

Bis-tetrahydrothiopheniumsalt of 1,4-bis(chloromethyl)-2-methoxy-5-(2-(2-(2-methoxy-ethoxy)-ethoxy)-ethoxy)-benzene 5c. Following the procedure described for **5a** using **4c** (22.6 g, 0.045 mol) as reagent and 72 h reaction time at ambient temperature, **5c** is obtained as a white solid (25.9 g, 82% yield). ^{1}H NMR (D_2O): δ = 7.13 (s, 2H), 4.45 (s, 4H), 4.19 (m, 4H), 3.84 (m, 4H), 3.48-3.67 (m, 16H), 3.36 (m, 8H), 3.25 (s, 6H), 2.21 (m, 8H).

1-Chloromethyl-2-(n-nonyloxy)-4-octylsulfanylmethyl-5-(2-(2-(2-methoxy-ethoxy)-ethoxy)-ethoxy)benzene and 1-chloromethyl-2-(2-(2-(2-methoxy-ethoxy)-ethoxy)-ethoxy)-4-octylsulfanylmethyl-5-(n-nonyloxy)benzene 6a. A mixture of n-octane thiol (3.4 g, 0.023 mol) and NaO*t*Bu (2.3 g, 0.023 mol) in MeOH (150 mL) was stirred for 30 min at room temperature after which a clear solution was obtained. This solution was added drop wise (during 1 h) to solution of **5a** (15.4 g, 0.023 mol) in MeOH (500 mL). The reaction mixture was stirred for 2 h, after which it was concentrated under reduced pressure. Subsequently, n-octane (100 mL) was added and evaporated again to remove the tetrahydrothiophene. This sequence was repeated three times. The residue was redissolved in CH_2Cl_2 (100 mL) and extracted with water (3 x 100 mL). The organic layers were dried over anhydrous $MgSO_4$ and concentrated under reduced pressure giving the crude product as a yellow viscous oil, which was used without further purification (13.2 g, 95% yield). ^{1}H NMR ($CDCl_3$): δ= 6.88+6.86 (2s, 2H), 4.62+4.60 (2s, 2H), 4.12 (m, 2H), 3.93 (m, 2H), 3.82(m, 2H), 3.64 (m, 10H), 3.36 (s, 3H), 2.43 (t, 2H), 1.54 (m, 26H), 0.85 (t, 6H).

1-Chloromethyl-2-methoxy-4-octylsulfanylmethyl-5-(2-(2-(2-methoxy-ethoxy)-ethoxy)-ethoxy)benzene and 1-chloromethyl-2-(2-(2-(2-methoxy-ethoxy)-ethoxy)-ethoxy)-4-octylsulfanylmethyl-5-methoxybenzene 6b. Using **5b** (10.0 g, 0.018 mol) as reagent and the same procedure as for **6a**, **6b** was obtained as a yellowish oil and used without further purification (8.50 g, 100% yield). ^{1}H NMR ($CDCl_3$): δ = 6.87 + 6.84 + 6.84 + 6.82 (4s, 2H), 4.62 + 4.58 (2s, 2H), 4.10 (m, 2H), 3.84-3.50 (m, 15H), 3.34 (s, 3H), 2.42 (t, 2H), 1.52 (m, 2H), 1.33-1.22 (m, 10H), 0.84 (t, 3H).

1-Chloromethyl-2,5-bis(2-(2-(2-methoxy-ethoxy)-ethoxy)-ethoxy)-4-octylsulfanylmethylbenzene 6c. Using **5c** (3.6 g, 0.0053 mol) as reagent and the same procedure as for **6a**, **6c** was obtained as a yellowish oil after column chromatographic purification (SiO_2, eluent diethylether) (2.36 g, 75% yield). ^{1}H NMR ($CDCl_3$): δ = 6.88+6.85 (2s, 2H), 4.62 (s, 2H), 4.12 (m, 4H), 3.83 (m, 4H), 3.75-3.52 (m, 18H), 3.36 (s, 6H), 2.43 (t, 2H), 1.59 (m, 2H), 1.29-1.20 (m, 10H), 0.86 (t, 3H).

Monomers

1-Chloromethyl-2-(n-nonyloxy)-4-octylsulfinylmethyl-5-(2-(2-(2-methoxy-ethoxy)-ethoxy)-ethoxy)benzene and 1-chloromethyl-2-(2-(2-(2-methoxy-ethoxy)-ethoxy)-ethoxy)-4-octylsulfinylmethyl-5-(n-nonyloxy)benzene 7a. An aqueous (35 wt-%) solution of H_2O_2 (5.1 g, 0.052 mol) was added drop wise to a solution of **6a** (15.4 g, 0.026 mol), TeO_2 (0.2 g, 0.0013 mol) and concentrated HCl (0.05 mL) in dioxane (170 mL). As soon as 6a was consumed (TLC), 100 mL of brine was added to quench the reaction. The reaction mixture was extracted with CH_2Cl_2 (3 x 50 mL), after which the combined organic extracts were dried over anhydrous $MgSO_4$. Evaporation of the solvent under reduced pressure gave the crude product. The pure product was obtained by column chromatography (SiO_2, eluent diethylether) as a yellow orange viscous oil (1/1 mixture of regio-isomers; 11.0 g, 71% yield). ^{1}H NMR ($CDCl_3$): δ= 6.96+6.93+6.89+6.88 (4s, 2H), 4.62+4.60 (2s, 2H), 4.12 (t, 2H), 3.96 (t, 2H), 3.88+3.87+3.85+3.84 (2dd, 2H), 3.65 (m, 8H), 3.54 (t, 2H), 3.36 (s, 3H), 2.89 (m, 2H), 1.77 (m, 4H), 1.25(m, 22H), 0.86 (t, 6H); FT-IR (NaCl, cm^{-1}): 2925($\nu_{C\text{-}H\ aliph}$), 2856, 1508, 1466, 1417, 1212, 1111, 1046 ($\nu_{C\text{-}S}$).

1-Chloromethyl-2-methoxy-4-octylsulfinylmethyl-5-(2-(2-(2-methoxy-ethoxy)-ethoxy)-ethoxy)-4-(octylsulfinylmethyl)-benzene and 1-chloromethyl-2-(2-(2-(2-methoxy-ethoxy)-ethoxy)-ethoxy)-4-octylsulfinylmethyl-5-methoxybenzene 7b. Starting from **6b** (8.6 g, 0.018 mol) and using the same procedure as for **7a**, **7b** was obtained as a yellow oil after column chromatographic purification (SiO_2, eluent ethylacetate:methanol 9:1) (1/1 mixture of regio-isomers; 6.6 g, 74% yield). ^{1}H NMR ($CDCl_3$): δ = 6.92+6.88+6.80+6.79 (4s, 2H), 4.60+4.56 (2s, 2H), 4.09 (t, 2H),

4.01+4.00+3.98+3.97 (2dd, 2H), 3.78+3.74 (2s, 3H), 3.64-3.32 (m, 10H), 3.32 (s, 3H), 2.58 (m, 2H), 1.83 (t, 2H), 1.31-1.20 (m, 10H), 0.85 (t, 3H); FT-IR (NaCl, cm^{-1}): 2926($\nu_{C\text{-}H\ aliph}$), 2857, 1510, 1464, 1407, 1217, 1110, 1044($\nu_{C\text{-}S}$).

1-Chloromethyl-2,5-bis(2-(2-(2-methoxy-ethoxy)-ethoxy)-ethoxy)-4-octylsulfinylmethylbenzene 7c. Starting from **6c** (3.0 g, 0.0049 mol) and using the same procedure as for **7a**, **7c** was obtained as a yellow oil after column chromatographic purification (SiO2, eluent EtOAc:MeOH 9:1) (2.4 g, 79% yield). ^{1}H NMR ($CDCl_3$): δ = 6.88+6.75 (2s, 2H), 4.54 (s, 2H), 4.05 (t, 4H), 4.02+3.98+3.90+3.86 (2dd, 2H), 3.78 (t, 4H), 3.64-3.45 (m, 16H), 3.27 (s, 6H), 2.52 (m, 2H), 1.63 (t, 2H), 1.33-1.16 (m, 10H), 0.77 (t, 3H); ^{13}C NMR (CDCl3): δ = 150.6 (1C), 150.3 (1C), 126.9 (1C), 120.1 (1C), 116.0 (1C), 114.3 (1C), 71.6 (1C), 70.6 (1C), 70.4 (1C), 70.3 (1C), 69.4 (1C), 68.7 (1C), 68.4 (1C), 58.8 (1C), 52.4 (1C), 51.0 (1C), 40.9 (1C), 31.5 (1C), 29.0 (1C), 28.7 (1C), 28.6 (1C), 22.4 (1C), 22.3 (1C), 13.8 (1C); FT-IR (NaCl, cm^{-1}): 2925($\nu_{C\text{-}H\ aliph}$), 2872, 1507, 1455, 1413, 12127, 1110, 1042($\nu_{C\text{-}S}$).

Precursor polymers

Precursor polymer 8a. To a solution of monomer **7a** (4.2 g, 0.0069 mol) in 2-BuOH (50 mL), a solution of Na*t*BuO (0.87 g, 0.009 mol) in 2-BuOH (20 mL) was added in one portion using a thermostatic flask and funnel (30 °C) after both solutions were purged with N_2. The polymerization was allowed to proceed for 1 h at 30 °C after which it was quenched by pouring the reaction mixture into a well-stirred amount of ice water (400 mL). After extraction with CH_2Cl_2 (3 x 200 mL), the combined organic layers were evaporated under reduced pressure giving the crude product, which was used without further purification (2.7 g, 69% yield). ^{1}H NMR ($CDCl_3$): δ= 7.0-6.5 (2H), 4.4 (1H), 4.1 (2H), 3.9-3.3 (17H), 2.6 (2H), 1.7-1.1 (26H), 0.8 (6H); ^{13}C NMR ($CDCl_3$): δ= 151.3 (1C), 150.4 (1C), 129.0 (1C), 128.2 (1C), 112.4 (1C), 111.5 (1C), 71.9 (1C), 70.7 (1C), 70.6 (1C), 69.8 (1C), 69.5 (1C), 69.3 (1C), 69.1 (1C), 68.8 (1C), 59.0 (1C), 53.6 (1C), 32.1 (1C), 32.0 (1C), 3.18 (1C), 31.0 (1C), 29.6 (1C), 29.3 (2C), 29.1 (1C), 28.9 (1C), 26.2 (1C), 23.0 (1C), 22.7 (1C), 14.1 (2C), 10.0 (2C); FT-IR (NaCl, cm^{-1}): 2920, 2856, 1506, 1467, 1413, 1378, 1213, 1112, 1047; SEC (THF) $M_w = 6 \times 10^4$ g/mol (PD = M_w/M_n = 2.0).

Precursor polymer 8b. Starting from monomer **7b** (4.1 g, 0.008 mol), the same polymerization procedure was employed as for **8a**. Precursor polymer **8b** was obtained as a yellow viscous oil (3.1 g, 82% yield). ^{1}H NMR ($CDCl_3$): δ= 7.0-6.3 (2H), 4.6-4.4 (1H), 4.1 (2H), 3.7 (3H), 3.6-3.4 (13H), 2.6 (2H), 2.2 (2H), 1.7-1.2 (12H), 0.8 (3H); ^{13}C NMR ($CDCl_3$): δ= 151.7 (1C), 150.4 (1C), 129.4 (1C), 128.6 (1C), 119.4 (1C), 116.0 (1C), 71.7 (1C), 70.4 (1C), 69.5 (1C), 69.4 (1C), 69.3 (1C), 68.5 (1C), 58.9 (1C), 56.0 (1C), 53.3 (1C), 51.3 (1C), 31.8 (1C), 29.1 (1C), 28.9 (1C), 28.7 (1C), 22.8 (1C), 22.5 (1C), 13.9 (1C), 9.9 (1C); FT-IR (NaCl, cm^{-1}): 2926, 2857, 1508, 1461, 1407, 1215, 1110, 1045; SEC (THF): $M_w = 21 \times 10^4$ g/mol (PD = M_w/M_n = 3.7).

Precursor polymer 8c. Starting from monomer **7c** (0.6 g, 0.001 mol), the same polymerization procedure was employed as for **8a**. Precursor polymer 8c was obtained as a yellow viscous oil (0.5 g, 92% yield). ^{1}H NMR ($CDCl_3$): δ= 7.0-6.4 (2H), 4.6-4.4 (1H), 4.1 (4H), 3.6-3.4 (22H), 3.2 (6H), 2.8 (2H), 2.2 (2H), 1.8 (2H), 1.6-1.2 (10H), 0.8 (3H); ^{13}C NMR ($CDCl_3$): δ= 151.4 (2C), 127.5 (2C), 111.0 (2C), 71.8 (2C), 70.8 (2C), 70.6 (2C), 70.5 (2C), 69.9 (2C), 69.1 (2C), 59.0 (2C), 56.8 (1C), 51.3 (1C), 31.7 (1C), 29.1 (1C), 28.8 (1C), 28.6 (1C), 22.7 (1C), 22.4 (1C), 13.9 (1C), 9.9 (1C); FT-IR (NaCl, cm^{-1}): 2925, 2871, 1509, 1456, 1420, 1215, 1109, 1042, 935; SEC (THF): $M_w = 28 \times 10^4$ g/mol (PD = M_w/M_n = 2.8).

Conjugated polymers

Poly(2-(n-nonyloxy)-5-(triethoxymethoxy)-1,4-phenylene vinylene) 9a. A stirred solution of **8a** (1 g) in toluene (45 mL) was purged with N_2 for 1 h, after which the elimination reaction was allowed to proceed at 110°C and stirred for 3 h. Subsequently, the total volume was reduced to 10 mL by evaporation and the resulting orange red solution was precipitated drop wise in cold hexane (100 mL). The resulting polymer was filtered off, washed with hexane and redissolved in toluene (45 mL). The elimination procedure was repeated after which crude **9a** was filtered off again and dried at room temperature under reduced pressure. For purification, the crude **9a** was dissolved in boiling THF (10 mL) and after cooling to 40 °C drop wise precipitated in hexane (100 mL), giving **9a** as a red, fibrous polymer (449 mg,

63% yield). Anal. Calcd. for $C_{24}H_{38}O_5$: C 70.9, H 9.4, O 19.7; Found C 70.9, H 9.9, O 19.2; ^{1}H NMR ($CDCl_3$): δ= 7.4 (2H), 7.2 (2H), 4.2 (2H), 4.0 (2H), 3.9 (2H), 3.7 (2H), 3.6 (4H), 3.4 (2H), 3.3 (3H), 1.9 (2H), 1.6 (2H), 1.2 (10H), 0.8 (3H); ^{13}C NMR ($CDCl_3$): δ= 151.4 (1C), 150.8 (1C), 127.9 (1C), 127.4 (1C), 123.5 (2C), 111.4 (1C), 110.4 (1C), 72.0 (1C), 71.0 (1C), 70.7 (1C), 70.6 (1C), 70.1 (1C), 69.6 (1C), 69.4 (1C), 59.2 (1C), 31.9 (1C), 29.7 (2C), 29.6 (1C), 29.4 (1C), 26.3 (1C), 22.7 (1C), 14.2 (1C); FT-IR (NaCl, cm^{-1}): 2922, 2856, 1506, 1467, 1422, 1355, 1255, 1208; SEC (THF): $M_w = 6 \times 10^4$ g/mol (PD = M_w/M_n = 3.8); UV-Vis $\lambda_{a,max}$= 495 nm ($CHCl_3$) and $\lambda_{a,max}$= 508 nm (as a film); Photoluminescence emission (PL) $\lambda_{em,\ max}$= 543 nm + 583 nm (λ_{exc}= 495 nm, $CHCl_3$) and $\lambda_{em,\ max}$= 587 nm (λ_{exc}= 508 nm; as a film); No T_g could be detected in classical DSC measurements.

Poly(2-methoxy-5-(triethoxymethoxy)-1,4-phenylene vinylene) 9b. Precursor polymer **8b** (4.3 g) was treated in the same way as **8a**. Conjugated polymer **9b** was obtained as a red, fibrous polymer (2.5 g, 91% yield). Anal. Calcd. for $C_{16}H_{22}O_5$: C 65.3, H 7.5, O 27.2; Found C 64.9, H 7.9, O 27.2; ^{1}H NMR ($CDCl_3$): δ= 7.4 (2H), 7.2 (2H), 4.2 (2H), 3.9 (3H), 3.8 (2H), 3.7 (2H), 3.6 (4H), 3.5 (2H), 3.3 (3H); ^{13}C NMR ($CDCl_3$): δ= 151.7 (1C), 150.6 (1C), 127.6 (1C), 126.9 (1C), 123.6 (1C), 123.1 (1C), 111.4 + 111.2 (1C), 108.9 + 108.6 (1C), 71.7 (1C), 70.7 (1C), 70.5(1C), 70.4 (1C), 69.8 (1C), 69.2 (1C), 58.8 (1C), 56.2 (1C); FT-IR (NaCl, cm^{-1}): 2929, 2873, 1511, 1448, 1400, 1366, 1250, 1210;); UV-Vis $\lambda_{a,max}$= 483 nm ($CHCl_3$) and $\lambda_{a,max}$= 508 nm (as a film); Photoluminescence emission (PL) $\lambda_{em,\ max}$= 546 nm (λ_{exc}= 483 nm, $CHCl_3$) and $\lambda_{em,\ max}$= 587 nm (λ_{exc}= 508 nm; as a film); SEC (THF): $M_w = 9 \times 10^4$ g/mol (PD = M_w/M_n= 4.8); No T_g could be detected in classical DSC measurements.

Poly(2,5-bis(triethoxymethoxy)-1,4-phenylene vinylene) 9c. Precursor polymer 8c (0.5 g) was treated in the same way as **8a**. Conjugated polymer 9c was obtained as a red, fibrous polymer (0.3 g, 87% yield). Anal. Calcd. for $C_{22}H_{34}O_8$: C 62.0, H 8.0, O 30.0; Found C 62.4, H 8.7, O 28.9; 1H NMR ($CDCl_3$): δ= 7.4 (2H), 7.2 (2H), 4.2 (4H), 3.9 (4H), 3.8 (4H), 3.7 (4H), 3.6 (4H), 3.5 (4H), 3.3 (6H); 13C NMR ($CDCl_3$): δ= 151.1 (2C), 127.8 (2C), 123.6 (2C), 111.2 (2C), 71.8 (2C), 70.9 (2C), 70.6 (2C), 70.5 (2C), 69.9 (2C), 69.1 (2C), 58.9 (2C); FT-IR (NaCl, cm^{-1}): 2925, 2861, 1512, 1448, 1400, 1366,

1250, 1210;); UV-Vis $\lambda_{a,max}$= 489 nm ($CHCl_3$) and $\lambda_{a,max}$= 509 nm (as a film); Photoluminescence emission (PL) $\lambda_{em,\ max}$= 543 nm (λ_{exc}= 489 nm, $CHCl_3$) and $\lambda_{em,\ max}$= 587 nm (λ_{exc}= 509 nm; as a film); SEC (THF): $M_w = 26 \times 10^4$ g/mol (PD =M_w/M_n = 3.1); No T_g could be detected in classical DSC measurements.

2.11 References

[1] Burroughes, J. H.; Bradley, D. D. C.; Brown, A. R.; Marks, R. N.; Mackay, K.; Friend, R. H.; Burns, P. L.; Holmes, A. B. *Nature* **1990**, *347*, 539.

[2] a) Friend, R. H.; Gymer, R. W.; Holmes, A. B.; Burroughes, J. H.; Marks, R. N.; Taliani, C.; Bradley, D. D. C.; Dos Santos, D. A.; Brédas, J. L.; Lögdlund, M.; Salaneck, W. R. *Nature* **1999**, *397*, 121. b) Scheinert, S.; Paasch, G. *Phys. Stat. Sol. (a)* **2004**, *201*, 1263. c) Tyler McQuade, D.; Pullen, A. E.; Swager, T. M. *Chem. Rev.* **2000**, *100*, 2537. d) Hoppe, H.; Niggemann, M.; Winder, C.; Kraut, J.; Hiesgen, R.; Hinsch, A.; Meissner, D.; Sariciftci, N. S. *Adv. Funct. Mat.* **2004**, *14*, 1005.

[3] a) Salbeck, J. *Ber. Bunsenges. Phys. Chem.* **1996**, *100*, 1666. b) Spreitzer, H.; Becker, H.; Kluge, E.; Kreuder, W.; Schenk, H.; Demandt, R.; Schoo, H. *Adv. Mater.* **1998**, *10*, 1340. c) Gelinck, G.H.; Warman, J.M.; Staring, E.G.J. *J. Phys. Chem.* **1996**, *100*, 5485.

[4] a) Brabec, C. J.; *Solar Energy Materials & Solar Cells* **2004**, *83*, 273-292. b) Mozer, A. J.; Sariciftci, N. S. C.R. Chimie **2006** Article in press.

[5] Gilch, H. G.; Wheelwright, W. L. *J. Polym. Sci.: A* **1966**, *4*, 1337.

[6] Swatos, W. J.; Gordon, B. *Polym. Prep.* **1990**, *31(1)*, 505.

[7] a) Hsieh, B. R.; Yu, Y.; VanLaeken, A. C.; Lee, H. *Macromolecules*, **1997**, *30*, 8094 b) Hsieh, B. R.; Yu, Y.; Forsythe, E. W.; Schaaf, G. M.; Feld, W. A. *J. Am. Chem. Soc.*, **1998**, *120*, 231.

[8] a) Neef, C. J.; Ferraris, J. P. *Macromolecules*, **2000**, *33*, 2311; b) Neef, C. J.; Ferraris, J. P. *Macromolecules*, **2004**, *37*, 2671.

[9] a) Wiesecke, J.; Rehahn, M. *Angew. Chem. Ind. Ed.*, **2003**, *42 (5)*, 567; b) J Wiesecke, J.; Rehahn, M., *Polym. Prep.* **2004**, *45 (1)*, 174.

[10] a) Hontis, L.; Lutsen, L.; Vanderzande, D.; Gelan, J. *Synth. Met.*, **2001**, *119*, 135. b) Hontis, L.; Vrindts, V.; Vanderzande, D.; Lutsen, L. *Macromolecules*, **2003**, *36 (9)*, 3035.

[11] Becker, H.; Spreitzer, H.; Ibrom, K.; Kreuder, W. *Macromolecules* **1999**, *32*, 4925.

[12] a) Louwet, F.; Vanderzande, D. J. M.; Gelan, J. M. J. V.; Mullens, J. *Macromolecules* **1995**, *28*, 1330. b) van Breemen, A. J. J. M.; Issaris, A. C. J.; de Kok, M. M.; Van Der Borght, M. J. A. N.; Adriaensens, P. J.; Gelan, J. M. J. V.; Vanderzande, D. J. M. *Macromolecules* **1999**, *32(18)*, 5728-5735.

[13] Lutsen, L.; Adriaensens, P.; Becker, H.; van Breemen, A. J.; Vanderzande, D. J. M.; Gelan, J. *Macromolecules* **1999**, *32(20)*, 6517-6525.

[14] a) Hontis, L.; Van Der Borght, M.; Vanderzande, D.; Gelan, J. *Polymer* **1999**, *40*, 6615-6617. b) Vanderzande, D. J. M.; Hontis, L.; Palmaerts, A.; Van Den Berghe, D.; Wouters, J.; Lutsen, L.; Cleij, T. *Proc. of SPIE* **2005**, *5937* 116-125.

[15] Kesters, E.; Vanderzande, D.; Lutsen, L.; Penxten, H.; Carleer, R. *Macromolecules* **2005** *38 (4),* 1141-1147.

[16] a) Van Der Borght, M.; Vanderzande, D.; Adriaensens, P.; Gelan, J. *J. Org. Chem.* **2000**, *65(2)*, 284-289.

[17] Van Severen, I.; Motmans, F.; Lutsen, L.; Cleij, T. J.; Vanderzande, D. *Polymer* **2005**, *46*, 5466.

[18] Van Breemen A. J. J. M.; Vanderzande, D. J. M.; Adriaensens, P. J.; Gelan, J. M. J. V. *J. Org. Chem.* **1999**, *64*, 3106.

[19] Keegstra, E. M. D.; Zwikker, J. W.; Roest, M. R.; Jenneskens, L. W. *J. Org. Chem.,* **1992**, *57*, 6678.

[20] Roex, H.; Adriaensens, P.; Vanderzande, D.; Gelan, J. *Macromolecules* **2003**, *36*, 5613.

[21] a) Onoda, M.; Tada, K. *Thin Solid Films* **2003**, *438-439*, 187-194. b) Leclerc, M. *Adv. Mater.* **1999**, *11 (18)*, 1491.

[22] Munters, T.; Martens, T.; Goris, L.; Vrindts, V.; Manca, J.; Lutsen, L.; De Ceuninck, W.; Vanderzande, D.; De Schepper, L.; Gelan, J.; Sariciftci, N. S.; Brabec, C. J. *Thin Solid Films* **2002**, *403-404*, 247.

[23] Wu, Z.; Wu, S.; Liang, Y. *Spectrochim. Acta Part A* **2003**, *59*, 1631.

[24] Chuah, B. S.; Hwang, D.-H.; Kim, S. T.; Moratti, S. C.; Holmes, A. B.; De Mello, J. C.; Friend, R. H. *Synth. Met.* **1997**, *91*, 279.

[25] Reichardt, C. *Solvents and Solvent Effects in Organic Chemistry*, VCH Weinheim: 1990, p. 408-410.

[26] Kim, J. *Pure Appl. Chem.* **2002**, *74*, 2031.

[27] Cleij, T. J.; Jenneskens, L. W. *J. Phys. Chem B* **2000**, *104*, 2237.

[28] Mihailetchi, V. D.; Koster, L. J. A.; Blom, P. W. M.; Melzer, C.; de Boer, B.; van Duren, J. K. J.; Janssen, R. A. J. *Adv. Funct. Mat.* **2005**, *15*, 795.

[29] Mihailetchi, V. D.; Koster, L. J. A.; Hummelen, J. C.; Blom, P. W. M. *Physical Review Letters.* **2004**, *93 (12)*, 216601-1.

[30] a) Blom, P. W. M.; de Jong, M. J. M.; van Munster, M. G. *Phys. Rev. B* **1997**, *55*, 656. b) Bozano, L.; Carter, S. A.; Scott, J. C.; Malliaras, G. G.; Brock, P. J. *APL* **1999**, *74 (8)*, 1132.

[31] Dimitrakopoulos, C.D.; Malenfant, P.R.L. *Adv. Mater*. **2002**, *14*, 99

[32] Lutsen, L.; Van Breemen, A.; Kreuder, W.; Vanderzande, D.; Gelan, J. *Helv. Chim. Acta* **2000**, *83*, 3113.

Chapter 3

Synthesis of New Non-Ionic, Non-Protic, Polar PPV Derivatives Soluble in Environmentally Friendly Solvents

Since it is within the objectives of this work to develop material systems which are compatible with processing from environmentally friendly solvent systems, two strategies are developed to further increase the polarity of PPV derivatives. As a first approach, two branched oligo(ethylene glycol) side chains are introduced at every repeating unit of a PPV backbone to form poly(2,5-bis(triethoxymethoxy)-2-glyceryl)-1,4-phenylene vinylene) (BTEMG-PPV). As a second approach, tetra-substituted conjugated materials are synthesized. To demonstrate the accessibility of tetra-substituted PPV derivatives, poly(2,3,5,6-tetrahexyloxy-1,4-phenylene vinylene) (TH-PPV) is prepared first. Although initially, this polymer was only prepared to optimize the synthesis of tetra-substituted PPV-type polymers, this material shows very interesting properties for application in photovoltaic applications. Finally, a PPV derivative with four polar oligo(ethylene oxide) chains, i.e. poly(2,3,5,6-tetra(triethoxymethoxy)-1,4-phenylene vinylene) (TTEM-PPV) is synthesized. All polymers described in this chapter are prepared via the dehydrohalogenation precursor method. The polar, non-ionic side chains of BTEMG-PPV and TTEM-PPV render the PPV backbone soluble in a variety of media at the most polar side of the polarity scale including alcohols and water.

3.1 Introduction

Polar conjugated polymers have become a very interesting topic in the field of conjugated polymers over the last few years. Different approaches have been developed to synthesize polar PPV derivatives and various side groups have

been added to the PPV backbone to make them more soluble and processable.[1] As a part of our work dedicated towards new functionalized, polar PPV derivatives, we are interested in the preparation of PPV-type polymers bearing non-protic, non-ionic polar side chains. The low reactivity of the non-protic, non-ionic polar side chains probably excludes the interference with other functionalities and makes these materials a worthwhile tool to develop the skills in handling this class of materials. An example of a non-protic, non-ionic side polar chain is the triethylene glycol derived side chain. In Chapter 2 we described the synthesis of two polar PPV derivatives bearing respectively one and two of such triethylene glycol derived side chains (Figure 3-1). We demonstrated that the polarity of the polymers can be altered without significantly affecting the conjugated backbone properties, *i.e.* the optical and electronic properties. However, the addition of these solubilizing side chains onto the conjugated backbone proved very effective in improving the solubility and processability of conjugated polymers.

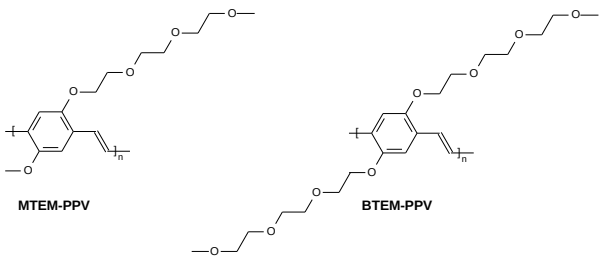

Figure 3-1 2,5-substituted PPV derivatives bearing polar side chains, which were prepared in Chapter 2

The capability to further fine-tune the solubility properties is important to find environmentally friendly processing solvents for this type of polymers. Recently, the use of alcohols or water as a reaction solvent is regarded as an important research topic in green chemistry. These solvents are low-cost, safe and environmentally benign solvents when compared with organic solvents which are normally used for organic reactions. In order to obtain water or alcohol dissolvable PPV derivatives, the compatibility of the materials with polar environments has to be enhanced. Therefore, two different strategies are worked out in this chapter. As a first strategy, two branched oligo(ethylene

glycol) side chains are introduced at every repeating unit of the PPV backbone. In this way poly(2,5-bis(triethoxymethoxy)-2-glyceryl)-1,4-phenylene vinylene) (BTEMG-PPV) is formed (Figure 3-2). A second method to increase the polarity, is the substitution of all the free positions of the phenylene unit in the PPV backbone with triethylene glycol derived side chains. Whereas BTEM-PPV (Figure 3-1), prepared in Chapter 2 is substituted with two polar side chains at the 2- and the 5-position of the PPV backbone, poly(2,3,5,6-tetra(triethoxymethoxy)-1,4-phenylene vinylene) (TTEM-PPV) is tetra-substituted with polar oligo(oxy ethylene) side chains (Figure 3-2).

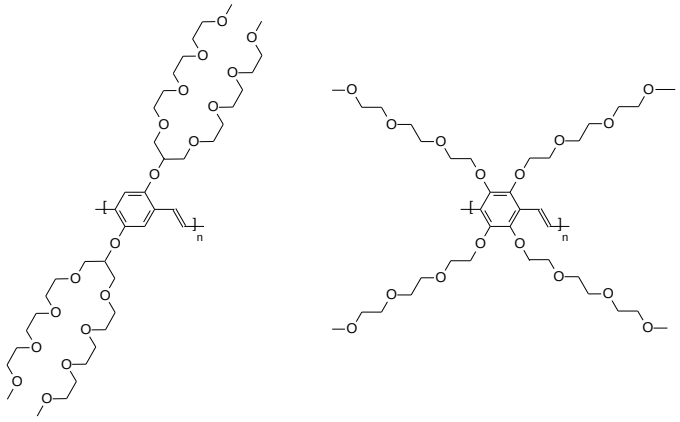

Figure 3-2 Two non-ionic, non-protic PPV derivatives with increased polarity which are prepared in this Chapter

3.2 A polar PPV derivative bearing two branched oligo(ethylene oxide) side chains

During the study of literature concerning polar, non-ionic conjugated materials, we encountered a communication which described the synthesis of a poly(*p*-phenylene ethynylene) (PPE) derivative with two branched oligo(ethylene glycol) side chains (Figure 3-3).[2] According to this report, the side chains introduce water solubility of the conjugated PPE backbone. Inspired by this observation, we became interested in the synthesis and solubility characteristics of a PPV derivative containing these branched polar

side chains, *i.e.* poly(2,5-bis(3,6,9-triethoxy-12-methoxy)-2-glyceryl)-1,4-phenylene vinylene) (BTEMG-PPV).

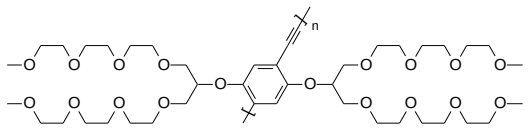

Figure 3-3 A PPE derivative containing branched oligo(ethylene oxide) side chains

▪ Synthesis of BTEMG-PPV

The practical synthetic route to the polar BTEMG-PPV is outlined in Scheme 3-2. In a first step, the fork of side chain arm **1** is prepared according to a literature procedure[3] starting from tri(ethylene glycol) monomethyl ether and epichlorohydrine (Scheme 3-1).

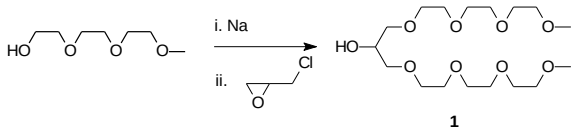

Scheme 3-1 Synthesis of the branched side chains

The 1,3-bis(3,6,9-trioxydecanyl)glycerol side chains **1** are coupled to the benzene ring using a Williamson etherification to form 1,4-bis(1,3-bis(3,6,9-trioxydecanyl)-2-glyceryl)benzene **3** (Scheme 3-2). For that purpose, the alcohol functionalized side chains are first activated to the corresponding tosylate ester **2** according to a procedure common in literature[4]. The functionalized benzene ring **3** is chloromethylated according to an adapted literature procedure[5] using concentrated HCl and formaldehyde in acetic anhydride to yield 2,5-bis-chloromethyl-1,4-bis(1,3-bis(3,6,9-trioxydecanyl)-2-glyceryl) benzene **4**.

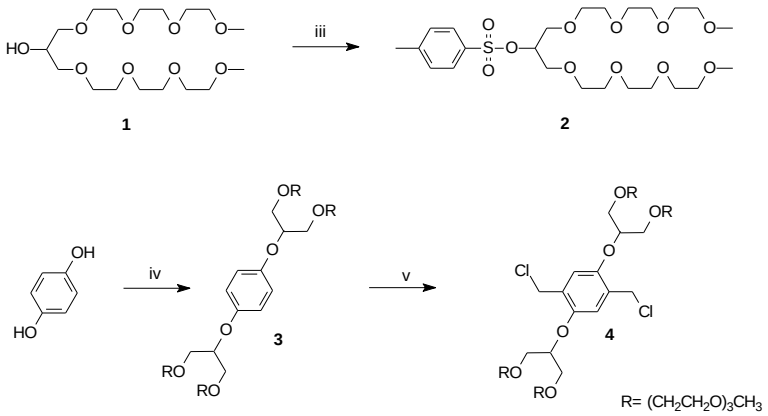

Scheme 3-2 Synthesis of monomer **4** (iii: TosCl, KOH, CH_2Cl_2, 0°C; iv: **2**, Na*t*BuO, EtOH; v: *p*-CH_2O, Ac_2O, HCl, 75°C)

- **Poly(2,5-bis(3,6,9-triethoxy-12-methoxy)-2-glyceryl)-1,4-phenylene vinylene) (BTEMG-PPV)**

Monomer **4** is polymerized according to the direct Gilch route[6] (Scheme 3-3). A typical Gilch polymerization is performed under a nitrogen atmosphere with dry and degassed 1,4-dioxane as the solvent, using the set-up depicted in Figure 3-4. After heating to 98 °C, the monomer is added, followed by a drop wise addition of an excess (larger then 2 equivalents) of K*t*BuO dissolved in dry 1,4-dioxane. During this addition, a change in colour of the reaction mixture from colourless to orange and an increase in viscosity are observed. After 5 minutes, a second solution of base is added. The polymerization is allowed to proceed for 2 hours at 98 °C. Poly(2,5-bis(3,6,9-triethoxy-12-methoxy)-2-glyceryl)-1,4-phenylene vinylene) (BTEMG-PPV) **5** is precipitated in cold cyclohexane. A red precipitation is formed which becomes oily and sticky during filtration. After drying overnight in a desiccator under vacuum, BTEMG-PPV is isolated in high yield (77%). Analytical Size Exclusion Chromatography (SEC) is performed using DMF as the eluent. This technique reveals that the obtained BTEMG-PPV has a very high polydispersity (PD=11.4). The presence of an oligomeric fraction is further confirmed by UV-Vis spectroscopy.

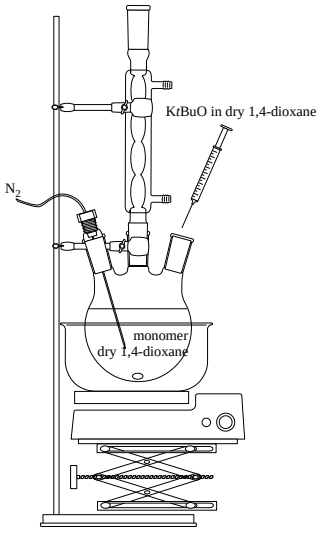

Figure 3-4 Set-up for the Gilch polymerization

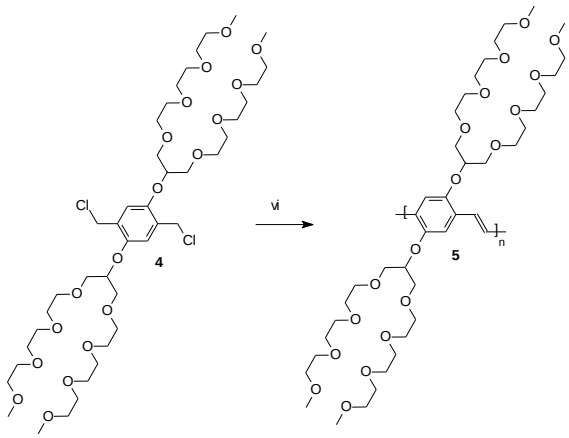

Scheme 3-3 Gilch polymerization of monomer **4** towards BTEMG-PPV **5** (vi: K*t*BuO, 1,4-dioxane)

In order to separate the polymer from the oligomeric fraction, a separation on Bio-Beads® S-X beads with DMF as eluent was performed. This separation was laborious since the polymer displayed strong adsorption to the column packing. As a result, the yields of the different fractions obtained after the Gel Permeation Chromatographic separation are low. Three fractions **5-1**, **5-2** and **5-3** are collected. The yield, molecular weight, polydispersity and UV-Vis absorption maximum λ_{max} in $CHCl_3$ of the different fractions are presented in Table 3-1. Approximately, 30 % of BTEMG-PPV could not be recuperated.

Polymer fraction	**Yield (%)**	**M_w (g/mol)**	**PD**	**λ_{max} (nm)**
5-1	23	200000	2.2	462
5-2	19	53000	7.4	331+459
5-3	27	28000	3.8	broad (shoulder at 455)

Table 3-1 Overview of the polymerization results and solution UV-Vis absorption maxima λ_{max} (solvent $CHCl_3$) for the collected fractions of BTEMG-PPV after separation on Bio-Beads® S-X beads using DMF as the eluent

Figure 3-5 shows the solution UV-Vis absorption spectra of the different fractions of BTEMG-PPV in $CHCl_3$ after separation on the Bio-Beads®. The UV-Vis absorption spectrum of the highest molecular weight fraction **5-1** exhibits a distinct transition with a maximum absorbance at λ_{max} = 462 nm. This value is low compared to BTEM-PPV (Figure 3-1, *cf.* Chapter 2) which exhibits a distinct absorption at λ_{max} = 489 nm in $CHCl_3$. The blue shift may be attributed to an increased steric hindrance between the bulky, branched side chains of BTEMG-PPV, which causes a more twisted conformation of the polymer backbone. However, it is very likely that higher λ_{max} values will be observed when BTEMG-PPV is prepared *via* the sulfinyl precursor route, as was demonstrated for other polar PPV derivatives in Chapter 2. The second fraction collected during the gel permeation chromatographic separation shows a transition in the UV-Vis absorption at λ_{max} = 459 nm, together with a transition at λ_{max} = 331 nm, which corresponds to an oligomeric fraction. The third fraction collected during the separation is the low molecular weight fraction and displays a broad band with a shoulder at 455 nm.

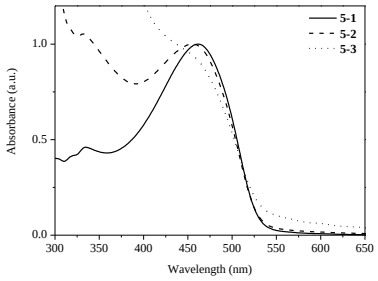

Figure 3-5 Solution UV-Vis absorption spectra (solvent $CHCl_3$) of the different fractions of BTEMG-PPV after separation on Bio-Beads® using DMF as the eluent

Fraction **5-1** is used to further characterize BTEMG-PPV by means of different analytical techniques. A thin film of **5-1** exhibits in the UV-Vis absorption spectrum a distinct absorption at λ_{max} = 469 nm (Figure 3-6). This transition is significantly blue shifted compared to the thin film absorption spectrum of BTEM-PPV (λ_{max} = 509 nm). It is again likely that these optical properties will improve when BTEMG-PPV is prepared *via* the sulfinyl precursor route. However, the blue shift might also be (partially) due to the

larger steric hindrance impacted by the more bulky side chains of BTEMG-PPV. In thin solid films these hindrance may play a more important role, leading to a significant reduction of the mean conjugation length.

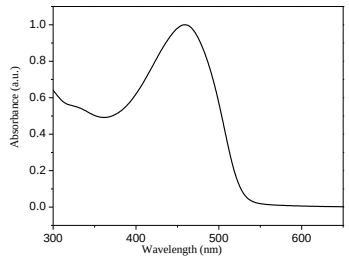

Figure 3-6 Thin film UV-Vis absorption spectrum of **5-1**

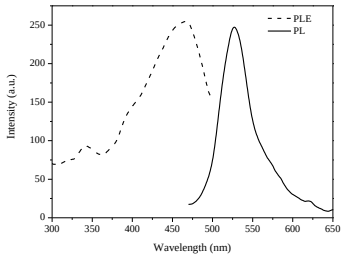

Figure 3-7 PL and PLE spectra of **5-1** in $CHCl_3$ solution

BTEMG-PPV **5-1** is also studied using fluorescence spectroscopy (Figure 3-7). In $CHCl_3$ solution, BTEMG-PPV exhibits a distinct fluorescence emission at λ_{em} = 528 nm (excitation wavelength λ_{exc} = 462 nm). This is again slightly blue shifted compared to BTEM-PPV, for which a distinct emission is found at λ_{em} = 543 nm in $CHCl_3$ solution (excitation wavelength λ_{exc} = 485 nm). The room temperature photoluminescence excitation (PLE) spectrum of a solution of **5-1** exhibits an excitation maxima at $\lambda_{ex,\ max}$= 459 nm (solvent $CHCl_3$; emission wavelength λ_{em}= 528 nm).

The solubility's and UV-Vis absorption characteristics of **5-1** in various solvents with different polarities, *i.e.* E_T^N values[7] are studied. For these studies a concentration of approximately 0.05 mM of **5-1** (based on the repeating unit) is employed. A distinct transition is found in the UV-Vis absorption spectrum for the solvents at the polar side of the polarity scale, ranging from the most polar solvent, *i.e.* water to the somewhat more apolar solvents often used in the manufacturing of organic photovoltaic devices[8], such as chlorobenzene. The solution absorption maxima range from λ_{max} = 459 to 465 nm (Table 3-2), indicating that the conformation of BTEMG-PPV is not much affected by the solvent, as expected for 'sterically crowded' conjugated polymer. Moreover, the solution characteristics do not change in the course of time, *i.e.* the same distinct transitions and solution absorption maxima are found for the prepared

solutions of **5-1** in the various solvents after one week at room temperature. No aggregation is observed.

Solvent	**Polarity[7] (E_T^N)**	**λ_{max} (nm)**
Water	1	459
Methanol	0.762	460
Ethanol	0.654	462
Acetic acid	0.648	459
2-Propanol	0.546	461
Acetonitrile	0.460	465
Dimethylsulfoxide	0.444	462
Acetic anhydride	0.407	461
Dimethylformamide	0.404	465
Acetone	0.355	462
Dichloromethane	0.309	459
Chloroform	0.259	462
Ethyl acetate	0.228	459
Tetrahydrofuran	0.207	463
Chlorobenzene	0.188	462
1,4-Dioxane	0.164	461

Table 3-2 Overview of solubility's and UV-Vis absorption maxima of **5-1** in selected solvents

Figure 3-8 shows the solution UV-Vis absorption spectra of **5-1** in selected polar and environmentally friendly solvents.[c] The solubility study shows that the introduction of the more polar branched oligo(ethylene glycol) side chains in poly(2,5-bis(triethoxymethoxy)-2-glyceryl)-1,4-phenylene vinylene) leads to an enhanced compatibility of PPV with polar environments, which makes processing of these materials from environmentally friendly polar solvent systems possible.

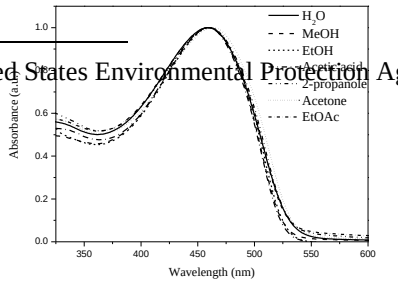

[c] According to the United States Environmental Protection Agency (EPA)

Figure 3-8 UV-Vis absorption spectra of **5-1** in environmentally friendly solvents[c]

The moderate optical properties are an indication for an increased defect level in the conjugated system, which can negatively influence the electronic characteristics such as the mobility of this material. Since BTEMG-PPV was prepared according to the dehydrohalogenation route, there is still room left for improvement of the purity of the material by synthesizing this material according to the sulfinyl precursor route.

3.3 Tetra-substituted PPV derivatives

A second approach to increase the compatibility of the PPV backbone with more polar environments, consists of the synthesis of a PPV derivative with four polar oligo(ethylene oxide) side chains. This implicates that we need to substitute all four positions of the phenylene unit in the PPV backbone with triethylene glycol derived side chains. Although extensive research has been carried out into the synthesis of a wide variety of substituted PPV derivatives in order to tune the characteristics of the polymer, up to now, efforts are mainly focussed on the modification of 2,5-substituted PPV derivatives. The literature concerning tetra-substituted PPV derivatives is very scarce. To our very best knowledge, there is only one report dated from 1993 on the synthesis of tetra-alkoxy-PPV derivatives,[9] *i.e.* poly(2,3,5,6-tetramethoxy-1,4-phenylene vinylene) (TM-PPV), of which the electrical conductivity after doping with $FeCl_3$ was studied.[10] 1,2,4,5-Tetramethoxybenzene was prepared from benzoquinone *via* 2,5-dimethoxy-1,4-benzoquinone and 2,5-dimethoxyhydroquinone.[11] TM-PPV was synthesized according to the Wessling route[12].

3.3.1 Poly(2,3,5,6-tetrahexyloxy-1,4-phenylene vinylene) (TH-PPV)

In order to get master of the synthesis of tetra-substituted PPV derivatives, a tetra-alkoxy-PPV derivative, poly(2,3,5,6-tetrahexyloxy-1,4-phenylene vinylene) (TH-PPV, Figure 3-9) is synthesized first.

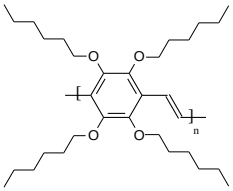

Figure 3-9 Poly(2,3,5,6-tetrahexyloxy-1,4-phenylene vinylene) (TH-PPV)

- **Synthesis of the Gilch monomer of TH-PPV**

The first step towards TH-PPV is the *in situ* hydrogenation of 2,5-dihydroxy-1,4-benzoquinone (Scheme 3-4). 1,2,4,5-Tetrahydroxybenzene **6** is obtained according to an adapted literature procedure[13] using the set-up depicted in Figure 3-10. A three-necked round-bottomed flask is charged with 2,5-dihydroxybenzene-1,4-benzoquinone, dimethylformamide (DMF) and platinum oxide as catalyst. A detailed procedure to guarantee a safe outcome of the hydrogenation reaction in the absence of air is given in the experimental section at the end of this chapter. After completion of the reaction, indicated by the amount of hydrogen gas consumed (Figure 3-10: level of the $CuSO_4$-solution **X**= $\mathbf{X_2}$ **=** constant) and by a change in colour of the reaction mixture from light brown to dark red-brown, cesium carbonate and the appropriate alkyl bromide are added under N_2 atmosphere. The reaction mixture is stirred for 6 days at 65 °C. In this way, tetrahydroxybenzene **6** is converted to tetrahexyloxybenzene **7** *via* a Williamson ether synthesis (Scheme 3-4). After work-up **7,** is purified by a twofold recrystallization from MeOH. 1,2,4,5-Tetrahexyloxybenzene is obtained in high yield (78 %) as white crystals.

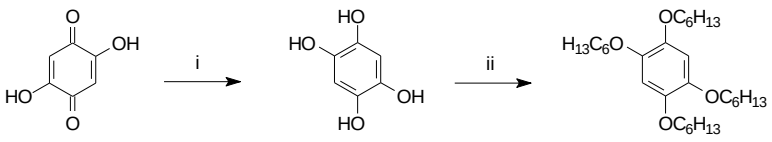

6 **7**

Scheme 3-4 Synthesis of 1,2,4,5-tetrahexyloxybenzene **7** (i: PtO_2, $H_{2(g)}$, DMF; ii: Cs_2CO_3, C_6H_{13}-Br)

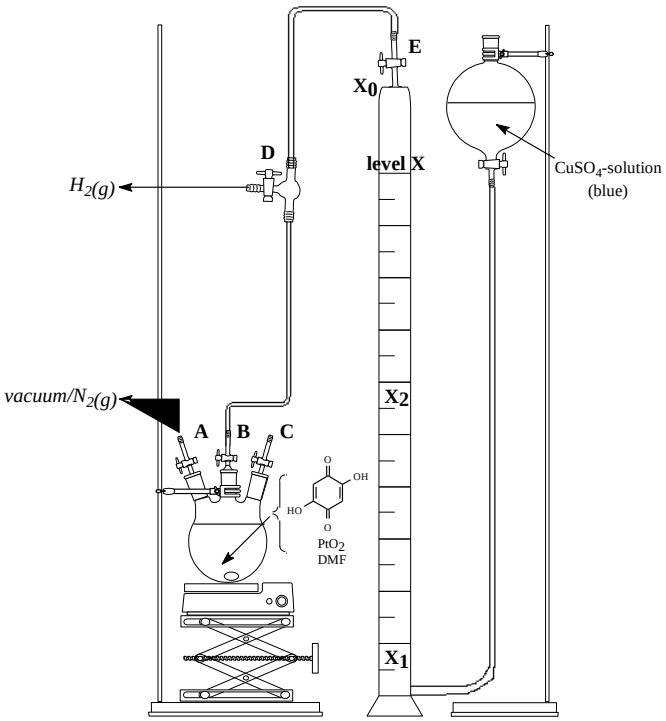

Figure 3-10 Set-up for the catalytic hydrogenation of 2,5-dihydroxybenzene-1,4-benzoquinone

7 is chloromethylated using concentrated HCl and formaldehyde in acetic anhydride to give 1,4-bischloromethyl-2,3,5,6-tetrahexyloxybenzene **8** (Scheme 3-5). However, when the reaction time and temperature described in literature (3 hours, 70 °C)[6] are used, a mixture of starting compound **7** and the monochloromethylated derivative are formed. Apparently, due to the sterical hindrance, this reaction proceeds extremely slow and high reaction time and temperature (6 days, 95 °C) are necessary in order to achieve the dichloro-compound in satisfying yield. After column chromatography, monomer **8** is

obtained in 68 % yield and with a high purity, as evidenced by the ^{1}H NMR and ^{13}C NMR NMR spectrum of **8** (Figure 3-11).

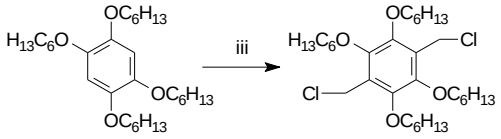

7 **8**

Scheme 3-5 Chloromethylation of tetrahexyloxybenzene **7** to monomer **8** (iii: *p*-CH_2O, Ac_2O, HCl)

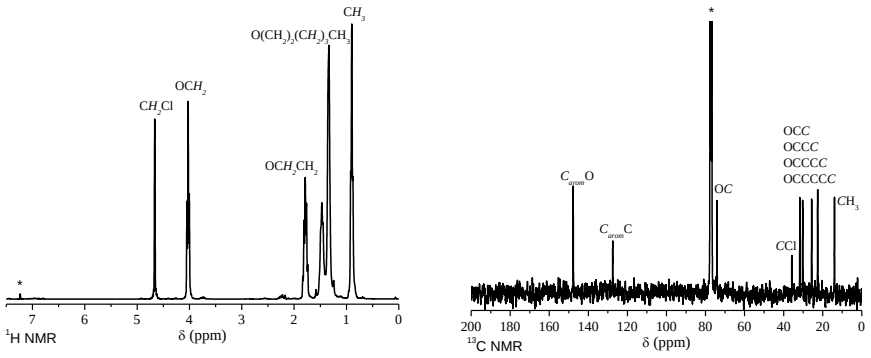

Figure 3-11 ^{1}H and ^{13}C NMR spectra of monomer **8** recorded in $CDCl_3$ at RT. The resonances marked with an asterisk result from the solvent residual peak of $CDCl_3$ (7.26 ppm for H atoms, δ = 77.16 ppm for C atoms)[14]

▪ Polymerization towards TH-PPV

Monomer **8** is brought in typical Gilch polymerization conditions[6], *i.e.* **8** is dissolved in dry and degassed 1,4-dioxane under a N_2 atmosphere (Scheme 3-6). After heating of the monomer solution to 98 °C, *tert*-butoxide dissolved in dry dioxane, is added, whereupon the solution turns from colourless to white. Addition of a second solution of base colours the solution bright yellow. The mixture is allowed to react for three hours and subsequently worked up by precipitation in cold methanol.

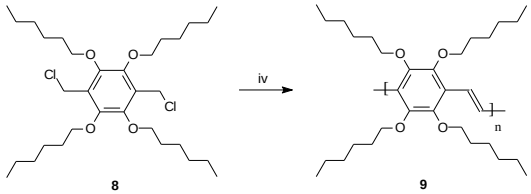

8 **9**

Scheme 3-6 Gilch polymerization of monomer **8** towards TH-PPV **9** (iv: K*t*BuO, 1,4-dioxane)

The resulting polymer is filtered off and washed thoroughly with methanol. Poly(2,3,5,6-tetrahexyloxy-1,4-phenylene vinylene) (TH-PPV) **9** is prepared in moderate yield (55 %) as a yellow, strongly fluorescent solid. TH-PPV is characterized using different analytical techniques. By means of ^{1}H NMR and ^{13}C NMR spectroscopy it is demonstrated that a pure material is obtained (Figure 3-12).

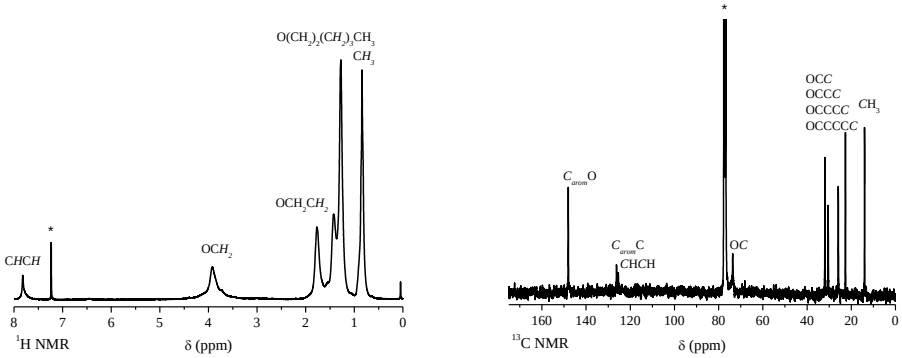

Figure 3-12 ^{1}H and ^{13}C NMR spectra of TH-PPV **9** recorded in $CDCl_3$ at RT. The resonances marked with an asterisk result from the solvent residual peak of $CDCl_3$ (7.26 ppm for H atoms, δ = 77.16 ppm for C atoms)[14]

An analytical SEC measurement of TH-PPV is performed in THF *versus* polystyrene standards. In addition to a high molecular weight polymer (M_w= 40 x 10^4 g/mol, polydispersity PD= 3.1), an oligomeric fraction is observed (M_w= 5 x 10^3 g/mol, PD= 1.3) (Figure 3-13). To the best of our knowledge, this is the first time that a bimodal behaviour is observed for a polymer prepared *via* the Gilch route. This phenomenon may shed some light on the exact nature of the polymerization mechanism. After all, as already mentioned in Chapter 2, the polymerization mechanism - either anionic or radical- is still under discussion. A broad community active in research on Gilch polymerizations is convinced

that an anionic polymerization process takes place.[15] Other research groups substantiate that radical processes are responsible for the formation of high molecular weight polymers.[16] Recently, our research group showed that both mechanisms are competing in the sulfinyl precursor route and that the high molecular weight fraction results from a radical chain process, while the anionic polymerization mechanism typically leads to lower molecular weight materials.[17] Although this discussion is beyond the scope of this work, the bimodal chromatogram obtained for TH-PPV is a strong indication that also in the Gilch route both mechanisms are in competition with each other.

Attempts to separate the oligomeric fraction from the high molecular weight fraction using Bio-Beads® S-X beads with THF as eluent, were unsuccessful. Therefore the mixture of TH-PPV is used for further characterization. UV-Vis spectra of the conjugated polymer **9** are taken at room temperature in $CHCl_3$ and as film. TH-PPV exhibits in the UV-Vis absorption spectrum a distinct absorption associated with the π–π^* transition, both in a thin film ($\lambda_{a,\,max}$= 442 nm) and in solution ($\lambda_{a,\,max}$= 430 nm) (Figure 3-14). This value is significantly blue shifted compared to BTEM-PPV (Figure 3-1) which exhibits a distinct absorption at λ_{max} = 489 nm in $CHCl_3$ and at λ_{max} =509 nm as thin film. The blue shift may be attributed to different factors. It is likely that the steric hindrance between the side chains of TH-PPV causes a twisted conformation of the polymer backbone and in this way a lower average conjugation length. However, the presence of low molecular weight fractions in the mixture of TH-PPV may also negatively influence the optical properties. Lower defect levels and therefore increased optical properties are likely obtained by preparing this material according to the sulfinyl precursor route.

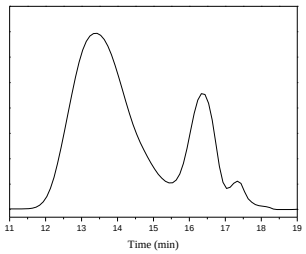

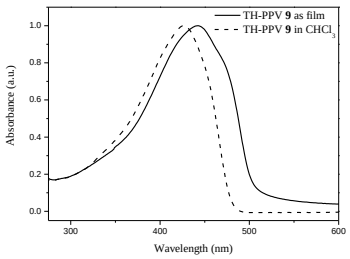

Figure 3-13 SEC chromatogram of **9**

Figure 3-14 UV-Vis absorption spectra of **9** as film and in $CHCl_3$

Furthermore, the solubility and UV-Vis absorption characteristics of TH-PPV in various solvents with different polarities, *i.e.* E_T^N values[7] are studied (Table 3-3). For these studies a concentration of approximately 0.05 mM (based on the repeating unit) of TH-PPV is employed. A distinct transition is found in the UV-Vis absorption spectrum for the solvents at the apolar side of the polarity scale. As with BTEMG-PPV, no significant dependence of λ_{max} on the polarity of the solvent was found, which also in this case probably can be contributed to the rather crowded substitution of the backbone. It should be noted that TH-PPV is soluble in cyclohexane, a very apolar solvent in which other PPV derivatives are usually insoluble.

Solvent	**Polarity[7] (E_T^N)**	**λ_{max} (nm)**
Cyclohexane	0.006	431
n-Hexane	0.009	426
Toluene	0.099	432
Diethyl ether	0.117	429
Chlorobenzene	0.188	433
Tetrahydrofuran	0.207	429
Ethyl acetate	0.228	426
Chloroform	0.259	430
Dichloromethane	0.309	427

Table 3-3 Overview of solution UV-Vis absorption maxima λ_{max} for **3** in selected solvents

TH-PPV is also studied using fluorescence spectroscopy (Figure 3-15). The photoluminescence emission (PL) spectrum of the conjugated polymer **9** exhibits two emission maxima at $\lambda_{em,max}$= 495 nm and 530 nm in a thin film (excitation wavelength λ_{exc}= 442 nm) and at $\lambda_{em,\ max}$= 488 nm and 519 nm in

solution (solvent $CHCl_3$; excitation wavelength λ_{exc}= 430 nm). Furthermore, the room temperature photoluminescence excitation (PLE) spectrum of a film of TH-PPV exhibits a distinct transition at λ_{em} = 438 nm (excitation wavelength λ_{exc} = 495 nm) and a solution of **9** exhibits an excitation maximum at $\lambda_{ex,\ max}$= 430 nm (solvent $CHCl_3$; emission wavelength λ_{em}= 488 nm). Currently, the PL quantum efficiency of this polymer is tested in co-operation with Dr. Henk J. Bolink of the Instituto de Ciencia Molecular (ICMol) (Universidad de Valencia, Spain).

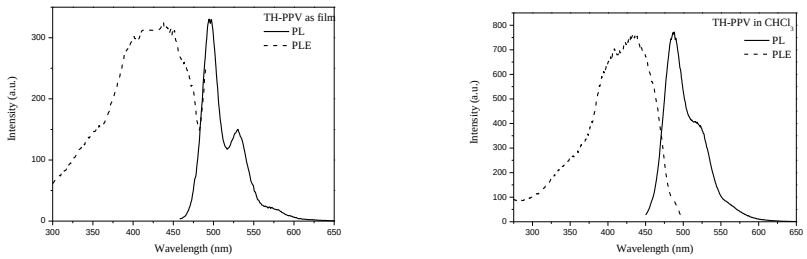

Figure 3-15 PL and PLE spectra of TH-PPV **9** as film and in $CHCl_3$

Two classical techniques are used to study the thermal stability of TH-PPV. The first technique is thermogravimetric analysis (TGA), in which the weight loss is recorded as a function of temperature at a heating rate of 20°C/min. A sample (10 mg) of **9** is inserted in the solid state. The change of mass of the sample is measured in real-time, while constantly increasing the temperature. The derivative of loss of weight to temperature shows one maximum at 378 °C, which accounts for the degradation of the conjugated PPV polymer (Figure 3-16). Note that we have to be careful with the interpretation of the results obtained, since we do not monitor the degradation of the conjugated system itself, but only keep track of loss of weight and thus the evaporation of the degradation products that are liberated during the degradation process. If the reaction product has a boiling point higher than the temperature at which the degradation reaction occurs, the observed loss of weight does not agree with the real reaction temperature.

A second technique used in the study of the thermal stability of TH-PPV is the thermal analysis by direct insert probe mass spectroscopy (DIP-MS). A heating rate of 10 °C/min is used. The total reconstructed ion chromatogram, in which the ion current is plotted *versus* increasing temperature, shows one signal at 293 °C related to the degradation of the conjugated polymer (Figure 3-17). The difference between TGA and DIP-MS analysis is the atmosphere in which the experiment is carried out. TGA is performed in argon atmosphere, whereas DIP-MS experiments are executed in high vacuum conditions (10^{-6} mm Hg). The high vacuum in the mass spectrometer causes a weight loss and a corresponding ion current at lower temperatures, because the evaporation is faster compared with a heating process in argon atmosphere (TGA). Hence the degradation temperature retrieved from DIP-MS is more realistic than that obtained from TGA. Still even the former measurements only allow a relative indirect observation of the degradation processes.

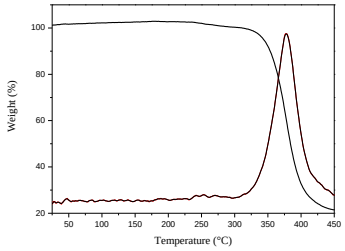

Figure 3-16 TGA plot of **9**

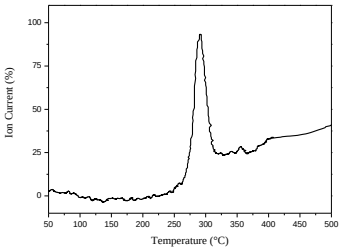

Figure 3-17 Ion chromatogram of **9**

To obtain more information about the stability of **9,** an *in situ* UV-Vis heating experiment is performed. A sample of **9** is heated using a dynamic heating program in which a thin film of **9** is heated at 2 °C/min from ambient temperature up to 120 °C and subsequently cooled down to room temperature. In the next run, the sample is heated to 140 °C and subsequently cooled down. This sequence is repeated up to 280 °C (Figure 3-18). After each heating run, the spectrum is cooled down and a UV-Vis absorption spectrum is taken at 25 °C (Figure 3-19). As shown in Figure 3-19, the maximum absorbance of **9** at room temperature is recovered for the heating runs between 120 °C and 220 °C. After 240°C, the maximum absorption is blue shifted. Further heating leads to a

further blue shift and to a steep decrease in the absorbance, indicating that degradation of the conjugated PPV polymer starts between 220 °C and 240 °C.

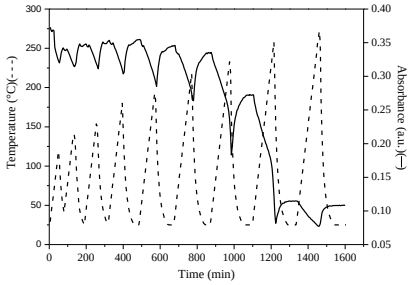

Figure 3-18 Plot demonstrating the dynamic heating program

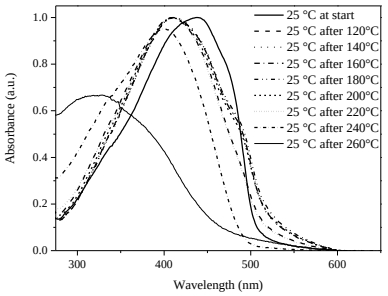

Figure 3-19 Thin film UV-Vis absorption spectra of **9** at RT after using a dynamic heating program

The phase behaviour of TH-PPV is investigated by means of differential scanning calorimetry (DSC) and polarized optical microscopy (POM). This tetra-alkoxy PPV derivative shows thermal liquid crystal behaviour. The existence of a thermotropic liquid crystalline phase is shown by POM. Polymer **9** is drop casted from a $CHCl_3$ solution onto a glass substrate which is made apolar by treatment with trimethylsilyl chloride at reflux temperature. The as-cast film is only weakly birefringent under cross-polarization. Nematic-like optical textures become more apparent upon cooling. During the subsequent thermal cycling between room temperature and 220 °C at a heating/cooling rate of 10°C/min, little variation in texture is observed. The birefringence weakens above 200 °C, due to isotropization. The optical texture is reversibly recovered upon cooling from 220 °C. Because the monomer of TH-PPV, *i.e.* 1,4-bis-chloromethyl-2,3,5,6-tetrahexyloxybenzene does not display liquid crystalline behaviour, it can be assumed that the observed liquid crystalline state originates from the rodlike nature of the main chain of TH-PPV. Therefore, TH-PPV is likely to be an example of a main chain-type liquid crystalline state. Mesophase formation is further evident from DSC measurements (Figure 3-20). The lower curve corresponds to a heating process and shows double melting endotherms (T_m= *circa* 51 °C and 89 °C). This is followed by a cooling process,

represented in the upper curve, which shows a clear crystallization peak around T_c= 71.5 °C.

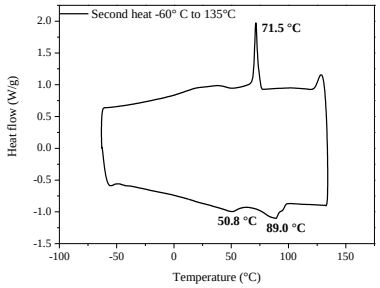

Figure 3-20 DSC plot of TH-PPV

The liquid crystalline behaviour of TH-PPV is a direct indication for the enhanced structural order of this material. It is likely that this order increases the mobility of charge carriers. The combination of a possible increased mobility and a high PL quantum efficiency makes TH-PPV a very interesting material for tests in photovoltaic applications. Currently this polymer is tested as active layer in organic light emitting devices (OLEDs) in co-operation with Dr. Henk Bolink (Universidad de Valencia, Spanje). Mobility measurements on TH-PPV are in progress in co-operation with the Materials Physics research group of the Institute for Materials Research (IMO) of UHasselt.

We can already conclude from this section that a breakthrough is realized towards a new class of semi-conductor material systems. The synthesis of the monomer 1,4-bischloromethyl-2,3,5,6-tetraalkoxybenzene is straightforward and feasible in high yields. The polymerization is accomplished using the well-known dehydrohalogenation route. TH-PPV is highly soluble in various solvents ranging from solvents at the apolar side of the polarity scale such as cyclohexane to the more common organic solvents such as dichloromethane. This result shows great promise towards the solubility characteristics of poly(2,3,5,6-tetra(triethoxymethoxy)-1,4-phenylene vinylene) (TTEM-PPV), a PPV derivative substituted with 4 polar oligo(ethylene glycol) side chains.

3.3.2 Poly(2,3,5,6-tetra(triethoxymethoxy)-1,4-phenylene vinylene) (TTEM-PPV)

The first step in the synthesis of TTEM-PPV is the preparation of the tri(ethylene glycol) side chains. Therefore, toluene-4-sulfonic acid 2-(2-(2-methoxy-ethoxy)-ethoxy)-ethyl ester **10** is prepared starting from the corresponding alcohol as is described in Chapter 2 (Scheme 3-7). The synthesis of 1,2,4,5-tetra(triethoxymethoxy)benzene **11** is similar to the synthesis 1,2,4,5-tetrahexyloxybenzene **7**, *i.e.* 1,2,4,5-tetrahydroxybenzene is obtained *in situ* by catalytic hydrogenation of 2,5-dihydroxybenzene-1,4-benzoquinone using the set-up depicted in Figure 3-10. Subsequently, 1,2,4,5-tetrahydroxybenzene is coupled with the tosylate ester **10** *via* a Williamson ether synthesis (Scheme 3-8). Excess of tosylate ester is removed by *Kugelrohr* distillation and after a flash column, pure **11** is obtained as a yellow oil in 79 % yield.

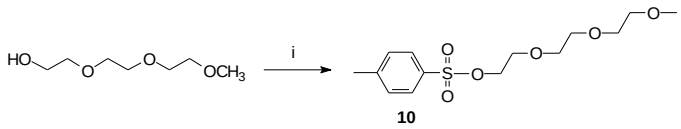

10

Scheme 3-7 Synthesis of the tosylate ester of the tri(ethylene glycol) side chains **10** (i: TosCl, KOH, CH_2Cl_2, 0°C)

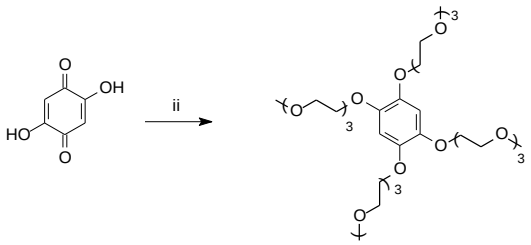

11

Scheme 3-8 Synthesis of 1,2,4,5-tetra(triethoxymethoxy)benzene **11** (ii: 1. PtO_2, $H_{2(g)}$, DMF; 2. Cs_2CO_3, **10**)

Tetra(triethoxymethoxy)benzene **11** is chloromethylated according to an adapted literature procedure[6] using concentrated HCl and formaldehyde in acetic anhydride towards monomer **12** (Scheme 3-9). However, while in the

reaction towards monomer **8** the sterical hindrance was overcome by using increased reaction temperature and time, in the case of tetra(triethoxymethoxy)benzene, these reaction circumstances lead to degradation of the ether functionalities of the side chains. Since low temperatures and short reaction times lead to monochloromethylation of 2,3,5,6-tetra(triethoxymethoxy)benzene **12** and high reaction temperatures and longer reaction times cause degradation of the side group functionalities, a compromise had to be reached. Pure monomer **12** is obtained in 28 % yield after a chloromethylation reaction during 26 hours at 70 °C and subsequent purification by column chromatography.

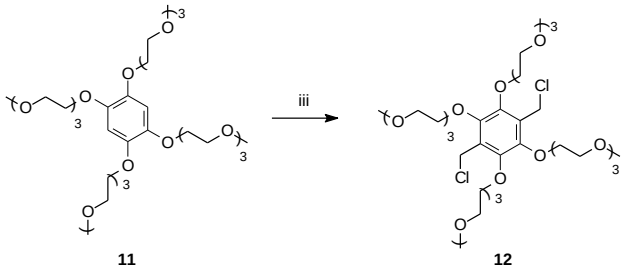

11 **12**

Scheme 3-9 Chloromethylation of tetra(triethoxymethoxy)benzene **11** to monomer **12** (iii: *p*-CH_2O, Ac_2O, HCl)

Monomer **12** is polymerized using the Gilch polymerization conditions[6], *i.e.* **12** is dissolved in dry dioxane under N_2 atmosphere, heated to 98 °C and an excess of base is added in two portions (Scheme 3-10). After a reaction time of 3 hours, poly(2,3,5,6-tetra(triethoxymethoxy)-1,4-phenylene vinylene) (TTEM-PPV) **13** is precipitated in cold hexane, filtered off and washed thoroughly with hexane. TTEM-PPV is obtained as a red solid in 63 % yield.

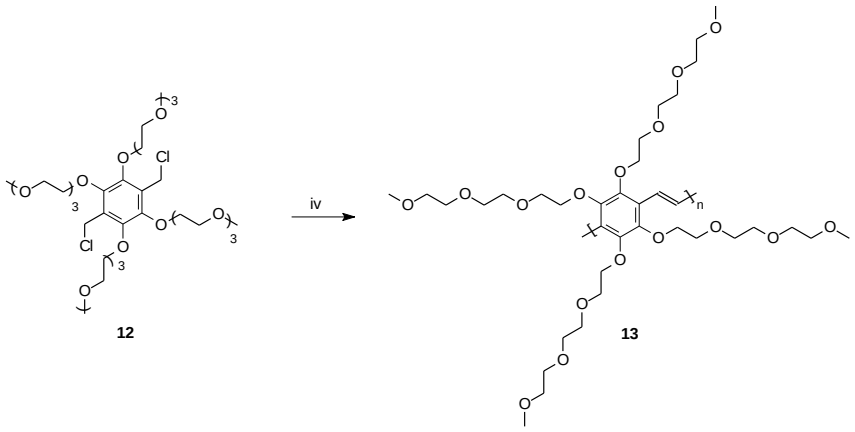

Scheme 3-10 Gilch polymerization of monomer **12** towards TTEM-PPV **13** (iv: K*t*BuO, 1,4-dioxane)

An analytical SEC measurement of TTEM-PPV is performed in DMF *versus* polystyrene standards. A very broad band is observed (M_w = 48 × 10^3 g/mol and PD = M_w/M_n = 5.9). Separation on Bio-Beads® S-X beads with DMF as eluent faild due to interactions of TTEM-PPV with the beads, so the polydisperse TTEM-PPV is used for further characterization. The high polydispersity is also demonstrated in the UV-Vis spectra of the conjugated polymer **13** (Figure 3-21). The spectra are taken at room temperature in $CHCl_3$ solution and as thin solid film. A solution of TTEM-PPV in $CHCl_3$ displays a broad band in the UV-Vis absorption a maximum absorbances at $\lambda_{a,max}$= 393 nm. A thin film of TTEM-PPV displays a similar absorbance band at $\lambda_{a,max}$= 397 nm. These values are markedly lower than the values obtained for BTEM-PPV (Figure 3-1) ($\lambda_{a,max}$= 489 nm in $CHCl_3$ and $\lambda_{a,max}$= 509 nm as thin film). Also compared to TH-PPV (Figure 3-9), a significant blue shift is observed ($\lambda_{a,max}$ of TH-PPV= 430 nm in $CHCl_3$ and $\lambda_{a,max}$= 442 nm as thin film). It is very likely that improved optical properties are obtained when the synthesis of TTEM-PPV is optimized. TTEM-PPV is also studied using fluorescence spectroscopy (Figure 3-22). The photoluminescence emission (PL) spectrum of the conjugated polymer **13** exhibits a distinct emission maximum at $\lambda_{em,max}$= 485 nm in solution (solvent $CHCl_3$; excitation wavelength λ_{exc}= 393 nm). Furthermore, the room temperature photoluminescence excitation (PLE)

spectrum of a solution of **13** exhibits an excitation maximum at $\lambda_{ex,\ max}$= 401 nm (solvent $CHCl_3$; emission wavelength λ_{em}= 485 nm).

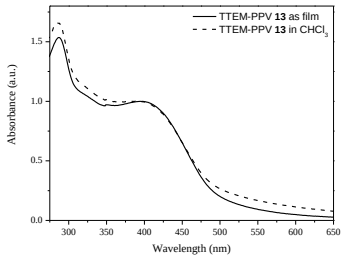

Figure 3-21 UV-Vis absorption spectra of **13** as film and in $CHCl_3$

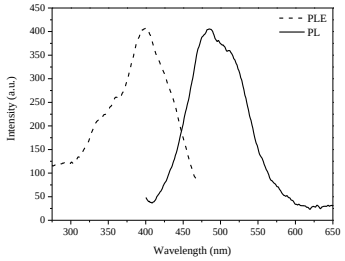

Figure 3-22 PL and PLE spectra of **13** in $CHCl_3$

The solubility and UV-Vis absorption characteristics of TTEM-PPV in various solvents with different polarities, *i.e.* E_T^N values[7] are studied. For these studies a concentration of approximately 0.05 mM (based on the repeating unit) of TTEM-PPV is employed. TTEM-PPV is soluble in the same solvents as BTEMG-PPV, *i.e.* all the solvents ranging from the most polar solvent of the polarity scale (water) to the somewhat more apolar solvents used in the manufacturing of organic PV devices[18], such as chlorobenzene. The solution absorption maxima range in the various solvents range from λ_{max} = 386 to 394 nm. Moreover, the solution characteristics do not change in the course of time, *i.e.* the same transitions and solution absorption maxima are found after one week at room temperature, which implicates that no aggregation of TTEM-PPV occurs in the tested solvents.

3.4 Conclusions

This chapter confirms the conclusions of Chapter 2, in which it was stated that by alternating the side chains, the solubility characteristics of PPV can be altered. Throughout this chapter, two strategies to further improve the polarity and to introduce compatibility with environmentally friendly environments, such as alcohols and water, were worked out. In the first strategy, two branched oligo(ethylene glycol) side chains were introduced at every repeating unit of a PPV backbone. The resulting conjugated material BTEMG-PPV is soluble in a

variety of media at the most polar side of the polarity scale, including alcohols and water. In a second approach, a tetra-substituted PPV derivative bearing four triethylene glycol derived side chains was prepared. In order to demonstrate the accessibility of tetra-substituted PPV derivatives, poly(2,3,5,6-tetrahexyloxy-1,4-phenylene vinylene) (TH-PPV) was prepared first. TH-PPV is highly soluble in solvents at the most apolar side of the polarity scale such as cyclohexane. In addition, TH-PPV is strongly fluorescent and shows interesting thermotropic liquid crystalline behaviour. This behaviour is characteristic for highly ordered structures. Since increased structural order enhances the mobility of charge carriers in a polymer, TH-PPV is a promising material for tests in advanced polymer based devices. So, a breakthrough was realized by the synthesis of tetra-substituted PPV derivatives. Not only is the synthesis very simple and straightforward, this new class of PPV derivatives allows for a simple generation of plethora of PPV derivatives. Replacement of the tetrahexyloxy side chains by polar tri(ethylene glycol) side chains, gave poly(2,3,5,6-tetra(triethoxymethoxy)-1,4-phenylene vinylene) (TTEM-PPV) which was characterized by the same solubility characteristics as BTEMG-PPV.

3.5 Experimental Section

Chemical and optical characterization

NMR spectra were recorded with a Varian Inova Spectrometer at 300 MHz using a 5 mm probe for ^{1}H NMR and at 75 MHz using a 5 mm broadband probe for ^{13}C NMR. Analytical Size Exclusion Chromatography (SEC) was performed using a Spectra series P100 (Spectra Physics) pump equipped with a pre-column (5 μm, 50 mm*7.5 mm, guard, Polymer Labs) and two mixed-B columns (10 μm, 2x300 mm*7.5 mm, Polymer Labs) and a Refractive Index (RI) detector (Shodex) at 40°C. THF or DMF were used as eluent at a flow rate of 1.0 mL/min. Molecular weight distributions are given relative to polystyrene standards. GC-MS data were obtained with a Varian TSQ 3400 Gas

Chromatograph and a TSQ 700 Finnigan Mat mass spectrometer. Direct insert probe mass spectroscopy (DIP-MS) analysis was carried out on a Finnigan TSQ 70, electron impact mode and a mass range of 35-500. Electron energy was 70 eV. A $CHCl_3$ solution of the polymer was applied on the heating element of the direct insert probe. A heating rate of 10 °C/min was used. TGA analysis was carried out on a TA INSTRUMENT 951 thermogravimetric analyser with a continuous flow of argon (80 mL/min). A heating rate of 20 °C/min was used. FT-IR spectra were collected with a Perkin Elmer Spectrum One FT-IR spectrometer (nominal resolution 4 cm^{-1}, summation of 16 scans). Fluorescence spectra were obtained with a Perkin Elmer LS-5B luminescence spectrometer. UV-Vis measurements were performed on a Cary 500 UV-Vis-NIR spectrophotometer (scan rate 600 nm/min, continuous run from 200 to 800 nm). *In situ* degradation reactions were performed in a variable temperature oven (Harrick), which can be positioned in the beam of the UV-Vis-NIR-spectrophotometer. Elemental analysis was performed with a Flash EA 1112 Series CHNS-O analyzer. Differential Scanning Calorimetry (DSC) was carried out on a TA instruments DSC 2920. The samples (10 mg) were heated from -100°C to 200°C at a heating rate of 10°C/min under N_2 atmosphere. The second heating curves were evaluated. Polarized Optical Light Microscopic observations were made by use of a Nikon 144040 OPTIPHOT POL microscope equipped with a temperature-controlled stage. Film specimens were drop casted from $CHCl_3$ solutions on a glass substrate which was made apolar by reflux in trimethylsilyl chloride for 10 minutes. All chemicals were purchased from Aldrich or Acros and used without further purification. The *in situ* elimination reactions were performed in a Harrick High Temperature Oven, which is positioned in the beam of a Perkin Elmer spectrum one FT-IR spectrometer (nominal resolution 4 cm^{-1}, summation of 16 scans). The temperature of the sample is controlled by a Watlow temperature controller (serial number 999, dual channel). The precursor polymer 6 was spin coated from a CHCl3 solution (6 mg/mL) on a KBr pellet at 500 rpm. The spin coated KBr pellet (diameter 25 mm, thickness 1 mm) is in direct contact with the heating element. All experiments were performed at 2°C/min under a continuous flow of nitrogen. “Timebase software” supplied by Perkin Elmer is

used to investigate regions of interest. *In situ* UV-Vis measurements were performed on a Cary 500 UV-Vis-NIR spectrophotometer, specially adopted to contain the Harrick high temperature cell (scan rate 600 nm/min, continuous run from 200 to 800 nm). The precursor polymer was spin coated from a $CHCl_3$ solution (6 mg/mL) on a quartz glass (diameter 25 mm, thickness 3mm) at 700 rpm. The quartz glass was heated in the same Harrick oven high temperature cell as was used in the FT-IR measurements. The cell was positioned in the beam of the UV-Vis-NIR-spectrophotometer and spectra were taken continuously. The heating rate was 2°C/min up to 300°C. All measurements were performed under a continuous flow of nitrogen. "Scanning Kinetics software" supplied by Varian is used to investigate regions of interest.

Chemicals

All chemicals were purchased from Aldrich or Acros and used without further purification unless otherwise stated. Dioxane was distilled from sodium/benzophenone.

Synthesis

1,3-Bis(3,6,9-trioxydecanyl)glycerol 1. Tri(ethylene glycol) monomethyl ether (200.0 g, 1.22 mol) was stirred under dry nitrogen at 100 °C while sodium (9.6 g, 0.42 mol) was added in small portions. After all sodium had reacted, the flask content was cooled to 80 °C and epichlorohydrine (37.0 g, 0.40 mol) was added drop wise. Stirring was continued at 100 °C for 12 h. After cooling to room temperature, the reaction mixture was filtered and purified by *Kugelrohr* distillation: the first fraction contains excess tri(ethylene glycol)monomethyl ether (p= 5 x 10^{-3} mbar, T= 180-200 °C), the second fraction is the pure product **1** (p= 5 x 10^{-3} mbar, T= 210°C) (81.6 g, 53%). ^{1}H NMR ($CDCl_3$): δ = 3.94 (m, 1H), 3.59 (m, 20H), 3.49 (m, 8H), 3.36 (s, 6H), 3.11 (broad, OH) ; MS (EI, m/z): 385 $[M+1]^+$

1,3-Bis(3,6,9-trioxydecanyl)glycerol-2-toluenesulfonic ester 2. A three-necked flask equipped with mechanical stirrer, thermometer and nitrogen inlet,

is charged with 1 (30.0 g, 78 mmol), *p*-toluenesulfonyl chloride (15.2 g, 79 mmol) and CH_2Cl_2 (75 mL). The homogeneous mixture is cooled to 0°C with a $CO_{2(s)}$-acetone bath. Freshly powdered KOH (17.4 g, 312 mmol) is added in small amounts under vigorous stirring while maintaining the reaction mixture below 5°C (exothermic reaction). The mixture is stirred for 3 h at 0°C after which CH_2Cl_2 (75 mL) and ice-water (100 mL) are added. The organic phase is separated and the aqueous phase is extracted with CH_2Cl_2 (2 x 50 mL). The combined organic layer is washed with water (50 mL), dried ($MgSO_4$) and concentrated under reduced pressure. The pure product 2 was obtained in 98% yield. ^{1}H NMR ($CDCl_3$): δ = 7.77 (d, 2H), 7.28 (d, 2H), 4.63 (m, 1H), 3.52 (m, 28H), 3.33 (s, 6H), 2.40 (s, 3H).

1,4-Bis(1,3-bis(3,6,9-trioxydecanyl)-2-glyceryl)benzene 3. A mixture of *p*-hydroquinone (3.2 g, 0.029 mol), Na*t*BuO (6.2 g, 0.064 mol) in EtOH (130 mL) was stirred for 1 h at ambient temperature under Ar atmosphere, after which **2** (34.6 g, 0.064 mol) was added. The reaction mixture was stirred for 48 h at reflux temperature. The total volume was reduced to 50 mL by evaporation, cooled down to ambient temperature and poured into water (100 mL). The product was extracted with CH_2Cl_2 (3 x 75 mL). The organic extracts were washed with 10 % NaOH-solution, dried over anhydrous $MgSO_4$ and the solvent was evaporated to give the crude product. After column chromatography (SiO_2, eluent diethyl ether/ MeOH 98/2) **3** was obtained as a yellow oil was obtained (18.0 g, 73 %). ^{1}H NMR ($CDCl_3$): δ = 6.85 (s, 4H), 4.35 (m, 1H), 3.56 (m, 56H), 3.34 (s, 12H). MS (EI, m/z): 843 [M+].

2,5-Bis-chloromethyl-1,4-bis(1,3-bis(3,6,9-trioxydecanyl)-2-glyceryl)benzene 4. To a stirred mixture of **3** (1.59 g, 1.9 mmol) and *p*-formaldehyde (0.16 g, 5.2 mmol), concentrated HCl (1.2 mL) was added drop wise under N_2 atmosphere. Subsequently, acetic anhydride (2.4 mL) was added at such a rate that the temperature did not exceed 70°C. After the addition was complete, the resulting solution was stirred at 75°C for 4 h after which it was cooled down to room temperature and poured into water (30 mL). The product was extracted with CH_2Cl_2 (3 x 30 mL). The organic extracts were washed with 10% $NaHCO_3$-solution, dried over anhydrous $MgSO_4$ and the solvent was evaporated to give the crude product, which was purified by column

chromatography. **4** was obtained as a yellow oil in 71% yield. (SiO_2, eluent diethyl ether/ MeOH 9/1). ^{1}H NMR (CD_3OD): δ = 7.24 (s, 2H), 4.89 (s, 4H), 4.50 (m, 2H), 3.61 (m, 56H), 3.35 (s, 12H); ^{13}C NMR ($CDCl_3$): δ= 150.3 (2C), 128.5 (2C), 117.4 (2C), 78.9 (2C), 71.6 (4C), 70.8 (8C), 70.4 (8C), 70.3 (8C), 68.9 (4C), 58.8 (4C), 40.9 (2C); MS (EI, *m/z*): 478 [M^+], 394, 309, 225, 141; MS (EI, m/z): 938 [M+].

Poly(2,5-bis(3,6,9-triethoxy-12-methoxy)-2-glyceryl)-1,4-phenylene vinylene) (BTEMG-PPV) 5. In a three-necked round-bottom flask fitted with a reflux condenser and a septum 0.34 g (0.36 mmol) of monomer **4** was dissolved in dry dioxane (20 mL) and flushed with N_2 for 15 min. Afterwards, a balloon filled with Ar was placed on top of the condenser. After heating to 98 °C, a solution of K*t*BuO (0.10 g, 0.94 mmol) in 1 mL dry dioxane was added. During this addition, the solution turned from colourless to green-orange. After 5 min., a second solution of K*t*BuO (0.08 g, 0.72 mmol) in 1 mL dry dioxane was added and the solution coloured dark-orange. After stirring for 2 h at 98 °C, the solution was cooled down to 50 °C and neutralized with acetic acid. The total volume was reduced to 10 mL by evaporation, and the polymer was precipitated in cyclohexane. A nice red precipitation was formed which became oily and sticky during filtration. After drying overnight in a desiccator, 240 mg (77%) of BTEMG-PPV was obtained. A gel permeation chromatographic separation on Biobeads® S-X beads with DMF as eluent was performed. Three different fractions were collected. The highest molecular weight fraction **5-1** was obtained in a yield of 18 % when calculated against the mol fraction of monomer **4**. SEC (DMF) $M_w = 20 \times 10^4$ g/mol (PD = M_w/M_n = 2.2); UV-Vis $\lambda_{a,max}$= 462 nm ($CHCl_3$) and $\lambda_{a,max}$= 469 nm (as a film) ^{1}H NMR ($CDCl_3$): δ= 8.0 (2H), 7.1 (2H), 4.5 (2H), 3.6 (56H), 3.3 (12H); ^{13}C NMR ($CDCl_3$): δ= 151.0 (2C), 129.2 (2C), 128.4 (2C), 119.8 (2C), 79.1 (2C), 71.8 (4C), 70.9 (8C), 70.8 (16C), 67.9 (4C), 59.0 (4C); FT-IR (NaCl, cm^{-1}): 2922, 2872, 1599, 1496, 1455, 1351, 1259, 1198, 1107,1039; DSC: T_g= -76 °C + -45 °C; TGA: degradation T_{max} = 301 °C; Photoluminescence emission (PL) $\lambda_{em,\ max}$= 528 nm (λ_{exc}= 462 nm, $CHCl_3$); Photoluminescence excitation (PLE) $\lambda_{ex,\ max}$= 459 nm (λ_{em}= 528 nm; $CHCl_3$).

1,2,4,5-Tetrahydroxybenzene 6 and 1,2,4,5-tetrahexyloxybenzene 7. In a three-necked round-bottomed flask 1,2,4,5-tetrahydroxybenzene **6** was generated quantitatively by *in situ* hydrogenation of 2,5-dihydroxy-1,4-benzoquinone (5.2 g, 37.0 mmol) in dry DMF (1220 mL) at atmospheric pressure (p_{H2}= 1 atm.) with PtO_2 (40 mg) as a catalyst. First the reaction set-up is made oxygen free. (Valve **A** and **B**: open, Valve **C**, **D** and **E**: closed; successively and repeatedly vacuum, N_2 inlet). Then the large column filled with a blue copper sulphate solution is charged with a known amount of hydrogen (1. Valve **A**, **B** and **E**: open, Valve **C** and **D**: closed; Vacuum, N_2 inlet, vacuum $\rightarrow$ level of the $CuSO_4$-solution **X**= $\mathbf{X_0}$ 2. Valve **D** and **E**: open, Valve **A**, **B** and **C**: closed; $H_{2(g)}$ [p(H_2)= 1 atm] $\rightarrow$ level of the $CuSO_4$-solution **X**= $\mathbf{X_1}$). The reaction mixture in the three-necked flask is subjected to hydrogenation with stirring (: Valve **A**, **C** and **D**: closed, Valve **B** and **E**: open). After completion of the reaction, indicated by the amount gas consumed (level of the $CuSO_4$-solution **X**= $\mathbf{X_2}$ **=** constant) and the change in colour of the reaction mixture from light brown to dark red-brown, the hydrogen atmosphere is replaced by nitrogen (Valve C is recommendable to ensure slow escape of the $H_{2\ (g)}$). Subsequently 1-bromohexane (27.0 g, 163.0 mmol) and cesium carbonate (72.4 g, 222.3 mmol) were added. The reaction mixture was stirred for 6 days at 65°C. After cooling to room temperature DMF was removed under reduced pressure and CH_2Cl_2 (600 mL) was added. The reaction mixture was washed with H_2O (3 x 100 mL), after which the organic extracts were dried upon anhydrous $MgSO_4$ and concentrated under reduced pressure to yield crude **7** as a brown solid which was recrystallized twice from MeOH giving 13.9 g (29.0 mmol, 78%) white

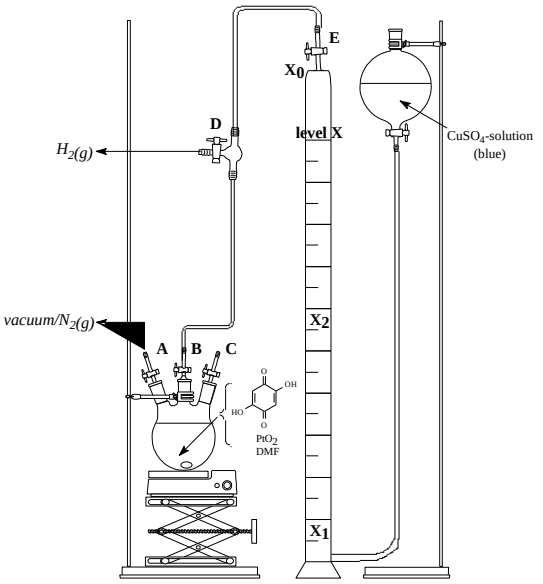

crystalline **7**. ^{1}H NMR ($CDCl_3$): δ = 6.55 (s, 2H), 3.91 (t, 8H), 1.74 (m, 8H), 1.43 (m, 8H), 1.30 (m, 16H), 0.89 (t, 12H) ; ^{13}C NMR ($CDCl_3$): δ= 143.4 (4C), 105.4 (2C), 70.4 (4C), 31.5 (4C), 29.4 (4C), 25.6 (4C), 22.5 (4C), 13.9 (4C); MS (EI, *m/*z): 478 [M^+], 394, 309, 225, 141.

1,4-Bis-chloromethyl-2,3,5,6-tetrahexyloxybenzene 8. To a stirred mixture of 7 (5.0 g, 10.4 mmol) and *p*-formaldehyde (3.1 g, 104 mmol) at 0 °C, concentrated HCl (9.6 mL, 114.8 mmol) was added drop wise under N_2 atmosphere. Subsequently, acetic anhydride (19.6 mL, 208.8 mol) was added slowly. After addition was complete, the resulting solution was stirred at 95°C for 6 days after which it was cooled down to room temperature and poured into water (100 mL). The reaction mixture was extracted with CH_2Cl_2 (3 x 100 mL) and dried over anhydrous $MgSO_4$. Evaporation of the solvent under reduced pressure gave the crude product. The pure product was obtained by column chromatography (SiO_2, eluent hexane/ethyl acetate 95/5) as a white solid (4.1 g, 68 %). ^{1}H NMR ($CDCl_3$): δ = 4.65 (s, 4H), 4.02 (t, 8H), 1.78 (m, 8H), 1.48 (m, 8H), 1.30 (m, 16H), 0.89 (t, 12H); ^{13}C NMR ($CDCl_3$): δ= 147.0 (4C), 126.9 (2C), 73.8 (4C), 35.6 (2C), 31.5 (4C), 30.1 (4C), 25.5 (4C), 22.5 (4C), 13.9 (4C); MS (EI, *m/*z): 574 [M^+], 539 [M^+]- Cl, 492 [M^+]- 2Cl-CH_2, 456, 370.

Poly(2,3,5,6-tetrahexyloxy-1,4-phenylenevinylene) (TH-PPV) 9. In a three-neck round-bottom flask fitted with a reflux condenser and a septum 1.5 g (3.1 mmol) of **8** was dissolved in dry dioxane (200 mL) and flushed with N_2 for 15 min. Afterwards, a balloon filled with N_2 was placed on top of the condenser. After heating to 96 °C, a solution of KtBuO (0.91 g, 8.1 mmol) in dry dioxane (9 mL) was added drop wise with a syringe while stirring. During this addition the solution turned from colourless to white. After 5 min, a second solution of K*t*BuO (0.70 g, 6.2 mmol) in dry dioxane (7 mL) was added at which the solution turned yellow. The polymerization was allowed to proceed for 3 h at 98 °C after which the total volume was reduced to 20 mL by evaporation and the solution was precipitated drop wise in cold MeOH (200 mL). The resulting polymer was filtered off, washed with MeOH and dried under reduced pressure at room temperature giving **9** as a yellow polymer (702 mg, 55% yield). Anal. Calcd. for $C_{32}H_{54}O_4$: C 76.4, H 12.7, O 10.8; Found C 76.7, H 11.4, O 11.9; ^{1}H NMR ($CDCl_3$): δ= 7.8 (2H), 3.9 (8H), 1.7 (8H), 1.4

(8H), 1.3 (16H), 0.8 (12H); 13C NMR (CDCl3): δ= 147.3 (4C), 126.2 (2C), 125.4 (2C), 73.3 (4C), 31.7 (4C), 30.3 (4C), 25.7 (4C), 22.5 (4C), 13.9 (4C); FT-IR (NaCl, cm^{-1}): 2955, 2859, 1445, 1378, 1301, 1266, 1121, 726; SEC (THF) Mw = 40×10^4 g/mol (PD = M_w/M_n = 3.1) + 5×10^3 g/mol (PD = M_w/M_n = 1.3); DSC: T_g= 51 °C + 89 °C, T_c= 71 °C; TGA: degradation T_{max} = 378 °C; DIP-MS: degradation T_{max}= 293 °C; UV-Vis $\lambda_{a,max}$= 430 nm ($CHCl_3$) and $\lambda_{a,max}$= 442 nm (as a film); Photoluminescence emission (PL) $\lambda_{em,\ max}$= 488 nm + a shoulder at 519 nm (λ_{exc}= 430 nm, $CHCl_3$) and $\lambda_{em,\ max}$= 495 nm + a shoulder at 530 nm (λ_{exc}= 442 nm; as a film); Photoluminescence excitation (PLE) $\lambda_{ex,\ max}$= 430 nm (λ_{em}= 488 nm; $CHCl_3$) and $\lambda_{ex,\ max}$= 438 nm (λ_{em}= 495 nm; as a film).

Toluene-4-sulfonic acid 2-(2-(2-methoxy-ethoxy)-ethoxy)-ethyl ester 10. **10** is synthesized starting from with 2-(2-(2-methoxy ethoxy)ethoxy)ethylalcohol and p-toluenesulfonyl chloride as described in Chapter 2. ^{1}H NMR (CDCl3): 7.60 (d, 2H), 7.17 (d, 2H), 3.96 (t, 2H), 3.49 (t, 2H), 3.42-3.38 (m, 8H), 3.17 (s, 3H), 2.25 (s, 3H); MS (EI, m/z): 318 [M^+], 273, 259, 243, 229, 199, 172, 155, 91, 59, 45.

1,2,4,5- Tetra(triethoxymethoxy)benzene 11. First, 1,2,4,5-tetrahydroxy-benzene **6** was generated by *in situ* hydrogenation of 2,5-dihydroxy-1,4-benzoquinone (5.2 g, 37.0 mmol) as described earlier in this experimental section. Subsequently **10** (51.9 g, 163.0 mmol) and cesium carbonate (72.4 g, 222.3 mmol) were added. The reaction mixture was stirred for 6 days at 65 °C. After cooling to room temperature DMF was removed under reduced pressure and CH_2Cl_2 (600 mL) was added. The reaction mixture was washed with H_2O (3 x 100 mL), after which the organic extracts were dried upon anhydrous $MgSO_4$ and concentrated under reduced pressure to yield crude **11** as a brown oil. The excess of starting material **10** was removed by *Kugelrohr* distillation (p= 0.13 mbar, T= 160 °C). After flash column (SiO_2, eluent diethylether/MeOH 4/1) pure **11** was obtained as a yellow oil (21.2 g, 79%). ^{1}H NMR ($CDCl_3$): δ = 6.55 (s, 2H), 4.01 (t, 8H), 3.70 (t, 8H), 3.58 (m, 8H), 3.54 (m, 8H), 3.45 (m, 16H), 3.27 (s, 12H) ; ^{13}C NMR ($CDCl_3$): δ= 143.4 (4C), 106.4 (2C), 71.7 (4C), 70.5 (4C), 70.4 (4C), 70.3 (4C), 69.8 (4C), 69.7 (4C), 58.8 (4C); MS (EI, *m/z*): 726 [M^+].

1,4-Bis-chloromethyl-2,3,5,6-tetra(triethoxymethoxy)benzene 12. To a stirred mixture of **11** (5.0 g, 6.9 mmol) and *p*-formaldehyde (2.1 g, 68.8 mmol) at 0 °C, concentrated HCl (7.3 mL, 75.6 mmol) was added drop wise under N_2 atmosphere. Subsequently, acetic anhydride (19.6 mL, 208.8 mmol) was added slowly. After addition was complete, the resulting solution was stirred at 70°C for 26 hours after which it was cooled down to room temperature and poured into water (150 mL). The reaction mixture was extracted with CH_2Cl_2 (3 x 100 mL) and dried over anhydrous $MgSO_4$. Evaporation of the solvent under reduced pressure gave the crude product. The pure product was obtained by column chromatography (SiO_2, eluent ether/MeOH 9/1) as a yellow oil (1.6 g, 28 %). ^{1}H NMR ($CDCl_3$): δ = 4.75 (s, 4H), 4.19 (t, 8H), 3.75 (t, 8H), 3.64 (m, 24H), 3.50 (m, 8H), 3.34 (s, 12H); ^{13}C NMR ($CDCl_3$): δ= 146.5 (4C), 127.1 (2C), 72.4 (4C), 71.7 (4C), 70.4 (4C), 70.3 (8C), 70.1 (4C), 58.8 (4C), 35.3 (2C); MS (EI, *m/z*): 822 [M^+].

Poly(2,3,5,6-tetra(triethoxymethoxy)-1,4-phenylene vinylene) (TTEM-PPV) 13. In a three-neck round-bottom flask fitted with a reflux condenser and a septum 1.2 g (1.4 mmol) of **12** was dissolved in dry dioxane (88 mL) and flushed with N_2 for 15 min. Afterwards, a balloon filled with N_2 was placed on top of the condenser. After heating to 96 °C, a solution of K*t*BuO (0.41 g, 3.7 mmol) in dry dioxane (4.4 mL) was added drop wise with a syringe while stirring. During this addition the solution turned from colourless to blue. After 5 min, a second solution of K*t*BuO (0.31 g, 2.9 mmol) in dry dioxane (3 mL) was added at which the solution turned orange-red. The polymerization was allowed to proceed for 3 h at 96 °C after which the total volume was reduced to 20 mL by evaporation and the solution was precipitated drop wise in cold hexane (200 mL). The resulting polymer was filtered off, washed with hexane and dried under reduced pressure at room temperature giving **13** as a red polymer (665 mg, 63% yield). ^{1}H NMR ($CDCl_3$): δ= 7.7 (2H), 4.2 (8H), 4.1 (8H), 3.6 (32H), 3.3 (12H); ^{13}C NMR ($CDCl_3$): δ= 147.1 (4C), 129.1 (2C), 125.8 (2C), 74.1 (4C), 72.3 (8C), 71.7 (8C), 70.4 (4C), 58.8 (4C); FT-IR (NaCl, cm^{-1}): 2874, 1575, 1447, 1397, 1350, 1258, 1198, 1107; SEC (DMF) M_w = 48×10^3 g/mol (PD = M_w/M_n = 5.9); DSC: T_g= -75 °C + -48 °C; TGA: degradation T_{max} = 279 °C; UV-Vis $\lambda_{a,max}$= 393 nm + 286 nm ($CHCl_3$) and

$\lambda_{a,max}$= 397 nm + 287 nm (as a film); Photoluminescence emission (PL) $\lambda_{em,max}$= 485 nm (λ_{exc}= 393 nm, $CHCl_3$); Photoluminescence excitation (PLE) $\lambda_{ex,max}$= 401 nm (λ_{em}= 485 nm; $CHCl_3$).

3.6 References

[1] Pinto, M. R.; Schanze, K. S. *Synthesis* **2002**, *9*, 1293.

[2] Khan, A.; Müller, S.; Hecht, S. *Chem. Commun.*, **2005,** 584-586.

[3] Lauter, W. H.; Meyer, V.; Enkelmann, G.; Wegner *Macromol. Chem. Phys.* **1998**, 199, 2129-2140.

[4] Keegstra, E. M. D.; Zwikker, J. W.; Roest, M. R.; Jenneskens, L. W. *J. Org. Chem.*, 1992, *57*, 6678-6680.

[5] Becker, H.; Spreitzer, H.; Ibrom, K.; Kreuder, W. *Macromolecules* **1999**, *32*, 4925.

[6] a) Gilch, H. G.; Wheelwright, W. L. *J. Polym. Sci.: A* **1966**, *4*, 1337 b) Spreitzer, H.; Becker, H.; Kluge, E.; Kreuder, W.; Schenk, H.; Demandt, R.; Schoo, H. *Adv. Mater.* **1998**, *10*, 1340.

[7] Reichardt, C. *Solvents and Solvent Effects in Organic Chemistry*, VCH Weinheim: 1990, p. 408-410.

[8] Munters, T.; Martens, T.; Goris, L.; Vrindts, V.; Manca, J.; Lutsen, L.; De Ceuninck, W.; Vanderzande, D.; De Schepper, L.; Gelan, J.; Sariciftci, N. S.; Brabec, C. J. *Thin Solid Films* **2002**, *403-404*, 247.

[9] Jin, J.-I; Park, C.-K *Macromolecules* **1993**, *26 (8)*, 1799.

[10] a) Donval, A.; Josse, D.; Kranzelbinder, G., Hierle, R.; Toussaere, J.; Zyss, J.; Perpelitsa, G.; Levi, O.; Davidov, D.; Bar-Nahum, I.; Neuman, R. *Synthetic Metals* **2001** *124*, 59-61. b) Hong, S. Y. *Bull. Korean Chem. Soc.* **1999**, *20(1)*, 42.

[11] Benington, F.; Morin, R. D.; Clark, L. C. *J. Org. Chem.* **1955,** *20*, 103.

[12] Wessling, R. A. *Journal of Polymer Science: Pol. Symp.***1985**, *72*, 55-66.

[13] a) Keegstra, E. M. D.; Huisman, B.-H.; Paardekooper, E. M., Hoogesteger, F. J.; Zwikker, J. W.; Jenneskens, L. W.; Kooijman, H.; Schouten, A., Veldman, N.; Spek, A. L. *J. Chem. Soc., Perkin Trans. 2* **1996**, 229-240. b) Schlotter, J. J. H.; Mertens, I. J. A.; van Wageningen, A. M. A.; Mulders, F. P. J.; Zwikker, J. W.; Buschman, H.-J.; Jenneskens, L. W. *Tetrahedron Letters*, **1994**, *35 (39)*, 7255-7258.

[14] Gottlieb, H. E.; Kotlyar, V.; Nudelman A. *J. Org. Chem*. **1997**, *62*, 7512-7515.

[15] a) Hsieh, B. R.; Yu, Y.; VanLaeken, A. C.; Lee, H. *Macromolecules*, **1997**, *30*, 8094 b) Hsieh, B. R.; Yu, Y.; Forsythe, E. W.; Schaaf, G. M.; Feld, W. A. *J. Am. Chem. Soc.*, **1998**, *120*, 231. c) Neef, C. J.; Ferraris, J. P. *Macromolecules*, **2000**, *33*, 2311; d) Neef, C. J.; Ferraris, J. P. *Macromolecules*, **2004**, *37*, 2671.

[16] a) Wiesecke, J.; Rehahn, M. *Angew. Chem. Ind. Ed.*, **2003**, *42 (5)*, 567; b) J Wiesecke, J.; Rehahn, M., *Polym. Prep.* **2004**, *45 (1)*, 174. c) Hontis, L.; Lutsen, L.; Vanderzande, D.; Gelan, J. *Synth. Met.*, **2001**, *119*, 135; b) Hontis, L.; Vrindts, V.; Vanderzande, D.; Lutsen, L. *Macromolecules*, **2003**, *36 (9)*, 3035.

[17] Vanderzande, D. J. M.; Hontis, L.; Palmaerts, A.; Van Den Berghe, D.; Wouters, J.; Lutsen, L.; Cleij, T. *Proc. of SPIE* **2005**, *5937* 116-125.

[18] Munters, T.; Martens, T.; Goris, L.; Vrindts, V.; Manca, J.; Lutsen, L.; De Ceuninck, W.; Vanderzande, D.; De Schepper, L.; Gelan, J.; Sariciftci, N. S.; Brabec, C. J. *Thin Solid Films* **2002**, *403-404*, 247.

Chapter 4

para-Phenylene Crown Ethers: Synthesis, Complexation and Polymerization

The objectives set for Chapter 4 concern the synthesis and further functionalization of the para-substituted crown ethers p-phenylene-20-crown-6 and p-phenylene-23-crown-7. So far, these products were never isolated in yields high enough to be of synthetic value; hitherto the latter was not even reported at all. In this chapter the synthesis is optimized and the crown ethers are fully characterized. Furthermore, their ability to form host–guest complexes with Na^+, K^+ and Rb^+ ions is investigated by ^1H NMR titration. Subsequently, the crown ether subunits are further functionalized to the corresponding Gilch monomers and polymerized to form the first 2,5-crown ether-substituted PPV derivatives.

4.1 Introduction

"Just as there is a field of molecular chemistry based on the covalent bond, there is a field of supramolecular chemistry, the chemistry of molecular assemblies and of the intermolecular bond. It is 'chemistry beyond the molecule'."

Lehn, J.-M.

The formation of a 'complex' by association of two or more chemical units is one of the most basic molecular processes of the field of supramolecular chemistry and of utmost importance in chemistry, physics and biology. An important area of complex formation involves synthetic 'host' molecules which coordinate 'guest' cations such as simple metal cations. The first neutral synthetic compounds to form stable complexes with alkali metal ions were macrocyclic polyethers, nicknamed crown compounds and discovered by C. J. Pederson in 1967.[1] As often happens in science, serendipity played an important role in the discovery of crown ethers and the appreciation of their intriguing characteristics. After all, the first crown compound was formed as an

unexpected by-product during an attempted preparation of the diphenol **3** from the dichloride **2** and the monoprotected catechol derivative **1a**. The presence of 10 % of catechol **1b** as an impurity led to the isolation of the unexpected by-product which was identified as the macrocyclic polyether **4**.[2] (Scheme 4-1) Given the trivial name dibenzo-18-crown-6 by Pedersen, it was found to be insoluble in methanol by itself, but became readily soluble on addition of a sodium salt. It was obtained in 45 % yield when pure catechol was employed in its synthesis.

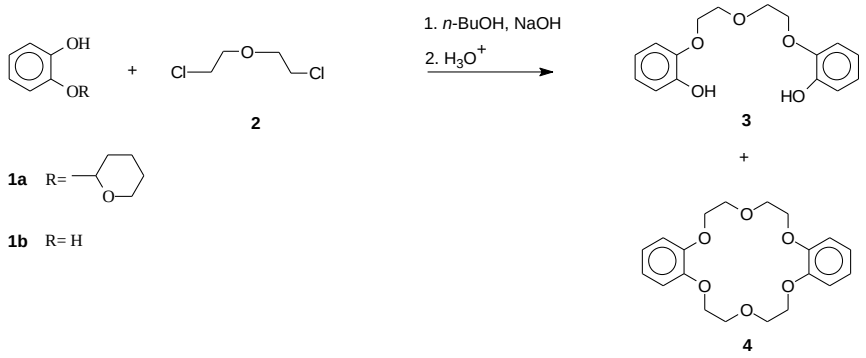

Scheme 4-1 Discovery of the synthesis of dibenzo-18-crown-6 **4**

The knowledge that these compounds selectively complex alkali and alkaline earth metal cations in their endopolarophilic cavity, incited scientist all over the world to modify the widely useful properties of crown ethers. Numerous crown compounds have been prepared by modification of all possible structural parameters in order to make accessible new ligand systems and to study the relationship between structure and cation selectivity.[3,4,5] One variable parameter is the introduction of aromatic systems in the ring. Following upon his initial discoveries, Pedersen prepared numerous other crown ethers, incorporating *ortho*-substituted benzene rings with up to four aromatic rings fused to the macrocycle (*e.g.* **5, 6** and **7** depicted in Figure 4-1).[6] A lot of research was also done on the complexing properties of host compounds containing 1,3-xylyl units (Figure 4-2).[7]

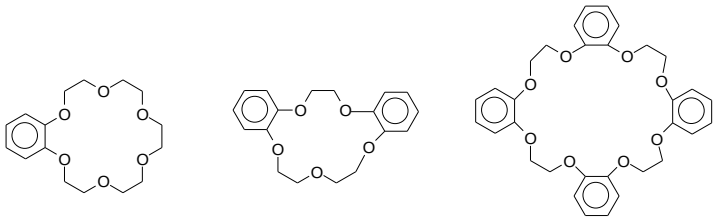

5 **6** **7**

Figure 4-1 Ortho-substituted macrocyclic polyethers

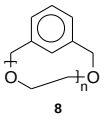

8

Figure 4-2 Meta-xylyl crown derivatives

Much less common in literature are the crown compounds containing *para*-phenylene units in the macrocycle. Moreover, hitherto *para*-substituted macrocyclic polyethers were never isolated in yields high enough to be of synthetic value. Cram *et al.* reported on the synthesis of *p*-phenylene-20-crown-6 **9** in a yield of 2 % along with its cyclic dimeer **10** (7 %) (Figure 4-3).[8] The highest yield of *p*-phenylene-20-crown-6 described in literature is 2.2 %.[9]

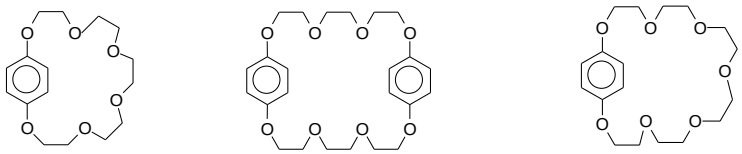

9 **10** **11**

Figure 4-3 Para-substituted macrocyclic polyethers

Yet, these macrocycles are interesting building blocks, as the aromatic subunit can serve as a π-donor for complexation with metal ions. Therefore, we set ourselves a target to optimize the synthesis of *p*-phenylene-20-crown-6 **9** in order to prepare this compound in a sufficient amount to allow further functionalization. Furthermore, we aim at synthesizing the larger *para*-substituted macrocyclic polyether *p*-phenylene-23-crown-7 (**11** in Figure 4-3), which has no precedent as far as we are aware. The ability of these *para*-substituted polyethers to form complexes with the alkali metal ions Na^+, K^+ and

Rb^+ ions can then readily be investigated by ^1H NMR spectroscopic titrations. The ultimate goal is to convert the crown ether subunits to the corresponding Gilch monomers in order to prepare the first 2,5-crown ether substituted conjugated PPV-type polymers.

▪ Conjugated polymers containing crown ether-subunits

Although crown ethers are the subject of an immense amount of papers, conjugated polymers with crown ether subunits are scarce.[10] And yet, attachment of these groups to a conjugated polymer does not reduce the basic function, but endows new interesting properties to the conjugated polymer. There exist various reasons which make crown ether-functionalized conjugated polymers a worthwhile material to develop and to investigate.

A first motive which makes these polymers worth the effort is the promising application in light-emitting electrochemical cells (LECs). The prototype LEC contains an ionically conducting polyelectrolyte with appropriate cations (*e.g.* poly(ethylene oxide) and $LiCF_3SO_3$) to enhance the cell conductivity for electrochemical doping of an electroluminescent (EL) active conjugated polymer, which is mostly a PPV derivative.[11] Owing to the large difference in polarity between the polyelectrolyte and the conjugated polymer, the prototype LECs often show phase separation, leading to a slow response, high turn-on voltages and short device lifetime. In order to overcome these drawbacks, considerable research has focused on the synthesis of PPV derivatives bearing oligo(ethylene oxide) side chains with a view to minimize the phase separation by covalently bind polyelectrolyte side chains onto the EL polymer backbones.[12] Crown ether-substituted non-conjugated polymers coupled with appropriate cations as ionically conducting polyelectrolytes have already demonstrated sufficient ionic conductivities for certain applications.[13] Clearly, conjugated crown ether-functionalized PPV-type polymers are very promising candidates for application in LECs.

Furthermore, the substitution of crown ethers in conjugated polymers could form an interesting subject for a study of polymer chain packing morphology. Understanding and ultimately controlling interchain interactions in conjugated polymers remains a key challenge to optimize the efficiency of PPV polymers for use in EL devices. It is generally accepted that interchain interactions play an important role in the luminescence processes of conjugated polymers. In most cases PPV-type polymers show greatly reduced photoluminescent (PL) quantum efficiencies in solid state relative to those obtained in dilute solution. This reduced efficiency is believed to be due to the strong interchain interactions which provide a rapid non-radiative decay mechanism.[14] To reduce interchain interactions, macrocycles can be build in. Indeed, initial PL studies on macrocycle containing polymers in literature showed improved efficiencies.[15]

In addition to the gain of ionic conductivities and the favourable interchain interactions of crown ether-functionalized conjugated polymers, crown ether substitution may serve as a feature for chemical sensing. There is a need for ion sensors since the concentrations of group I and II ions are extensively measured in biological sciences and in health care field. Host-guest interaction between crown ether-functionalized conjugated polymer and a given cation may lead to modifications of the characteristic properties of the conjugated polymers, making these polymers possible candidates for sensor application.[16] Interesting ionochromic effects have indeed been obtained with some new crown ether-substituted polythiophenes (PT) in solution. Non-covalent interactions between crown ether-substituted PT and ions can modify the side-chain organization and then affect the conformation of the polymer backbone and its fluorescence intensity or absorption in the UV-Vis range.[17] Depending upon the nature of the side chains, ordering,[18] disordering[19] or aggregation[20] of these macromolecules can be induced through complexation with alkali metal ions. Besides changes in the UV-Vis absorption or fluorescence spectra, the ionochromic response of conjugated crown ether containing polymers to alkali metal ions in solution can be demonstrated by changes in conductivity. It is well known that twisting of the conjugated polymer's backbone from planarity can result in a conductivity

drop as high as 10^5 or greater.[21] Hence, conductivity changes in conjugated polymers provide a large dynamic range which, if harnessed effectively, can result in very sensitive sensory materials. Towards this goal, Swager *et al.* designed a conjugated crown ether-substituted PT that undergoes stimulus-induced conformational changes. Metal complexation of this crown ether-substituted PT forces a rotation of the thiophene rings in order to accommodate maximum chelation which reduces π-orbital overlap (Figure 4-4).[22] Ionochromic effects are measured in salt solutions and large shifts in λ_{max} with the appropriate ion are observed. Complexation of a specific ion induces the desired twist in the polymer's backbone which impedes intrachain carrier transport.[23] Further, since the shifts occur in the visible region, a dramatic colour change is observed.

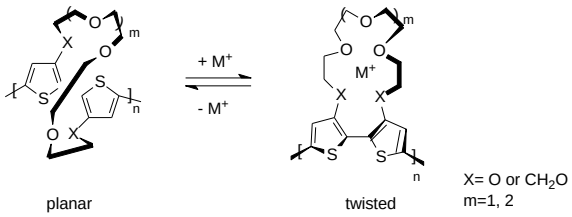

Figure 4-4 Conformational change of crown ether-substituted polythiophenes induced by the cation complexation

Recently, PPV derivatives with crown ether units in direct π-conjugation at the 2,3-position have attracted interest based on the electrical conductivity of the main chain and the cation-binding ability of the crown cavity (Figure 4-5).[24]

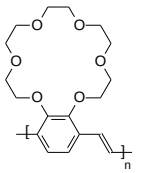

Figure 4-5 PPV derivative substituted with crown ether units at 2,3-position prepared in literature *via* a modified Gilch route

These *ortho*-crown ether substituted PPV-type polymers show unique self-assembling features attributed to the complexation with K^+ and are found to

form nanoribbons through supramolecular assembly with K^+ in dilute solution.[25] The binding of the metal ions in the crown ether rings make these macrocycles and the polymer backbone more rigid, favouring their π-stacking interactions with each other. Furthermore, fluorescence attenuation of this polymer is found upon K^+, Na^+ or Li^+ binding.

We set ourselves a target to prepare *p*-phenylene-20-crown-6 **9** and *p*-phenylene-23-crown-7 **11** (Figure 4-3) with the ultimate goal to synthesize tailored polymers containing crown ether units and sensing alkali metals ions (Figure 4-6). Since the macrocyclic ligands of *para*-substituted macrocyclic polyether PPV derivatives are in close proximity to the conjugated backbone, one may expect that the interactions between cations and the π–face of the aromatic structure during host-guest are 'recognized' by the polymer, leading to modifications of the characteristic properties of the conjugated polymer. Therefore, if the cationic complexation is efficient and rapid, these *para*-crown ether-substituted PPV derivatives could find use as novel polymer based sensor systems. In addition, this new class of PPV derivatives could form an interesting subject for a study of polymer chain packing morphology and shows interesting properties for application in LECs.

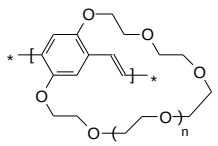

Figure 4-6 PPV derivatives containing *para*-substituted macrocyclic polyethers in the backbone (n= 1 or 2)

4.2 Synthesis and characterization of *p*-phenylene-20-crown-6 and *p*-phenylene-23-crown-7

The general method to prepare macrocyclic polyethers is the Williamson ether synthesis which involves the displacement of halide ions from a dihaloalkane by the dianion derived from a diol.[26] For the synthesis of the crown ethers **7 (n=1)** and **7 (n=2)**, dihydroquinone is used as the nucleophile

towards the bisbrominated ethylene glycols **6 (n=5)** and **6 (n=6)** (Scheme 4-3). **6 (n=5)** and **6 (n=6)** are prepared starting from the corresponding bistosylated compounds **5 (n=5)** and **5 (n=6)**, which are prepared according to a literature procedure (Scheme 4-3).[27] Since hexa(ethylene glycol) **4 (n=6)** is not commercially available, a highly selective synthesis for chain-extended monodisperse oligo(ethylene glycols) is used, starting from di(ethylene glycol) to obtain the α, ω-ditritylated hexa(ethylene glycol) **3**.[27] Deprotection occurs in methanol using acetyl chloride as a catalyst (Scheme 4-2).

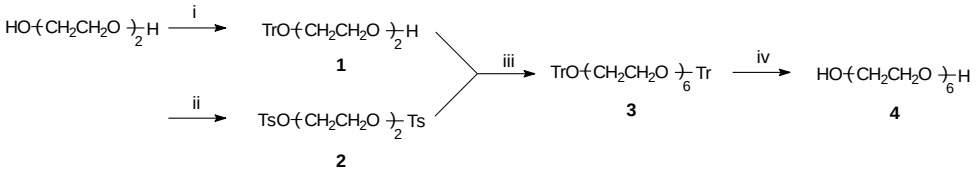

Scheme 4-2 Synthesis of hexa(ethylene glycol) **4** (i: TrCl, C_5H_5N; ii: TsCl, KOH, CH_2Cl_2; iii: NaH, THF; iv: CH_3COCl, MeOH)

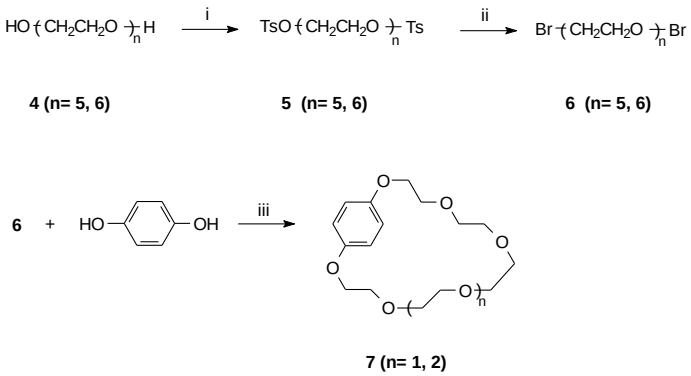

Scheme 4-3 Synthesis of the *p*-phenylene crown ethers **7 (n=1)** and **7 (n=2)** (i: TsCl, KOH, CH_2Cl_2; ii: LiBr, THF; iii: Cs_2CO_3, DMF)

Using the described procedure, *p*-phenylene-20-crown-6 **7 (n=1)** and *p*-phenylene-23-crown-7 **7 (n=2)** are prepared in yields high enough to be of synthetic value, *i.e.* 29 % for **7 (n=1)** and 16 % for **7 (n=2)**, contrary to the yields reported in literature which are at utmost 2.2 %.[8,9] Furthermore, the obtained macrocyclic crown ethers are of high purity. The purity of **7 (n=1)** and **7 (n=2)** is checked by mass spectroscopy and by ^1H and ^{13}C NMR spectroscopy

in CD_3OD and $CDCl_3$. Figure 4-7 shows the ^1H and ^{13}C NMR assignments of both compounds.

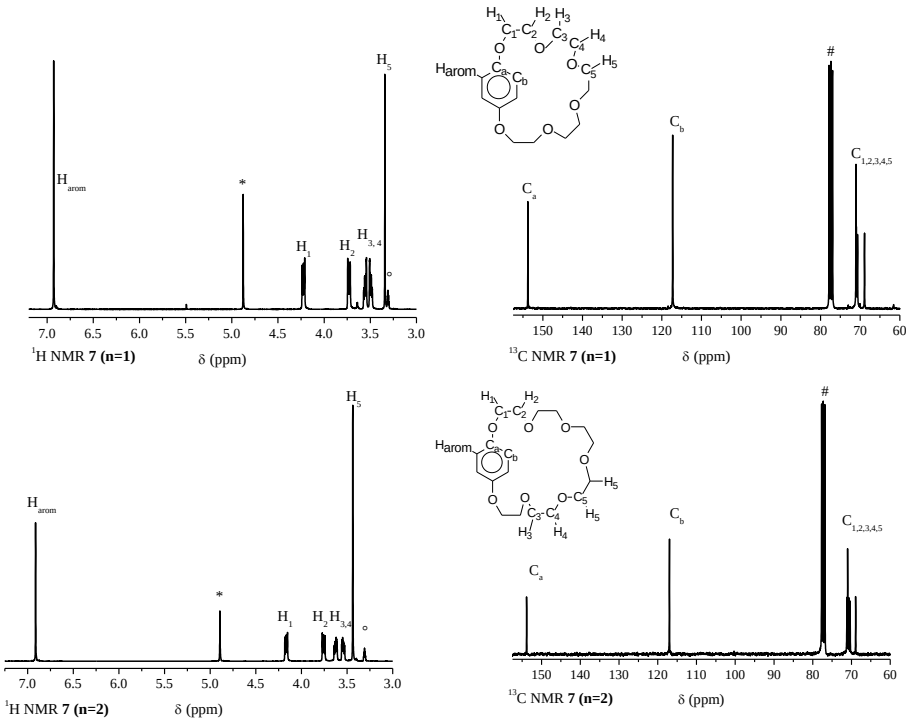

Figure 4-7 ^1H NMR spectra (recorded at 300 MHz) in CD_3OD and ^{13}C NMR spectra (recorded at 75 MHz) in $CDCl_3$ of **7 (n=1)** and **7 (n=2)** at RT. (°: Solvent residual peak CD_3OD: 3.31 ppm; *: D_2O peak: 4.79 ppm; #: $CDCl_3$: 77.16 ppm)[28] (Inset: Chemical structures of **7 (n=1)** and **7 (n=2)**)

4.3 Study of the host-guest complexation using NMR titration

- **Complexation studies**

Having achieved a considerable improvement in the synthesis of *para*-phenylene crown ethers, attention is now focused on the complexing ability of these compounds. When host (H) and guest (G) interact in solution forming a

complex (C), the stability constant (K) in equilibrium can be expressed as in equation **(2)**, where $[H]_0$ and $[G]_0$ are the analytical concentrations of respectively the crown ether host and the ionic guest and [C] is the equilibrium concentration of the crown ether : metal ion complex.

$$H + G \underset{k_{-1}}{\overset{k_1}{\rightleftharpoons}} C \qquad \textbf{(1)}$$

$$K = \frac{k_1}{k_{-1}} = \frac{[C]}{[H][G]} = \frac{[C]}{([H]_0-[C])([G]_0-[C])} \qquad \textbf{(2)}$$

Nuclear magnetic resonance (NMR) spectroscopy is one of the most useful techniques available to chemists for the investigation of dynamic molecular processes. The ^{1}H NMR titration method has been extensively employed to determine binding constants of complex formation in host-guest complexes.[29] The method involves the titration of the host until there is no significant change in the chemical shift of a monitored signal in successive NMR spectra. In early reports, one erroneous claimed that the study using NMR spectroscopy as detection technique for the determination of complexation constants requires the presence of protons either in the cation or in the anion of the salt.[30] However, to use NMR methods to study complexation phenomena, it is sufficient that at least one site in the uncomplexed host (or guest) molecule gives rise to a signal at chemical shift δ_H (δ_G) that is significant different from the same site in the complexed host (or guest) molecule δ_C.

Since it is well-known that the commercially available benzo-18-crown-6 (B18C6, Figure 4-11) cavity preferably accommodates potassium cations,[4] this cation is also used for the initial titration experiments of **7 (n=1)** and **7 (n=2)**. All ^{1}H NMR spectra are recorded in CD_3OD, which is chosen as solvent since all reactants are sufficiently soluble in this medium. By comparing the ^{1}H NMR spectra of the uncomplexed **7 (n=1)** with **7 (n=1)** in presence of K^+ (left-hand side of Figure 4-8), it becomes clear that the resonances of all the protons of **7 (n=1)** shift downfield ($\Delta\delta > 0$) upon addition of KSCN. The reason for the

observed downfield shifts upon complexation seems clear; the positive charge on the cation induces deshielding of the crown ethers protons. The downfield shift of the aromatic protons is mainly due to a decrease in the π-electron density of the benzene ring when complexed. The ^{1}H NMR titration of **7 (n=2)** with K^{+} (presented on the right-hand side of Figure 4-8) likewise shows a downfield shift upon complexation for the protons H_1, H_2, H_5 and H_{arom}. On the other hand, the progressive addition of K^{+} ions produces an upfield shift of the protons $H_{3,4}$. This conflicting behaviour cannot be directly related to the cation binding, since in that case the shift of all protons should have the same sign.[31] It shows that cation complexation by the macrocyclic cavity indirectly produces a modification of the electronic environment of the protons. This modification is presumably due to conformational changes of the oligo(ethylene oxide) loop upon complexation as a result of which $H_{3,4}$ is influenced by the anisotropic effect produced by the π-system of the aromatic ring.

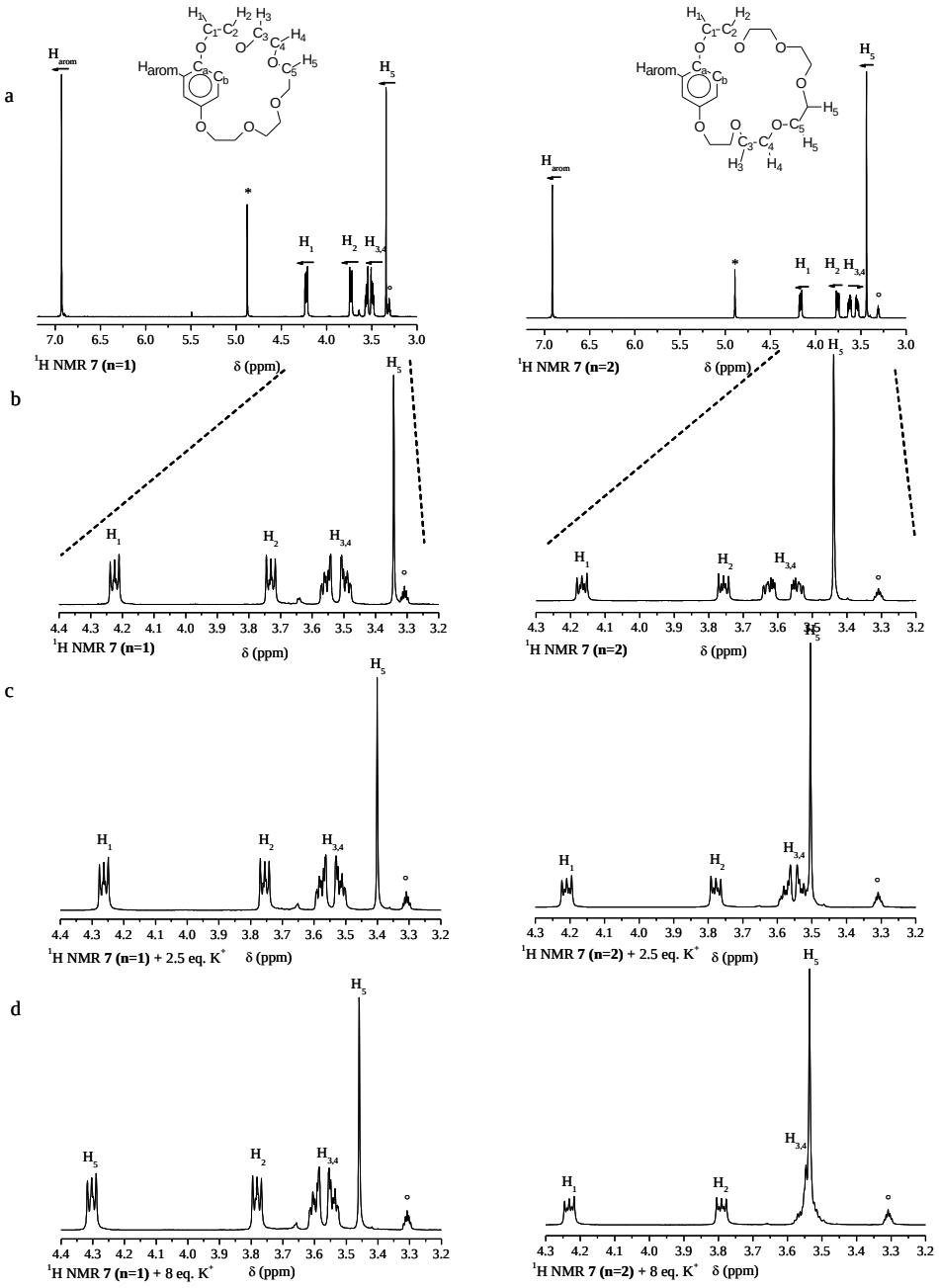

Figure 4-8 (a)-(b) ^{1}H NMR spectrum of **7 (n=1)** (left) and **7 (n=2)** (right) recorded at 300 MHz in CD_3OD at RT. The direction of the change in chemical shifts of the protons (← downfield, → upfield) in a ^{1}H NMR titration experiment with KSCN is shown. *(c)-(d)* The observed shifts of protons $H_{1\text{-}5}$ during complexation with KSCN. (°: Solvent residual peak CD_3OD: 3.31 ppm, *: D_2O peak: 4.79 ppm).[28]

▪ Evaluation of binding constants

In order to further understand the host-guest interactions involved in the complexes, an attempt is made to quantify them by using the gradual changes in the chemical shifts of **7 (n=1)** and **7 (n=2)** upon complexation to calculate the stability constants. In addition to the titration experiments of **7 (n=1)** and **7 (n=2)** with K^+ ions, the complexation of the two crown ethers with Na^+ and Rb^+ cationsis examined. The magnitude of $\Delta\delta_{lim}$ provides a measure for the complexation strength between the crown ether moiety and the particular cation in the solvent medium used. In fact, it is the curvature of the change in chemical shift *versus* molar host:guest ratio plot that reflects complex stability.[32] Figure 4-9 and Figure 4-10 show the NMR titration curves of **7 (n=1)** and **7 (n=2)** with the studied metal ions. Since a gradual downfield shift of the host proton resonances with increasing cation concentration is indicative for host-guest 1:1 complex formation,[33] it is likely that the type of complex formed between **7 (n=1)** and **7 (n=2)** and the metal ions is 1:1. However, this does not always indicate that the metal cation is located in the cavity of the polyether. The metal ion may have directed valencies which preclude bonding to all the oxygen atoms or it may be too large or too small to fit 'exactly' in the hole.[5] No attempts are made to investigate the exact nature and structure of the complexes. Figure 4-9 and Figure 4-10 show that the changes in chemical shift of **7 (n=1)** and **7 (n=2)** upon complexation with the different ions will only reach a limiting value at very high mole ratios of salt. This is indicative of the formation of weak complexes with low K values. The changes in the chemical shift of both crown ethers with the ion sodium cation are negligible, which implicates that **7 (n=1)** and **7 (n=2)** do not form complexes with Na^+ ions. Therefore, all further attention is focused on the complexation of **7 (n=1)** and **7 (n=2)** with the metal cations of potassium and rubidium.

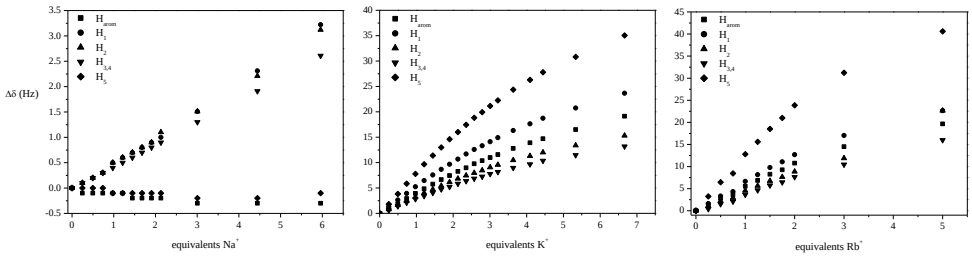

Figure 4-9 NMR titration curve of **7 (n=1)** with (from left to right**)** Na^+, K^+ and Rb^+

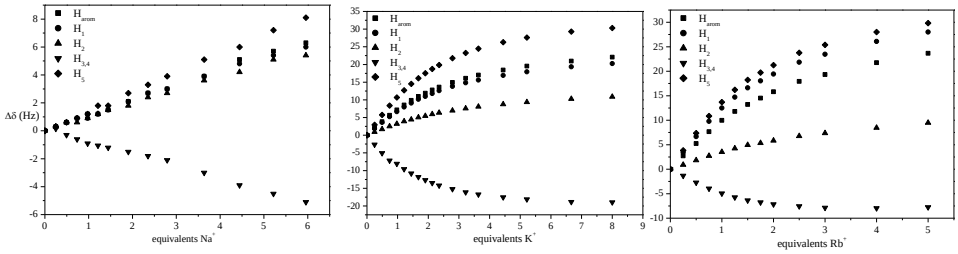

Figure 4-10 NMR titration curve of **7 (n=2)** with (from left to right**)** Na^+, K^+ and Rb^+

To produce evidence that the NMR titration method is carried out correctly, the exact same titration procedure is applied to the commercially available benzo-18-crown-6 (B18C6). The B18C6 : K^+ complex possess a high binding constant since the six oxygens of B18C6 are fully complementary in their locations to the K^+-ion.[3] Therefore, above equimolar cation : crown ether ratio no significant changes occur in the chemical shift. This behaviour is demonstrated in Figure 4-11; K^+-induced shifts are found only up to addition of 1 equivalent K^+. This corroborates the accuracy of the applied titration procedure.

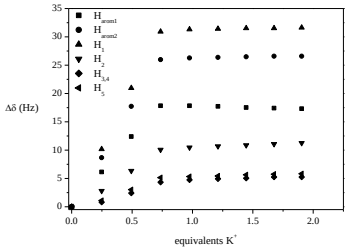

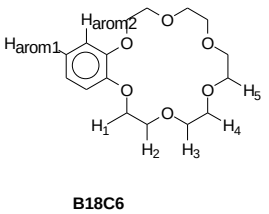

B18C6

Figure 4-11 NMR titration curve of **B18C6** with K^+

Via procedures[32,34,35] in which the value of the binding constant is fitted to minimize a function expressing the difference between calculated and observed chemical shift changes, binding constants for 1:1 complexes can been derived. It should be stipulated that, since cation complexation is based on weak non-covalent interactions, the choice of solvent medium, the type of counter anion as well as the temperature can profoundly affect complexation characteristics. The rate constants for complexation and decomplexation are often very large so that the observed chemical shift is the weighted average of the shifts δ_C and δ_H. Under these fast exchange conditions, the observed chemical shift can be rewritten as a complicated function of $[H]_0$, $[G]_0$, δ_H, δ_C and K:[35]

$$\delta_{obs} = \delta_H - \frac{(\Delta\delta)}{2}\,(b - \sqrt{b^2 - 4R})$$

where $\Delta\delta = \delta_H - \delta_C$

$R = [G]_0 / [H]_0$

$b = 1 + R + 1/(K[H]_0)$

This equation describes the complexation-induced shift of an NMR signal. The variation of δ with changing R forms the basis of the NMR titration technique for the determination of K values. However, the equation requires that both δ_H and δ_C are known. The former is easily determined by direct measurement in the absence of guest. The latter, on the other hand, cannot usually be determined directly since – as mentioned before- the rate constants for complexation and decomplexation are often very large, making it impossible to reach the slow-exchange limit. Furthermore, unless the value of K is substantially greater than 10, it is difficult to approach the δ_c limit at any readily attainable ratio of $[G]_0$ to $[H]_0$. So, we are left with two unknown parameters, δ_C and K. It is possible to use non linear curve fitting to iteratively determine the values of K and δ_C that best simulate an experimental set of δ_C *versus* R data.[36] The input includes the experimental values of δ_{obs} *versus* $[G]_0$ and $[H]_0$, along with the value of δ_H and an estimate of the value of K and δ_C. Table 4-1 lists the logarithmic values of the complexation constants estimated

by treatment of the data collected from the chemical shifts of H_1, H_5 and H_{arom} with the program MathCad. As expected, the binding constants of **7 (n=1)** and **7 (n=2)** with K^+ and Rb^+ are low, compared to the log K value for interaction of **B18C6** with K^+ in MeOH as determined spectrophotometric in literature as 5.27.[37] The log K of **B18C6** with K^+ estimated by treatment of the data collected from the NMR titration with the program MathCad, is found to be 3.89. This large difference with the value reported in literature reflects the limitations of the fitting program. Values of K greater than 5 lead to rapid 'saturation' of the host sites at relatively low ratios of $[G]_0$ to $[H]_0$ and consequent rapid changes in δ, which causes significant errors in the non linear iterative curve fitting and the derived K values.[35]

	Log K			
	7 (n=1):K^+	**7 (n=1):Rb^+**	**7 (n=2):K^+**	**7 (n=2):Rb^+**
H_5	0.172	0.591	0.881	1.127
H_1	0.147	0.360	0.800	1.071
H_{arom}	/	0.365	0.789	0.972
Average	0.16	0.44	0.82	1.06

Table 4-1 Log K estimated by treatment of the data collected from the changes in chemical shifts of H_1, H_5 and H_{arom} with changing R, using. MathCad for the non linear curve fitting

Although values of K cannot be determined accurately if log K is less than *circa* 1.5,[38] the values listed in Table 4-1 can be used to show the general trend. For spherical metal ions, such as K^+ and Rb^+, the optimum charge-shell should also have a spherical form. The insertion of the *p*-xylylene aromatic unit leads to a more pronounced spatial stretch of individual donor atom pairs and therefore to more unfavourable complexation. In other words, the rigid ligands **7 (n=1)** and **7 (n=2)** give definite and only slightly alterable coordination cavities. The small size of the cavity of **7(n=1)** is too tight and discomforting for inclusion of the host. The somewhat larger K value of **7(n=2)** with the metal ions suggests that the longer oligo(ethylene oxide) loop of **7(n=2)** allows more pronounced conformational changes and a somewhat better adaptation of the size and geometry of the macrocyclic cavity to the size of the metal cation.

4.4 PPV derivatives bearing *para*-substituted macrocyclic polyethers in the backbone

4.4.1 Monomer synthesis and characterization

p-Phenylene-20-crown-6 **7 (n=1)** and *p*-phenylene-23-crown-7 **7 (n=2)** are chloromethylated according to an adapted literature procedure[39] using concentrated HCl and formaldehyde in acetic anhydride. The mixture is allowed to react for 3.5 hours at 75 °C. After work-up and purification by column chromatography, pure 2,5-bischloromethyl-1,4-phenylene-20-crown-6 **8 (n=1)** and 2,5-bischloromethyl-1,4-phenylene-23-crown-7 **8 (n=2)** are obtained in respectively 62 % and 42 % yield (Scheme 4-4).

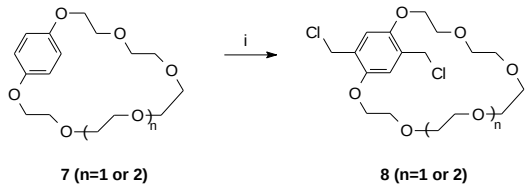

Scheme 4-4 Synthesis of the *p*-phenylene crown ether monomers **8 (n=1)** and **8 (n=2)** (i: *p*-CH_2O, Ac_2O, HCl)

Figure 4-12 shows the ^1H and ^{13}C NMR assignments of the Gilch monomer **8 (n=2)**. The spectra are very similar to the spectra of **7 (n=2)**, with an additional singulet, corresponding to the CH_2Cl protons in the ^1H spectrum and two extra peaks in the ^{13}C NMR spectrum, one in the aromatic region and one peak corresponding to the *C*H_2Cl carbons. On the other hand, the ^1H NMR spectrum of **7 (n=1)**, becomes much more complicated upon the chloromethylation reaction towards **8 (n=1)** (Figure 4-13). In all probability, the short, relatively non-flexible chains of the small cavity of **8 (n=1)** slows the rotation, as a result of which the different protons on each carbon will appear as separate signals. In contrast, the larger oligo(ethylene oxide) loop of **8 (n=2)** has a more flexible oligo(ethylene oxide) loop in which the protons undergo a faster exchange resulting in a much simpler ^1H NMR spectrum. To be able to

make the signal assignments in the solution ^{1}H NMR spectrum of **8 (n=1)**, the proton spectrum is correlated with the more unequivocal carbon spectrum using heteronuclear correlation (HETCOR) spectroscopy (Figure 4-14). A correlation is achieved between the easily assigned ^{13}C's and the protons to which they are directly attached. In this way, the more complicated ^{1}H spectrum of **8 (n=1)** is resolved and it is found that also **8 (n=1)** is obtained very pure.

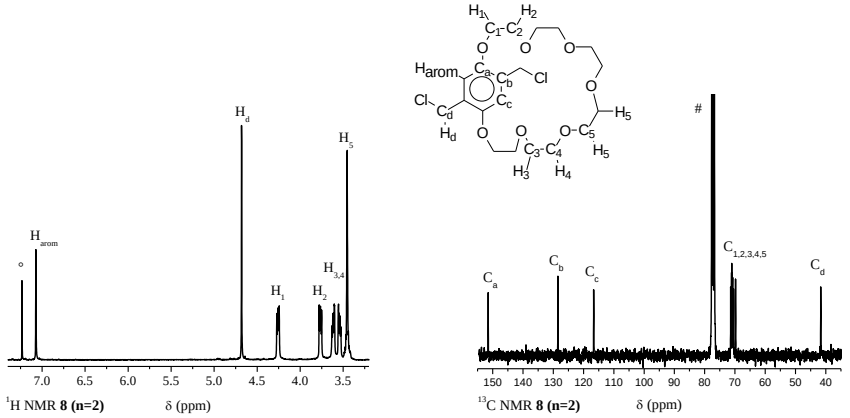

Figure 4-12 ^{1}H NMR spectrum (recorded at 300 MHz) and ^{13}C NMR spectrum (recorded at 75 MHz) of **8 (n=2)** in $CDCl_3$ at RT. (°: Solvent residual peak $CDCl_3$ in ^{1}H: 7.24 ppm; #: $CDCl_3$ in ^{13}C: 77.16 ppm)[28] (Inset: chemical structure of **8 (n=2)**)

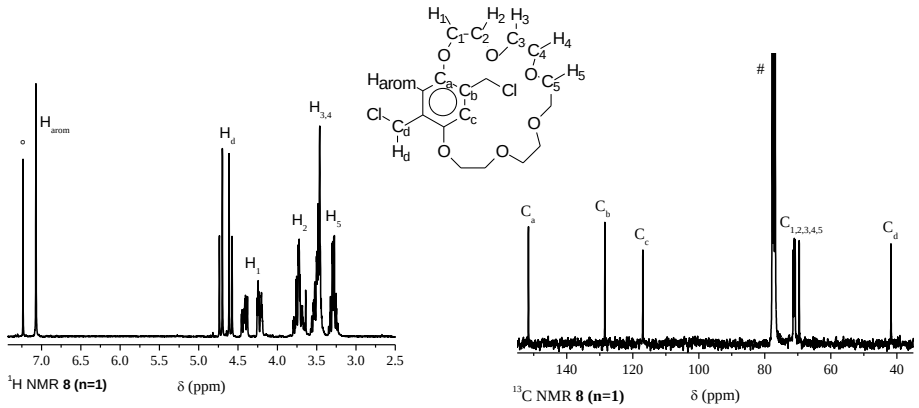

Figure 4-13 ^{1}H NMR spectrum (recorded at 300 MHz) and ^{13}C NMR spectrum (recorded at 75 MHz) of **8 (n=1)** in $CDCl_3$ at RT. (°: Solvent residual peak $CDCl_3$ in ^{1}H: 7.24 ppm; #: $CDCl_3$ in ^{13}C: 77.16 ppm)[28] (Inset: chemical structure of **8 (n=1)**)

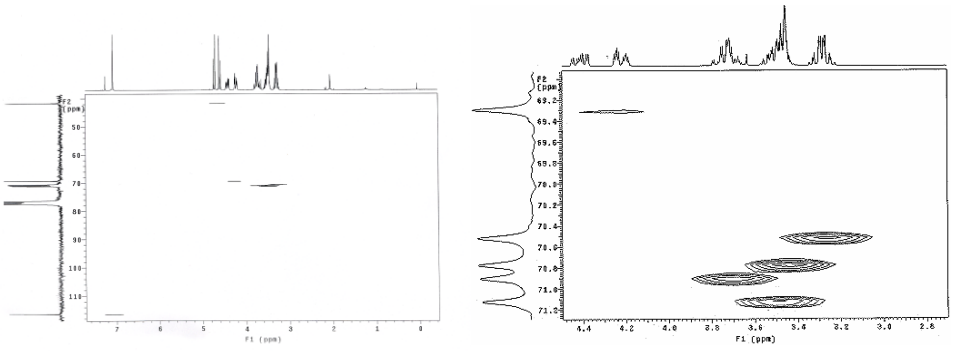

Figure 4-14 One bond optimized HETCOR spectrum of **8 (n=1)** in $CDCl_3$ at RT

4.4.2 Synthesis and characterization of PPV derivatives containing *para*-substituted crown ethers

Poly(*para*-(2,5-phenylene-23-crown-7) vinylene) **9 (n=1)** and poly(*para*-(2,5-phenylene-20-crown-6) vinylene) **9 (n=2)** are prepared according to the Gilch route **(**Scheme 4-5).[40] The *para*-crown ether monomers **8 (n=1)** and **8 (n=2)** are polymerized in dioxane at 98 °C using potassium *tert*-butoxide as the base. After precipitation in hexane and thoroughly washing with water, both conjugated polymers are obtained in moderated yields with considerable high molecular weights and low polydispersities (Table 4-2).

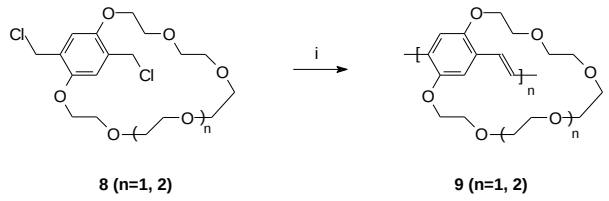

Scheme 4-5 Gilch polymerization of the *p*-phenylene crown ether monomers **8 (n=1)** and **8 (n=2)** towards the conjugated polymers **9 (n=1)** and **9 (n=2)** (i: K*t*BuO, 1,4-dioxane)

Polymer	Yield (%)	M_w (g/mol)	PD
9 (n=1)	54	210000	2.3
9 (n=2)	65	80000	2.0

Table 4-2 Polymerization results of **9 (n=1)** and **9(n=2).** Analytical SEC measurements are performed in DMF *versus* polystyrene standards

Poly(*p*-(2,5-phenylene-20-crown-6) vinylene) **9 (n=1)** as well as poly(*p*-(2,5-phenylene-23-crown-7) vinylene) **9 (n=2)** are soluble in the polar, aprotic solvents DMSO and DMF and to some extent in $CHCl_3$. The conjugated polymers **9 (n=1)** and **9(n=2)** are characterized using ^1H and ^{13}C NMR spectroscopy (*cf.* experimental section), as well as UV-Vis and fluorescence spectroscopy. UV-Vis spectra of the conjugated polymers **9 (n=1)** and **9(n=2)** are taken at room temperature in $CHCl_3$ and as thin film. The crown ether-substituted PPV-type polymers exhibit in the UV-Vis absorption spectrum a distinct absorption associated with the π–π^* transition, both in a thin film ($\lambda_{a,\ max}$= 486 nm for both **9 (n=1)** and **9 (n=2)**) and in solution ($\lambda_{a,\ max}$= 469 nm for **9 (n=1)** and $\lambda_{a,\ max}$= 480 nm for **9 (n=2)**) (Figure 4-15). These values are blue shifted compared to the values obtained for BTEM-PPV, *i.e.* the PPV derivative containing two oligo(ethylene oxide) side chains prepared in chapter 2 ($\lambda_{a,max}$= 489 nm in $CHCl_3$ and $\lambda_{a,max}$= 509 nm as thin film). This shift is likely due to defects caused during the Gilch polymerization reaction.

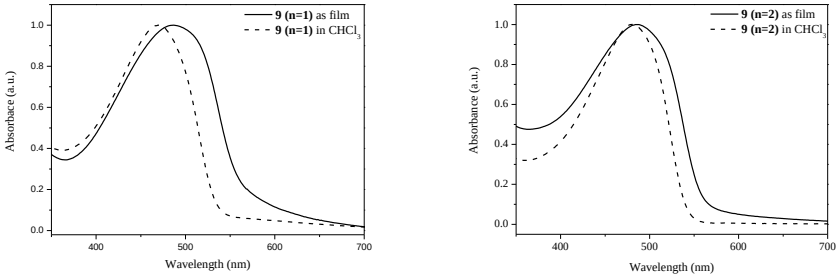

Figure 4-15 UV-Vis absorption spectra of **9 (n=1)** and **9 (n=2)** in $CHCl_3$ and as film

The crown ether-functionalized polymers are also studied using fluorescence spectroscopy. In $CHCl_3$ solution, for polymers **9 (n=1)** and **9 (n=2)**, a distinct emission is found at λ_{em} = 533 nm and 537 nm, respectively

(excitation wavelength λ_{exc}= 469 nm and λ_{exc}= 480 nm respectively) (Figure 4-16). Furthermore, the room temperature photoluminescence excitation (PLE) spectra of a $CHCl_3$-solution of **9 (n=1)** and **9 (n=2)** exhibit distinct transitions at λ_{em} = 470 nm and 473 nm respectively (emission wavelength λ_{exc} = 533 nm and 537 nm respectively) (Figure 4-16). These observations indicate that fluorescence properties of the two *para*-crown ether PPV-type polymers are similar to each other and comparable to the fluorescence characteristics of *e.g.* BTEM-PPV, for which a distinct emission is found at λ_{em} = 543 nm in $CHCl_3$ solution (excitation wavelength λ_{exc}= 485 nm).

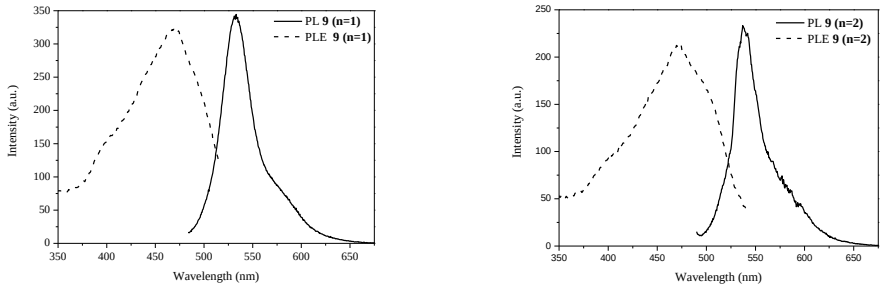

Figure 4-16 PL and PLE spectra in $CHCl_3$ of **9 (n=1)** and **9 (n=2)**

4.4.3 Complexation of crown ether-substituted PPV derivatives with metal ions

After the successful optimization of the synthesis of *p*-phenylene-20-crown-6, the preparation of the hitherto unreported *p*-phenylene-23-crown-7, the complexation study of these two crown ethers and the polymerization towards the first PPV derivatives containing *para*-phenylene crown ethers, the last point at issue is the examination of the effects of metal cation binding on the absorbance and fluorescence spectra of the conjugated crown ether containing polymers in solution. To that end, UV-Vis as well as PL and PLE spectra in $CHCl_3$ after addition of an excess of metal ions (Na^+, K^+ and Rb^+) are taken and compared to the spectra of **9 (n=1)** and **9 (n=2)** before addition. It is found that the UV-Vis absorbance spectra of **9 (n=1)** and **9 (n=2)** are indifferent to the addition of metal cations. This is illustrated for the addition of rubidium cations to a $CHCl_3$ solution of **9 (n=2)** in Figure 4-17.

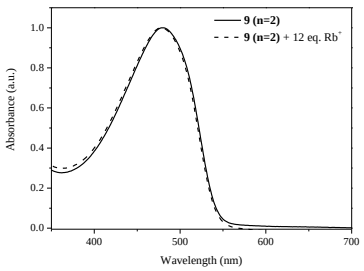

Figure 4-17 UV-Vis absorption spectra of **9 (n=2)** in $CHCl_3$ before and after addition of Rb^+ ions

Similar observations have been made in literature for the conjugated *ortho*-substituted crown ether PPV derivative (Figure 4-5), which also displays unchanged absorbance spectra in the presence of K^+, Na^+ and Li^+ relative to the maximum absorbance band in the absence of metal ions.[24] However, the report on the *ortho*-substituted crown ether PPV derivative describes how the fluorescence intensity decreases as the molar ratio of K^+, Na^+ or Li^+ increases. The emission is dramatically reduced to near background level when the molar ratio of K^+ to the *ortho*-crown ether unit is 6. This fluorescence attenuation is attributed to electron-transfer from the excited polymer to the analyte K^+. At the same time, the appearance of a second maximum emission is described, which is attributed to the formation of excimers.[41] In the case of the fluorescence spectra of the PPV derivatives substituted with crown ether units at the 2,5-position, the reduction of the emission upon addition of metal ions is only moderate, even when a very large excess of metal ions is added, *e.g.* the emission of **9 (n=1)** and **9 (n=2)** is only reduced for 17 % and for 35 % respectively after addition of 12 equivalents rubidium cations (Figure 4-18 and Figure 4-19). Furthermore, no excimer formation is observed.

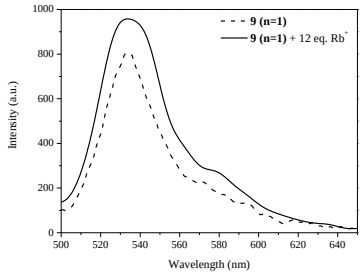

Figure 4-18 PL spectra of **9 (n=1)** in $CHCl_3$ after addition of Rb^+ ions

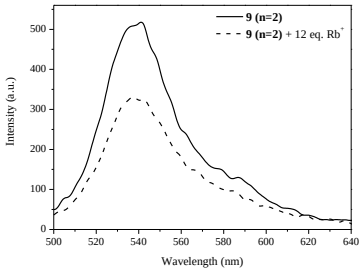

Figure 4-19 PL spectra of **9 (n=2)** in $CHCl_3$ after addition of Rb^+ ions

The limited attenuation of fluorescence and the lack of excimer formation of **9 (n=1)** and **9 (n=2)** upon exposure to metal ions is probably due to the low complexation ability of these crown ether PPV derivatives. However, another possible cause can not be ruled out yet. The limited changes of the fluorescence spectra of the crown ether PPV derivatives upon complexation may be (partially) attributed to the fact that the *para*-substituted macrocyclic polyethers already captured the potassium ions of the base used in the polymerization reaction. Although the conjugated polymers are thoroughly washed with water after filtration in order to remove the ions, it is conceivable that the crown ethers in **9 (n=1)** and **9 (n=2)** are still complexed with potassium cations. If this is the case, it is obvious that addition of more and different ions has a reduced effect on the characteristic properties of the polymer. An interesting remark made by the authors of the *ortho*-derivative of **9** corroborates this assumption.[41] They mention how the solvent used in the polymerization is an important factor for the solubility of the resultant polymers. When THF, dioxane and xylene or a mixture of xylene and *tert*-butanol are used, the *ortho*-crown ether substituted PPV derivatives obtained, exhibits very poor solubility in common organic solvents. However, when DMF is used as the solvent during polymerization, the obtained 2,3-crown ether containing PPV polymer is soluble in $CHCl_3$. In the case of the *para*-substituted crown ether PPV-type polymers, dioxane is used as the solvent and the resulting polymers have a limited solubility. The solubility characteristics may be attributed to the extent of complexation with

metal ions (K^+) during polymerization. Since potassium cations have a poor solubility in dioxane compared to the solubility in DMF, it is likely that the crown ether complexation occurs more readily during polymerization in dioxane. This implicates that the *para*-substituted macrocyclic polyethers may have captured already K^+ cations during polymerization and therefore are less sensitive to further addition of metal ions. Further examination is necessary to confirm these statements.

4.5 Conclusions

The synthesis of two neutral crown ethers containing *para*-phenylene units was optimized, so that the products were isolated in yields high enough to be of synthetic value *i.e.* 29 % for **7 (n=1)** and 16 % for **7 (n=2)**. The ability of these *para*-substituted polyethers to form complexes with the alkali metal ions Na^+, K^+ and Rb^+ ions was investigated by ^1H NMR spectroscopic titrations. Low complexation constants were found. The crown ethers were then further functionalized and polymerized. The resulting *para*-substituted crown ether PPV-type polymers only showed moderate reduction of emission upon addition of metal cations. Further studies are necessary to find out if this limited attenuation is due to the premature complexation of the macrocycles during polymerization or a result of the low complexation constants.

4.6 Experimental Section

Chemical and optical characterization

NMR spectra were recorded with a Varian Inova Spectrometer at 300 MHz using a 5 mm probe for ^1H NMR and at 75 MHz using a 5 mm broadband probe for ^{13}C NMR. GC-MS data were obtained with a Varian TSQ 3400 Gas Chromatograph and a TSQ 700 Finnigan Mat mass spectrometer. Analytical Size Exclusion Chromatography (SEC) was performed using a Spectra series P100 (Spectra Physics) pump equipped with a pre-column (5 μm, 50 mm*7.5

mm, guard, Polymer Labs) and two mixed-B columns (10 μm, 2x300 mm*7.5 mm, Polymer Labs) and a Refractive Index (RI) detector (Shodex) at 40°C. DMF was used as eluent at a flow rate of 1.0 mL/min. Molecular weight distributions are given relative to polystyrene standards. GC-MS data were obtained with a Varian TSQ 3400 Gas Chromatograph and a TSQ 700 Finnigan Mat mass spectrometer. FT-IR spectra were collected with a Perkin Elmer Spectrum One FT-IR spectrometer (nominal resolution 4 cm-1, summation of 16 scans). Fluorescence spectra were obtained with a Perkin Elmer LS-5B luminescence spectrometer. UV-Vis measurements were performed on a Cary 500 UV-Vis-NIR spectrophotometer (scan rate 600 nm/min, continuous run from 200 to 800 nm).

Experimental procedure for NMR titration

All ^{1}H NMR titration experiments were recorded on a Varian Inova Spectrometer at 300 MHz using a 5 mm probe in CD_3OD at room temperature. The spectrum of a sample containing a known amount (1 eq., in the order of 0.05 mmol) of the host **7 (n=1, 2)** in 800 μL CD_3OD was recorded. To this sample, *circa* 0.25 eq. of the guest in 7.5 μL CD_3OD was added and the spectrum was recorded again. The process was repeated. Typically eight to fourteen spectra were recorded for each host. ^{1}H NMR titration experiments of the host **7 (n=1, 2)** were performed with KSCN, NaSCN and RbI. RbI was added as a solid. As a reference, the ^{1}H NMR titration experiments were also performed for B18C6 with KSCN in CD_3OD. The Δδ values were calculated by subtracting the chemical shift of the mixture host-guest from that of the pure host. The titration curve of the Δδ *vs.* the guest to host ratio was plotted.

Chemicals

All chemicals were purchased from Aldrich or Acros and used without further purification. Dioxane and THF were distilled from sodium/benzophenone. The crown ether benzo-18-crown-6 (B18C6) was commercially available (Acros) and used without further purification.

Synthesis

2-(2-trityloxy-ethoxy)ethanol 1. A three-necked flask equipped with mechanical stirrer, thermometer and N_2-inlet, was charged with diethylene glycol (1061.2 g, 10.0 mol) and pyridine (118.6 g, 1.5 mol). The solution was heated at 45°C and triphenylmethylchloride (278.8 g, 1.0 mol) was added under vigorous stirring. After additional stirring for 16 h, the reaction mixture, which contained white precipitate, was extracted with toluene at 40°C. The combined toluene extract was concentrated under reduced pressure. The solid residue was dissolved in boiling CH_2Cl_2 (500 mL) from which the desired product crystallized upon slowly cooling to -15 °C. The crude product is filtrated and recrystallized by dissolving it in boiling EtOAc, followed by addition of n-hexane and slowly cooling to -15 °C (1 g of **1**: 2 mL EtOAc/ 1mL hexane). A white crystalline solid was obtained in 73% yield. T_m= 113 °C. ^{1}H NMR ($CDCl_3$): δ = 7.45 (d, 6H), 7.26 (m, 9H), 3.73 (t, 2H), 3.67 (t, 2H), 3.60 (t, 2H), 3.25 (t, 2H). Mass (GC-MS, EI): 348 $[M+1]^+$, 271 $[M+1]^+$- C_6H_5, 259 $[M+1]^+$- $C_4H_9O_2$, 243 $[M+1]^+$- $C_4H_9O_3$, 165 $[M+1]^+$- $C_4H_9O_3$- C_6H_5, 105 $[M+1]^+$- 3x C_6H_5, 77 C_6H_5.

1,5-Bis(tosyloxy)-3-oxapentane 2. A three-necked flask equipped with mechanical stirrer, thermometer and N_2-inlet, was charged with *Bis*(2-hydroxyethyl)ether (53.1 g, 0.5 mol), *p*-toluenesulfonyl chloride (194.5 g, 1.02 mol) and CH_2Cl_2 (500 mL). The homogeneous mixture was cooled with a $CO_{2(s)}$-acetone bath. Freshly powdered KOH (224.4 g, 4.0 mol) was added in small amounts under vigorous stirring while maintaining the reaction mixture below 5 °C (exothermic reaction). The mixture was stirred for 3 h at 0 °C after which CH_2Cl_2 (500 mL) and ice-water (600 mL) were added. The organic phase was separated and the aqueous phase was extracted with CH_2Cl_2 (2 x 150 mL). The combined organic layer was washed with water (100 mL), dried ($MgSO_4$) and concentrated under reduced pressure. The pure product was obtained as a white crystalline solid in 98% yield. ^{1}H NMR ($CDCl_3$): δ = 7.76 (d, 4H), 7.34 (d, 4H), 4.07 (t, 4H), 3.59 (t, 4H), 2.43 (s, 6H).

1,1,1,21,21,21-hexaphenyl-2,5,8,11,14,17,20-heptaoxaheneicosane 3. A 3-L one-necked flask equipped with a N_2-inlet was charged with NaH (18.0 g,

0.75 mol) and dry THF (1200 mL). Subsequently **1** (155.0 g, 0.6 mol) was added to the magnetically stirred suspension. After stirring for 24 h, the reaction vessel was cooled to 0 °C in an ice-bath and **2** (124.3 g, 0.3 mol) dissolved in THF (1200 mL) was added drop wise over a period of 1 h. The reaction mixture was stirred for an additional 96 h. Then the solvent was removed under reduced pressure, dry CH_2Cl_2 (600 mL) was added, and the reaction mixture was poured into a stirred mixture of CH_2Cl_2 (600 mL) and ice-water (1200 mL). The organic phase was separated, and the aqueous layer is extracted with water (3 x 300 mL). The combined organic phase was washed with water (2 x 150 mL), dried ($MgSO_4$), and concentrated under reduced pressure to obtain **3** as a clear viscous oil in 96 % yield. ^{1}H NMR ($CDCl_3$): δ = 7.45 (d, 12H), 7.24 (m, 18H), 3.64 (m, 20H), 3.21 (t, 4H).

2-(2-(2-(2-(2-(2-hydroxy-ethoxy)-ethoxy)-ethoxy)-ethoxy)-ethoxy)-ethanol 4 (n=6). To a solution of **3** (50.0 g, 0.065 mol) in MeOH (250 mL), acetyl chloride (10 drops) was added as a catalyst. The mixture was cooled down to -15 ^{o}C and the progress of the reaction was followed by TLC in a $CHCl_3$-aceton (10:1) system. As soon as the starting material was consumed (*circa* 2 days), the reaction mixture was filtered off to remove the side products. After concentration under reduced pressure, **4** was obtained as a clear colourless oil in 98% yield. ^{1}H NMR ($CDCl_3$): δ = 3.70 (t, 4H), 3.65 (s, 16H), 3.58 (t, 4H), 2.96 (s, 2H).

1,14-Bis(tosyloxy)-3,6,9,12-tetraoxatetradecaan 5 (n=5) and **1,17-bis(tosyloxy)-3,6,9,12,15-pentaoxaheptadecaan 5 (n=6)** were prepared according to the same procedure as described for **2** with **4 (n=5)** and **4 (n=6)** as the respectively ethylene glycols. **5** was obtained as a yellow viscous oil in high yields (> 98%). ^{1}H NMR (300 MHz, $CDCl_3$) of **5 (n=5):** δ = 7.75 (d, 4H), 7.31 (d, 4H), 4.12 (t, 4H), 3.65 (t, 4H), 3.57 (m, 12H), 2.41 (s, 6H). ^{1}H NMR ($CDCl_3$) of **5 (n=6):** δ = 7.75 (d, 4H), 7.31 (d, 4H), 4.12 (t, 4H), 3.65 (t, 4H), 3.57 (m, 16H), 2.41 (s, 6H).

1,14-dibromo-3,6,9,12-tetraoxatetradecaan 6 (n=5) and 1,17-dibromo-3,6,9,12,15-pentaoxaheptadecaan 6 (n=6). A three-necked flask, equipped with a mechanical stirrer, reflux cooler and thermometer, was charged with **5 (n= 5)** (25.0 g, 45.8 mmol) or **5 (n= 6)** (27.0 g, 45.8 mmol) and freshly distilled

THF (85 mL). Under vigorous stirring a solution of lithium bromide (8.6 g, 98.9 mmol) in dry THF (85 mL) was added to the solution. A white suspension was obtained which was stirred at 50 °C for six days. Filtration of the reaction mixture gave a light-brown filtrate, which was concentrated under reduced pressure. Extraction of the crude product with toluene (150 mL) followed by filtration and concentration yielded the corresponding dibromide as a yellow oil in high yields (95% for **6 (n=5)** and 92% of **6 (n=6)**). ^{1}H NMR ($CDCl_3$) of **6 (n=5)**: δ = 3.79 (t, 4H), 3.65 (s, 16H), 3.46 (t, 4H); ^{1}H NMR ($CDCl_3$) of **6 (n=6)**: δ = 3.79 (t, 4H), 3.65 (s, 12H), 3.46 (t, 4H).

***p*-phenylene-20-crown-6 7 (n=1).** A mixture of the dibromide **6 (n=5)** (34.2 g, 94.0 mmol) and *p*-hydroquinone (10.3 g, 94.0 mmol) in DMF (700 mL) was added drop wise over a period of 6 days to a white suspension of cesium carbonate (91.8 g, 281.8 mmol) in DMF (700 mL) at 65 °C. After a few hours, the reaction mixture turned brown. Stirring was continued for another six days at 65 °C. After cooling to room temperature DMF was removed under reduced pressure and CH_2Cl_2 (400 mL) was added. Subsequently, the suspension was filtered over Celite® 512 and the brown residue was thoroughly washed with CH_2Cl_2 (3 x 200 mL). The combined filtrate was washed with water (3 x 300 mL), dried upon $MgSO_4$ and concentrated under reduced pressure to yield crude 7 (n=1) as a brown, viscous oil. The crude product was purified by *Kugelrohr* distillation (195 °C; 0.05 mbar) to give 8.4 g (29%) of **7 (n=1)** as a colourless oil. ^{1}H NMR (CD_3OD): δ = 6.93 (s, 4H), 4.23 (t, 4H), 3.74 (t, 4H), 3.53 (m, 8H), 3.37 (s, 4H); ^{13}C NMR ($CDCl_3$): δ= 153.0 (2C), 116.7 (4C), 70.7 (2C), 70.6 (2C), 70.3 (2C), 68.5 (2C); Mass (GC-MS, EI): 312 $[M+1]^+$, 268 $[M+1]^+$-C_2H_4O, 226 $[M+1]^+$-$C_4H_8O_2$.

***p*-phenylene-23-crown-7 7 (n=2)**. **7 (n=2)** was prepared according to the same procedure as described for 7 (n=1) with **6 (n=6)** as the dibromide. After *Kugelrohr* distillation (211°C; 0.05 mbar) and column purification (SiO_2, eluent diethylether /MeOH 9/1), **7 (n=2)** was obtained as a colourless oil in a yield of 16%. ^{1}H NMR (CD_3OD): δ = 6.81 (s, 4H), 4.16 (t, 4H), 3.76 (t, 4H), 3.61 (m, 4H), 3.56 (m, 4H), 3.46 (s, 8H); ^{13}C NMR ($CDCl_3$): δ= 153.1 (2C), 116.4 (4C), 70.8 (2C), 70.6 (4C), 70.3 (2C), 70.0 (2C), 68.6 (2C); Mass (GC-

MS, EI): 356 $[M+1]^+$, 312 $[M+1]^+$-C_2H_4O, 268 $[M+1]^+$-$C_4H_8O_2$, 180 $[M+1]^+$-$C_8H_{16}O_4$.

Monomers

2,5-Bischloromethyl-1,4-phenylene-20-crown-6 8 (n=1). To a stirred mixture of **7 (n=1)** (4.0 g, 12.8 mmol) and *p*-formaldehyde (1.06 g, 35.2 mmol), concentrated HCl (6.8 mL) was added drop wise under N_2 atmosphere. Subsequently, acetic anhydride (12.1 mL) was added at such a rate that the temperature did not exceed 70°C. After the addition was complete, the resulting solution was stirred at 75°C for 3.5 h after which it was cooled down to room temperature and poured into water (100 mL). The product was extracted with CH_2Cl_2 (3 x 75 mL). The organic extracts were combined and the solvent was evaporated to give the crude product, which was purified by column chromatography. **8 (n=1)** was obtained as a yellow solid in 62% yield (3.2 g). (SiO_2, eluent hexane/ EtOAc 6/4). ^{1}H NMR ($CDCl_3$): δ = 7.07 (s, 2H), 4.74+ 4.70+ 4.62+ 4.58 (dd, 4H), 4.41 (m, 2H), 4.25+ 4.20 (dt, 2H), 3.73 (m, 4H), 3.48 (m, 8H), 3.29 (m, 4H); ^{13}C NMR ($CDCl_3$): δ= 150.9 (2C), 127.9 (2C), 116.4 (2C), 71.1 (2C), 70.9 (2C), 70.8 (2C), 70.5 (2C), 69.3 (2C), 41.6 (2C); Mass (GC-MS, EI): 408 $[M^+]$, 372 $[M^+]$-Cl, 336 $[M^+]$-2Cl.

2,5-Bis-chloromethyl-1,4-phenylene-23-crown-7 8 (n=2). With **7 (n=2)** as reagent (1.0 g, 2.85 mol) and using the same procedure as for **8 (n=1)**, **8 (n=2)** was obtained after column chromatography (SiO_2, eluent diethylether/MeOH 97/3) as an oil (556 mg, 42% yield). ^{1}H NMR ($CDCl_3$): δ = 7.08 (s, 2H), 4.68 (s, 4H), 4.26 (t, 4H), 3.77 (t, 4H), 3.61+3.56 (dt, 8H), 3.48 (m, 8H); ^{13}C NMR ($CDCl_3$): δ= 150.7 (2C), 127.8 (2C), 116.1 (2C), 71.0 (2C), 70.8 (2C), 70.7 (2C), 70.4 (2C), 70.1 (2C), 69.4 (2C), 41.5 (2C); Mass (GC-MS, EI): 452 $[M^+]$, 417 $[M^+]$-Cl, 382 $[M^+]$-2Cl.

Polymers

Poly(*para*-(2,5-phenylene-20-crown-6) vinylene) 9 (n=1). In a three-necked round-bottom flask fitted with a reflux condenser and a septum, monomer **8 (n=1)** (1.44 g, 3.52 mmol) was dissolved in dry dioxane (220 mL) and flushed with N_2 for 15 min. Afterwards, a balloon filled with Ar was

placed on top of the condenser. After heating to 98 °C, a solution of K*t*BuO (1.02 g, 915.2 mmol) in 10 mL dry dioxane was added. During this addition, the solution turned from colourless to orange. After 5 min., a second solution of K*t*BuO (0.79 g, 7.04 mmol) in 7.5 mL dry dioxane was added and the solution coloured dark-orange. After stirring for 2 h at 98 °C, the solution was cooled down to 50 °C and neutralized with acetic acid. The total volume was reduced to 10 mL by evaporation, and the polymer was precipitated in hexane. A nice red precipitation was formed and thoroughly washed with water. After drying overnight in a desiccator, 639 mg (54%) of **9 (n=1)** was obtained. SEC (DMF) $M_w = 21\times10^4$ g/mol (PD = M_w/M_n = 2.3); UV-Vis $\lambda_{a,max}$= 478 nm ($CHCl_3$) and $\lambda_{a,max}$= 490 nm (as a film) ^{1}H NMR ($CDCl_3$): δ= 7.3 (2H), 6.5 (2H), 4.2 (4H), 3.8 (4H), 3.5 (8H), 3.3 (4H); ^{13}C NMR (deuterated-DMSO): δ= 150.8 (2C), 127.8 (2C), 123.9 (2C), 112.1 (2C), 70.0 (6C), 68.4 (4C); FT-IR (NaCl, cm^{-1}): 2864, 1599, 1498, 1455, 1350, 1248, 1192, 1113, 1056, 974, 931, 751; Photoluminescence emission (PL) $\lambda_{em,\ max}$= 533 nm (λ_{exc}= 478 nm, $CHCl_3$); Photoluminescence excitation (PLE) $\lambda_{ex,\ max}$= 468 nm (λ_{em}= 533 nm; $CHCl_3$).

Poly(*para*-(2,5-phenylene-23-crown-7) vinylene) 9 (n=2). 9 (n=2) was prepared according to the standard Gilch procedure as described for **9 (n=1)**, using **8 (n=2)** (394.3 mg, 0.86 mmol) as the monomer. **9 (n=2)** was obtained as a red solid in a yield of 65 %. SEC (DMF) $M_w = 8\times10^4$ g/mol (PD = M_w/M_n = 2.0); UV-Vis $\lambda_{a,max}$= 480 nm ($CHCl_3$) and $\lambda_{a,max}$= 485 nm (as a film) ^{1}H NMR ($CDCl_3$): δ= 7.5 (2H), 6.5 (2H), 4.2 (4H), 3.9 (8H), 3.5 (8H); ^{13}C NMR (deuterated-DMSO): δ= 151.9 (2C), 127.3 (2C), 120.3 (2C), 111.5 (2C), 69.8 (12C); FT-IR (NaCl, cm^{-1}): 2929, 2858, 1619, 1500, 1457, 1417, 1352, 1253, 1200, 1115, 1063, 943; Photoluminescence emission (PL) $\lambda_{em,\ max}$= 537 nm (λ_{exc}= 480 nm, $CHCl_3$); Photoluminescence excitation (PLE) $\lambda_{ex,\ max}$= 473 nm (λ_{em}= 537 nm; $CHCl_3$).

4.7 References

[1] Pedersen, C. J. *J. Amer. Chem. Soc*., **1967**, *89 (10)*, 2495 -2496.

[2] Pedersen, C. J. *Aldrichim. Acta*, **1971**, *4 (1)*, 1-7.

[3] Lehn, J.M. *Science*, **1993**, *260*, 1762.

[4] Christensen, J. J.; Hill J. O.; Izatt, R. M. *Science* **1971**, *174*, 459-467.

[5] Christensen, J. J.; Eatough D. J.; Izatt, R. M. *Chem. Rev.* **1974**, *74*, 351-384.

[6] a) Pedersen, C. J. *J. Amer. Chem. Soc*., **1967**, *89 (26)*, 7017 -7036. b) Pedersen, C. J. *J. Amer. Chem. Soc*., **1970**, *92 (2)*, 391-394.

[7] a) Reinhoudt, D. N.; Gray, R. T. *Tetrahedron Letters*, **1975**, *25*, 2105-2109. b) Koenig, K. E.; Helgeson, R. C.; Cram, D. J. *J. Amer. Chem. Soc*., **1976**, *98 (13)*, 4018-4020. c) Moore, S. S.; Tarnowski, T. L.; Newcomb, M.; Cram, D. J. *J. Amer. Chem. Soc*., **1977**, *99 (19)*, 6398-6410.

[8] a) Helgeson, R. C.; Tarnowski, I. L.; Timko, J. M.; Cram, D. J. *J. Amer. Chem. Soc*., 1977, *99 (19)*, 6411-6418. b) Timko, J. M.; Moore, S. S.; Walba, D. M.; Hiberty, P. C.; Cram, D. J. *J. Amer. Chem. Soc*., **1977**, *99 (13)*, 4207-4219.

[9] Kawashima, N.; Kawashima, T.; Otsubo, T.; Misumi, S. *Tetrahedron Letters*, **1978**, *50*, 5025-5028.

[10] Fabre, B.; Simonet, J. *Coord. Chem. Rev.* **1998**, *178-180*, 1211-1250.

[11] a) Pei, Q.; Yang, Y.; Yu, G.; Zhang, C.; Heeger, A. J. *J. Am. Chem. Soc.* **1996**, *118*, 3922. b) Leger, J. M.; Carter, S. A.; Ruhstaller, B. *J. Appl. Phys.* **2005**, *98*, 124907.

[12] a) Huang, C.; Huang, G.; Guo, J.; Huang, W.; Kang, E. T.; Yang, C.-Z. *Polym. Prepr.* **2002**, *43 (2)*, 574. b) Morgado, J.; Cacialli, F.; Friend, R. H.; Chuah, B. S.; Rost, H.; Holmes, A. B. *Macromolecules* **2001**, *34*, 3094-3099. c) Huang, C.; Huang, W.; Guo, J.; yang, C.-Z.; Kang, E.-T. *Polym.* **2001**, *42*, 3929-3938. d) Xiang, D.; Shen, Q.; Zhang, S.; Jiang, X. *J. Appl. Polym. Sci.* **2003**, *88*, 1350-1356.

[13] Collie, L.; Parker, D.; Tachon, C.; Hubbard, H. V. S. A.; Davies, G. R.; Ward, I. M. Wellings, S. C. *Polymer* **1993**, *37 (7)*, 1541.

[14] a) Jenekhe, S. A.; Osaheni, J. A. *Science* **1994**, *265*, 765. b) Nguyen, T. Q.; Doan, V.; Schwarz, B. J. *J. Chem. Phys.* **1999**, *110*, 4068. c) Nguyen, T. Q.; Martini, I. B.; Liu, J.; Schwarts, B. J. *J. Chem. Phys. B* **2000**, *104*, 237. d) Lemmer, U.; Heun, S.; Mahrt, R. F.; Scherf, U.; Hopemie, M.; Siegner, U.; Göbel, E. O.; Müllen, K.; Bässler, H. *Chem. Phys.Lett.* **1995**, *240*, 373.

[15] Fu, D.-K.; Xu, B.; Swager, T. M.; *Tetrahedron*, **1997**, *45*, 15487-15494.

[16] McQuade, T. D.; Pullen, A. E.; Swager, T. M. *Chem. Rev.* **2000**, *100*, 2537-2574 and references cited herein.

[17] Leclerc, M. *Adv. Mater.* **1999**, *11 (18)*, 1491-1498.

[18] Boldea, A.; Lévesque, I.; Leclerc, M. *J. Mater. Chem.*, **1999**, *9*, 2133-2138.

[19] a) Lévesque, I.; Leclerc, M. *J. Chem. Soc. Commun.*, **1995**, 2293 b) Lévesque, I.; Leclerc, M. *Chem. Mater.*, **1996**, *8*, 2843-2849.

[20] Béra-Abérem, M.; Ho, H.-A.; Leclerc, M. *Tetrahedron* **2004**, *60*, 11169-11173.

[21] *Supramolecular Chemistry I- Directed Synthesis and Molecular Recognition;* Wever, E.; Ed.; Springer-Verlag: New York, 1993.

[22] Marsella, M. J.; Swager, T. M. *J. Amer. Chem. Soc*., **1993**, *115*, 12214-12215.

[23] Swager, T. M.; Marsella, M. J. *Macromol. Symp*., **1995**, *98*, 855-858.

[24] Liu, H.; Wang, S.; Luo, Y.; Tang, W.; Yu, G.; Li, L.;Chen, C.; Xi, F. *J. Mater. Chem.*, **2001**, *11*, 3063-3067.

[25] Luo, Y.-H.; Liu, H.-W.; Xi, F.; Li, L.; Jin, X.-G.; Han, C.C.; Chan; C.-M *J. Amer. Chem. Soc*., **2003**, *125*, 6447-6451 and references cited herein.

[26] Williamson, A. W. *J. Chem. Soc.*, **1852**, *4*, *229.*

[27] Keegstra, E. M. D.; Zwikker, J. W.; Roest, M. R.; Jenneskens, L. W. *J. Org. Chem.*, **1992**, *57*, 6678-6680.

[28] Gottlieb, H. E.; Kotlyar, V.; Nudelman A. *J. Org. Chem*. **1997**, *62*, 7512-7515.

[29] Wilcox, C. S. *Frontiers in Supramolecular Organic Chemistry and Photochemistry* **1991**, Weinheim VCH.

[30] Reinhoudt, D. N.; Gray, R. T.; De Jong, F.; Smit, C. J. *Tetrahedron* **1977**, *33*, 563-571.

[31] Jousselme, B.; Blanchard, P.; Levillin, E.; Delaunay, J.; Allain, M.; Richomme, P.; Rondeau, D.; Galledo-Planas, N.; Roncali, J. *J. Amer. Chem. Soc*., **2003**, *125*, 1363-1370.

[32] Zhu, C. Y.; Bradshaw, J. S.; Oscarson, J. L.; Izatt, R. M. *J. Incl. Phenom.* **1992**, *12*, 275.

[33] Diederich, F. *Angew. Chem. Internat. Ed.* **1988**, *27 (3)*, 362-386.

[34] Hynes, J. H. *J. Chem. Soc. Dalton Trans.* **1993**, 311-312.

[35] Macomber, R. S. *J. Chem. Educ.* **1992**, *69 (5)*, 375-378

[36] Sprague, E. D. Larrabee, C. E. Jr . *J. Chem. Educ.* **1988**, *65 (3)*, 238-242.

[37] a) Izatt, R. M.; Bradshaw, J. S.; Nielsen, S. A.; Lamb, J. D.; Christensen, J. *J. Chem. Rev.* **1985**, *85*, 271-339. b) Ercolani, G.; Mandolini, L.; Masci, B. *J. Amer. Chem. Soc*., **1981**, *103*, 7484-7489.

[38] Wang, T.; Bradshaw, J. S.; Izatt, R. M. *J. Heterocyclic Chem*. **1997**, *31*, 1097-1114.

[39] Becker, H.; Spreitzer, H.; Ibrom, K.; Kreuder, W. *Macromolecules* **1999**, *32*, 4925.

[40] Spreitzer, H.; Becker, H.; Kluge, E.; Kreuder, W.; Schenk, H.; Demandt, R.; Schoo, H. *Adv. Mater.* **1998**, *10*, 1340.

[41] Yang, J.; Swager, T. M. *J. Amer. Chem. Soc*., **1998**, *120*, 11864-11873.

Chapter 5

Alcohol-functionalized PPV derivatives

Chapter 5 describes the synthesis of alcohol-functionalized PPV (co)polymers according to the sulfinyl precursor route. As a first approach, poly(2-methoxy-5-(hydroxy-triethoxy)-1,4-phenylene vinylene) (MHTE-PPV) is prepared. This homopolymer appears insoluble, presumably because the polar side chains in this polymer cause aggregation due to hydrogen bonding. In order to overcome the solubility problems, a copolymer is prepared between the sulfinyl monomer towards poly(2,5-bis(triethoxymethoxy)-1,4-phenylene vinylene) (BTEM-PPV) and the sulfinyl monomer towards MHTE-PPV. This copolymer is soluble in the common organic solvents. The exact composition of the copolymer is determined using ^{13}C NMR spectroscopy. Moreover, in order to understand the composition of the copolymer, the formation rates of the actual comonomers - the p-quinodimethane derivatives- are determined. The results obtained in this UV-Vis study are in good accordance with the results of NMR spectroscopy.

5.1 Introduction

Introducing chemical functionalities to PPV-type polymers provides access to a wide variety of material properties that stem from the functional groups used. As already mentioned, currently much interest exists in polar functionalized PPV derivatives.[1] These functionalized polymers significantly expand the application range compared to their non-functional counterparts and therefore exhibit promising properties for a variety of nano-technological applications such as conjugated self-assembled multilayers[2] as well as organized hybrid systems[3]. An important functionality in organic chemistry is the alcohol function. Alcohols are readily converted into a variety of other

functional groups such as halides, aldehydes, esters and carboxylic acids with outstanding efficiency. Therefore, the presence of an alcohol function in a PPV derivative could allow for post-polymerization functionalization of the polymer and form a platform to obtain PPV derivatives with more complex tailored substituents. Furthermore, alcohol-functionalized polymers show self-assembling behaviour *via* hydrogen bonding.[4] Despite the promising surplus value of alcohol side chains on PPV-type polymers, articles on alcohol-functionalized PPV derivatives are very scarce in literature. We found one article, dated from 1998, that reports on the synthesis of an alcohol-functionalized PPV derivative and the copolymerization reactions with plain PPV using the Wessling route.[5] Copoly(5-(2-hydroxyethoxy)-2-methoxy-1,4-phenylene vinylene/1,4-phenylene vinylene) is used to form self-assembled multilayer films based on hydrogen bonding interactions. However, neither molecular weights, nor NMR results of the alcohol-functionalized (co)polymers are reported. We prefer to use the sulfinyl precursor route to prepare alcohol-substituted PPV derivatives, since this route has proven its versatility for several different monomer systems and leads to materials with improved opto-electronic characteristics compared to other routes (*cf.* Chapter 2).[6,7] As a first approach, the homopolymer poly(2-methoxy-5-(hydroxy-triethoxy)-1,4-phenylene vinylene) (MHTE-PPV) is prepared.

5.2 Synthesis of poly(2-methoxy-5-(hydroxy-triethoxy)-1,4-phenylene vinylene) (MHTE-PPV)

5.2.1 Monomer synthesis

The various steps towards the alcohol-functionalized sulfinyl monomer are outlined in Scheme 5-1. The first synthetic step is a Williamson etherification between the two commercially available compounds 4-methoxy-phenol and 2-(2-(2-chloro-ethoxy)-ethoxy)-ethanol. During the next step concentrated HCl and formaldehyde in acetic anhydride are used to chloromethylate 2-(2-(2-(4-methoxy-phenoxy)-ethoxy)-ethoxy)-ethanol **1**. As a side reaction the alcohol function of **1** is converted to the corresponding acetic ester **2**. Deprotection to

chloromethylated alcohol 2-(2-(2-(2,5-bis-chloromethyl-4-methoxy-phenoxy)-ethoxy)-ethoxy)-ethanol **3** is accomplished quantitatively by hydrolyzation with an aqueous K_2CO_3-solution. The asymmetrically substituted monomer **6** is prepared *via* the symmetrical bissulfonium salt **4**. Treatment of this salt with an equimolar amount of an alkylthiolate anion generates the mono-substituted thioether **5**. A selective tellurium-catalyzed oxidation of this thioether yields a mixture of the two sulfinyl regio-isomers **6**. No attempts are made to separate the regio-isomers.

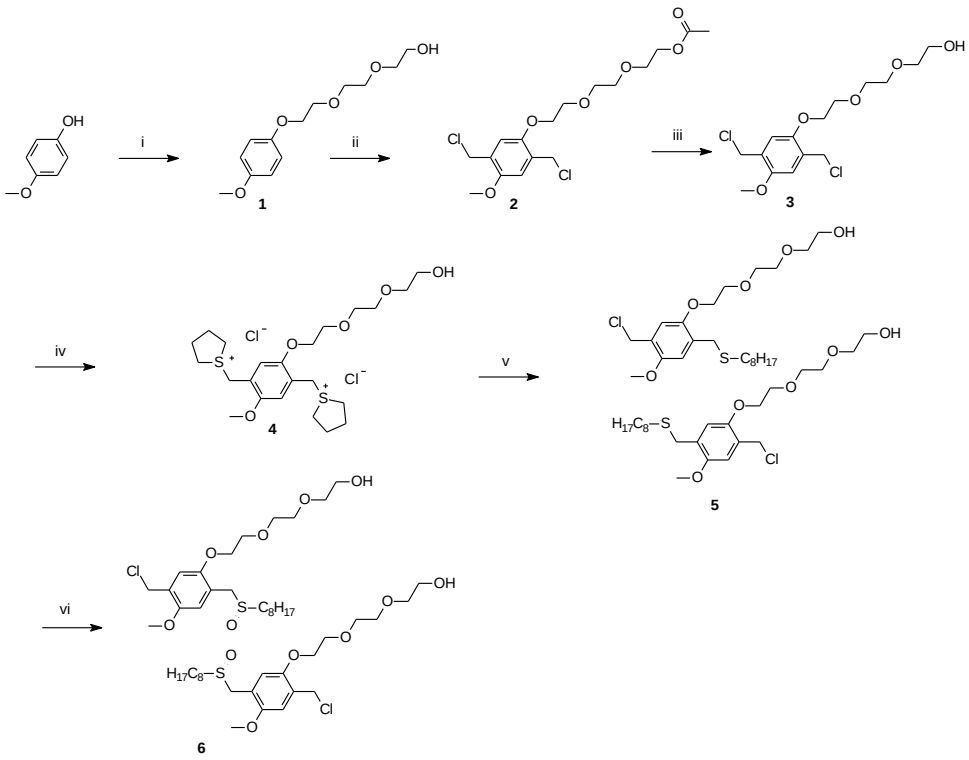

Scheme 5-1 Synthesis of the alcohol-functionalized sulfinyl monomer **6** (Na*t*BuO, NaI_{cat}, 2-(2-(2-chloro-ethoxy)-ethoxy)-ethanol**,** EtOH; ii: *p*-CH_2O, Ac_2O, HCl, 70°C; iii: K_2CO_3-solution in H_2O, MeOH; iv: THT, MeOH; v: octane-1-thiol, Na*t*BuO, MeOH; vi: H_2O_2, TeO_2, HCl_{cat}, 1,4-dioxane)

5.2.2 Polymer synthesis

Sulfinyl monomer **6** is polymerized at 30 °C in *sec*-BuOH according to the standard procedure (Scheme 5-2).[8] The concentration of the monomer is 0.1 M when the total amount of solvent is taken into account. After 1 h the polymerization reaction is stopped and the reaction mixture is poured into ice water, neutralized to pH=7 and subsequently extracted with CH_2Cl_2. The combined organic layers are evaporated and precipitated in a hexane to yield a soluble precursor polymer **7** in good yield (72 %). An analytical SEC measurement of **7** reveals the formation of a polymer with a molecular weight of 9×10^4 g/mol and a polydispersity of 1.9 *versus* polystyrene standards in DMF.

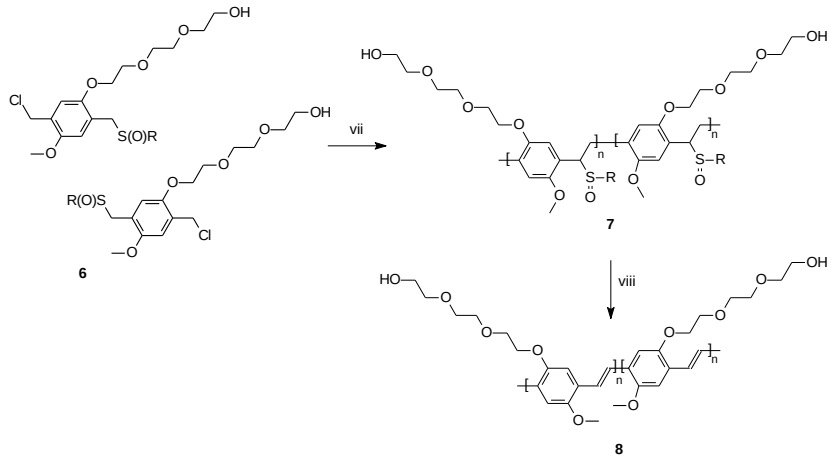

Scheme 5-2 Polymerization of **6** towards precursor polymer **7** and thermal elimination of **7** to the conjugated alcohol-functionalized polymer **8** (vii: Na*t*BuO, *sec*-BuOH; viii: toluene, reflux)

The thermal elimination is performed according to the two-step elimination procedure[9] in toluene solution as a result of which the precursor polymer **7** converts into the conjugated structure MHTE-PPV **8** (Scheme 5-2). However, during the first elimination the conjugated polymer precipitates from the toluene solution. After filtration, washing and drying under vacuum, the conjugated material **8** is insoluble in all tested solvents, even so when **8** is

refluxed overnight in the various solvents. Presumably, aggregation occurs due to strong hydrogen bonding. Similar phenomena are reported in literature:

- Benjamin *et al.* describe how the use of hydroxyl monomers towards copoly(5-(2-hydroxyethoxy)-2-methoxy-1,4-phenylene vinylene/1,4-phenylene vinylene) (Compound **A** in Figure 5-1) leads to the formation of low molecular weight oligomers. The precursor polymer of **A** aggregates, presumably because the polar side chains interact by hydrogen bonding.[5]
- According to a report of 2003, the polymerization yield of aryl-ethynylene polymers bearing 11-undecanol benzoate groups (Polymer **B** in Figure 5-1) is very low due to an insoluble polymer fraction, which is formed mainly by an aggregation phenomenon.[10]
- Homopolymers of poly(ω-hydroxyalkyl)thiophene (Polymer **C** in Figure 5-1) are described in literature as insoluble, while copolymers with 3-alkylthiophenes become soluble in common solvents.[11]

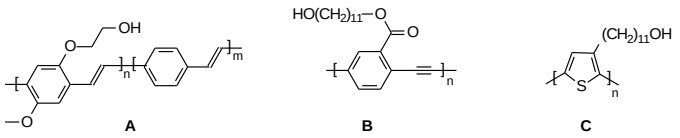

Figure 5-1 Alcohol-functionalized polymers known in literature

To substantiate the statement that the solubility problem of MHTE-PPV is intrinsic to the alcohol-functionality in the side chains of the PPV polymer, a second approach to obtain an alcohol-functionalized PPV derivative is used. In this approach poly(1,4-(2-(pentyloxy-5-carboxymethylester)-5-methoxy phenylene) vinylene)[a] is converted to poly(1,4-(2-(6-hydroxyhexyloxy)-5-methoxy phenylene) vinylene) using lithium alumium hydride (Scheme 5-3). Comparison of the FT-IR data of the ester-functionalized and the hydroxy-functionalized polymer demonstrates a quantitative reduction of the ester functionalities. While the ester-functionalized polymer is readily soluble in

[a] The synthesis of this polymer is described in Chapter 6.

common solvents such as $CHCl_3$, THF, 1,4-dioxane and toluene, the hydroxy-functionalized polymer is insoluble in all tested solvents.

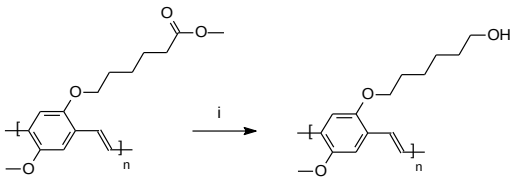

Scheme 5-3 Reduction of an ester-functionalized PPV to an alcohol-functionalized PPV (i: $LiAlH_4$, THF)

In order to overcome the solubility problem of the homopolymer MHTE-PPV, we could opt for the protection of the hydroxyl groups as a tetrahydropyranyl (THP) ethers. This approach is succesfully applied in literature for polythiophene polymers containing ω-hydroxyalkyl side chains (compound **C** in Figure 5-1).[12] In this chapter, we choose an alternative strategy, namely diluting the amount of hydroxy-functionalities by the synthesis of a copolymer. As the alcohol-functionalities in a copolymer are diluted by the comonomer, less interference can be expected.

5.3 The copolymer (MHTE-BTEM)-PPV

In order to improve the solubility of the homopolymer MHTE-PPV, the copolymer copoly(2-methoxy-5-(hydroxy-triethoxy)-1,4-phenylene vinylene/ 2,5-bis(triethoxymethoxy)-1,4-phenylene vinylene) ((MHTE-BTEM)-PPV) is prepared *via* the sulfinyl precursor route using on the one hand the monomer towards the alcohol-functionalized PPV derivative and on the other hand the monomer towards poly(2,5-bis(triethoxymethoxy)-1,4-phenylene vinylene) (BTEM-PPV) (Figure 5-2). BTEM-PPV is selected because the oligo(ethylene oxide) side chains guarantee good solubility, even in the conjugated form. Furthermore, the monomer and polymer synthesis of BTEM-PPV is well established.[b]

[b] The synthesis of the sulfinyl monomer of BTEM-PPV is described in Chapter 2.

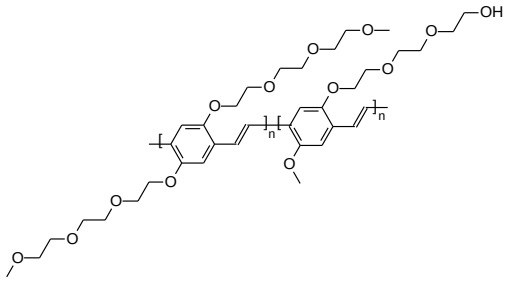

Figure 5-2 The copolymer (MHTE-BTEM)-PPV

5.3.1 Study of the formation of the different p-quinodimethane systems in (MHTE-BTEM)-PPV

- **Introduction**

Before to start with the synthesis of (MHTE-BTEM)-PPV, the reactivity of the different comonomers is checked. As mentioned in Chapter 1 and 2, the actual monomer in the sulfinyl precursor route is a *p*-quinodimethane (*p*-QM) system, which is formed by basic treatment of the premonomer (Scheme 5-4).

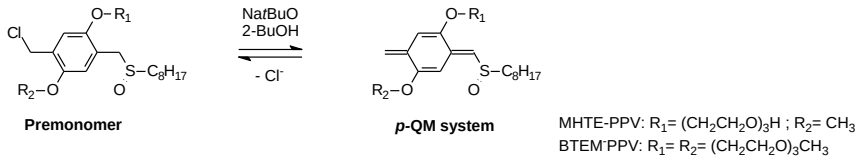

Scheme 5-4 Formation of actual monomers - the *p*-QM systems- of (MHTE-BTEM)-PPV

Kinetic data obtained from a mechanistic study on the *p*-QM formation can be of interest to access the possible outcome of copolymerization reactions involving monomers with different *p*-QM formation rates. Indeed, in the extreme case in which the *p*-QM system of one monomer is consumed before a sufficient amount of the other *p*-QM system is formed, one would end up with a mixture of homopolymers. If we assume that the formed *p*-QM structures are immediately consumed in the spontaneous polymerization process, the copolymer composition is explained by the differences in formation rate of the actual comonomers. This implies at the same time that there is no difference in

reactivity of the *p*-QM system towards either radical species of the two comonomers.

Since a *p*-QM intermediate has a strong absorbance in the UV-Vis spectrum, the formation of the actual monomer is readily monitored by UV-Vis spectroscopy. UV-Vis spectroscopy studies on the *p*-QM formation towards BTEM-PPV and MHTE-PPV are performed in *sec*-butanol. A large excess of base (Na*t*BuO) is used to guarantee fast and complete formation of the *p*-QM system. The monomer concentrations used in these UV-Vis measurements are too low (10^{-4} M) to self-initiate polymerization. Therefore, the decrease in *p*-QM absorption only occurs by solvent-substitution on the quinoid structure to yield the solvent-substituted monomer (Scheme 5-5). The formation of the solvent-substituted compound is proven with mass spectroscopy.

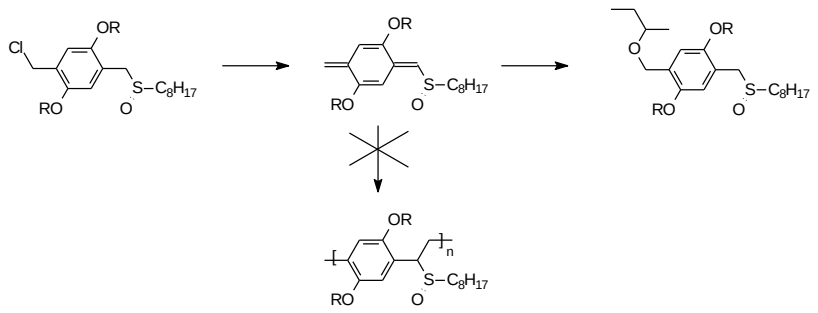

Scheme 5-5 Reaction scheme of the *p*-QM formation and solvent-substitution

When an excess of base is added to a diluted solution of a sulfinyl monomer in *sec*-BuOH, a typical plot is observed in the UV-Vis spectrum (Figure 5-3). Three different signals can be distinguished. The signal around 230 nm corresponds to the premonomer, the signal around 260 nm originates from the solvent-substituted premonomer and the signal around 315 nm is assigned to the *p*-QM system. The premonomer signal decreases in time. The signal of the *p*-QM system first increases rapidly and subsequently decreases. The signal of the solvent-substituted product only increases as the reaction progresses.

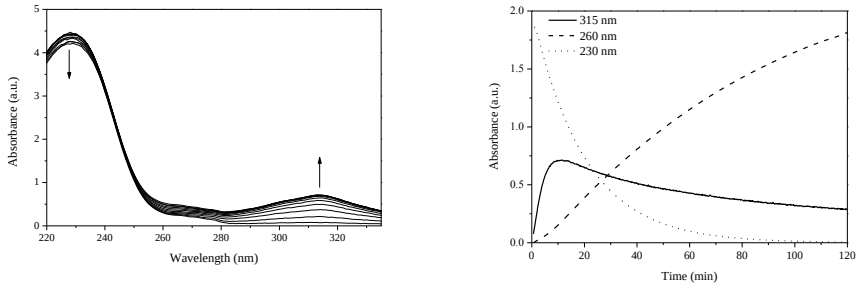

Figure 5-3 Typical UV-Vis spectrum of the *p*-QM formation (left) and plots of the absorptions at 230, 260 and 315 nm (right)

▪ Set-up and procedure used in the study of the *p*-QM formation

To allow very fast and accurate measurements of the kinetics of the *p*-QM systems in solution, the UV-Vis spectrophotometer is equipped with a so-called stopped-flow accessory. A simplified schematic representation of the basic components of a stopped-flow is depicted in Figure 5-4. The two syringes **1** and **2** are used to introduce the base and monomer solutions into the mixing chamber **3**. The flow of the mixed solution is then rapidly transferred into the sample cell **4**. When driving forward syringe **1** and **2**, syringe **5** is driven out to hit an electric switch **6** which starts recording of the measurement. With this equipment UV-Vis detection starts within a few milliseconds.

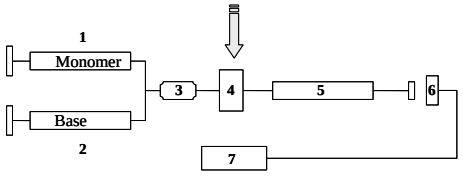

Figure 5-4 Set-up of the UV-Vis stopped-flow accessory

To obtain the rate constants of the *p*-QM formation towards BTEM-PPV, a 10^{-4} M solution of the sulfinyl monomer towards BTEM-PPV in *sec*-BuOH is placed in syringe **1**. Successively 10^{-3} M, 2 x 10^{-3} M, 4 x 10^{-3} M and 8 x 10^{-3} M solutions of Na*t*BuO in *sec*-BuOH are charged in syringe **2**. The maximum absorbance of the *p*-QM system (λ_{max}= 315 nm) is detected in function of the

time. Similar measurements are performed using the sulfinyl monomer towards MHTE-PPV (λ_{max} of the QM-system= 312 nm). All measurements were performed in threefold to insure good reproducibility. Figure 5-5 shows the outcome of these UV-Vis stopped-flow measurements. Each time, a typical curve is observed: the absorption signal rapidly rises and subsequently decreases somewhat slower.

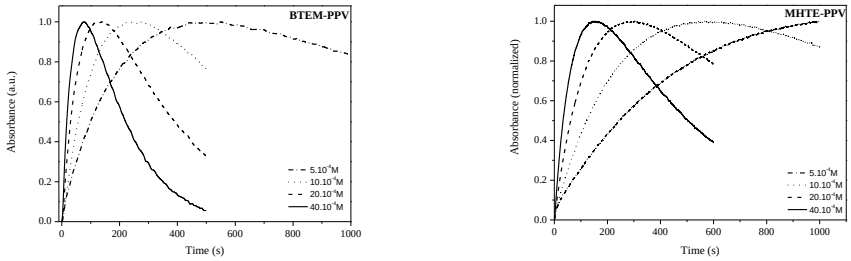

Figure 5-5 Formation of the *p*-QM systems towards BTEM-PPV (left) and MHTE-PPV (right) at different base concentrations

These qualitative measurements already give a first indication of the reactivity of the different monomers. When the absorbance of both *p*-QM systems at the same base concentration (2 x 10^{-3} M) is plotted in function of time, the general trend becomes clear. The *p*-QM system towards BTEM-PPV reaches a maximum absorbance after 130 s, compared to MHTE-PPV which reaches a maximum around 300 s, indicating that the QM formation rate of BTEM is higher (Figure 5-6).

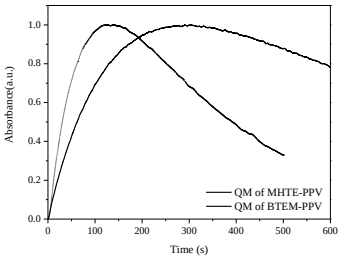

Figure 5-6 Comparison of the formation rate of the two *p*-QM systems for a base concentration of 2 x 10^{-3} M

▪ Quantitative study on *p*-QM formation

The data obtained from the UV-Vis stopped-flow measurements can be used to determine the rate constants of the *p*-QM formation reactions. For this purpose a non linear least-squares method[13] is used. Since the *p*-QM system is formed by an elimination reaction of the premonomer after addition of a base and subsequently consumed to yield the solvent-substituted product (Scheme 5-5), the reaction is said to proceed in a consecutive way. Actually the consecutive reactions are second-order reactions; therefore we should follow second-order kinetics to determine the rate constants of the *p*-QM formation. However, when one of the reagents in a second-order reaction is present in large excess compared to the other reagent, the change in its concentration is only a fraction of the total concentration and hence this concentration may be considered to be constant throughout the reaction.[14] Since first-order data are easier to process than data from higher-order systems, one often arranges conditions deliberately so that the reaction under study will follow first-order kinetics. The higher-order rate constants are found by performing subsequent experiments at different constant concentrations of the reagent in excess. This is worked-out on the basis of the general reaction: A + B → C.

The decrease of compound A is reflected in the equation: $-\frac{d[A]}{dt} = k_2 [A][B]$

When [B] >>[A], the equation becomes $-\frac{d[A]}{dt} = k_{obs} [A]$ where $k_{obs} = k_2 [B]$

Integration yields: $\ln [A] = - k_{obs} t + \text{constant}$

By this, the plot of ln [A] *versus* time yields a straight line with a slope= $-k_{obs}$. When k_{obs} is plotted at different concentrations of B a straight line is obtained with a slope= k_2, the second order rate constant.

In our case, a large excess of base is used, so the base concentration is considered to be constant throughout the consecutive reactions. The second-order rate constants of the *p*-QM formations are found by performing subsequent reactions using different base concentrations.

The consecutive first-order reaction kinetics are determined for the reaction

$$\text{PM (premonomer)} \xrightarrow[k_1]{} \text{QM} \xrightarrow[k_2]{} \text{solvent-substituted product}$$

The decrease of the premonomer is written as

$$\frac{d[PM]}{dt} = -k_1[PM]$$

The formation and subsequent decrease of the *p*-QM system is given as

$$\frac{d[QM]}{dt} = k_1[\text{premonomer}] - k_2[QM]$$

Integration of both equations yields[15]:

$$[PM] = [PM]^\circ \, e^{-k_1 t}$$

$$[QM] = \frac{k_1}{k_2 - k_1} [PM]^\circ \left(e^{-k_1 t} - e^{-k_2 t}\right) \qquad \textbf{(1)}$$

The absorbance originating from the *p*-QM system is proportional to the concentration of the *p*-QM system according to Beer's law (A= ε.c.l). Hence it is not necessary to know the exact concentration of the QM system; we just need the change in a proportional physical constant to determine the rate constants of the *p*-QM formation. From equation ***(1)***, it can be derived that

$$Abs_{QM} = k_3 \left(e^{-k_{1obs} t} - e^{-k_{2obs} t}\right) + k_4 \qquad \textbf{(2)}$$

With:

- Abs_{QM} = The maximum absorbance of the *p*-QM system (λ_{max}= 315 nm and 312 nm for the *p*-QM system towards BTEM-PPV and MHTE-PPV respectively)
- k_{1obs} and k_{2obs} = The observed pseudo first-order rate constants for the *p*-QM formation and solvent-substitution respectively
- k_3 and k_4 = Constant values to fit the equation using a non linear least-squared computational program

The different curves shown in Figure 5-5 are analyzed by means of a non linear least-squares method, where k_{1obs} and k_{2obs} are used as unknown parameters to fit equation ***(2***). Table 5-1 shows the observed pseudo first-order rate constants k_{1obs} for the *p*-QM formation towards BTEM- and MHTE-PPV at different base concentrations.

[Base] (10^{-4} M)	**k_{1obs} (10^{-2} sec^{-1}) BTEM-PPV**	**k_{1obs} (10^{-2} sec^{-1}) MHTE-PPV**
5.00	0.469 ± 0.004	0.168 ± 0.003
10.00	0.756 ± 0.012	0.344 ± 0.001
20.00	1.458 ± 0.013	0.715 ± 0.003
40.00	2.596 ± 0.028	1.281 ± 0.003

Table 5-1 The observed pseudo first-order rate constants k_{1obs} for the *p*-QM formation towards BTEM- and MHTE-PPV at different base concentrations

To get the absolute second order rate constants k_1 for the *p*-QM formation, the observed k_{1obs} values are plotted *versus* the different base concentrations (Figure 5-7). Straight lines with excellent correlation factors are obtained. The slope of the line is determined as the second order rate constant k_1. The values of the absolute rate constant are depicted in Table 5-2.

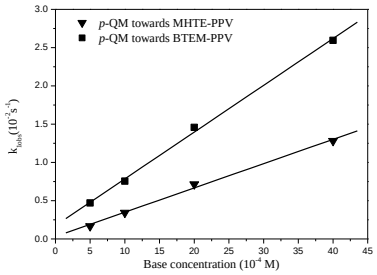

Figure 5-7 Plot of the observed pseudo first-order rate constants k_{1obs} *versus* different base concentrations to determine the absolute rate constants k_1 for the *p*-QM formation towards BTEM- and MHTE-PPV

***p*-QM towards**	**k_1 (mol^{-1} s^{-1})**	**R**
BTEM-PPV	0.0611 ± 0.0019	0.999
MHTE-PPV	0.0317 ± 0.0015	0.998

Table 5-2 Second-order rate constants k_1 for the *p*-QM formation towards BTEM- and MHTE-PPV

Apparently, the two monomers involved in the copolymerization reaction of (BTEM-MHTE)-PPV have different *p*-QM formation rates. The chemical differentiations on the monomer stage clearly affect the formation rate of the actual monomer and these differences on their turn will influence the copolymer composition. The reason for the faster *p*-QM formation of the sulfinyl monomer of BTEM-PPV is unknown.

5.3.2 Synthesis of the copolymer (MHTE-BTEM)-PPV

The copolymerization is performed according to the general procedure of the sulfinyl precursor route using the sulfinyl monomers of MHTE-PPV and BTEM-PPV (Scheme 5-6). Note that the monomer towards MHTE-PPV is a mixture of two regio-isomers. For reasons of simplicity only one isomer is depicted in Scheme 5-6. The molar monomer feed ratio of the copolymerization is 3 BTEM-PPV/ 1 MHTE-PPV. After polymerization in *sec*-BuOH, the reaction mixture is poured into water whereupon long, white strings are formed. After extraction with CH_2Cl_2 and reduction of the solvent, precursor polymer **12** is precipitated in hexane and dried *in vacuum*. **12** is prepared in good yield (69 %) and with a high M_w (20 x 10^4 g/mol). The final step in the sulfinyl precursor route is the thermal elimination of the sulfinyl group according to the two-step elimination procedure, as a result of which the precursor polymer converts into the conjugated structure (MHTE-BTEM)-PPV **13** (Scheme 5-6).

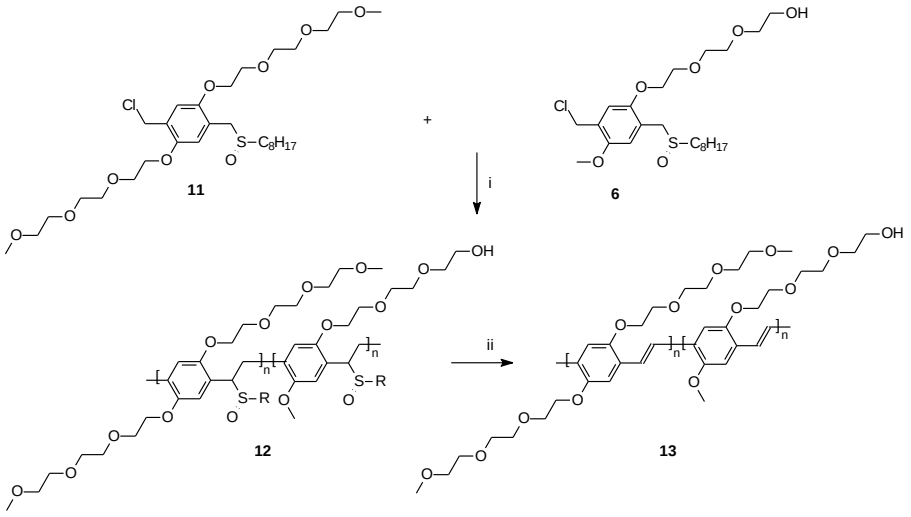

Scheme 5-6 Copolymerization reaction of monomer **11** with monomer **6** (i: Na*t*BuO, *sec*-BuOH; ii: toluene, reflux)

5.4 Characterization of the copolymer (MHTE-BTEM)-PPV

Contrary to the homopolymer MHTE-PPV, the copolymer (MHTE-BTEM)-PPV is soluble in the common organic solvent such as $CHCl_3$, CH_2Cl_2, chlorobenzene, THF, DMF and 1,4-dioxane and therefore can be fully characterized using different analytical techniques (*cf*. experimental section). (MHTE-BTEM)-PPV exhibit in the UV-Vis absorption spectrum a distinct absorption associated with the π–π* transition, both in a thin film (λ_{max} = 506 nm) and in solution (λ_{max} = 490 nm, $CHCl_3$) (Figure 5-8). These values are very similar to the homopolymer BTEM-PPV, which displays a distinct transition at λ_{max} = 509 nm as thin film and at λ_{max} = 489 nm in $CHCl_3$ solution. The copolymer is also studied using fluorescence spectroscopy. In a $CHCl_3$, **13** exhibits a distinct fluorescence emission at λ_{em}= 540 nm (excitation wavelength λ_{exc} = 490 nm) (Figure 5-9). For the homopolymer BTEM-PPV, the fluorescence emission is comparable (λ_{em} = 543 nm, excitation wavelength λ_{exc} = 489 nm, $CHCl_3$).

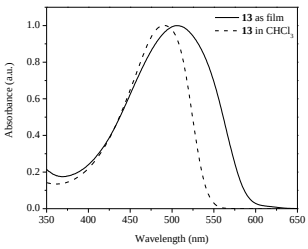

Figure 5-8 UV-Vis absorption spectra of (MHTE-BTEM)-PPV **13** in $CHCl_3$ and as film

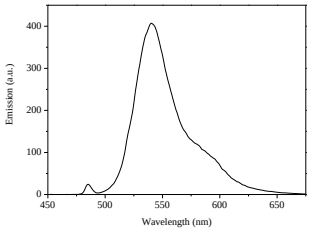

Figure 5-9 Fluorescence emission spectra of (MHTE-BTEM)-PPV **13** in $CHCl_3$

The exact chemical composition and the comonomer distribution in (MHTE-BTEM)-PPV is determined with quantitative ^{13}C NMR measurements. Earlier, the sulfinyl monomer of MHTE-PPV and the monomer and homopolymer of BTEM-PPV were characterized with ^{13}C NMR (*cf.* also experimental section at the end of this chapter). By comparing the different spectra, all peaks in the spectrum of (MHTE-BTEM)-PPV can be assigned. The signal at 61.6 ppm is assigned to the CH_2OH in MHTE-PPV. The signal at 58.9 ppm originates from the OCH_3 in BTEM-PPV. The ratio between these signals determines the copolymer composition. Copolymer **13** consists for 80 percent out of BTEM-PPV units and only for 20 percent out of MHTE-PPV units while the initial comonomer feed ratio was 75/25 BTEM-PPV/ MHTE-PPV. When the results obtained from the ^{13}C NMR composition analysis of the actual conjugated copolymer are compared with the UV-Vis stopped-flow study, the relationship between the *p*-QM formation rate and the copolymer composition becomes clear. The copolymer contains more repeating units of the monomer that reaches its maximum absorbance first. The difference between the initial comonomer feed and the actual copolymer composition is rather small but the trend is visible in the accurate composition determination by quantitative ^{13}C NMR spectroscopy. The copolymer composition can directly be correlated to the differences in formation rate between the actual monomers in the sulfinyl polymerization process as was demonstrated by UV-Vis spectroscopy measurements on the various monomers.

5.5 Conclusions

This chapter further demonstrated the versatility of the sulfinyl precursor route by the synthesis of an alcohol-substituted PPV derivative. Due to aggregation, the conjugated homopolymer was insoluble. A successful approach to improve the solubility properties of the alcohol-substituted homopolymer was the use of a copolymer. An alcohol-functionalized monomer and a monomer bearing two oligo(ethylene oxide) side chains were copolymerized *via* the sulfinyl precursor route and the copolymer composition was characterized using ^{13}C NMR spectroscopy. In order to explain the compositions of the copolymers, a UV-Vis study on the actual monomer – a *p*-quinodimethane derivative - was performed. Results obtained in this UV-Vis study were in good accordance with the actual copolymer composition as determined with ^{13}C NMR spectroscopy.

5.6 Experimental Section

Chemical and optical characterization.

NMR spectra were recorded with a Varian Inova Spectrometer at 300 MHz using a 5 mm probe for ^{1}H NMR and at 75 MHz using a 5 mm broadband probe for ^{13}C NMR. Analytical Size Exclusion Chromatography (SEC) was performed using a Spectra series P100 (Spectra Physics) pump equipped with a pre-column and two mixed-B columns (Polymer Labs) and a Refractive Index (RI) detector (Shodex) at 40°C. DMF was used as the eluent at a flow rate of 1.0 mL/min. Molecular weight distributions are given relative to polystyrene standards. GC-MS data were obtained with a Varian TSQ 3400 Gas Chromatograph and a TSQ 700 Finnigan Mat mass spectrometer. UV-Vis measurements were performed on a Cary 500 UV-Vis-NIR spectrophotometer (scan rate 600 nm/min, continuous run from 200 to 800 nm). FT-IR spectra were collected with a Perkin Elmer Spectrum One FT-IR spectrometer (nominal resolution 4 cm^{-1}, summation of 16 scans). Fluorescence spectra were obtained with a Perkin Elmer LS-5B luminescence spectrometer. For the

qualitative UV-Vis measurements on the different *p*-quinodimethane systems a CARY 500 UV-VIS-NIR spectrophotometer was used equipped with a stopped-flow module allowing very fast measurements. A 10^{-4} M solution of the different monomers in 2-BuOH and a 10^{-3} M solution of Na*t*BuO in the same solvent were prepared and both solutions were injected simultaneously whereupon the monitoring of the signals of interest was started. For the quantitative kinetic measurements the base solutions were prepared from a stock solution. Both monomer and base solutions were degassed by nitrogen flushing. The obtained data were fitted using a non-linear least-squares method using the program Kaleidagraph 3.0 for Macintosh computer.

Chemicals

All chemicals were purchased from Aldrich or Acros and used without further purification unless otherwise stated. Tetrahydrofuran (THF) was distilled from sodium/benzophenone.

Synthesis

2-(2-(2-(4-Methoxy-phenoxy)-ethoxy)-ethoxy)-ethanol 1. A mixture of 4-methoxy-phenol (10.0 g, 0.081 mol), Na*t*BuO (9.3 g, 0.097 mol) in EtOH (150 mL) was stirred for 2 h at ambient temperature under Ar atmosphere, after which 2-(2-(2-chloro-ethoxy)-ethoxy)-ethanol (16.2 g, 0.097 mol) and a catalytic amount of sodium iodide (0.5 g, 0.003 mol) was added. The reaction mixture was stirred for 6 h at reflux temperature and overnight at 50 °C. After the total volume was reduced to 30 mL by evaporation and the solution was cooled down to ambient temperature, the product was extracted with CH_2Cl_2 (3 x 75 mL). The organic extracts were dried over anhydrous $MgSO_4$ and the solvent was evaporated to give the crude product. The excess of starting material were removed by *Kugelrohr* distillation. Pure product **1** was obtained as an oil (16.8 g, 81 % yield). ^{1}H NMR ($CDCl_3$): δ = 6.83 + 6.81 (dd, 4H), 4.07 (t, 2H), 3.82 (t, 2H), 3.73 (m, 11H), 3.60 (t, 2H); MS (EI, m/z): 256 [M^+], 163, 151, 133, 124, 109.

Acetic acid 2-(2-(2-(2,5-bis-chloromethyl-4-methoxy-phenoxy)-ethoxy)-ethoxy)-ethyl ester 2. To a stirred mixture of **1** (20.0 g, 0.078 mol) and *p*-formaldehyde (6.4 g, 0.21 mol), concentrated HCl (36.6 mL) was added drop wise under N_2 atmosphere. Subsequently, acetic anhydride (77.3 mL) was added at such a rate that the temperature did not exceed 70 °C. After addition was complete, the resulting solution was stirred at 70 °C for 4 h after which it was cooled down to room temperature and poured into water (250 mL). The reaction mixture was extracted with CH_2Cl_2 (3 x 150 mL). The combined organic layers were carefully washed with a 10% $NaHCO_3$ solution till a pH of 7 was obtained and then dried over anhydrous $MgSO_4$. Evaporation of the solvent under reduced pressure gave a white solid (28.9 g, 94 % yield). ^{1}H NMR ($CDCl_3$): δ = 6.94 + 6.90 (2s, 2H), 4.63 + 4.60 (2s, 4H), 4.21 (t, 2H), 4.15 (t, 2H), 3.85 (t, 2H), 3.83 (s, 3H), 3.70 (m, 6H), 2.02 (s, 3H); MS (EI, m/z): 394 [M^+], 359 [M^+]-Cl, 323 [M^+]-2Cl, 281 [M^+]-2Cl-$COCH_3$; FT-IR (NaCl, cm^{-1}): 2915, 1735, 1639, 1514, 1249, 1225, 1180, 1141, 1058, 1040.

2-(2-(2-(2,5-Bis-chloromethyl-4-methoxy-phenoxy)-ethoxy)-ethoxy)-ethanol 3. The acetic acid **2** (11.9 g, 0.030 mol) is dissolved in 125 mL MeOH. A 10% K_2CO_3-solution in water is added until the begin product is completely disappeared on TLC. After acidification with 1% HCl-solution, extraction with CH_2Cl_2, drying over anhydrous $MgSO_4$ the free alcohol **3** is obtained as an oil (10.3 g, 97 % yield). ^{1}H NMR ($CDCl_3$): δ = 6.91 + 6.90 (2s, 2H), 4.65 + 4.60 (2s, 4H), 4.16 (t, 2H), 3.86 (t, 2H), 3.84 (s, 3H), 3.60 (m, 6H), 3.70 (t, 2H), 1.87 (broad, OH); MS (EI, m/z): 352 [M^+], 317 [M^+]-Cl, 282 [M^+]-2Cl, 281 [M^+]-2Cl-$COCH_3$; FT-IR (NaCl, cm^{-1}): 3447(broad, H-bonding), 2931, 2868, 1515, 1414, 1264, 1228, 1181, 1124, 1060, 1034.

Bis-tetrahydrothiopheniumsalt of 2-(2-(2-(2,5-Bis-chloromethyl-4-methoxy-phenoxy)-ethoxy)-ethoxy)-ethanol 4. To a solution of **3** (5.0 g, 0.014 mol) in MeOH (30 mL), tetrahydrothiophene (6 mL, 0.067 mol) was added, after which the white solution turned bright yellow. The mixture was allowed to react for 16 h at 50 °C, after which the total volume was reduced to 10 mL by evaporation. Subsequently the product was precipitated in cold aceton (100 mL) after which the bissulfonium salt was filtered off, washed with aceton (3 x 50 mL) and dried under vacuum. A white solid was obtained (5.0 g,

66 % yield). ^{1}H NMR (D_2O): δ= 7.11+7.10 (2s, 2H), 4.46 + 4.42 (2s, 4H), 4.18 (t, 2H), 3.85 (t, 2H), 3.81 (s, 3H), 3.67 (t, 2H), 3.62 (m, 4H), 3.51 (t, 2H), 3.41 (m, 8H), 2.24 (m, 8H).

1-Chloromethyl-2-(methoxy)-4-octylsulfanylmethyl-5-(2-(2-(2-hydroxy-ethoxy)-ethoxy)-ethoxy)benzene and 1-chloromethyl-2-(2-(2-(2-hydroxy-ethoxy)-ethoxy)-ethoxy)-4-octylsulfanylmethyl-5-(methoxy)benzene 5. A mixture of n-octane thiol (1.3 g, 0.0091 mol) and NaO*t*Bu (0.88 g, 0.0091 mol) in MeOH (50 mL) was stirred for 30 min at room temperature after which a clear solution was obtained. This solution was added drop wise (during 1 h) to solution of **4** (5.0 g, 0.0091 mol) in MeOH (165 mL). The reaction mixture was stirred for 2 h, after which it was concentrated under reduced pressure. Subsequently, n-octane (100 mL) was added and evaporated again to remove the tetrahydrothiophene. This sequence was repeated three times. The residue was redissolved in CH_2Cl_2 (100 mL) and extracted with water (3 x 100 mL). The organic layers were dried over anhydrous $MgSO_4$ and concentrated under reduced pressure giving the crude product. Pure thioether **5** was obtained as a yellow viscous oil after purification by column chromatography (SiO_2, eluent diethylether) (1/1 mixture of regio-isomers; 2.0 g, 46 % yield). ^{1}H NMR ($CDCl_3$): δ= 6.84+6.83+6.79+6.78 (4s, 2H), 4.64+4.60 (2s, 2H), 4.15 (m, 2H), 3.83 (m, 9H), 3.82 (m, 4H), 2.46 (m, 2H), 1.56 (m, 2H), 1.24 (m, 10H), 0.84 (t, 3H). MS (EI, m/z): 427 [M^+]- Cl.

1-Chloromethyl-2-(methoxy)-4-octylsulfinylmethyl-5-(2-(2-(2-hydroxy-ethoxy)-ethoxy)-ethoxy)benzene and 1-chloromethyl-2-(2-(2-(2-hydroxy-ethoxy)-ethoxy)-ethoxy)-4-octylsulfinylmethyl-5-(methoxy) benzene 6. An aqueous (35 wt-%) solution of H_2O_2 (0.25 g, 0.0026 mol) was added drop wise to a solution of **5** (0.60 g, 0.0013 mol), TeO_2 (0.1 g, 0.65 mmol) and concentrated HCl (0.05 mL) in dioxane (15 mL). As soon as **5** was consumed (TLC), 30 mL of brine was added to quench the reaction. The reaction mixture was extracted with CH_2Cl_2 (3 x 30 mL), after which the combined organic extracts were dried over anhydrous $MgSO_4$. Evaporation of the solvent under reduced pressure gave the crude product. The pure product **6** was obtained by column chromatography (SiO_2, eluent diethylether) as a yellow viscous oil (1/1 mixture of regio-isomers; 0.44 g, 71 % yield). ^{1}H NMR ($CDCl_3$): δ=

6.95+6.93+6.81+6.78 (4s, 2H), 4.61+4.58 (2s, 2H), 4.03 (t, 2H), 3.96 (t, 2H), 3.88+3.87+3.85+3.84 (2dd, 2H), 3.76 (m, 5H), 3.65 (m, 4H), 3.57 (m, 2H), 2.59 (m, 2H), 1.75 (m, 2H), 1.28 (m, 10H), 0.82 (t, 3H); ^{13}C NMR (CDCl3): 151.4+151.3 (1C), 150.5+150.2 (1C), 126.9+126.4 (1C), 120.5+120.1 (1C), 119.6+119.4 (1C), 113.8+112.5 (1C), 72.6+72.5 (1C), 69.7 (1C), 68.9 (1C), 67.3 (1C), 66.8 (1C), 61.3 (1C), 55.9+55.8 (1C), 53.2+52.9 (1C), 52.0+51.1 (1C), 41.2+41.0 (1C), 31.5 (1C), 29.0 (1C), 28.8 (1C), 28.6 (1C), 22.4 (2C), 13.8 (1C).; FT-IR (NaCl, cm^{-1}): 3439 (broad, H-bonding), 2925, 2866, 1518, 1417, 1262, 1132, 1045 ($\nu_{C\text{-}S}$).

Homopolymer MHTE-PPV

Precursor polymer of MHTE-PPV 7. The polymerization of monomer **6** (500 mg, 1.0 mmol) in 2-BuOH (7 mL) was performed in a thermostatic flask (30 °C). Na*t*BuO (0.25 g, 1.3 mmol), dissolved in the same solvent (3 mL), was added in one portion *via* a thermostatic funnel after both solutions were purged with N_2. Polymerization was allowed to proceed for 1 h at 30°C. The reaction is terminated by pouring the reaction mixture in a well stirred amount of ice water (100 mL) and then neutralized with 1M HCl-solution whereupon the precursor polymer precipitated. After extraction with CH_2Cl_2 (3 x 50 mL), the combined organic layers were evaporated and precipitated in a hexane to yield precursor polymer **7** (332 mg, 72 % yield). ^{1}H NMR ($CDCl_3$): δ= 7.0-6.3 (2H), 4.5 (1H), 4.1-3.3 (12H), 2.6 (2H), 1.8-1.2 (14H), 0.8 (3H); FT-IR (NaCl, cm^{-1}): 3411, 2926, 2859, 1506, 1463, 1411, 1213, 1122, 1047; SEC (DMF) M_w = 9×10^4 g/mol (PD = M_w/M_n = 1.9).

Poly(2-methoxy-5-(hydroxy-triethoxy)-1,4-phenylene vinylene) (MHTE-PPV) 8. A stirred solution of **7** (0.3 g) in toluene (20 mL) was purged with N_2 for 30 min., after which the elimination reaction was allowed to proceed at 110°C and stirred for 3 h. During this time, the polymer precipitated from the toluene solution. After 3h, the total volume was reduced to 10 mL by evaporation and the resulting orange red solution which already contained solid, was precipitated in cold hexane (100 mL). The resulting polymer was filtered off, and the elimination procedure was repeated after which crude **8** was filtered off again and dried at room temperature under reduced pressure.

The resulting red polymer (238 mg, 86 %) was insoluble. FT-IR (KBr, cm^{-1}): 3411, 2926, 2859, 1506, 1462, 1352, 1295, 1209.

Poly(1,4-(2-(5-carboxypentyloxy)-5-methoxyphenylene)vinylene 9. The synthesis of this ester-functionalized PPV derivative is described in Chapter 6. FT-IR (NaCl, cm^{-1}): 2952, 2869, 2700 (broad, ν_{O-H}), 1709 (ν_{C-O}), 1503, 1464, 1412, 1207, 1036, 972.

Poly(1,4-(2-(6-hydroxyhexyloxy)-5-methoxyphenylene)vinylene 10. A round-bottomed flask was charged with $LiAlH_4$ (0.014 g, 0.37 mmol) and dry THF (5 mL) under argon atmosphere. This slurry was cooled to 0°C and a solution of **9** dissolved in a minimal amount of dry THF was added portion wise in such a way that the reaction did not proceed too vigorously. When the addition is complete a reflux condenser was fitted and the reaction mixture was heated at reflux temperature for 2 h. After cooling down, air was allowed in the system and the reaction mixture was placed in an ice bath. Subsequently, a minimal amount of saturated ammonium chloride solution was added until no more gas development could be detected. The precipitated polymer **10** was filtered of and washed with water. After drying overnight under vacuum the alcohol-functionalized PPV **10** was obtained as a red, insoluble solid. FT-IR (NaCl, cm^{-1}): 3429, 2926, 2861, 1606, 1498, 1454, 1403, 1211, 1056.

1-Chloromethyl-2,5-bis(2-(2-(2-methoxy-ethoxy)-ethoxy)-ethoxy)-4-octylsulfinylmethylbenzene 11. The synthesis of this compound is described in the experimental section of Chapter 2. ^{1}H NMR ($CDCl_3$): 6.88+6.75 (2s, 2H), 4.54 (s, 2H), 4.05 (t, 4H), 4.02+3.98+3.90+3.86 (2dd, 2H), 3.78 (t, 4H), 3.64-3.45 (m, 16H), 3.27 (s, 6H), 2.52 (m, 2H), 1.63 (t, 2H), 1.33-1.16 (m, 10H), 0.77 (t, 3H); ^{13}C NMR ($CDCl_3$): 150.6 (1C), 150.3 (1C), 126.9 (1C), 120.1 (1C), 116.0 (1C), 114.3 (1C), 71.6 (1C), 70.6 (1C), 70.4 (1C), 70.3 (1C), 69.4 (1C), 68.7 (1C), 68.4 (1C), 58.8 (1C), 52.4 (1C), 51.0 (1C), 40.9 (1C), 31.5 (1C), 29.0 (1C), 28.7 (1C), 28.6 (1C), 22.4 (1C), 22.3 (1C), 13.8 (1C); FT-IR (NaCl, cm^{-1}): 3421, 2925, 2872, 1507, 1455, 1413, 12127, 1110, 1042(ν_{C-S}).

Copolymer (MHTE-BTEM)-PPV

Precursor polymer 12 towards (MHTE-BTEM)-PPV. The molar monomer feed ratio of the copolymerization was 3 equivalents of monomer **11**

to 1 equivalent of monomer **6**. A thermostatic flask (30 °C) was charged with a mixture of monomer **6** (734 mg, 1.2 mmol) and monomer **11** (187 mg, 0.4 mmol) in 2-BuOH (10 mL). Na*t*BuO (0.20 g, 2.0 mmol), dissolved in the same solvent (6 mL), was added in one portion *via* a thermostatic funnel after both solutions were purged with N_2. Polymerization was allowed to proceed for 1 h at 30°C. The reaction is terminated by pouring the reaction mixture in a well stirred amount of ice water (100 mL). Long, white strings are formed during this precipitation. After extraction with CH_2Cl_2 (3 x 50 mL), the combined organic layers were evaporated and precipitated in a hexane to yield precursor polymer **12** (596 mg, 69 % yield). ^{1}H NMR ($CDCl_3$): δ= 7.0-6.3, 4.6-4.4, 4.1-3.2, 2.8-2.6, 2.2, 1.8-1.3, 0.8; ^{13}C NMR ($CDCl_3$): δ= 151.4, 151.1, 150.8, 150.6 126.9, 126.5, 120.0, 115.8, 112.6, 111.3, 72.6, 71.8, 70.6, 70.1, 69.9, 69.8, 69.4, 69.0, 68.7, 68.1, 67.3, 66.9, 62.0, 59.3, 56.8, 55.3, 53.5, 51.3, 31.7, 31.5, 29.1, 28.9, 28.8, 28.6, 22.7, 22.4, 13.9, 9.9; FT-IR (NaCl, cm^{-1}): 3418, 2928, 2869, 1508, 1460, 1418, 1214, 1112, 1043; SEC (DMF) $M_w = 20 \times 10^4$ g/mol ($PD = M_w/M_n = 2.5$).

(MHTE-BTEM)-PPV 13. A stirred solution of **12** (0.4 g, 7.2 mmol) in toluene (30 mL) was purged with N_2 for 30 min., after which the elimination reaction was allowed to proceed at 110°C and stirred for 3 h. Subsequently, the total volume was reduced to 10 mL by evaporation and the resulting orange red solution was precipitated drop wise in cold MeOH (100 mL). The resulting red polymer was filtered off, washed with hexane and redissolved in toluene (40 mL). The elimination procedure was repeated after which crude **13** was filtered off again and dried at room temperature under reduced pressure. For purification, **13** was dissolved in boiling THF (20 mL) and after cooling to 40°C drop wise precipitated in MeOH (200 mL), giving **12** as a red, fibrous polymer (120 mg, 67 % yield). ^{1}H NMR ($CDCl_3$): δ= 7.4-7.2, 4.3-4.1, 3.9-3.8 3.7-3.3; ^{13}C NMR ($CDCl_3$): δ= 151.0, 127.8, 123.5, 111.2, 71.8, 70.8, 70.6, 70.5, 69.8, 69.1, 61.6, 58.9, 56.3; The signal at 61.6 ppm is assigned to the *C*H_2OH in MHTE-PPV. The signal at 58.9 originates from the O*C*H_3 in BTEM-PPV. The ratio between these signals determines the copolymer composition. It is found that monomer **11** is built in 4 times more than monomer **6**. FT-IR (NaCl, cm^{-1}): 3429, 2925, 2861, 1607, 1494, 1451, 1404,

1205, 1106, 1050; SEC (DMF) $M_w = 15 \times 10^4$ g/mol (PD = M_w/M_n = 2.4). UV-Vis $\lambda_{a,max}$= 490 nm ($CHCl_3$) and $\lambda_{a,max}$= 506 nm (as a film); Photoluminescence emission (PL) $\lambda_{em,\ max}$= 540 nm (λ_{exc}= 490 nm, $CHCl_3$).

5.7 References

[1] Pinto, M.R.; Schanze, K.S. *Synthesis* **2002**, 9, 1293.

[2] a) Liang, Z.; Cabarcos, O.M.; Allara, D.L.; Wang, Q. *Adv. Mater.* **2004**, *16*, 823. b) Liang, Z.; Rackaitis, M.; Li, K.; Manias, E.; Wang, Q. *Chem. Mater.* **2003**, *15*, 2699.

[3] Chan, E.W.L.; Lee, D-C.; Ng, M-K.; Wu, G.; Lee, K.Y.C.; Yu, L. *J. Am. Chem. Soc.* **2002**, *124*, 12238.

[4] Ajayaghosh, A.; George, S. J. *J. Am. Chem. Soc*. **2001**, *123*, 5148-5149.

[5] Benjamin, I.; Hong, H.; Avny, Y.; Davidov, D.; Neumann, R. *J. Mater. Chem.* **1998**, *8 (4)*, 919-924.

[6] Van Severen, I.; Motmans, F.; Lutsen, L.; Cleij, T. J.; Vanderzande, D. *Polymer* **2005**, *46*, 5466.

[7] a) Roex, H.; Adriaensens, P.; Vanderzande, D.; Gelan, J. *Macromolecules* **2003**, *36*, 5613. b) Munters, T.; Martens, T.; Goris, L.; Vrindts, V.; Manca, J.; Lutsen, L.; De Ceuninck, W.; Vanderzande, D.; De Schepper, L.; Gelan, J.; Sariciftci, N. S.; Brabec, C. J. *Thin Solid Films* **2002**, *403-404*, 247.

[8] Lutsen, L.; Adriaensens, P.; Becker, H.; van Breemen, A. J.; Vanderzande, D. J. M.; Gelan, J. *Macromolecules* **1999**, *32 (20)*, 6517-6525.

[9] Roex, H.; Adriaensens, P.; Vanderzande, D.; Gelan, J. *Macromolecules* **2003**, *36*, 5613.

[10] Arias-Marin, E.; Le Moigne, J.; Maillou, T.; Guillon, D.; Moggio, I.; Geffroy, B. *Macromolecules*, **2003**, *36*, 3570-3579.

[11] a) Lowe, J.; Holdcroft, S. *Polym. Prepr*. **1994**, *35(1)*, 297. b) Della Casa, C.; Salatelli, E.; Andreani, F.; Costa Bizarri, P. *Makromol. Chem., Makromol. Symp.* **1992**, *59*, 233.

[12] Murray, K. A.; Moratti, S. C.; Baigent, D. R.; Greenham, N. C.; Pichler, K.; Holmes, A. B.; Friend, R. H. *Synth. Met.* **1995**, *69*, 395-396.

[13] a) Cai, R.; Wu, X.; Liu, Z.; Ma, W.; *Anal.*, **1999,** *124*, 751-754. b) Reich, L; *Thermochim. Act.*, **1997**, *293*, 179.

[14] Fundamentals of Analytical Chemistry, Skoog, West en Holler, 7th Ed., Saunders College Publishing, **1996**.

[15] Chemical reactor theory: an introduction. Denbigh, K.G.; Turner, J.C.R.; Cambridge University Press, Great Britain, **1971**.

Chapter 6

Ester- and Carboxylic Acid-Functionalized PPV Derivatives[a]

Chapter 6 presents the synthesis of the ester-functionalized PPV derivative poly(1,4-(2-(pentyloxy-5-carboxymethylester)-5-methoxy phenylene)vinylene) via the sulfinyl precursor route. By basic hydrolysis of the ester side groups, the corresponding polar carboxylic acid-containing PPV derivative, i.e. poly(1,4-(2-(5-carboxypentyloxy)-5-methoxy phenylene)vinylene) (CPM-PPV) is readily obtained. This carboxy-substituted polymer exhibits significantly improved optical properties as compared to previously reported similar polymers. Furthermore, copolymers are prepared between on the one hand CPM-PPV and on the other hand MDMO- or MTEM-PPV.

6.1 Introduction

Chapter 5 described the synthesis, characterization and copolymerization behaviour of an alcohol-functionalized PPV derivative. This chapter describes the synthesis and the characterization of a polar carboxylic acid-containing PPV derivative. A literature study reveals that only a limited number of articles is devoted to carboxylic acid-tethered PPV-type polymers. Mostly, the polar carboxy-functionalities are build in with a view to form self-assembled multilayer films. For instance, Benjamin *et al.* prepared PPV homo- and copolymers with carboxy-moieties attached *via* an ethyl chain to the aromatic phenyl ring (**1** in Figure 6-1) according to the standard Wessling method, albeit without clear characterization of the polymers.[1] They used the presence of the polar side chains to form self-assembled multilayer films based on hydrogen

[a] Part of this chapter is published in *Polymer* **2005**, *46*, 5466-5475.

bonding interactions. Poly(1,4-(2-(5-carboxypentyloxy)-5-methoxy phenylene)vinylene) (CPM-PPV) (**2** in Figure 6-1), the subject matter of this chapter, was prepared earlier in literature *via* the Gilch route for fabrication of organic multilayer structures by the self-assembly technique.[2] Peng *et al.* wanted to overshoot the mark of self-assembled multilayer films and set the ultimate goal to achieve stable, nanoporous polymer networks with controllable and uniform pore sizes.[3] For this purpose, the polar carboxylic acid functional groups were anchored in geometrically-fixed positions, rather than on flexible side chains such as for **1** and **2** in Figure 6-1. Oxadiazole rings were used to tether the isophtalic acids to the polymer backbone to assure shape persistence during self-assembly (**3** in Figure 6-1). The rigid arm and the polymer backbone are electronically cross-conjugated to enable the electronic and optical properties of the polymer backbone to change in response to the self-assembly process. The copolymer was prepared *via* the Heck coupling reaction and by subsequent hydrolysis of the ester side groups. The structure of the polymer was confirmed using ^{1}H NMR spectroscopy. A band at 1731 cm^{-1} in the FT-IR spectrum is reported. This is typical for the stretching vibrations of the carbonyl group of an ester functionality and therefore suggesting that the hydrolysis was incomplete.

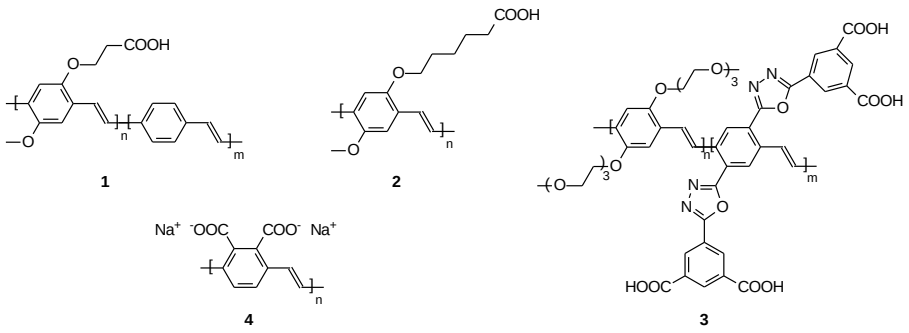

Figure 6-1 Carboxylic acid containing PPV derivatives reported in literature

An isolated case is the article of Wagaman and Grubbs that reports on the synthesis of a dicarboxylate PPV derivative (**4** in Figure 6-1) *via* ring-opening

metathesis polymerization (ROMP) starting from barrelene monomers.[4] The electron-withdrawing carboxylic acid groups are directly bond on the aromatic phenyls rings on purpose to improve PPVs electron injection and electron transport properties and therefore, enhance device efficiency.

We prepared poly(1,4-(2-(5-carboxypentyloxy)-5-methoxy phenylene) vinylene) (CPM-PPV) (**2** in Figure 6-1) with a view to use it as a platform for further functionalization. Different post-polymerization approaches are put to the test in Chapter 7, starting from CPM-PPV. Chapter 8 will investigate the immobilization of antibodies on the carboxylic acid functionalities and the impact of these polymers as a sensing mechanism for antibody-antigen affinity reactions.

As was already indicated in Chapter 2 and the references cited herein, polymers prepared *via* the sulfinyl precursor route display a notable improvement of properties as compared to the same materials prepared *via* the Gilch route. These improved properties were attributed to the higher chemical selectivity during polymerization. Within this context, the sulfinyl route is also the route of choice to obtain the polar carboxylic acid-functionalized PPV derivative. The optical properties of CPM-PPV prepared *via* the sulfinyl precursor route are compared to previously reported similar polymers obtained *via* other routes. To avoid solubility problems, the corresponding methylester is used during the synthesis of the monomer and precursor polymer. After formation of the ester-substituted PPV derivative, the ester side groups are hydrolyzed using basic conditions. In order to dilute the amount of functionalities of in the polymer, two copolymers are synthesized, respectively using the sulfinyl monomer of MDMO-PPV and the sulfinyl monomer of MTEM-PPV as comonomer with the sulfinyl monomer of CPM-PPV. For the copolymer (MDMO-CPM)-PPV two different monomer feed ratios are used, *i.e.* 9/1 and 1/1.

6.2 Synthesis and characterization of poly(1,4-(2-(5-carboxy pentyloxy)-5-methoxy phenylene)vinylene) (CPM-PPV)

6.2.1 Monomer synthesis

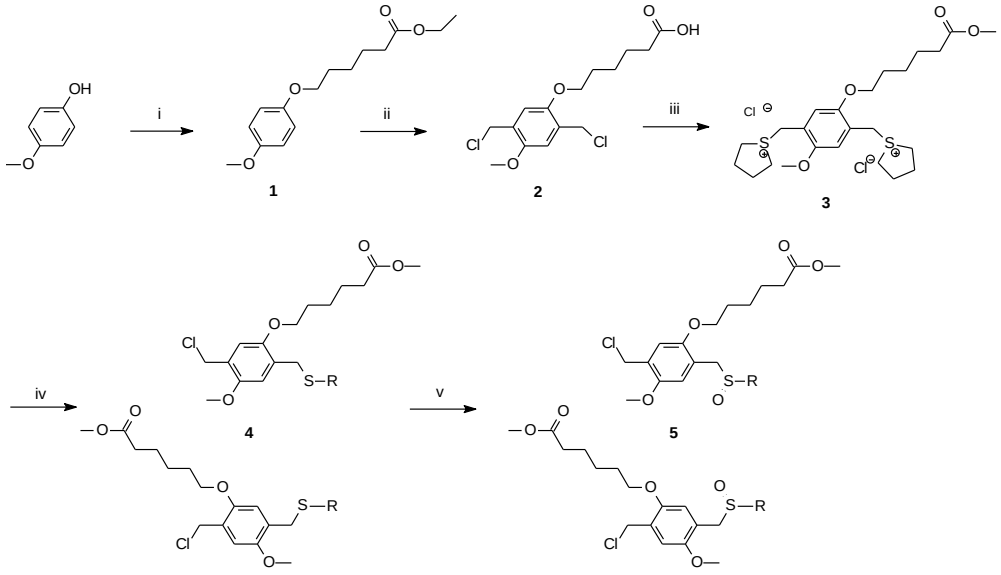

Scheme 6-1 Synthesis of the sulfinyl monomer **5** (i: Na*t*BuO, ethyl 6-bromohexanoate, NaI_{cat}, EtOH(reflux); ii: *p*-CH_2O, Ac_2O, HCl, 60°C; iii: THT, MeOH, 50°C; iv: RSH, Na*t*BuO, MeOH; v: H_2O_2, TeO_2, HCl_{cat}, 1,4-dioxane)

The monomer 6-(5-chloromethyl-4-methoxy-2-octylsulfinylmethyl-phenoxy)-hexanoic acid methyl ester **5** is prepared in a five step reaction according to Scheme 6-1. Starting from 4-methoxyphenol and ethyl 6-bromohexanoate, a Williamson etherification gives 6-(4-methoxy-phenoxy)-hexanoic acid ethyl ester **1**. Subsequently, **1** is chloromethylated using concentrated HCl and formaldehyde in acetic anhydride to give 6-(2,5-bischloromethyl-4-methoxy-phenoxy)-hexanoic acid **2**, according to a literature procedure.[2] During this reaction the ester converts into the corresponding carboxylic acid. The next step involves the formation of the bissulfonium salt

3. This procedure is well documented in literature for comparable systems.[5] An interesting feature of this synthetic procedure is that during this reaction, in addition to the formation of a bissulfonium salt, the carboxylic acid converts into the corresponding methyl ester. The crucial step in the monomer synthesis is the introduction of a thioether group by reaction of the symmetrical bissulfonium salt **3** with an equimolar amount of an alkylthiolate anion. Azeotropic removal of tetrahydrothiophene affords the mono-substituted thioether **4**, which can be selectively oxidized to the desired sulfinyl monomer **5** using mild oxidation conditions. It should be noted that both **4** and **5** are present in a 1/1 mixture of regio-isomers, which is used without further separation.

6.2.2 Polymer synthesis

6-(5-Chloromethyl-4-methoxy-2-octylsulfinylmethyl-phenoxy)-hexanoic acid methyl ester **5** is polymerized in sec-butanol using the standard procedure of the sulfinyl precursor route (Scheme 6-2).[6] The polymerization is allowed to proceed for 1 h at 30 °C, after which it is quenched by pouring the reaction mixture in water. After extraction with dichloromethane, the organic layers are evaporated under reduced pressure giving crude precursor polymer **6** (64 % yield), which is used without further purification. An analytical SEC measurement of **6**, performed *versus* polystyrene standards using THF as the eluent, reveals that a high molecular weight polymer is obtained with a low polydispersity (M_w = 2.51 x 10^5 g/mol; PD= 2.1). Previously for MDMO-PPV a molecular weight of 3.1 × 10^5 g/mol was reported.[6] So it is demonstrated that the polymerization using the sulfinyl precursor route of monomer **5** with side groups containing a polar ester is straightforward and comparable to the polymerization of similar monomers with apolar alkyl substituents. The ester side groups are not affected by the polymerization conditions as noticed from FT-IR spectroscopy where the signal at 1728 cm^{-1} remains unaffected.

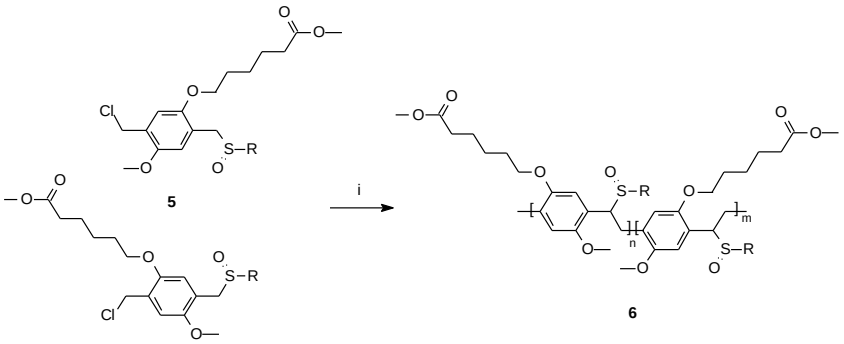

Scheme 6-2 Synthesis of the sulfinyl precursor polymer **6** towards the ester-substituted PPV derivative (i: Na*t*BuO, 2-BuOH)

6.2.3 Thermal conversion of the precursor polymer to the conjugated structure

The final step in the sulfinyl precursor route is the thermal elimination of the sulfinyl group as a result of which the precursor polymer **6** converts into the conjugated structure **7** (Scheme 6-3).

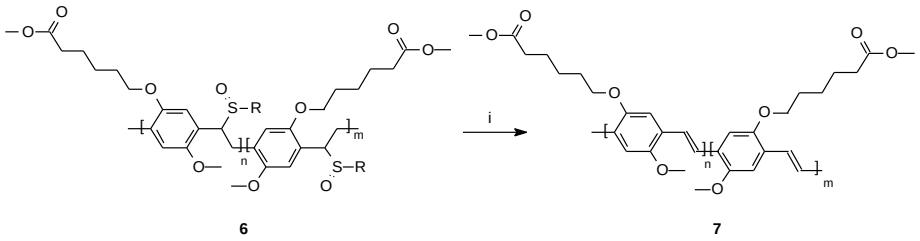

Scheme 6-3 Thermal elimination towards the conjugated ester-functionalized PPV derivative **7** (i: toluene (reflux))

The conjugated polymer poly(1,4-(2-(pentyloxy-5-carboxymethylester)-5-methoxy phenylene)vinylene) **7** can be prepared *via* two methods, *i.e.* thermal conversion in a thin film (**7a**) and thermal conversion in solution (**7b**) (Scheme 6-3). Polymer **7a** is specifically prepared to study the elimination process of the sulfinyl groups by *in situ* UV-Vis spectroscopy in a thin film. At room temperature, thin films of the precursor polymer **6** exhibit a strong absorbance with a maximum at λ_{max} = 300 nm (Figure 6-2). Upon heating from room

temperature to 250°C, a new absorption band appears which is associated with the conjugated system. During the elimination process, this band exhibits a gradual red shift (λ_{max} = 470 nm at 110°C) with increasing temperature due to an increase of the average conjugation length (Figure 6-3). When the absorbance at this maximum wavelength (λ_{max} = 470 nm) is monitored *versus* temperature, it is evident that the conjugated structure starts to develop around 75°C. From Figure 6-3 it is evident that the elimination process of a thin film of **6** heated at 2 °C/min to 110 °C is incomplete (*i.e.* residual absorption of **6** at λ_{max} = 300 nm remains present). Apparently the presence of elimination products in the thin film results in an incomplete conversion and either a slower heating rate at this temperature or a higher temperature is required to complete the thin film process. Notwithstanding, the elimination can successfully be performed in toluene solution at 110 °C. After a two-step elimination procedure, **7b** is obtained in excellent yield and UV-Vis spectroscopy of a solution of **7b** reveals that the elimination is virtually complete (Figure 6-2; only minimal absorption of **6** at λ_{max} = 300 nm remains). Hence, for all further chemical conversions only **7b** is used.

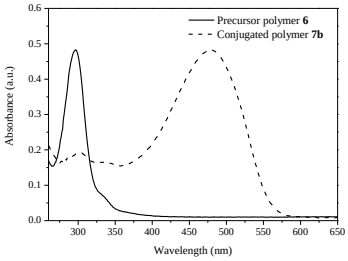

Figure 6-2 Solution UV-Vis absorption spectra of polymers **6** and **7b** (solvent THF)

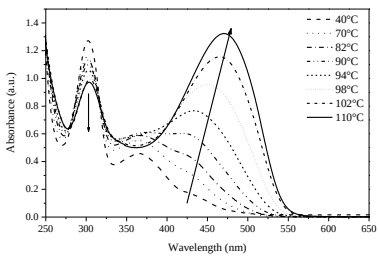

Figure 6-3 Thin film UV-Vis absorption spectra of the gradual formation of the conjugated polymer **7a**

Polymer **7b** exhibits all characteristics typical for alkoxy-substituted PPV derivatives, indicating that the incorporation of polar groups does not lead to significant problems in the solution elimination process. The solution UV-Vis absorption maximum of **7b** is λ_{max} = 479 nm (THF). The apparent molecular weight of **7b** as obtained by analytical SEC *versus* polystyrene standards using THF as the eluent (2.90 x 10^5 g/mol) is slightly higher than that of the

precursor polymer **6**, as a result of the increase in hydrodynamic volume of **7b** due to the rigidity of its conjugated backbone. This increased rigidity is also reflected in the glass transition temperature T_g as determined through Differential Scanning Calorimetry. It is found that the T_g of **7b** (55°C) is substantially higher than the T_g of **6** (-39°C).

Polymer **7b** shows a typical thermochromic effect,[7] which is clearly visible in the temperature dependent UV-Vis absorption spectra (Figure 6-4). Whereas at room temperature the absorption maximum of **7b** in a thin film is positioned around λ_{max}= 510 nm, upon increase of temperature a reversible shift is observed to lower wavelength (*i.e.* λ_{max} = 470 nm at 110°C). The same phenomenon is observed with FT-IR spectroscopy where the double bond signal at 970 cm^{-1} decreases upon heating and increases to its initial value when the sample is cooled to room temperature.

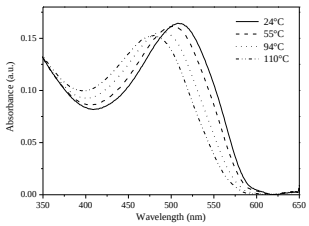

Figure 6-4 Thin film UV-Vis absorption spectra of polymer **7b** demonstrating the thermochromic effect

An additional heating/cooling experiment was performed to study the thermal degradation process of **7b**. From the UV-Vis spectra it is evident that the conjugated structure exhibits thermal stability up to only 160 °C, whereas for example, alkoxy-substituted PPV derivatives are stable up to 190 °C.[8] Notwithstanding, thermal stability up to 160 °C is sufficiently high for virtually all applications.

6.2.4 Hydrolysis of 7b towards CPM-PPV

Poly(1,4-(2-(pentyloxy-5-carboxymethylester)-5-methoxy phenylene) vinylene) **7b** is hydrolyzed using a base (K*t*BuO in H_2O), giving poly(1,4-(2-

(5-carboxypentyloxy)-5-methoxy phenylene)vinylene) (CPM-PPV) **8** in 79 % yield (Scheme 6-4).

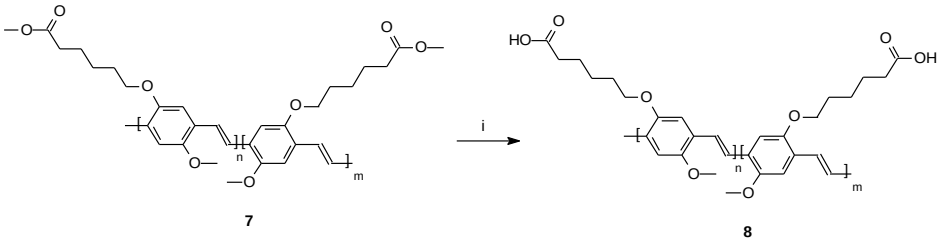

Scheme 6-4 Hydrolysis of **7b** to CPM-PPV **8** (i: K*t*BuO, H_2O, 1,4-dioxane)

The carboxylic acid-substituted polymer is soluble in the common organic solvents, such as acetone, THF, DMF and even in basic water. The molecular weight of **8** (2.23 x 10^5 g/mol) is only slightly lower than that of **7b**, indicating that the conjugated system does not degrade during hydrolysis. This is also corroborated by the solution UV-Vis absorption spectrum of **8**, which exhibits a distinct transition at λ_{max} = 490 nm (solvent DMSO, Figure 6-5). Furthermore, the glass transition temperature of **8** (T_g= 51 °C) remains virtually unchanged as compared to **7b** (T_g= 51 °C), as determined through Differential Scanning Calorimetry.

It is noteworthy that previous researchers have claimed the successful synthesis of CPM-PPV using the Gilch precursor route, albeit without documenting the polymer properties and analytical data.[2] The only evidence provided in these reports for the existence of the carboxy-substituted PPV is a thin film UV-Vis absorption spectrum, displaying a broad band with a shoulder at 430 nm.[5b] In marked contrast polymer **8** displays a well defined transition at λ_{max} = 490 nm in solution (solvent DMSO) as well as in a thin film (Figure 6-5). This comparison further supports the versatility of the sulfinyl precursor route in the synthesis of polar substituted PPV derivatives. In addition, this improvement in optical properties, exemplifies the importance of the sulfinyl precursor route in general, to obtain high purity conjugated polymers.

Additional analyses have been carried out to verify the complete hydrolysis of the ester side groups. FT-IR spectroscopy of polymer **7b** shows a strong absorption band at 1728 cm^{-1}, which is characteristic of the carbonyl absorption of the ester side group. As the polymer **7b** is hydrolyzed into the desired carboxy-substituted polymer **8**, the peak shifts to 1709 cm^{-1}, characteristic of the carbonyl absorption of the carboxylic acid (Figure 6-6). In addition, a broad band at approximately 2800 cm^{-1} is observed for the OH-stretch of the hydrogen bonded carboxylic acid groups of **8**. The complete hydrolysis of **7b** is even better observed using quantitative ^{13}C NMR. Whereas methyl esters exhibit a distinct resonance at δ = *circa* 50 ppm (O-*C*H_3), this resonance is entirely absent in the hydrolyzed polymer **8**.

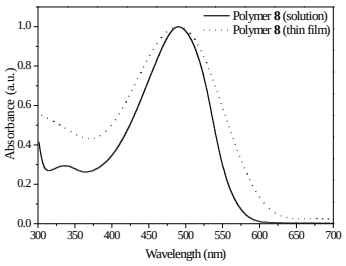

Figure 6-5 Solution (DMSO) and thin film UV-Vis absorption spectra of **8**

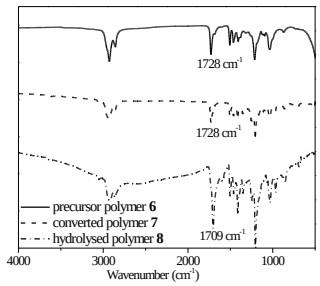

Figure 6-6 FT-IR spectra of precursor polymer **6**, conjugated polymer **7b** and hydrolyzed polymer **8**

6.3 Copolymerizations

The ultimate goal of the synthesis of poly(1,4-(2-(5-carboxypentyloxy)-5-methoxy phenylene)vinylene) (CPM-PPV) is to use this polymer as a platform for further functionalization. One can imagine that the amount of carboxylic acid functionalities in the homopolymer CPM-PPV is too high to achieve a quantitative functionalization in the case of highly tailored or large, complex side groups such as phthalocyanine functionalities (Chapter 7). Also with a view to covalently attach complex biomolecules to the PPV backbone (Chapter 8), one does not want to take any chances of unreacted carboxylic acid side groups since they may give rise to adverse interactions. As already mentioned

in Chapter 5, a synthetic strategy to dilute the amount of functionalities of a polymer is the synthesis of a copolymer. To this end, two copolymers are prepared, respectively using the sulfinyl monomer of MDMO-PPV and the sulfinyl monomer of MTEM-PPV as comonomer with the sulfinyl monomer of CPM-PPV.

6.3.1 (MDMO-CPM)-PPV

The copolymer (MDMO-CPM)-PPV is synthesized *via* the sulfinyl precursor route using on the one hand the monomer towards poly(1,4-(2-methoxy-5-(3,7-dimethyloctyloxy)) phenylene vinylene) (MDMO-PPV) and on the other hand, the monomer towards the carboxylic acid-functionalized PPV derivative CPM-PPV (Scheme 6-5). The sulfinyl monomer of MDMO-PPV is selected as comonomer since MDMO-PPV is a typical representative of the class of PPV-type materials and constitutes the bench-mark material in conjugated polymer research and development. The copolymerizations are performed in *sec*-BuOH according to the same standard procedure as for **6**. Two different molar monomer feed ratios are used in the copolymerization *i.e.* 9/1 and 1/1 MDMO-PPV/CPM-PPV. Note that both monomers are a mixture of regio-isomers. For reasons of simplicity in each case only one isomer is depicted in Scheme 6-5.

After polymerization, the reaction mixture is poured into water whereupon long, white strings are formed. After extraction with CH_2Cl_2 and evaporation of the solvent, the precursor copolymers **9 (n/m=1)** and **9 (n/m= 9)** are precipitated in cold methanol and dried *in vacuum*. The precursor copolymers are prepared in good yield and with high molecular weights M_w (Table 6-1). After isolation, **9 (n/m=1)** and **9 (n/m= 9)** are converted to the conjugated form by reflux in toluene (Scheme 6-5). After a two-step elimination procedure[9] and purification in boiling toluene, the conjugated copolymers **10 (n/m=1)** and **10 (n/m=9)** are obtained in excellent yield with molecular weights in the same order of magnitude as those found for the corresponding precursor polymers (Table 6-1). The increase in the polydispersity values reflects different

hydrodynamic volumes for the more rigid conjugated polymers, as compared to the precursor polymers. The same effect was observed for the polar polymers described in Chapter 2.

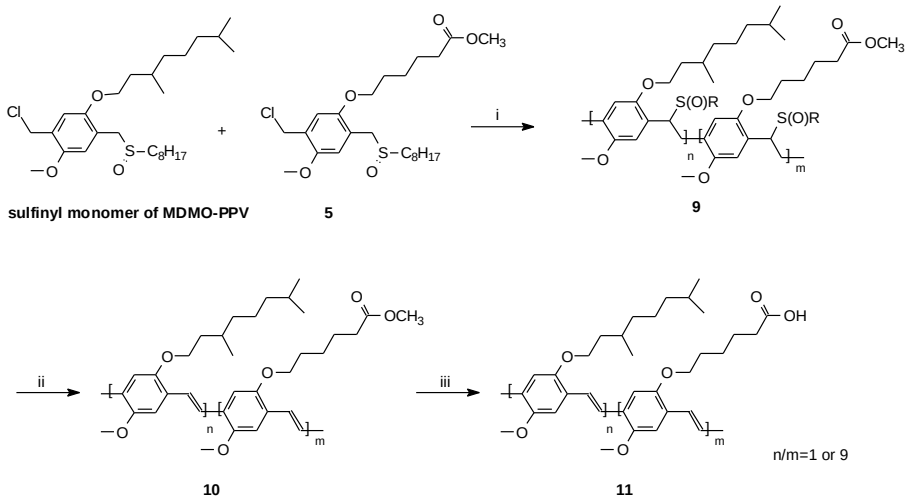

Scheme 6-5 Synthesis of the copolymer (MDMO-CPM)-PPV **11 (n/m=1)** and **11 (n/m=9)** *via* the sulfinyl precursor route (i: Na*t*BuO, 2-BuOH; ii: toluene (reflux); iii: K*t*BuO, H_2O, 1,4-dioxane)

Polymer	Yield (%)	M_w (g/mol)	PD	λ_{max} (nm) (as film)	λ_{max} (nm) (in THF)
9 (n/m=1)	84	240000	2.7	301	/
9 (n/m=9)	87	225000	3.1	300	/
10 (n/m=1)	89	350000	5.8	513	503
10 (n/m=9)	95	310000	5.3	520	514
11 (n/m=1)	93	250000	4.6	510	502
11 (n/m=9)	79	265000	4.4	520	510

Table 6-1 Polymerization results for precursor ester-functionalized copolymers **9 (n/m=1 or 9)**, the ester-functionalized conjugated copolymers **10 (n/m=1 or 9)** and the carboxylic acid-functionalized copolymers **11 (n/m=1 or 9)**. SEC measurements were performed *versus* polystyrene standards using THF as eluent

The elimination processes of the sulfinyl groups of the precursor copolymers **9 (n/m=1)** and **9 (n/m= 9)** are monitored by *in situ* UV-Vis

spectroscopy using a dynamic heating program of 2 °C/min from ambient temperature up to 300 °C under a continuous N_2 flow. The elimination process of **9 (n/m=1 or 9)** is similar to that of the ester-functionalized homopolymer **7** and illustrated for **9 (n/m=9)** in Figure 6-7 and Figure 6-8. At room temperature, thin films of **9 (n/m=1)** and **9 (n/m=9)** exhibit a strong absorbance with a maximum at λ_{max} = 300 nm. Upon heating, a new absorption band appears related to the conjugated system. At increasing temperatures, this band exhibits a gradual red shift (λ_{max} = 477 nm for **10 (n/m=1)** and at λ_{max} = 474 nm for **10 (n/m=9)** at 110 °C (Figure 6-7)). When the absorbance at this maximum wavelength (λ_{max} = 474 nm for **10 (n/m=9)**) is monitored *versus* temperature, it becomes evident that the conjugated structure starts to develop around 65 °C (Figure 6-8). At temperatures above 110 °C, the absorption at 474 nm starts to decrease as a result of the thermochromic effect. After *circa* 200 °C, a fast decrease in the absorbance is observed, related to the degradation of the conjugated system.

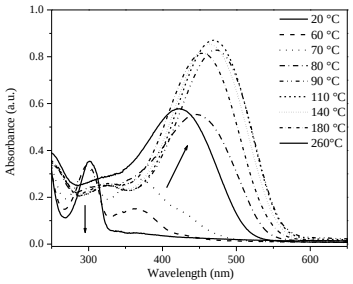

Figure 6-7 Thin film UV-Vis absorption spectra of the gradual formation of the conjugated copolymer **10 (n/m=9)**

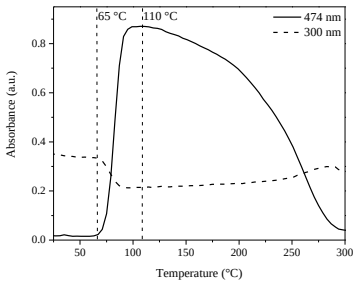

Figure 6-8 Absorbance at 474 nm and at 300 nm as a function of temperature for **10 (n/m=9)**

The elimination from the precursor copolymers to the conjugated copolymers **10 (n/m=1 or 9)** is also followed by *in situ* FT-IR spectroscopy *via* the formation of the *trans* vinylene double bond (965 cm^{-1}) as well as by the vanishing of the IR absorbances of the sulfinyl group (1044 cm^{-1}). This is illustrated for **10 (n/m=9)** in Figure 6-9. These measurements confirm that the elimination starts around 65 °C and is complete at 110 °C. In the region between 120 and 200°C there is a slight decrease in the absorbance of the

double bond, related to the thermochromic effect. Around 200 °C (fast decrease in the absorbance at 965 cm^{-1}), degradation of the conjugated system occurs. Similar observations are made for **10 (n/m=1)**.

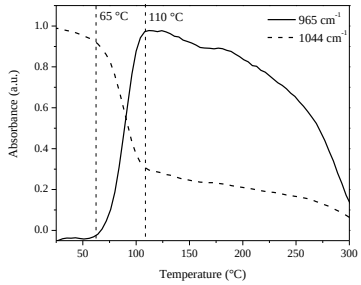

Figure 6-9 IR absorbances at 965 cm^{-1} and at 1044 cm^{-1} as a function of temperature for **10 (n/m=9)**

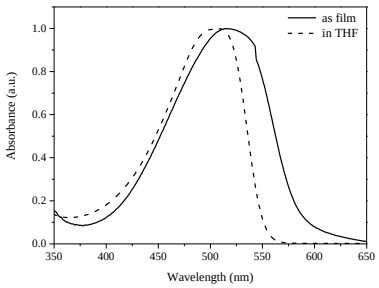

Figure 6-10 Thin film and solution (THF) UV-Vis absorption spectra of **10 (n/m=9)**

The exact chemical composition and comonomer distribution in (MDMO-CPM)-PPV is determined with quantitative ^{1}H NMR measurements. The ^{1}H NMR results of the sulfinyl monomer and homopolymer MDMO-PPV are described in literature[6, 10] and earlier in this chapter, the homopolymer CPM-PPV was characterized by ^{1}H NMR spectroscopy. By comparing these different ^{1}H NMR spectra, all the peaks in the spectrum of the ester-functionalized copolymer **10 (n/m=1 or 9)** can be assigned. The signals at 0.99 ppm are assigned to the CHCH_3 groups in MDMO-PPV. The triplet at 2.32 ppm originates from the CH_2COOCH$_3$ in CPM-PPV. The ratio between these signals determines the copolymer composition. It is found that the ratio of the two comonomers built in is *circa* 9% ester monomer and *circa* 91% MDMO-monomer for **10 (n/m= 9)** and *circa* 42% ester monomer and thus *circa* 58% MDMO-monomer for **10 (n/m= 1)**.

The ester-functionalized conjugated polymer **10 (n/m=1 or 9)** is then hydrolyzed using the same procedure as for the homopolymer CPM-PPV giving **11 (n/m=1 or 9)** in excellent yields (Scheme 6-5, Table 6-1). The hydrolyzations are verified by FT-IR and complete for more than 90 %. As is the case for **8**, the molecular weight of **11 (n/m=1 or 9)** is only slightly lower

than that of **10 (n/m=1 or 9)**, which is again an indication that the conjugated system does not degrade during hydrolysis (Table 6-1). This is even more corroborated by the solution and thin film UV-Vis absorption spectra of **11 (n/m=1 or 9)**, which exhibit distinct transitions at maximum wavelengths similar to those of **10 (n/m=1 or 9)** (Table 6-1, Figure 6-10, Figure 6-11, Figure 6-12).

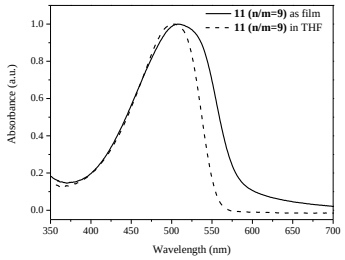

Figure 6-11 Thin film and solution (THF) UV-Vis absorption spectra of **11 (n/m=9)**

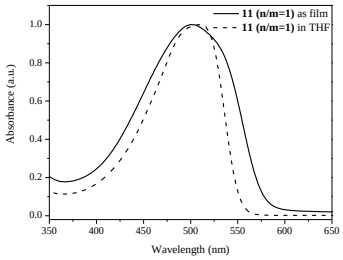

Figure 6-12 Thin film and solution (THF) UV-Vis absorption spectra of **11 (n/m=1)**

6.3.2 (MTEM-CPM)-PPV

This copolymer is prepared within the scope of Chapter 8, in which the interaction of biomolecules with a selection of functionalized PPV-type (co)polymers is studied. The monomer synthesis of poly(2-methoxy-5-(triethoxymethoxy)-1,4-phenylene vinylene) (MTEM-PPV) is described in Chapter 2. The copolymerization is performed according to the same standard procedure as for (MDMO-CPM)-PPV with molar monomer feed ratio of 9 MTEM-PPV and 1 CPM-PPV (Scheme 6-6, only one of the two regio-isomers of the sulfinyl monomers of MTEM- and CPM-PPV are represented).

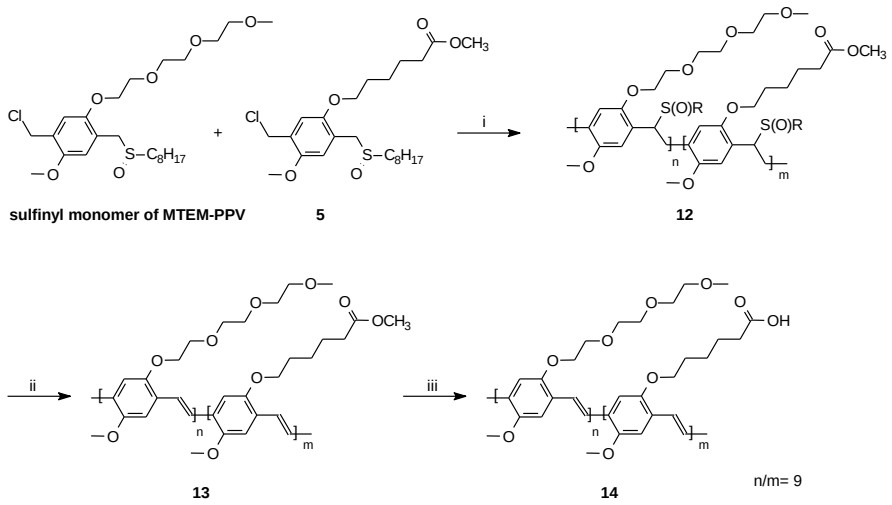

Scheme 6-6 Synthesis of the copolymer (MTEM-CPM)-PPV **14** *via* the sulfinyl precursor route (i: Na*t*BuO, 2-BuOH; ii: toluene (reflux); iii: K*t*BuO, H_2O, 1,4-dioxane)

The precursor copolymer **12** is prepared in excellent yield and with a high M_w (Table 6-2). After isolation, the precursor copolymer is converted to the conjugated form according to the two-step elimination procedure (Scheme 6-6). The conjugated copolymer **13** is obtained in good yield with a high molecular weight M_w (Table 6-2).

Polymer	**Yield (%)**	**M_w (g/mol)**	**PD**	**λ_{max} (nm) (as film)**	**λ_{max} (nm) (in THF)**
12 (n/m=9)	94	362000	3.4	302	/
13 (n/m=9)	85	535000	5.4	519	495
14 (n/m=9)	58	445000	4.8	512	495

Table 6-2 Polymerization results for precursor ester-functionalized copolymer **12**, the ester-functionalized conjugated copolymer **13** and the carboxylic acid-functionalized copolymer **14**. SEC measurements were performed *versus* polystyrene standards using DMF as eluent

The exact chemical composition and comonomer distribution in (MTEM-CPM)-PPV is again determined with quantitative ^{1}H NMR measurements. The signal at 3.32 ppm is assigned to the $CH_2OC\mathit{H}_3$ group in MTEM-PPV. The triplet at 2.35 ppm originates from the $C\mathit{H}_2COOCH_3$ in CPM-PPV. The ratio between these signals determines the copolymer composition. Approximately 7 % ester monomer and *circa* 93 % MTEM-monomer is build in.

The ester-functionalized conjugated copolymer **13** is hydrolyzed to yield **14**. The yield of **14** is somewhat lower (Table 6-2) due to the fact that the hydrolyzation reaction is done in duplicate to ensure a complete hydrolyzation which is verified using FT-IR spectroscopy. The solution and thin film UV-Vis absorption spectra of **13** and **14** display distinct transitions (Figure 6-13, Figure 6-14 and Table 6-2).

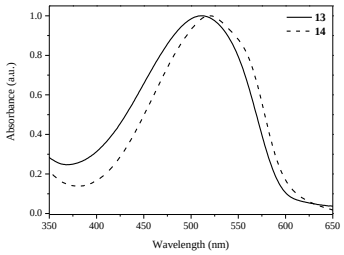

Figure 6-13 Thin film UV-Vis absorption spectra of **13** and **14**

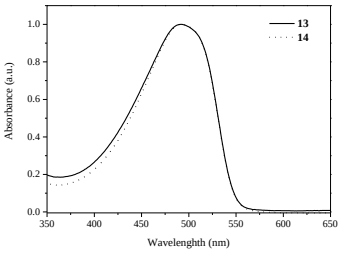

Figure 6-14 Solution (THF) UV-Vis absorption spectra of **13** and **14**

6.4 Conclusions

In conclusion, the synthesis of poly(1,4-(2-(5-carboxypentyloxy)-5-methoxy phenylene)vinylene) (CPM-PPV) has been demonstrated. CPM-PPV was obtained by quantitative hydrolysis of the corresponding ester-substituted PPV derivative, which was prepared *via* the sulfinyl precursor route. The ester- as well as the carboxylic acid-functionalized PPV-type polymers were fully characterized using different analytical techniques as well as UV-Vis absorption spectroscopy. CPM-PPV is soluble in common organic solvents,

such as DMSO, acetone, THF and even in basic water. Furthermore, this polymer exhibits a significantly improved λ_{max} value as compared to previous reports, indicating its improved purity and lower defect levels. In addition, copolymers are prepared between on the one hand CPM-PPV and on the other hand MDMO- or MTEM-PPV.

6.5 Experimental Section

Chemical and optical characterization.

NMR spectra were recorded with a Varian Inova Spectrometer at 300 MHz for ^{1}H NMR and at 75 MHz for ^{13}C NMR. Analytical Size Exclusion Chromatography (SEC) was performed using a Spectra series P100 (Spectra Physics) pump equipped with a pre-column (5 μm, 50 mm*7.5 mm, guard, Polymer Labs) and two mixed-B columns (10 μm, 2x300 mm*7.5 mm, Polymer Labs) and a Refractive Index (RI) detector (Shodex) at 40°C. Either THF or DMF was used as the eluent at a flow rate of 1.0 mL/min. Molecular weight distributions are given relative to polystyrene standards. GC-MS data were obtained with a Varian TSQ 3400 Gas Chromatograph and a TSQ 700 Finnigan Mat mass spectrometer. Glass transition temperatures (T_g) were determined through Differential Scanning Calorimetry (DSC) on a DSC 910-2000 analyzer. The samples (10 mg) were heated from -100°C to 150°C at a heating rate of 10°C/min under N_2 atmosphere. The second heating curves were evaluated. UV-Vis measurements were performed on a Cary 500 UV-Vis-NIR spectrophotometer (scan rate 600 nm/min, continuous run from 200 to 800 nm). FT-IR spectra were collected with a Perkin Elmer Spectrum One FT-IR spectrometer (nominal resolution 4 cm^{-1}, summation of 16 scans). Fluorescence spectra were obtained with a Perkin Elmer LS-5B luminescence spectrometer. *In situ* elimination reactions were performed in a variable temperature oven (Harrick). This oven can be positioned in the beam of either the FT-IR spectrometer or the UV-Vis-NIR-spectrophotometer. Elemental analysis was performed with a Flash EA 1112 Series CHNS-O analyzer.

Chemicals

All chemicals were purchased from Aldrich or Acros and used without further purification unless otherwise stated. The MDMO-PPV monomer was synthesized and polymerized as described elsewhere.[11]

Synthesis

6-(4-methoxy-phenoxy)-hexanoic acid ethyl ester 1. A mixture of 4-methoxyphenol (15.0 g, 120 mmol), NaO*t*Bu (13.9 g, 145 mmol) and EtOH (125 mL) was stirred for 1 h at room temperature under N_2 atmosphere, after which ethyl 6-bromohexanoate (32.1 g, 145 mmol) and sodium iodide (0.5 g, 3.3 mmol) were added. The resulting solution was stirred for 4 h at reflux temperature. The reaction was quenched with water (125 mL), and then extracted with CH_2Cl_2 (3 x 50 mL). The combined organic extracts were dried over anhydrous $MgSO_4$. Evaporation of the solvent under reduced pressure gave the crude product. The pure product was obtained by column chromatography (SiO_2, eluent CH_2Cl_2) as a colourless oil (29.3 g, 92% yield). ^{1}H NMR ($CDCl_3$): δ = 6.74 + 6.76 (dd, 4H), 3.97 (t, 2H), 3.72 (t, 2H), 3.65 (t + s, 5H), 3.54 (t, 2H), 3.23 (s, 1H); Mass (GC-MS, EI): 266 $[M+1]^+$, 221 $[M+1]^+$-C_2H_5O.

6-(2,5-bis-chloromethyl-4-methoxy-phenoxy)-hexanoic acid 2. To a stirred mixture of **1** (7.2 g, 27 mmol) and *p*-formaldehyde (2.23 g, 74 mmol), concentrated HCl (13 mL) was added drop wise under N_2 atmosphere. Subsequently, acetic anhydride (26 mL, 0.28 mol) was added at such a rate that the temperature did not exceed 70°C. After the addition was complete, the resulting solution was stirred at 60°C for 3 h after which it was cooled down to room temperature and poured into water (100 mL). The resulting precipitate was filtered off, redissolved in CH_2Cl_2 (100 mL) and dried over anhydrous $MgSO_4$. Evaporation of the solvent under reduced pressure gave the carboxylic acid as a white solid (9.16 g, 93%). ^{1}H NMR ($CDCl_3$): δ = 6.89+6.88 (2s, 2H),

4.61+4.60 (2s, 4H), 3.97 (t, 2H), 3.83 (s, 3H), 3.39 (t, 2H), 1.81 (m, 2H), 1.72 (m, 2H), 1.58 (m, 2H).

Bis-tetrahydrothiophenium salt of 6-(2,5-bis-chloromethyl-4-methoxy-phenoxy)-hexanoic acid methyl ester 3. To a solution of **2** (3.0 g, 9 mmol) in MeOH (30 mL), tetrahydrothiophene (3 mL, 36 mmol) was added. The mixture was allowed to react for 14 h at 50°C, after which the total volume was reduced to 15 mL by evaporation at room temperature. Subsequently the product was precipitated in cold acetone (150 mL) after which the bissulfonium salt was filtered off as a white solid (3.25 g, 69% yield). ^{1}H NMR (D_2O): δ= 7.12+7.11 (2s, 2H), 4.44+4.43 (2s, 4H), 4.03 (t, 2H), 3.81 (s, 3H), 3.58 (s, 3H), 3.40 (m, 8H), 2.34 (t, 2H), 2.24 (m, 8H), 1.75 (m, 2H), 1.59 (m, 2H), 1.42 (m, 2H); ^{13}C NMR (75 MHz, $CDCl_3$): δ= 177.5, 151.9, 151.3, 119.7, 119.6, 116.2, 115.4, 69.1, 56.2, 52.1, 43.0, 41.5, 33.5, 28.3, 28.0, 24.9, 23.9; FT-IR (NaCl, cm^{-1}): 3000, 2943, 2877, 1734(ν_{C-O}), 1513, 1465, 1447, 1400, 1314, 1230 ,1165 ,1103 ,1035, 910.

6-(5-chloromethyl-4-methoxy-2-octylsulfanylmethyl-phenoxy)-hexanoic acid methyl ester and 6-(2-chloromethyl-4-methoxy-5-octylsulfanylmethyl-phenoxy)-hexanoic acid methyl ester 4. A mixture of *n*-octane thiol (1.0 g, 7 mmol) and NaO*t*Bu (0.67 g, 7 mmol) in MeOH (40 mL) was stirred for 30 min at room temperature after which a clear solution was obtained. This solution was added dropwise to a solution of **3** (3.8 g, 7 mmol) in MeOH (130 mL). The reaction mixture was stirred for 2 h after which it was concentrated under reduced pressure. Subsequently, *n*-octane (100 mL) was added and evaporated again to remove the tetrahydrothiophene. This sequence was repeated three times. After removal of the solvents under reduced pressure, the residue was redissolved in CH_2Cl_2 (100 mL) and the organic layer was extracted with water (3 x 100 mL). The organic layer was dried over anhydrous $MgSO_4$. Evaporation of the solvent under reduced pressure gave the crude product. The pure product was obtained by column chromatography (SiO_2, eluent CH_2Cl_2) as a yellow viscous oil (1/1 mixture of regio-isomers; 2.8 g, 88% yield). ^{1}H NMR ($CDCl_3$): δ= 6.90+6.88+6.84+6.82 (4s, 2H), 4.61+4.60 (2s, 2H), 3.94 (m, 2H), 3.83+3.81 (2s, 3H), 3.69+3.68 (2s, 2H), 3.65 (s, 3H), 2.44 (t, 2H), 2.33 (t, 2H), 1.79 (m, 2H), 1.71 (m, 2H), 1.52 (m, 2H), 1.30-1.23 (m, 12H), 0.85 (t, 3H); ^{13}C

NMR ($CDCl_3$): δ= 174.1, 151.1, 150.5, 128.7, 124.7, 114.3, 113.3, 68.6, 56.2, 51.5, 39.2, 34.0, 31.9, 31.8, 30.2, 29.2, 29.0, 28.5, 25.7, 24.6, 22.6, 14.1; Mass (GC-MS, EI): 458 $[M+1]^+$, 423 $[M+1]^+$- HCl, 329 $[M+1]^+$- $C_7H_{13}O_2$, 313 $[M+1]^+$- $C_8H_{17}S$, 277 $[M+1]^+$-$C_8H_{17}S$ – HCl, 185 $[M+1]^+$- $C_8H_{17}S$ – $C_7H_{13}O_2$, 129 $C_7H_{13}O_2$.

Monomer

6-(5-chloromethyl-4-methoxy-2-octylsulfinylmethyl-phenoxy)-hexanoic acid methyl ester and 6-(2-chloromethyl-4-methoxy-5-octylsulfinylmethyl-phenoxy)-hexanoic acid methyl ester 5. An aqueous (35 wt%) solution of H_2O_2 (1.2 g, 12.4 mmol) was added drop wise to a mixture of **4** (2.8 g, 6 mmol), concentrated HCl (0.05 mL) and TeO_2 (0.06 g, 0.36 mmol) in dioxane (50 mL). As soon as **4** was consumed (TLC), 100 mL of brine was added to quench the reaction. The reaction mixture was extracted with $CHCl_3$ (3 x 50 mL) after which the combined organic extracts were dried over anhydrous $MgSO_4$. Evaporation of the solvent under reduced pressure gave the crude product. The pure product was obtained by column chromatography (SiO_2, eluent CH_2Cl_2/MeOH 19/1) as an orange viscous oil (1/1 mixture of regio-isomers; 2.6 g, 93% yield). Anal. Calcd. For $C_{24}H_{39}ClO_5S$: C 60.67, H 8.27, O 16.83, S 6.75; Found C 59.84, H 8.32, O 17.23, S 5.08; ^{1}H NMR ($CDCl_3$): δ= 6.88+6.86+6.85+6.84 (4s, 2H), 4.56+4.55 (2s, 2H), 4.13+4.11+4.20+4.00 (2dd, 2H), 3.91(m, 2H), 3.77+3.75 (2s, 3H), 3.60 (s, 3H), 2.67 (m, 2H), 2.29 (t, 2H), 1.78-1.61 (m, 6H), 1.49-1.18 (m, 12H), 0.81 (t, 3H); ^{13}C NMR ($CDCl_3$): δ= 173.7, 173.6, 151.0, 150.7, 150.5, 150.2, 126.4, 126.2, 119.7, 119.6, 115.5, 114.5, 113.6, 112.7, 68.4, 68.2, 55.9, 55.8, 52.7, 52.3, 51.3, 51.2, 41.1, 41.0, 33.7, 33.6, 31.5, 30.6, 28.9, 28.7, 28.6, 28.5, 25.4, 25.3, 24.4, 22.3, 13.8; FT-IR (NaCl, cm^{-1}): 2928 (ν_{C-H} aliph), 1738(ν_{C-O}), 1045(ν_{C-S}).

Sulfinyl monomer of MTEM-PPV. The synthesis and characterization of this compound is described in the experimental section of Chapter 2. ^{1}H NMR ($CDCl_3$): δ= 7.4 (2H), 7.2 (2H), 4.2 (2H), 3.9 (3H), 3.8 (2H), 3.7 (2H), 3.6 (4H), 3.5 (2H), 3.3 (3H); FT-IR (NaCl, cm^{-1}): 3421, 2925, 2872, 1507, 1455, 1413, 12127, 1110, 1042(ν_{C-S}).

Precursor polymer towards CPM-PPV

Precursor polymer of 6-(5-chloromethyl-4-methoxy-2-octylsulfinyl methyl-phenoxy)-hexanoic acid methyl ester 6. To a solution of monomer **5** (2.0 g , 4.21 mmol) in 2-BuOH (30 mL), a solution of Na*t*BuO (0.53 g, 5.47 mmol) in 2-BuOH (12 mL) was added in one portion using a thermostatic flask and funnel (30°C) after both solutions were purged with N_2. The polymerization was allowed to proceed for 1 h at 30°C after which it was quenched by pouring the reaction mixture in a well stirred amount of ice water (200 mL). After extraction with CH_2Cl_2 (3 x 200 mL), the combined organic layers were evaporated under reduced pressure giving the crude product, which was used without further purification (1.18 g, 64% yield). ^{1}H NMR ($CDCl_3$): δ= 7.0-6.3 (2H), 4.5 (2H), 4.1-3.6 (6H), 3.4 (3H), 2.4-1.8 (4H), 1.8-1.2 (18 H), 0.9 (3H); FT-IR (NaCl, cm^{-1}): 2929, 2856, 1728(ν_{c-o}), 1506, 1463, 1409, 1212, 1032; SEC (THF) M_w = 2.51 x 10^5 g/mol (PD = M_w/M_n = 2.1); DSC T_g = -39 °C.

Conjugated ester-functionalized PPV-polymer

Poly(1,4-(2-(pentyloxy-5-carboxymethylester)-5-methoxy phenylene) vinylene 7. The conjugated polymer **7** was prepared *via* two methods, *i.e.* thermal conversion in a thin film (**7a**) and thermal conversion in solution (**7b**). However, for all further chemical conversions only **7b** was used.

- To prepare **7a,** precursor polymer **6** was spin coated from a $CHCl_3$ solution (6 mg/mL) on a KBr (diameter 25 mm, thickness 1 mm) or quartz (diameter 25 mm, thickness 3 mm) substrate at 500-700 rpm. Subsequently the spin coated substrate was placed in an oven and heated at 2°C/min up to 300°C under a continuous flow of N_2 during which the samples were in direct contact with the heating element.
- To prepare **7b**, a stirred solution of **6** (2.19 g, 4.99 mmol) in toluene (125 mL) was purged with N_2 for 1 h, after which the elimination reaction was allowed to proceed at 110°C for 3 h. Subsequently, the total volume was reduced to 50 mL by evaporation and the resulting orange red solution was precipitated drop wise in cold EtOH (1250 mL). The resulting polymer was filtered off, washed with EtOH and redissolved in toluene (125 mL). The

elimination procedure was repeated after which crude 7b was filtered off again and dried at room temperature under reduced pressure. For purification, the crude 7b was dissolved in boiling THF (25 mL) and after cooling to 40°C drop wise precipitated in EtOH (250 mL), giving 7b as a red, fibrous polymer (1.02 g, 78% yield). ^{1}H NMR ($CDCl_3$): δ= 7.5-7.3 (2H), 7.2-6.9 (2H), 4.2 (2H), 3.8 (3H), 3.6 (3H), 2.3 (2H), 1.8-1.3 (6H); ^{13}C NMR ($CDCl_3$): δ= 173.1, 151.3, 150.8, 127.2, 123.2, 110.4, 109.1, 69.0, 56.1, 49.5, 33.8, 28.6, 25.5, 24.7; FT-IR (NaCl, cm^{-1}): 2934, 2866, 1728(ν_{C-O}), 1505, 1463, 1413, 1205, 1034, 969; SEC (THF) M_w = 2.90 x 10^5 g/mol (PD = M_w/M_n = 2.0); UV-Vis λ_{max}= 479 nm (THF), λ_{max}= 459 nm ($CHCl_3$); Photoluminescence emission maximum 546 nm (λ_{ex}= 459 nm, $CHCl_3$); DSC T_g = 55°C.

Hydrolysis

Poly(1,4-(2-(5-carboxypentyloxy)-5-methoxyphenylene)vinylene (CPM-PPV) 8. A solution of polymer **7b** (200 mg, 0.72 mmol repeating units) and dioxane (40 mL) was heated to reflux temperature after which a solution of K*t*BuO (0.87 g, 7.6 mmol) in water (1 mL) was added. After 4 h stirring at reflux temperature the reaction mixture was added drop wise to a well stirred amount of ice water (400 mL), neutralized with aqueous HCl (1 M) and the resulting precipitate was filtered off and washed with water (3 x 50 mL). The polymer was dried at room temperature under reduced pressure giving 8 as a red fibrous polymer (0.149 g, 79 % yield). Anal. Calcd. for $C_{15}H_{18}O_4$: C 68.69, H 6.92, O 24.40; Found C 68.83, H 7.33, O 23.55; ^{1}H NMR (DMSO): δ= 7.7-7.5 (4H), 7.2 (1H), 4.2-3.7 (5H), 2.2 (2H), 2.0-1.2 (6H); ^{13}C NMR (DMSO): δ= 174.5, 151.2, 150.7, 126.3, 124.4, 110.8, 109.9, 68.6, 56.0, 33.7, 28.8, 25.3, 24.4; FT-IR (NaCl, cm^{-1}): 2952, 2869, 2700 (broad, ν_{O-H}), 1709 (ν_{C-O}), 1503, 1464, 1412, 1207, 1036, 972; SEC (DMF) M_w = 2.23 x 10^5 g/mol (PD = M_w/M_n = 2.5); UV-Vis λ_{max}= 490 nm (DMSO), λ_{max}= 490 nm (as film); Photoluminescence emission maximum 540 nm (λ_{ex}= 470 nm, $CHCl_3$); DSC T_g = 51°C.

Copolymers

- **(MDMO-CPM)-PPV**

Precursor copolymer 9 (n/m= 9) towards (MDMO-CPM)-PPV. The molar monomer feed ratio of the copolymerization reaction was 1 equivalent of monomer 5 to 9 equivalents of the MDMO monomer. A thermostatic flask (30 °C) was charged with a mixture of monomer 5 (217 mg, 0.46 mmol) and the MDMO monomer (2.0 g, 4.1 mmol) in 2-BuOH (32 mL). Na*t*BuO (0.57 g, 5.9 mmol), dissolved in the same solvent (13 mL), was added in one portion *via* a thermostatic funnel after both solutions were purged with N_2. Polymerization was allowed to proceed for 1 h at 30°C. The reaction was terminated by pouring the reaction mixture in a well stirred amount of ice water (100 mL). Long, white strings were formed during this precipitation. After extraction with CH_2Cl_2 (3 x 50 mL), the combined organic layers were evaporated and precipitated in cold MeOH to yield precursor copolymer **9 (n/m=9)** (1.90 g, 87 % yield). ^{1}H NMR ($CDCl_3$): δ= 7.6-7.4, 7.3-7.1, 6.3, 4.5-4.1, 4.1-3.6, 3.4, 2.4-1.8, 1.8-0.6; FT-IR (NaCl, cm^{-1}): 2932, 2864, 1727(ν_{c-o}), 1506, 1444, 1413, 1208, 1027; SEC (THF) $M_w = 23 \times 10^4$ g/mol (PD = M_w/M_n = 3.1). UV-Vis λ_{max}= 300 nm (as film).

Precursor copolymer 9 (n/m= 1) towards (MDMO-CPM)-PPV. This compound was synthesized according to the same procedure as for **9 (n/m=9)**, starting from a molar monomer feed ratio of 1 equivalent of monomer 5 (0.97 g, 2.05 mmol) to 1 equivalent of the MDMO monomer (1.0 g, 2.05 mmol). 9 (n/m=9) was obtained after precipitation in cold hexane (1.53 g, 84 % yield). ^{1}H -NMR ($CDCl_3$): δ= 7.6-7.4, 7.3-7.1, 6.3, 4.5-4.1, 4.1-3.6, 3.4, 2.4-1.8, 1.8-0.6; FT-IR (NaCl, cm^{-1}): 2929, 2859, 1728(ν_{c-o}), 1508, 1444, 1410, 1210, 1023; SEC (THF) $M_w = 24 \times 10^4$ g/mol (PD = M_w/M_n = 2.7). UV-Vis λ_{max}= 301 nm (as film).

Ester-functionalized copolymer 10 (n/m= 1 or 9). A stirred solution of **9 (n/m= 1 or 9)** (3.9 mmol) in toluene (100 mL) was purged with N_2 for 30 min., after which the elimination reaction was allowed to proceed at 110°C and stirred for 3 h. Subsequently, the total volume was reduced to 30 mL by evaporation and the resulting orange red solution was precipitated drop wise in cold EtOH (300 mL). The resulting red polymer was filtered off, washed with

MeOH and redissolved in toluene (100 mL). The elimination procedure was repeated after which crude **10 (n/m= 1 or 9)** was filtered off again and dried at room temperature under reduced pressure. For purification, **10 (n/m= 1 or 9)** was dissolved in boiling THF (20 mL) and after cooling to 40°C drop wise precipitated in EtOH (200 mL), giving **10 (n/m= 1 or 9)** as a red, fibrous polymer (89 % for **10 (n/m= 1)** and 95% yield for **10 (n/m= 9)**). ^{1}H NMR ($CDCl_3$) of **10 (n/m= 1 or 9)**: δ= 7.5, 7.2, 4.1, 3.9, 2.32, 1.9-1.5, 1.3-1.1, 0.99, 0.9-0.8. The signal at 0.99 ppm is assigned to the three CHC*H*$_3$ methyl groups in MDMO-PPV. The signal at 2.32 ppm originates from the C*H*$_2$COO in CPM-PPV. The ratio between these signals determines the copolymer composition. It is found that monomer **5** is built for 42 % in **10 (n/m= 1)** and for 9 % in **10 (n/m= 9)**; FT-IR of **10 (n/m= 1)** (NaCl, cm^{-1}): 2927, 1731, 1504, 1464, 1414, 1353, 1255, 1038, 965; FT-IR of **10 (n/m= 9)** (NaCl, cm^{-1}): 2925, 2868, 1731, 1592, 1503, 1463, 1413, 1352, 1254, 1204, 1038, 966; SEC of 10 (n/m= 1) (DMF): M_w = 35 × 10^4 g/mol (PD = M_w/M_n = 5.8); SEC of **10 (n/m= 9)** (DMF): M_w = 31 × 10^4 g/mol (PD= 4.6). UV-Vis of **10 (n/m= 1):** $\lambda_{a,max}$= 503 nm (THF) and $\lambda_{a,max}$= 514 nm (as film). UV-Vis of **10 (n/m= 9):** $\lambda_{a,max}$= 514 nm (THF) and $\lambda_{a,max}$= 520 nm (as film).

(MDMO-CPM)-PPV 11 (n/m=1 or 9). The hydrolysis of polymer **10 (n/m= 1 or 9)** was performed using the same procedure as for **8**, taking the molar ester ratio into account. To ensure a quantitative conversion, the procedure was done in duplicate. **11 (n/m= 1 or 9)** was obtained as a red fibrous polymer (93 % yield for **11 (n/m= 1)** and 79% yield for **11 (n/m= 9)**). ^{1}H NMR ($CDCl_3$) of **11 (n/m= 1 or 9)**: δ= 7.5, 7.2, 4.2-3.9, 2.2, 1.9-1.2, 1.3-1.1, 1.0, 0.9-0.7; FT-IR of 11 (n/m= 1) (NaCl, cm^{-1}): 3059, 2958, 2868, 1710 (ν_{C-O}), 1505, 1463, 1430, 1414, 1356, 1254, 1205, 1037, 968; FT-IR of **11 (n/m= 9)** (NaCl, cm^{-1}): 2956, 2868, 1714 (ν_{C-O}), 1504, 1464, 1452, 1259, 1036, 968; SEC of **11 (n/m= 1)** (DMF) M_w = 2.50 x 10^5 g/mol (PD = M_w/M_n = 4.6); SEC of **11 (n/m= 9)** (DMF) M_w = 2.65 x 10^5 g/mol (PD = M_w/M_n = 4.4); UV-Vis of **11 (n/m= 1)**: λ_{max}= 502 nm (THF) and λ_{max}= 510 nm (as film); UV-Vis of **11 (n/m= 9):** λ_{max}= 510 nm (THF) and λ_{max}= 520 nm (as film).

- **(MTEM-CPM)-PPV**

Precursor copolymer 12 towards (MTEM-CPM)-PPV. The copolymerization is performed according to the same standard procedure as for **9 (n/m=9)**, using a molar monomer feed ratio of 1 equivalent of monomer **5** (0.2 g, 0.45 mmol) and 9 equivalents of the MTEM-monomer (2.0 g, 4.05 mmol). **12** was obtained in 94 % yield. ^{1}H NMR ($CDCl_3$): δ= 7.6-7.4, 6.5-6.3, 4.6-4.4, 4.1, 3.7, 3.6-3.4, 2.6, 2.3, 2.2, 1.7-1.2; FT-IR (NaCl, cm^{-1}): 2922, 2873, 1729(ν_{c-o}), 1593, 1504, 1463, 1413, 1351, 1254, 1044; SEC (DMF) M_w = 3.62 x 10^5 g/mol (PD = M_w/M_n = 3.4). UV-Vis λ_{max}= 302 nm (as film).

Ester-functionalized copolymer 13. This conjugated polymer was synthesized according to the same procedure as for **10**, using hexane as the non-solvent during precipitation. **13** was obtained as a red, fibrous polymer in 85 % yield. ^{1}H NMR ($CDCl_3$): δ= 7.4, 7.1, 4.2, 3.9, 3.8-3.5, 3.32, 2.35, 1.7-1.2; The signal at 3.32 ppm is assigned to the $CH_2OC\mathit{H_3}$ group in MTEM-PPV. The triplet at 2.35 ppm originates from the $C\mathit{H_2}COOCH_3$ in CPM-PPV. The ratio between these signals determines the copolymer composition. Approximately 7% ester monomer 5 and ~93% MTEM-monomer is build in. FT-IR (NaCl, cm^{-1}): 3058, 2924, 2871, 1727, 1590, 1505, 1463, 1413, 1352, 1254, 1206, 1109, 968; SEC (DMF) M_w = 5.53 x 10^5 g/mol (PD = M_w/M_n = 5.4). UV-Vis $\lambda_{a,max}$= 495 nm (THF) and $\lambda_{a,max}$= 519nm (as a film).

(MTEM-CPM)-PPV 14. The hydrolysis of polymer **13** was performed using the same procedure as for **8**, taking the molar ester ratio into account. To ensure a quantitative conversion, the procedure was done in duplicate. **14** was obtained as a red fibrous polymer in 58 % yield. ^{1}H NMR ($CDCl_3$): δ= 7.4, 7.2, 4.2, 3.8-3.5, 3.3, 1.8-1.2; FT-IR (NaCl, cm^{-1}): 3059, 2951, 2872, 1713 (ν_{C-O}), 1593, 1504, 1413, 1351, 1254, 1206, 1108, 967; SEC (DMF) M_w = 4.45 x 10^5 g/mol (PD = M_w/M_n = 4.8); UV-Vis: λ_{max}= 495 nm (THF) and λ_{max}= 512 nm (as film).

6.6 References

[1] Benjamin, I.; Hong, H.; Avny, Y.; Davidov, D.; Neumann, R. *J. Mater. Chem.* **1998**, *8 (4)*, 919-924.

[2] a) Fujii, A.; Sonoda, T.; Yoshino, K. *Jpn. J. Appl. Phys.* **2000**, *39*, L249. 9. b) Fujii A.; Sonoda T.; Fujisawa T.; Ootake R.; Yoshino K. *Synth. Met.* **2001**, 119, 18. c) Sonoda, T.; Fujisawa, T.; Fujii, A.; Yoshino, K. *Appl. Phys. Let* **2000**, *76 (22)*, 3227.

[3] Peng, Z.; Xu, B.; Zhang, J.; Pan, Y. *Chem. Commun.* **1999**, 1855.

[4] Wagaman, M. W.; Grubbs, R. H. *Macromolecules* **1997**, *30*, 3978-3985.

[5] Van Breemen, A. J. J. M.; Issaris A. C. J.; De Kok M. M.; Van Der Borght M. A. N.; Adriaensens P. J.; Gelan J. M. J. V.; Vanderzande, D. J. M. *Macromolecules* **1999**, 32, 5728-5735.

[6] Lutsen, L.; Adriaensens, P.; Becker, H.; Van Breemen, A. J. ; Vanderzande, D.; Gelan, J. *Macromolecules* **1999**, *32 (20)*, 6517-6525.

[7] a) Onoda, M.; Tada, K. *Thin Solid Films* **2003**, *438-439*, 187-194. b) Leclerc, M. *Adv. Mater*. **1999**, *11 (18)*, 1491

[8] Kesters, E.; Lutsen, L.; Vanderzande, D.; Gelan, J.; Nguyen, T.P., Molinié, P. *Thin Solid Films* **2002**, *403-404*, 120.

[9] Roex, H.; Adriaensens, P.; Vanderzande, D.; Gelan, J. *Macromolecules* **2003**, *36*, 5613.

[10] Roex, H. *Ph.D Dissertation* **2003** Limburgs Universitair Centrum Diepenbeek, Belgium.

[11] a) Lutsen, L.; Van Breemen, A.; Kreuder, W.; Vanderzande, D.; Gelan, J. *Helvetica Chimica Acta* **2000**, *83*, 3113. b) Lutsen, L.; Adriaensens, P.; Becker, H.; van Breemen, A. J.; Vanderzande, D. J. M.; Gelan, J. *Macromolecules* **1999**, *32 (20)*, 6517-6525.

Chapter 7

Post-Polymerization Functionalization as a Route towards Complex Ester- and Amide-Functionalized PPV Derivatives

This chapter demonstrates that the direct polymerization of complex tailored functionalized monomers is cumbersome, in fact often impossible. As a solution, the ambitious and versatile synthetic strategy of post-polymerization functionalization is tested, using the carboxylic acid-substituted PPV (co)polymers prepared in chapter 6 as the platform for the introduction of a library of molecules which can be attached to the conjugated polymer via their alcohol or amine-functionalities. The first post-polymerization functionalization method tested, is based on Mitsunobu reaction conditions. Using these reaction conditions various more complex tailored alcohol-functionalized substituents can be covalently attached to the phenylene ring. Analytical data of the functionalized polymers are consistent with a quantitative functional group substitution. Further improvements in reproducibility and solubility are made using the DCC/DMAP-esterification method. This straightforward method even allows covalent tethering of bulky phthalocyanine-functionalities on a PPV backbone. In addition, this chapter shows how carboxylic acid-bearing copolymers can be converted into amide-bearing PPV derivatives in a straightforward manner.

7.1 Introduction

As already mentioned in Chapter 1, there are two main methods to introduce functionality into a PPV backbone. In the first approach, the desired side chain is incorporated into the reactive monomer. The pre-functionalized monomer is subsequently polymerized. This strategy was successfully applied in the previous chapters for a number of polar substituents. However, this chapter will show that the range of functionalities that can be build into a PPV

derivative using the direct polymerization method, is limited. This chapter describes the synthesis of monomers functionalized with large and more complex side groups for application in organic solar cells. It is demonstrated that functional group incompatibility with the polymerization reaction results in insufficiently high molecular weights or may even hamper polymerization altogether. Another problem of the direct polymerization of functionalized monomers is the decomposition or transformation of the side group substituents towards other functionalities.

In order to overcome these problems, a second approach to introduce functionality into a PPV backbone, is put to the test. In this approach, functionalities are introduced to a preformed polymer scaffold *via* post-polymerization reactions. This method has the advantage of being applicable to a wide variety of functionalities. Thus far, most reported post-polymerization functionalization reactions on conjugated PPV-type polymers have been limited to the deprotection of functional groups after polymerization,[1] a method which only allows for the introduction of a limited number of functionalities. Here, a versatile novel approach is tested which allows for the incorporation of a sheer unlimited number of polar molecules as substituents. The carboxylic acid containing PPV derivative, poly(1,4-(2-(5-carboxypentyloxy)-5-methoxy phenylene)vinylene) (CPM-PPV) and copolymers of CPM-PPV, which are prepared as described in chapter 6, are used as the platform for further functionalization. Different functionalization methods are elaborated. First, the carboxylic acid groups of the PPV-type polymers are brought under the mild, neutral conditions of the Mitsunobu reaction.[2] This approach is tested with various alcohol-functionalized molecules *i.e.* 5-(hydroxy methyl)furfural , 2- as well as 4-nitrobenzylalcohol and 3-N,N-dimethylamino-1-propanol. Also a so-called 'push-pull' molecule that has electron donor and acceptor groups in electronic communication through a π-conjugated bridge, is introduced *via* this method. Secondly, the DCC/DMAP-esterification method is put to the test, using the same alcohol-functionalized model compounds as in the Mitsunobu-approach. In addition, phthalocyanine-molecules are brought under the DCC-activation method in order to covalently graft the conjugated PPV-backbone

with these functionalities. Finally, preliminary results are presented of the conversion of carboxylic acid-substituted PPV copolymers into amide-bearing PPV derivatives.

7.2 Direct polymerization of complex tailored functionalized monomers towards application in organic solar cells

Photovoltaic (PV) devices are one of the most promising sustainable energy sources for the mid- and long-term future. Organic solar cells have the potential to realize a significant cost reduction for PV energy conversion. However, there are still some crucial obstacles to be overcome before large-scale production of plastic solar cells can be considered. As a part of our work dedicated to the functionalization of PPV towards application in advanced polymer based devices, this section presents two possible interesting functionalized PPV-type polymers for application in organic solar cells.

7.2.1 PPV derivatives bearing push-pull like molecules

- **Introduction**

A limitation of today's organic solar cells is the low mobility of charge carriers as a result of the large degree of disorder inherent to organic films deposit by techniques exploitable at the industrial scale. It is of great importance to understand, and more, to control the assembly process. Several classical approaches can be followed to introduce structural order at the nano-scale or molecular level: regioregularity, use of hydrogen bonding, liquid crystal groups, etc. An innovative molecular organization technique is based on polar order.[3] Polar order can be introduced by orientation of molecules with a large ground-state dipole, which are grafted on a conjugated polymer. Orientation is performed through dc-field ordering of the polar molecules, the so-called DπA-molecules that have electron donor and acceptor groups in electronic communication through a π-conjugated bridge (also called push-pull molecules and used in nonlinear optics[4]) (Figure 7-1). By application of an

external static electric field through the polymer film, while heating near the glass transition temperature (T_g), the molecules with a large ground-state dipole are oriented in the field. When the functionalized polymer film is subsequently cooled while the field is still applied, the orientation is frozen and an internal field is stored in the polymeric semi-conductor.[5]

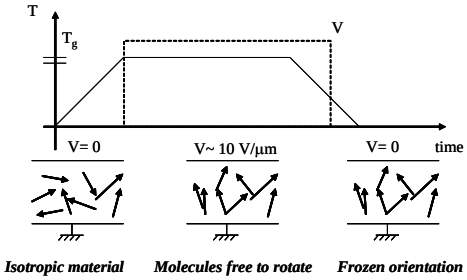

Figure 7-1 Mechanism of the dc-field ordering of the polar molecules covalently tethered to a polymer

The storage of an internal field in a polymeric semi-conductor device should be of significant interest for PV solar cell applications as it will facilitate exciton dissociation. Whereas the efficiency of usual p-n junction devices is limited by the weak extension of the depletion zone (typically 10 to 50 nm)[6], in which the majority of charge separation or recombination processes take place, the depletion zone of polar ordering of push-pull like molecules grafted on a conjugated polymer extends over the whole polymer film thickness. Hence, all photogenerated excitons are likely to find a junction and split before recombination. We have set ourselves a target to introduce push-pull dipoles as side chains on the rigid polyconjugated PPV backbone in order to investigate the molecular orientation concept for PV applications. This study is done in co-operation with the CEA Saclay, France.

- **Direct polymerization routes towards PPV derivatives bearing push-pull like molecules**

The first push-pull-functionalized monomers are prepared using 6-(2,5-bis-chloromethyl-4-methoxy-phenoxy)-hexanoic acid (BCMH-acid), which is

synthesized as described in Chapter 6. BCMH-acid is functionalized with the DπA-molecules 2-((4-nitro-phenyl)-ethyl-amino)ethanol **1**, 4-(N-(2-hydroxyethyl)-N-ethyl)-amino-4'-nitrostilbene **2** and ethyl(4-((4-nitrophenyl)azo)phenyl)amino) ethanol (Disperse Red 1) **3** using Mitsunobu reaction conditions[2] (Scheme 7-1). **1**-**3** are typical DπA-molecules with a donor/transmitter/acceptor structure and possess a large ground state dipole moment μ which is necessary for efficient DC-field orientation.[7] We received these molecules from the CEA Saclay, France.

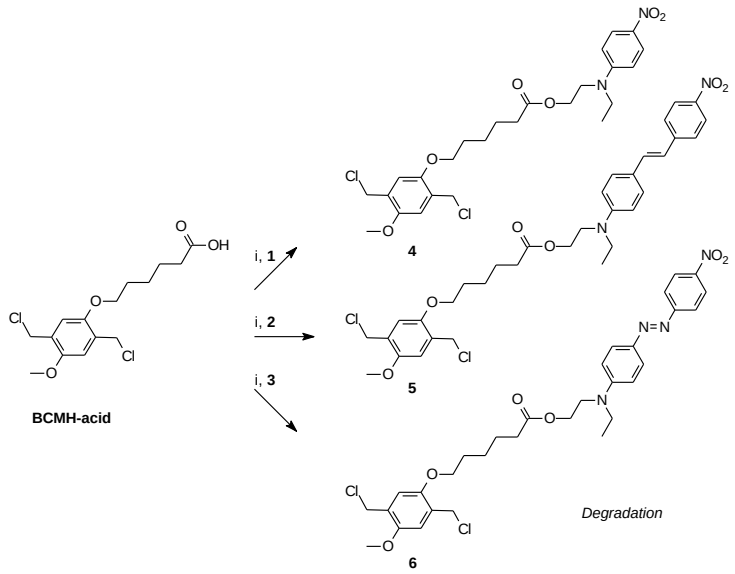

Scheme 7-1 Synthesis of the Gilch monomers functionalized with push-pull molecules **4**-**6** (i: DEAD, PPh_3, THF; **1**: 2-((4-nitro-phenyl)-ethyl-amino)ethanol **2**: 4-(N-(2-hydroxyethyl)-N-ethyl)-amino-4'-nitrostilbene **3**: Disperse Red 1)

After column chromatography, monomer **4** and **5** are obtained as respectively a yellow and a red oil. Pure monomer **6** could not be isolated due to degradation during column chromatography. Monomer **4** and **5** are polymerized according to the standard Gilch polymerization procedure[8] at 98 °C (Scheme 7-2). During the addition of the base (K*t*BuO), the solution turns from bright yellow to black under the formation of dark fumes, *i.e.* decomposition occurs. Lowering the temperature during the Gilch polymerization of monomer **4** leads to the same degradation phenomenon. Therefore, the dithiocarbamate precursor route[9] is tested. To that end, Gilch

monomer **4** is converted to the corresponding dithiocarbamate monomer **7**. In spite of the strong base used during the polymerization reaction, no polymerization is observed. Even at increased temperature using dioxane as the reaction solvent, intact **7** is recovered after reaction (Scheme 7-2).

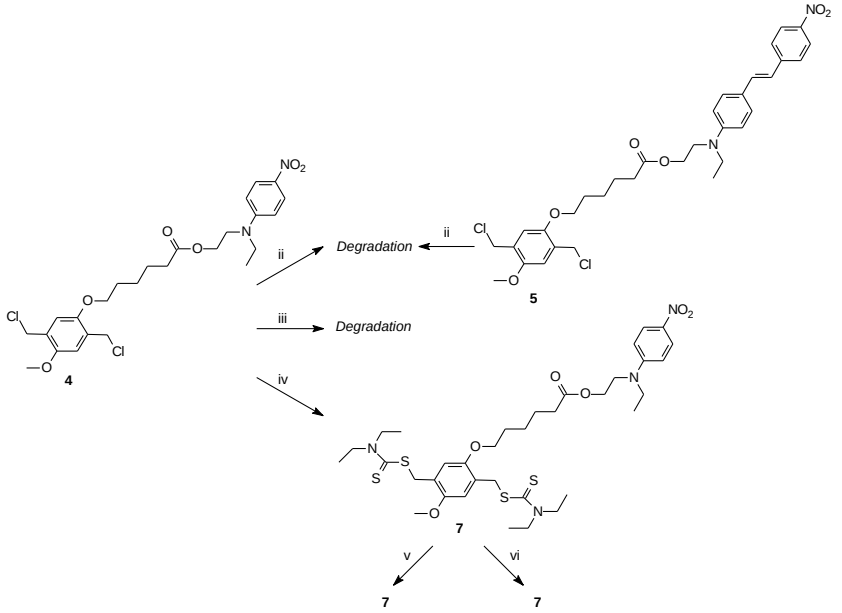

Scheme 7-2 Attempted polymerization of the Gilch monomers **4** and **5** (ii: K*t*BuO, dioxane (dry), 98 °C; iii: K*t*BuO, dioxane (dry), RT); Conversion of **4** to the corresponding dithiocarbamate monomer **7** (iv: $NaSC(S)NEt_2.3H_2O$, EtOH); Attempted polymerization of **7** (v: LDA, THF (dry), RT; vi: LDA, dioxane (dry), 98 °C)

As neither the Gilch nor the dithiocarbamate precursor route is suitable to polymerize the push-pull-functionalized monomers, the versatile sulfinyl precursor route is put to the test. Starting from *p*-(N-butyl-N-2-hydroxyethyl)-nitrobenzene and *p*-hydroxyanisol, sulfinyl monomer **11** is prepared in co-operation with Iris Duyssens (Scheme 7-3). A direct synthesis involving a two-phase reaction with a transfer catalyst (Aliquat 336®) is used to obtain the mono-substituted thioether since the commonly used route *via* the symmetrical α,α'-bissulfonium-*p*-xylene produces only very low yields. Sulfinyl monomer **11** is obtained with high purity in an overall yield of 28 % yield in relation to the dichloride **9**.

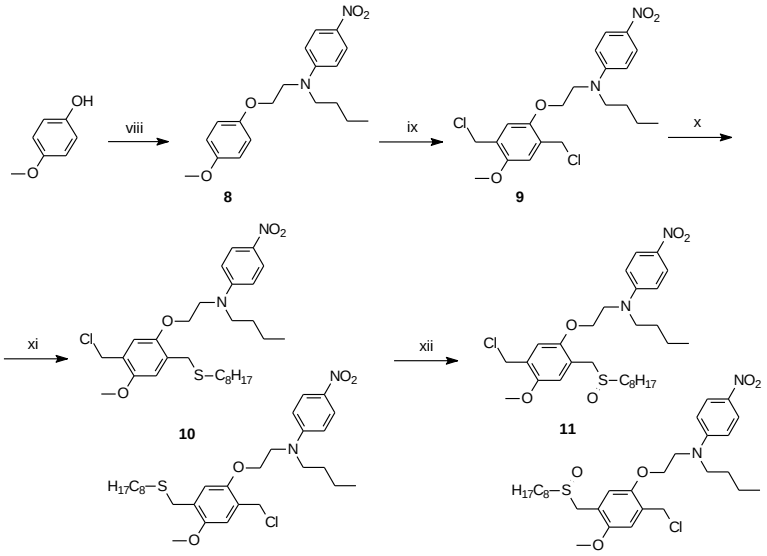

Scheme 7-3 Synthesis of the sulfinyl monomer **11** functionalized with a push-pull molecule (viii: PPh_3, DEAD, *p*-(N-butyl-N-2-hydroxyethyl)-nitrobenzene, diethyl ether; ix: *p*-CH_2O, Ac_2O, HCl, 70 °C; x: $C_8H_{17}SH$, NaOH, Aliquat 336, toluene; xii: H_2O_2, TeO_2, HCl_{cat}, dioxane)

Sulfinyl monomer **11** is polymerized in *sec*-BuOH according to the standard procedure (Scheme 7-4). The final step towards a conjugated PPV derivative functionalized with DπA-molecules is the thermal elimination of the sulfinyl group according to the two-step elimination procedure, as a result of which the precursor polymer **12** converts into the conjugated structure **13** (Scheme 7-4). After conversion, a material insoluble in the common organic solvents is obtained. Refluxing this material in THF yields a soluble fraction with a molecular weight of $M_w = 3.2 \times 10^4$ g/mol. However, this fraction appeared impure and attempts to purify the polymer failed. It should be noted that it has been shown by Iris Duyssens that the copolymerization reaction between the sulfinyl monomer **11** and the monomer towards MDMO-PPV in a ratio of 1:1 yields a soluble conjugated PPV-type copolymer tethering push-pull molecules. However, to obtain the desired homo-polymers, further studies have focused on the post-polymerization functionalization approach (*cf.* section 7.3).

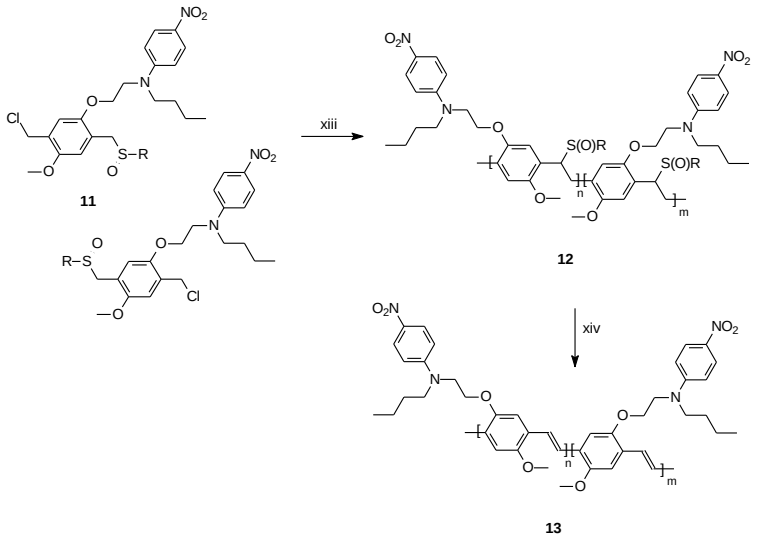

Scheme 7-4 Synthesis of the sulfinyl precursor polymer **12** (xiii: Na*t*BuO, 2-BuOH) and thermal elimination towards the conjugated push-pull-functionalized PPV derivative **13** (xiv: toluene (reflux))

7.2.2 Phthalocyanine-containing PPV derivatives

- **Introduction**

Besides a possible improvement in efficiency of organic solar cells by incorporation of push-pull dipoles as side chains on the conjugated PPV backbone, PPV derivatives bearing phthalocyanine (Pc) molecules as pendant groups are promising candidates for electron and energy transfer processes applied to PV devices. Pc's are planar aromatic macrocycles constituted by four isoindole units linked together through nitrogen atoms.[10] Their 42 π-electrons are distributed over 32 carbon and 8 nitrogen atoms but the electronic delocalization mainly takes place on the inner ring, which is constituted by 16 atoms and 18 π-electrons (Figure 7-2). These molecular materials are characterized by an outstanding stability and high polarizability. The hydrogen atoms of the central cavity can be replaced by more than 70 elements, generating the metallo-phthalocyanines (MPc's).

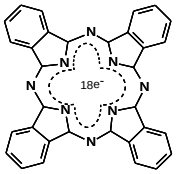

Figure 7-2 Electronic delocalization in phthalocyanines

Pc's show interesting optical properties. Figure 7-3 depicts the electronic absorption spectrum of a MPc. Two main bands are present, *i.e.* the Q-band, located at the 620-700 nm region and responsible for the green-blue colour of these compounds and the Soret or B-band, located between 320 and 360 nm. Especially the high extinction coefficient (log ε is *circa* 5.2) for the absorption of electromagnetic radiation between 620 and 700 nm (Q-band) is intriguing. After all, one of the biggest existing hurdles to reach high-efficiency PV cells with conjugated polymers is the mismatch between the absorption spectrum of the organic semi-conductors and the solar spectrum. The absorption bandwidth of PPV-type materials is too narrow to absorb a large fraction of the solar spectrum. While the photon flux of the AM1.5G solar spectrum peaks around 700 nm, PPV-type polymers absorb strongly over the wavelength range 350-650 nm.[11] Pc's on the other hand, absorb strongly in the area where the photon flux of the AM1.5G solar spectrum peak is maximum. Therefore, they act as efficient antennas which collect the solar light by the harvest of light in the lower energy region of the visible spectrum, leading to a better match with the solar spectrum of the polymers.

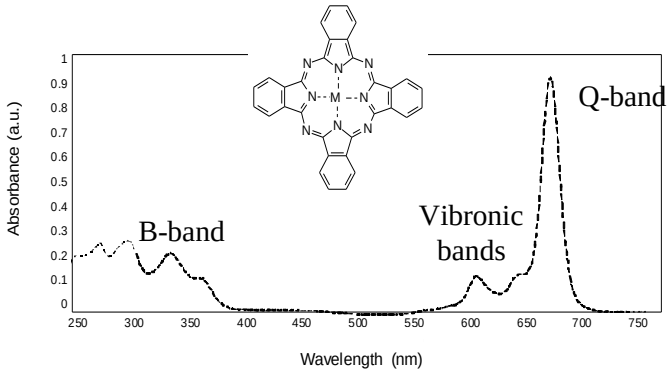

Figure 7-3 Typical UV-Vis spectrum of a MPc (Inset: Chemical structure of a MPc)

In addition, the chemical versatility of Pc-compounds allows different transformations, which give access to a wide variety of materials with different electrochemical properties. By peripheral functionalization with electron-withdrawing groups or substitution of one of the isoindoles by an acceptor heterocyclic unit such as 1,2,4-triazole,[12] electron accepting Pc-components are created. As already mentioned in Chapter 1, a breakthrough in realizing a promising efficient conversion of solar energy into electrical energy has been achieved by using blends of soluble electron donor type conjugated polymers with fullerenes as electron acceptor, transporting component.[13] These bulk heterojunctions still suffer from a morphological instability. An elegant way to overcome these drawbacks is offered by the design and the synthesis of p-type conjugated backbones (*donor-cable*) bearing acceptor groups (*acceptor-cable*). In this way, the effective donor/acceptor interfacial area will be maximized, and phase separation and clustering phenomena should be prevented as well.[14] It is indeed intriguing to think of single materials with intrinsic donor–acceptor properties as well as the capability of both electron and hole transport (p/n-type material) (*double-cable polymer*). Even though fullerenes indicate to be specially interesting electron acceptor materials, the search for other alternative electron accepting components is also being pursued. Such an interesting alternative are the Pc's. By covalently attaching acceptor Pc-molecules to a polymer backbone, the Pc's may play the role of photo-sensitizer, allowing the formation of excitons within the polymeric framework by energy transfer.

As a part of our work towards the functionalization of PPV for application in advanced polymer based devices, we are interested in PPV derivatives with Pc-molecules as side chains on the conjugated backbone. In literature, only a very few examples of Pc-units covalently attached to a polymer backbone have been reported. A recent report describes the preparation of a donor–acceptor copolymer comprising a polythiophene backbone and bearing electron-acceptor Pc-chromophores on the side chains.[15] Although the Pc-content in this literature copolymer necessarily had to be kept low (1/9 molar ratio mixture of the Pc-thiophene monomer and 3-decylthiophene) in order to maintain a sufficient solubility of the material, preliminary studies on the photo-induced charge

transfer properties of these copolymers already provided an indication for a good charge photo-generation arising from the photo-induced electron transfer from the polythiophene backbone to the Pc-moieties.

This research is done in co-operation with the research group of Phthalocyanines and Molecular Materials of the Universidad Autónoma de Madrid (UAM). Pc-functionalized Gilch monomers (Figure 7-4) are synthesized in cooperation with Juan José Cid of the UAM. Pc-monomer **1** and **2** are synthesized starting from the carboxylic acid-functionalized Gilch monomer BCMH-acid as depicted for Pc-monomer **1** in Scheme 7-5. All Pc-monomers are tested in the direct polymerization method using the Gilch precursor route. It may be noticed that only a general description of this research is given. Further details will be presented in the dissertation of Juan José Cid.

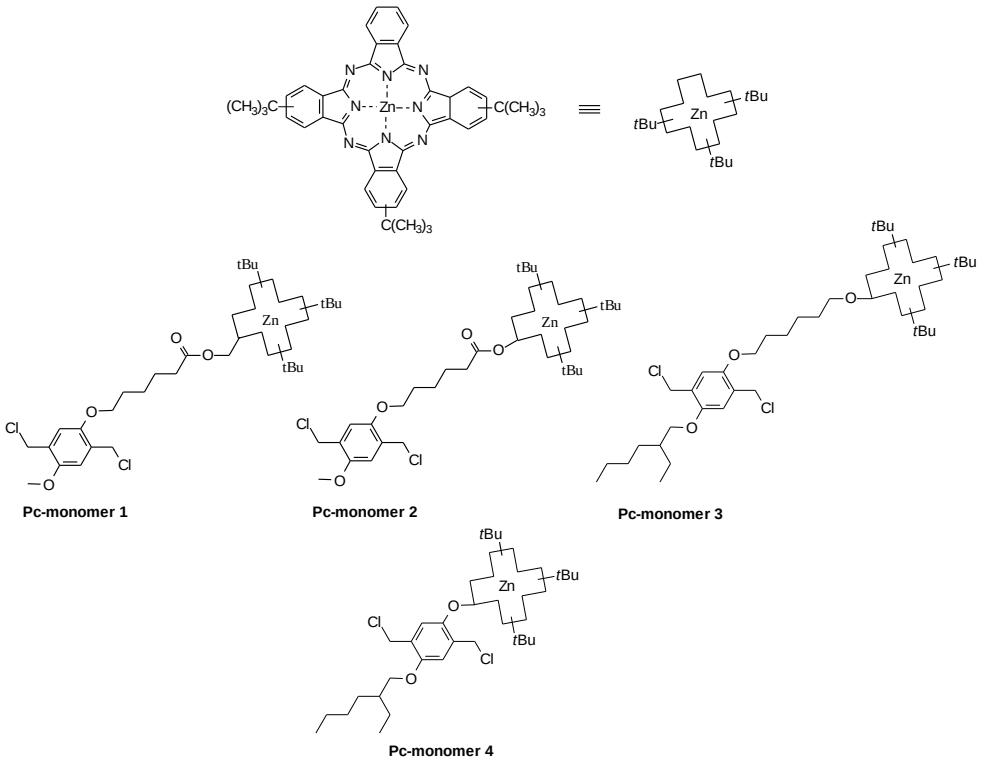

Figure 7-4 Pc-functionalized Gilch monomers

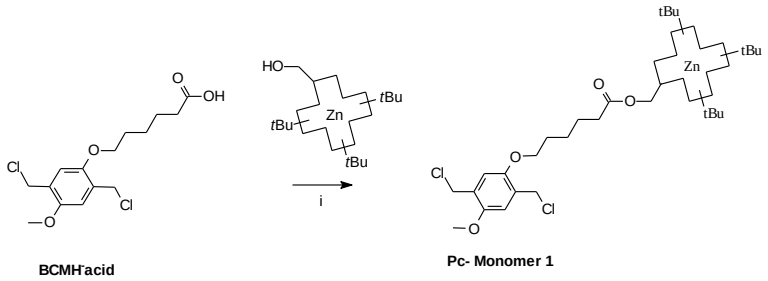

Scheme 7-5 Synthesis of Pc-monomer **1** (i: DCC, DMAP, CH_2Cl_2)

- **Direct polymerization of Pc-functionalized Gilch monomers**

As a first approach towards Pc-functionalized PPV-type polymers, Pc-monomer **1** is brought in typical Gilch polymerization conditions, *i.e.* Pc-monomer **1** is dissolved in dry and degassed 1,4-dioxane under a nitrogen atmosphere (Scheme 7-6). The reaction temperature of the standard Gilch polymerization (98 °C) is lowered to 40 °C. After heating of the monomer solution to 40 °C, *tert*-butoxide dissolved in dry dioxane, is added, followed by addition of a second solution of base. The mixture is allowed to react for three hours and subsequently worked up by precipitation in methanol. The resulting polymer is filtered off and washed thoroughly with methanol, whereupon the methanol turns blue and the polymer more and more red. This is an indication that the ester bond is broken during the polymerization. Indeed, the retention factor (R_f, *i.e.* the distance travelled by the compound on the TLC plate divided by the distance travelled by the solvent) of the blue methanol solution is identical to the R_f value of the starting alcohol-functionalized Pc-compound (depicted in Scheme 7-5). A UV-Vis spectrum of the purified polymer shows a distinct absorption maximum at 482 nm arising from the $\pi-\pi^*$ transition of the conjugated backbone of the polymer, but the typical bands of the Pc-functionalities are absent. Apparently, due to the basic conditions, hydrolysis of the ester takes place mainly, despite the steric hindrance. Similar unwanted side-reactions are observed during the copolymerization reaction of Pc-monomer **1** with the Gilch monomer towards MDMO-PPV (Scheme 7-6).

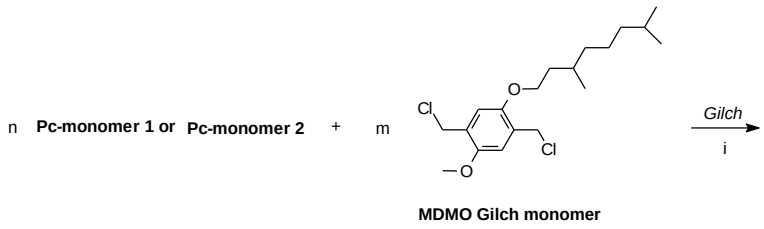

Scheme 7-6 Attempts to (co)polymerize Pc-monomer **1** (i: K*t*BuO, dioxane (dry), 40°C 1. n=1, m=0; 2. m/n=3) and Pc-monomer **2** (i: K*t*BuO, dioxane (dry), 50°C; m/n=3)

Pc-monomer **2** is synthesized with the purpose to increase the steric hindrance of the ester bond in order to circumvent the hydrolysis and favour the polymerization reaction. In a first attempt, Pc-monomer **2** is brought in the typical Gilch polymerization conditions together with the Gilch monomer towards MDMO-PPV in a ratio of 1:3 (Scheme 7-6). The polymerization temperature is lowered to 50 °C. After work-up and washing, a green-red polymer is obtained with a molecular weight of 4.2 x 10^4 g/mol and a polydispersity of 3.8. The UV-Vis spectrum of this polymer not only shows the characteristic PPV at 477 nm, but also the typical Pc-bands (B-band at 349 nm and Q-band at 672 nm) (Figure 7-5). However, the carbonyl absorption of the ester functionality is absent in the FT-IR spectrum. In order to examine if the Pc-compounds are still covalently attached to the PPV repeating units, a GPC analysis with UV–Vis detection using THF as the eluent is performed. Figure 7-6 shows the UV-Vis absorbance of the eluate from the column at two selected wavelengths. Clearly, the distinctly different absorption maxima arising from the π–π* transition of the conjugated backbone of the copolymer (477 nm) and the typical Q-band of the Pc-functionalities (672 nm) appear at different time intervals. The elution of the polymer backbone is observed with a maximum intensity around 16.0 minutes (Figure 7-7). At this time no absorption of the Pc-functionality is observed. This is a clear indication that the Pc's are no longer covalently attached to the PPV backbone. Several other polymerization experiments are performed with Pc-monomer **2** in which reaction time, reaction temperature and comonomer ratios are varied. None of

these polymerizations has led to a PPV-type polymer with Pc-functionalities covalently attached to the backbone.

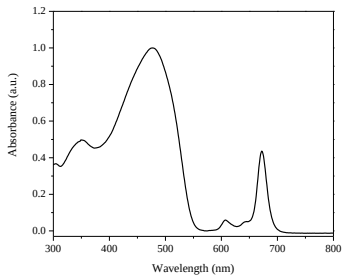

Figure 7-5 Solution UV-Vis absorption spectrum of the copolymer between Pc-monomer **2** and the Gilch monomer towards MDMO-PPV (solvent: THF)

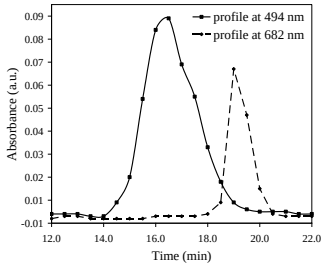

Figure 7-6 SEC chromatograms obtained *via* UV-Vis detection at selected wavelengths of the copolymer between Pc-monomer **2** and the MDMO Gilch monomer (solvent: THF)

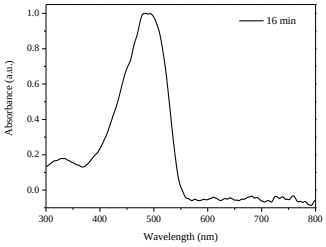

Figure 7-7 SEC chromatogram obtained *via* UV-Vis detection at a selected elution time of the copolymer between Pc-monomer **2** and the MDMO Gilch monomer (solvent: THF)

Obviously, the ester bond is unsuitable for the preparation of Pc-bearing PPV derivatives. Therefore, the ester bond is replaced by the stronger ether bond in the synthesis of Pc-monomer **3** and **4** (Figure 7-4). The copolymerizations of Pc-monomer **3** with the Gilch monomer towards MDMO-PPV are performed under typical Gilch conditions using again lower reaction temperatures (Scheme 7-7). A solution of the comonomers in dry 1,4-dioxane is heated to 50 °C and an excess of base is added in two batches. After polymerization for three hours, the solution is quenched by adding water, a 0.1 M HCl-solution and finally MeOH whereupon a green solid precipitates. Washing the polymer in a Soxhlet extraction with methanol does not cause

colouring of the extraction solvent. However, for both comonomer ratios, a material insoluble in the common organic solvents is obtained.

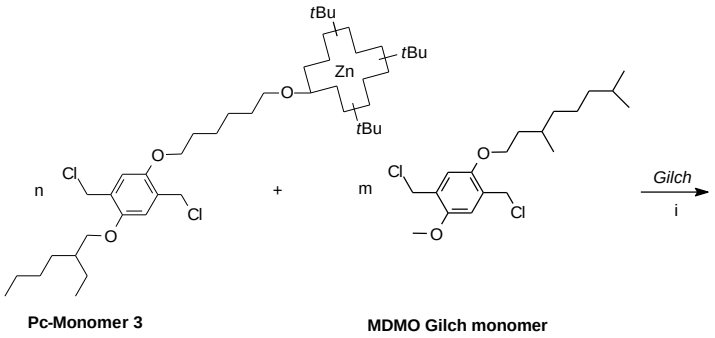

Scheme 7-7 Attempts to polymerize Pc-monomer **3** (i: K*t*BuO, dioxane (dry), 50°C; 1. m/n=2; 2. m/n=4)

Copolymerization of Pc-monomer **4** with the Gilch MDMO-PPV monomer at 40 °C also yields an insoluble material (Scheme 7-8). Homopolymerization reactions of Pc-monomer **4** at different reaction times and temperatures reveal that the solubility increases with increasing reaction time and temperature (Scheme 7-8).

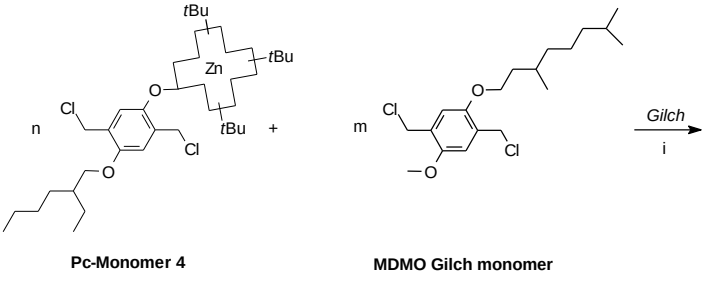

Scheme 7-8 Attempts to polymerize Pc-monomer **4** (i: K*t*BuO, dioxane (dry) 1. m/n=4 40°C 2. n=1; m=0, 50°C, 48 h; 3. n=1; m=0, 98°C, 18 h)

Figure 7-8 shows the UV-Vis absorption spectrum in THF of the polymer obtained after Gilch polymerization at 98°C for 18 hours. The $\pi-\pi*$ transition of the conjugated PPV backbone appears as a shoulder (*circa* 480 nm) of the broad Soret-band of the Pc-functionality (342 nm). Also the typical Q-band (688 nm) is broadened. This can be an indication of aggregate formation, either

with the π-conjugated polymer backbone or with other Pc-functionalities. GPC analysis with UV–Vis detection using THF as the eluent is performed in order to examine if the Pc-compounds are covalently attached to the PPV backbone. Figure 7-9 shows the UV-Vis absorbance of the eluate from the column at different elution times. The distinctly different absorption maxima arising from the π–π* transition of the conjugated backbone of and the typical Q-band of the Pc-functionalities appear at different time intervals (Figure 7-9 and Figure 7-10). The elution of the PPV backbone is observed with a maximum intensity around 17.5 minutes (Figure 7-11), which corresponds to a molecular weight of 1.0 x 10^5 g/mol. At this time only a small absorption of the Pc-functionality is observed.

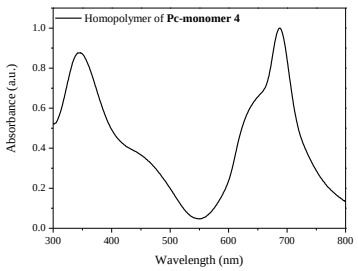

Figure 7-8 UV-Vis absorption spectrum in THF of the homopolymer of Pc-monomer **4**

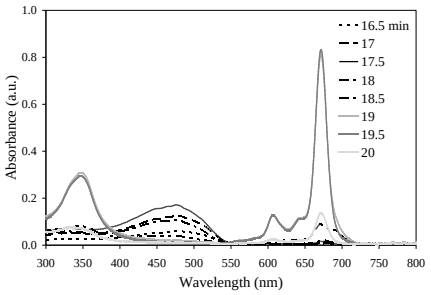

Figure 7-9 SEC chromatograms obtained *via* UV-Vis detection in THF of the homopolymer of Pc-monomer **4**

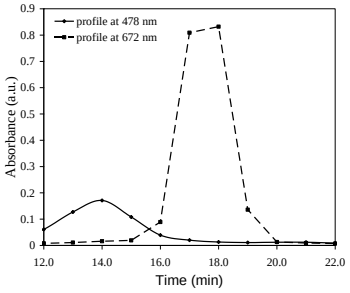

Figure 7-10 SEC chromatograms obtained *via* UV-Vis detection in THF at selected wavelengths of the homopolymer of Pc-monomer **4**

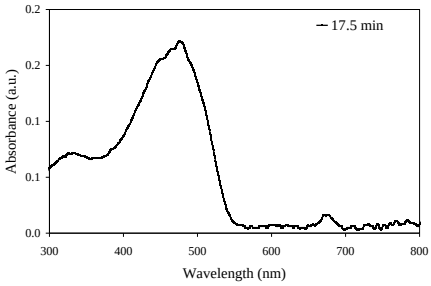

Figure 7-11 SEC chromatogram obtained *via* UV-Vis detection in THF at a selected elution time of the homopolymer of Pc-monomer **4**

We can use the Beer-Lambert law (Abs_{max}= ε_{max} x c x l) to determine the ratio of Pc-functionalities which are still covalently attached to the PPV

repeating units. After all, the concentration of Pc-functionalities (c) covalently attached to the polymer is directly proportional to the maximum absorbance (Abs_{max}) at 688 nm in Figure 7-11, the path length of the sample (l) and the molar extinction coefficient (ε_{max}) of the Pc at peak maximum in the solvent used. The extinction coefficient ε_{max} of MDMO-PPV is 31000 M^{-1} cm^{-1} (log ε_{max}= 4.5) in THF, as determined by means of UV-Vis spectroscopy. The ε_{max} value of the Pc-functionality in THF, on the other hand, is 230000 M^{-1} cm^{-1} (log ε_{max}= 5.4). Using these values for ε_{max} and the maximum absorbances at 480 nm and 688 nm, we can derive the values for the concentration of respectively the repeating units of the PPV backbone and the Pc-functionalities. The ratio of these concentrations determines the amount of Pc's covalently attached to the PPV backbone. A substitution ratio of approximately 1.2 % is found. Although unexpected from scientific point of view, everything seems to indicate that the strong ether bond does not survive the polymerization at 98 °C.

Clearly, the reaction conditions of the direct polymerization of Pc-functionalized monomers are still far from optimal and a lot of effort and study are necessary before all questions and problems are solved and well-defined Pc-bearing PPV derivatives are obtained. However, as will be demonstrated in section 7.3, the post-polymerization functionalization method might offer a straightforward alternative approach.

7.3 Post-polymerization functionalization of CPM-PPV towards complex ester-functionalized PPV-type polymers

7.3.1 Using Mitsunobu reaction conditions[a]

In 1967 Mitsunobu and Yamada reported that carboxylic acids can be esterified with primary and secondary alcohols using the redox system diethyl azodicarboxylate (DEAD) and triphenylphosphine.[2] The reaction was reviewed

[a] Part of this section was published in *Polymer* **2005**, *46*, 5466-5475.

by Mitsunobu in 1981,[16] and since then its use in organic synthesis has mushroomed, as evidenced by more than 2000 citations of the Mitsunobu papers. The compatibility of the reaction conditions with a wide range of functional groups and the simplicity of the experimental protocol are primary reasons for the popularity the reaction has enjoyed. Although the reaction is discovered almost four decades ago, new applications are still being found.

A possible application of this route is the reaction of the carboxylic acid function of CPM-PPV with alcohol-functionalized molecules. In order to test this, a solution of CPM-PPV in dry THF is cooled to 0°C. To this solution an alcohol-functionalized molecule and triphenylphosphine are added. Subsequently DEAD is slowly dripped. The mixture is then allowed to warm to room temperature over a period of 2 h and stirred at room temperature for an additional 24 h, after which the reaction mixture is added drop wise to a non-solvent and filtered off. Four hydroxy-bearing model compounds are used: 5-(hydroxymethyl)furfural, 2-nitrobenzylalcohol, 4-nitrobenzylalcohol and 3-N,N-dimethylamino-1-propanol to yield respectively the ester-substituted polymers **A**, **B**, **C** and **D** (Scheme 7-9).

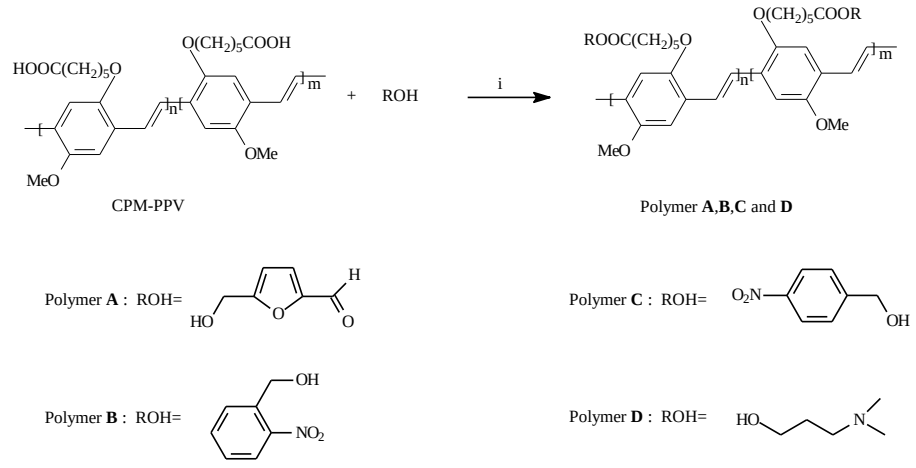

Scheme 7-9 General scheme of the synthesis of the grafted polymers **A-D** *via* the Mitsunobu reaction (i: DEAD, PPh_3, THF)

The solubility of **A-D** is limited, with polymer **D** being entirely insoluble in common organic solvents. Therefore it is difficult to fully characterize the new

ester-functionalized PPV derivatives. However, the quantitative functional group substitution after post-polymerization functionalization of CPM-PPV can be proven by comparison of the FT-IR-spectra. As shown in Figure 7-12, the carbonyl absorption at 1709 cm^{-1} of the carboxylic acid shifts to higher frequency upon formation of the ester bond in polymers **A**-**D** (1725 cm^{-1}- 1739 cm^{-1}). In addition, it should be noted that the broad band centered at 2800 cm^{-1} of the OH-stretch has entirely disappeared in the FT-IR spectra of the ester-functionalized PPV derivatives **A**-**D**. Furthermore, all the characteristic bands corresponding to the functional groups in the new ester-substituted polymers are present:

- The band at 1680 cm^{-1} in polymer **A** corresponds to the stretching vibrations of the carbonyl group of the α,β-unsaturated aldehyde and the band at 1522 cm^{-1} corresponds to the absorption of the hetero-aromatic ring.
- The band at 1613 cm^{-1} in polymer **B** corresponds to the attached phenyl group. In addition, the two bands at 1528 cm^{-1} and 1343 cm^{-1} are typical for a conjugated nitro-group.
- Similar to polymer **B**, the spectrum of polymer **C** displays a band at 1606 cm^{-1} and two bands at 1520 cm^{-1} and 1341 cm^{-1}.

Hence, all FT-IR spectra are consistent with a full conversion of the carboxylic acid functionalities.

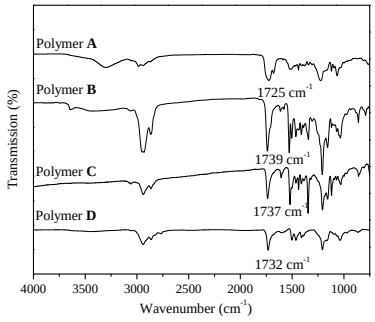

Figure 7-12 FT-IR spectra of the polymers **A**, **B**, **C** and **D**

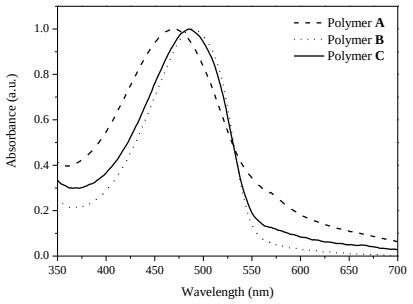

Figure 7-13 Solution UV-Vis absorption spectra of **A**, **B** and **C** (solvent THF)

The apparent molecular weights as observed by SEC of the soluble ester-functionalized PPV derivatives **A**, **B** and **C** (1.3 x 10^4 g/mol, 5.1 x 10^4 g/mol and 1.8 x 10^4 g/mol respectively, *cf.* experimental section) are lower than the molecular weight found for the carboxy-substituted PPV derivative CPM-PPV (2.2 x 10^5 g/mol, *cf.* Chapter 6). However, it should be noted that strong tailing is observed in the SEC analysis indicating that the grafted polymers **A-C** exhibit interactions with the SEC column. Such interactions result in a lower apparent molecular weight. Hence, the apparent molecular weights are unsuitable to judge the presence or absence of substantial polymer degradation during the Mitsunobu reaction. To resolve this issue, two additional experiments have been performed.

In the first experiment, the well-known MDMO-PPV, which does not contain the carboxylic acid functionalities, is subjected to the same Mitsunobu conditions as used for the preparation of the ester-functionalized PPV-type polymers **A-C**. 4-Nitrobenzylalcohol is used as the alcohol-functionalized molecule (Scheme 7-10). A SEC analysis before and after this treatment yields no significant changes in the molecular weight of MDMO-PPV, indicating that the conjugated structure of MDMO-PPV is not affected by the reaction conditions.

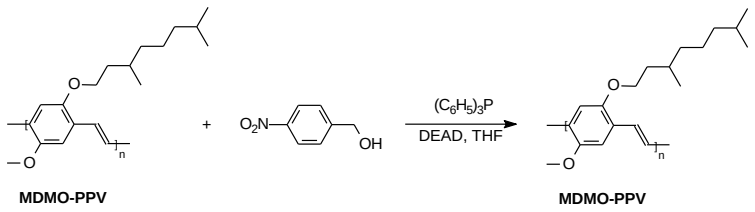

Scheme 7-10 MDMO-PPV in the Mitsunobu reaction

In a second experiment, the furfural containing polymer **A** is subjected to basic hydrolysis (Scheme 7-11). Analytical FT-IR data confirm the full hydrolysis of the ester side groups, giving back the carboxylic acid-substituted polymer CPM-PPV (Figure 7-14). The analytical SEC result of this recovered CPM-PPV exhibits an increase in apparent molecular weight as compared to polymer **A**, although the final molecular weight remains lower than that

observed for the original CPM-PPV. Notwithstanding, this increase in apparent molecular weight further corroborates our observation that the anomalous analytical SEC results of the ester-functionalized polymers **A-C** are likely the result of column interactions during SEC analysis.

To further confirm the presence of the conjugated system in the grafted PPV derivatives **A-C**, UV-Vis solution spectra are made (Figure 7-13). The shape and peak positions of λ_{max} are strongly dependent on the solvent used as a result of solubility issues. In THF solution for polymers **A-C** well defined transitions are observed at λ_{max} = 469, 488 and 486 nm respectively, which is in the same spectral region as the transition observed for CPM-PPV. This observation further confirms our finding that no substantial degradation of the conjugated system occurs during the Mitsunobu reaction.

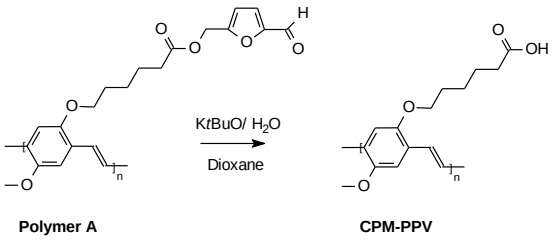

Scheme 7-11 Hydrolysis of polymer **A** towards CPM-PPV

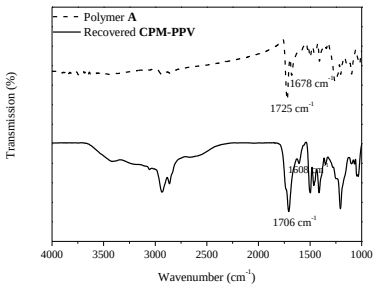

Figure 7-14 FT-IR spectra of polymer **A** and 'recovered' CPM-PPV obtained by hydrolysis of **A**

From the previous observations it can be concluded that the Mitsunobu reaction conditions can be used to graft the carboxylic acid functionalities of CPM-PPV with more complex alcohol-functionalized molecules. This makes

the Mitsunobu reaction worthwhile to test as an approach to tether push-pull substituents to CPM-PPV. 4-(N-(2-Hydroxyethyl)-N-ethyl)-amino-4'-nitrostilbene is used as the active polar molecule. In order to graft CPM-PPV with this DπA-molecule, a solution of CPM-PPV in dry dioxane is cooled to 15 °C. Then the push-pull molecule and triphenylphosphine are added to the solution. Subsequently DEAD is slowly dripped (Scheme 7-12). The mixture is allowed to warm to room temperature and stirred for 24 h, after which the reaction mixture is added drop wise to diethyl ether. The push-pull molecule-substituted PPV derivative is filtered off and purified using a Soxhlet extraction with diethyl ether as the extraction solvent.

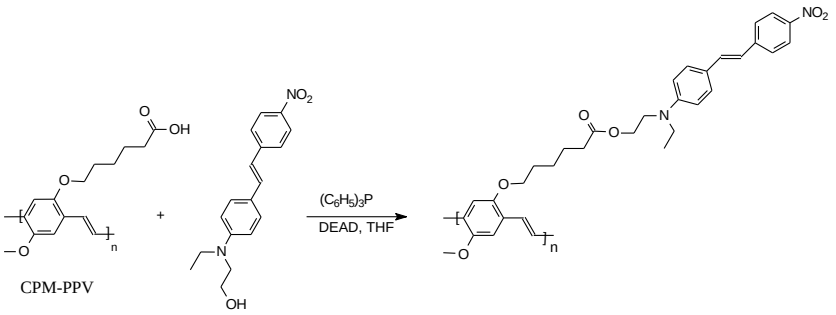

Scheme 7-12 Grafting of CPM-PPV with push-pull molecules using the Mitsunobu reaction conditions

The grafting of the carboxy-substituted polymer is confirmed by comparison of the FT-IR-spectra of CPM-PPV, the DπA-molecule and the PPV derivative after the Mitsunobu reaction. As shown in Figure 7-15, the carbonyl absorption at 1708 cm^{-1} of the carboxylic acid shifts to higher frequency upon formation of the ester bond (1729 cm^{-1}). In addition, all the characteristic bands corresponding to the push-pull functional groups in the new ester-substituted polymer are present: The band at 1608 cm^{-1} corresponds to the attached phenyl group. In addition, the two bands at 1522 cm^{-1} and 1336 cm^{-1} are typical for a conjugated nitro-group. Molecular weight determination by SEC in DMF against polystyrene gives a molecular weight of 3.0 x 10^5 g/mol. Strong tailing in the SEC results suggests that the grafted polymer interacts with the SEC column, which implicates that the apparent molecular

weight is unreliable. The push-pull-grafted PPV derivative shows a broad transition in the UV-Vis spectrum with a maximum absorbance at a wavelength at *circa* 450 nm in film. The glass transition temperature of this functionalized PPV derivative grafted with DπA-molecules is 110 °C as determined by Differential Scanning Calorimetry measurements. This is substantially higher than the T_g observed for CPM-PPV (51 °C). This may be attributed to the increased steric hindrance caused by the bulky push-pull side chains. The obtained T_g is sufficiently high to maintain a stable dipole alignment after dc-field ordering of the polar molecules. Currently, the molecular orientation concept for photovoltaic applications is investigated in co-operation with the CEA Saclay, France.

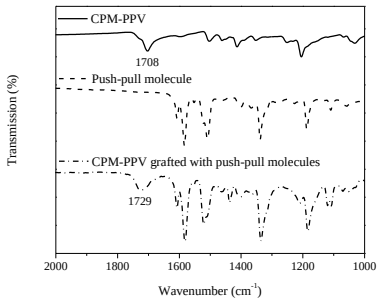

Figure 7-15 Detailed FT-IR spectrum of the starting compounds and the grafted polymer

7.3.2 Using DCC/DMAP-esterification method

Notwithstanding the first results of the application of the Mitsunobu reaction are a good proof of principle for the possibility of post-polymerization functionalization of CPM-PPV, there is still room left for improvement. In order to overcome solubility problems and enhance the reproducibility, the so-called DCC/DMAP-esterification method is put to the test. This carbodiimide coupling reaction is a mild one pot esterification method, in which carboxylic acid groups are converted *in situ* by N,N-dicyclohexylcarbodiimide (DCC) to an anhydride-type of functionality that reacts with the alcohol to the corresponding ester at room temperature under neutral conditions.[17] Addition

of N,N-dimethyl-4-aminopyridine (DMAP) accelerates the DCC-activated esterification of carboxylic acids with alcohols to such an extent that formation of side products is suppressed and even sterically esters are formed in good yields at room temperature.[18]

In order to allow a proper comparison with the post-polymerization functionalization results obtained *via* the Mitsunobu reaction, CPM-PPV is grafted with the same hydroxy-bearing model compounds as shown in Scheme 7-9, using the DCC/DMAP-esterification method. The esterification reactions are conducted in CH_2Cl_2 under argon atmosphere. To a solution of CPM-PPV and the respective alcohol-functionalized reagent, DCC and DMAP are added as effective esterification promoting agents. The reactions are allowed to proceed for 1 h at 0 °C and for an additional 24 h at room temperature after which the solutions are precipitated drop wise to a non-solvent. The resulting polymers **A'-C'** are filtered off, washed and dried under reduced pressure. The successful conversion is proven using FT-IR spectroscopy, since the carbonyl absorption at 1709 cm^{-1} of the carboxylic acid shifts to higher frequency upon formation of the ester bond in **A'-C'**. The DCC-activation method appears straightforward and reproducible. Contrary to the Mitsunobu reaction, this esterification method does not suffer from solubility problems, so this time, the quantitative functional group substitution of the soluble polymers **A'**, **B'** and **C'** can be further confirmed using ^{1}H NMR spectroscopy. For all three polymers, a characteristic peak is found around δ= 5.1-5.4 ppm, for the protons of the COOCH_2-R groups. In addition, all characteristic peaks for the attached substituents are present (see experimental section). Although the ^{1}H NMR peaks are broad due to the polymeric nature of **A'-C'**, integration of the signals is consistent with a quantitative conversion of the carboxylic acid functionalities to the corresponding esters.

7.3.3 Using the DCC/DMAP-esterification reaction for the preparation of Pc-containing PPV derivatives

In the previous section, it is demonstrated that the DCC/DMAP-esterification reaction allows for the grafting of model compounds to a PPV backbone. Hence, a preliminary experiment was conducted to assess whether it is possible to prepare Pc-containing PPV-type polymers *via* this method. Since Pc-functionalities are bulky molecules, a copolymer of CPM-PPV is used (Scheme 7-13; molar ratio of *circa* 42% acid-functionalized repeating units and and *circa* 58% MDMO-monomer as determined by NMR spectroscopy). Hydroxymethyl phthalocyanine, prepared by our collaborators at UAM, is used as the alcohol-functionalized reagent in the DCC/DMAP-esterification reaction. The coupling reaction is conducted in dry THF for 3 days. After precipitation in methanol, the resulting (MDMO-Pc)-PPV polymer is washed in a Soxhlet extraction using methanol as the extraction solvent. Subsequently, THF is used as the extraction solvent in a Soxhlet extraction, so that a soluble polymeric fraction is obtained after redistillation of the solution in the flask. This soluble polymer is used for analysis.

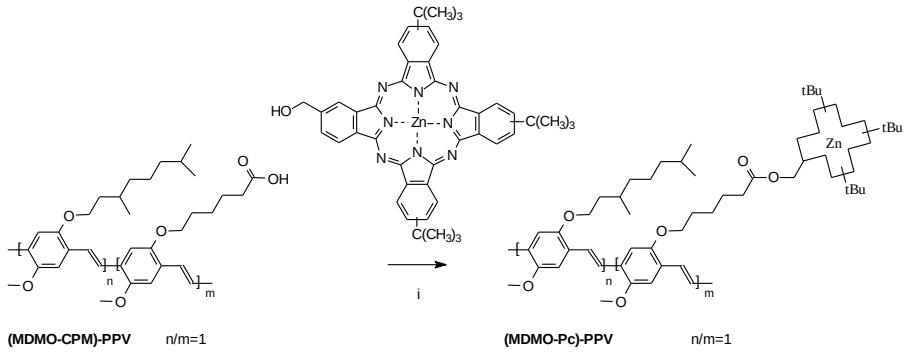

Scheme 7-13 Grafting of phthalocyanine-functionalities on (MDMO-CPM)-PPV *via* the DCC/DMAP-esterification method (i: DCC, DMAP, THF)

The successful conversion is proven by FT-IR spectroscopy. The FT-IR spectra show that the carbonyl absorption at 1709 cm^{-1} of the carboxylic acid functionalities of (MDMO-CPM)-PPV shifts to 1730 cm^{-1} upon formation of the ester bond in (MDMO-Pc)-PPV. An unambiguous proof that the Pc-

functionalities are covalently attached to the PPV backbone comes from a GPC analysis with UV–Vis detection using THF as the eluent. Figure 7-16 shows the UV-Vis absorbance of the eluate from the GPC column at different selected elution times. Clearly, the distinctly different absorption maxima arising from the $\pi-\pi*$ transition of the conjugated backbone of the copolymer (494 nm) as well as the typical Q-band of the Pc-functionalities (672 nm) appear and disappear simultaneous, indicating that the Pc's are covalently attached to the PPV backbone. The elution of the Pc-grafted copolymer is observed with a maximum intensity around 16.0 minutes (Figure 7-17), which corresponds to a molecular weight of 9.8×10^4 g/mol.

We can again apply Beer's law to determine the ratio of Pc-functionalities covalently built in the copolymer. The molar extinction coefficient ε_{max} of (MDMO-CPM)-PPV in THF is 28000 $M^{-1} cm^{-1}$ ($\log \varepsilon_{max} = 4.4$), as is determined from a Beer's law plot. Using the ε_{max} values and the maximum absorbances at 494 nm and 672 nm, we can derive the values for the concentration of respectively the repeating units of the PPV backbone and the Pc-functionalities. The substitution ratio derived in this manner is 9 %, whereas theoretically 42 % would have been possible based on the composition of the starting copolymer. Although this implicates that the post-polymerization functionalization of (MDMO-CPM)-PPV with Pc-functionalities is not yet quantitative, this method still forms a significant improvement compared to direct polymerization of Pc-functionalized monomers. Besides, this substitution ratio already is comparable with the Pc-content of the polythiophene copolymer prepared in literature (1/9 molar ratio mixture of the Pc-thiophene monomer and 3-decylthiophene).[15] In addition, it should be noted that the above results originate from a preliminary experiment. Hence, undoubtedly further improvements are possible.

As is evident from Figure 7-18, a smaller fraction of the phthalocyanine-functionality is eluted around 19.5 minutes, which is an indication that a part the starting Pc-compound is still present in the sample, in spite of the thorough purification by Soxhlet extraction. In order to remove this starting material and obtain a polymeric fraction with a low polydispersity, gel permeation

chromatographic separation on Biobeads® S-X beads using THF as eluent might be a viable solution. Still, the presence of the unreacted Pc-functionalities in the Soxhlet-purified polymer sample can be to our advantage since it forms an indication that Pc-molecules interact *via* π–π stacking with the Pc-macrocycles covalently attached to the PPV backbone. Therefore, it may be possible that the addition of more Pc-molecules to a Pc-containing copolymer causes π–π stacking phenomena of the additional Pc-molecules with the covalently attached Pc-units in the PPV-material which could mean a further enhancement of the promising electron and energy transfer processes of the Pc-molecules.

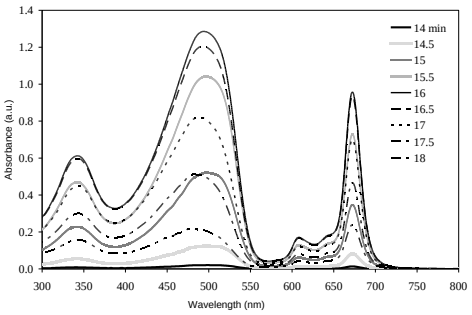

Figure 7-16 SEC elution curves of (MDMO-Pc)-PPV obtained *via* UV-Vis detection

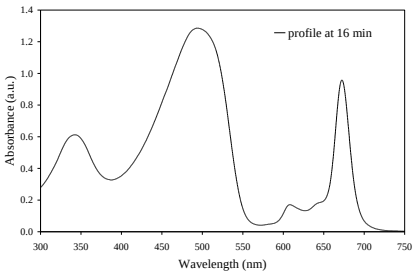

Figure 7-17 SEC chromatogram of (MDMO-Pc)-PPV obtained *via* UV-Vis detection at a selected elution time (solvent: THF)

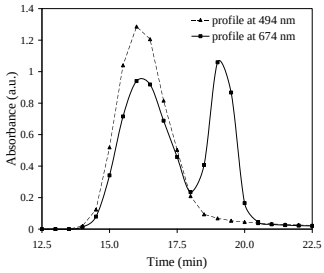

Figure 7-18 SEC chromatograms of (MDMO-Pc)-PPV obtained *via* UV-Vis detection at selected wavelengths (solvent: THF)

7.4 Post-polymerization functionalization of (MDMO-CPM)-PPV towards amide-functionalized PPV-type polymers

Amide-functionalized PPV-type polymers are extremely rare in literature. To our very best knowledge, literature on PPV derivatives bearing amide-functionalities is restricted to oligo(*p*-phenylene vinylene) derivatives bearing amide end groups[19] and a copolymer containing PPV conjugated blocks and poly(acrylamide) segments.[20] In this section, a straightforward manner is described to obtain PPV-type polymers containing amide-groups in the side chains starting from the carboxylic acid-bearing (co)polymers prepared in chapter 6. In view of the large amount of various amines commercially available, the post-polymerisation functionalization is a very interesting and versatile approach to prepare a multiplicity of amide-functionalized PPV derivatives. Furthermore, as will be described in chapter 8, this method is very promising for the preparation of antibody-functionalized PPV-type polymers for application as transducer layer in a biosensor.

Initial results which are obtained in co-operation with Dr. Jérôme Husson confirm that amide-functionalized PPV-type polymers can be prepared by post-polymerization functionalization of carboxylic acid containing PPV derivatives using a large excess of an amine-functionalized molecule and a coupling reagent X[b] in THF for 144 hours. By-products generated during the course of the reaction are water-soluble, contrary to the polymer. Therefore by-products and excess reagents are easily removed by precipitation of the amide-bearing polymer in a MeOH/water-solution. Scheme 7-14 depicts the conversion of the carboxylic acid side groups of (MDMO-CPM)-PPV into amide-functionalities using di-n-butylamine as the amine-functionalized reagent. The reaction proceeds under mild conditions and with high yields (>90 %). Effectiveness of the procedure is demonstrated by NMR analysis (see experimental section) and

[b] Since currently, a procedure is in progress to patent this approach, no details on the coupling reagent are given

FT-IR spectroscopy (Figure 7-19). The carbonyl absorption at 1709 cm^{-1} is completely absent after functionalization with the amine groups, which confirms a quantitative conversion. In addition, the spectrum shows the strong carbonyl absorption of a tertiary amide at 1645 cm^{-1}. Furthermore, no substantial degradation of the conjugated system occurs during the amide-functionalization reaction since no significant changes are observed in the molecular weight. This is further corroborated by the shape and peak positions of the UV-Vis spectra. A well-defined transition is observed at λ_{max} = 500 nm for the amide-functionalized copolymer in $CHCl_3$ solution (Figure 7-20), which is in the same spectral region as the transition observed for the starting (MDMO-CPM)-PPV.

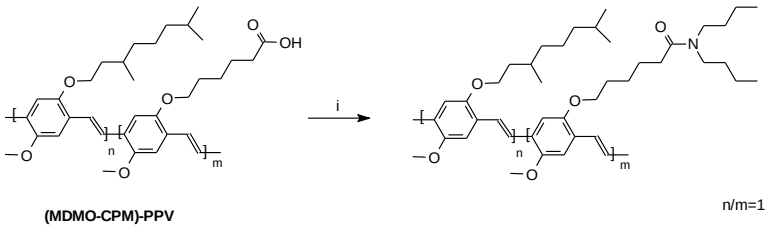

Scheme 7-14 Synthesis of an amide-functionalized PPV-type polymer by post-functionalization in solution (i: di-n-butylamine, coupling reagent X, THF, 144 h)

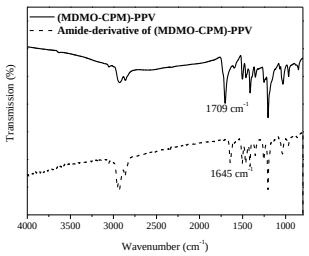

Figure 7-19 FT-IR spectra of (MDMO-CPM)-PPV before and after post-polymerization functionalization with dibutylamine

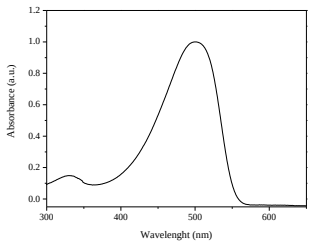

Figure 7-20 Solution UV-Vis absorption spectra of the amide-bearing PPV copolymer (solvent $CHCl_3$)

For the moment excess amine and coupling reagent are used to insure a quantitative conversion. Experiments are currently in progress in order to reduce the amount of reagents. This optimization is necessary to make the protocol suitable for more expensive amine-functionalized molecules.

7.5 Conclusions

In this chapter it has been demonstrated that poly(1,4-(2-(5-carboxypentyloxy)-5-methoxy phenylene)vinylene) (CPM-PPV) and copolymers of CPM-PPV form an excellent starting platform to obtain polar functionalized PPV derivatives with more complex tailored substituents *via* post-polymerization functionalization of the carboxylic acid side groups. Using the Mitsunobu reaction conditions, various substituents were covalently attached to the PPV backbone in a quantitative way *via* an ester linkage. Further improvements were achieved using the DCC activation method. This method even showed promising results for the covalent tethering of phthalocyanine molecules onto the PPV backbone. In addition, it has been demonstrated that amide-functionalized PPV-type polymers can be prepared by post-polymerization functionalization of the carboxylic acid containing PPV derivatives.

7.6 Experimental Section

Chemical and optical characterization.

NMR spectra were recorded with a Varian Inova Spectrometer at 300 MHz for ^{1}H NMR and at 75 MHz for ^{13}C NMR. Analytical Size Exclusion Chromatography (SEC) was performed using a Spectra series P100 (Spectra Physics) pump equipped with a pre-column (5 μm, 50 mm*7.5 mm, guard, Polymer Labs) and two mixed-B columns (10 μm, 2x300 mm*7.5 mm, Polymer Labs) and a Refractive Index (RI) detector (Shodex) at 40°C. For the phthalocyanine-functionalized PPV-type polymers, an Ocean Optics USB2000

UV-Vis absorbance detector equipped with a Z-type flow cell was used during the Size Exclusion Chromatography. Either THF or DMF was used as the eluent at a flow rate of 1.0 mL/min. Molecular weight distributions are given relative to polystyrene standards. Differential Scanning Calorimetry measurements were performed on a TA instruments DSC 2920. The samples (10 mg) were heated from -100 °C to 150 °C at a heating rate of 10 °C/min under N_2 atmosphere. GC-MS data were obtained with a Varian TSQ 3400 Gas Chromatograph and a TSQ 700 Finnigan Mat mass spectrometer. UV-Vis measurements were performed on a Cary 500 UV-Vis-NIR spectrophotometer (scan rate 600 nm/min, continuous run from 200 to 800 nm). FT-IR spectra were collected with a Perkin Elmer Spectrum One FT-IR spectrometer (nominal resolution 4 cm^{-1}, summation of 16 scans). Fluorescence spectra were obtained with a Perkin Elmer LS-5B luminescence spectrometer. Elemental analysis was performed with a Flash EA 1112 Series CHNS-O analyzer. All chemicals were purchased from Aldrich or Acros and used without further purification. Tetrahydrofuran (THF) and dioxane were distilled from sodium/benzophenone. Dichloromethane (CH_2Cl_2) was dried by distillation from phosphorus pentoxide.

Synthesis

Direct polymerization of complex functionalized monomers

6-(2,5-Bis-chloromethyl-4-methoxy-phenoxy)-hexanoic acid. This Gilch monomer was prepared and characterized as described in Chapter 6.

6-(2,5-Bis-chloromethyl-4-methoxy-phenoxy)-hexanoic acid 2-(ethyl-(4-nitro-phenyl)-amino)-ethyl ester 4. A solution of 6-(2,5-bis-chloromethyl-4-methoxy-phenoxy)-hexanoic acid (1.3 g, 3.81 mmol) in dry THF (40 mL) was cooled to 0 °C under Ar atmosphere. To this solution 2-((4-nitro-phenyl)-ethyl-amino)ethanol 1 (0.8 g, 3.81 mmol) and triphenylphosphine (1.2 g, 4.57 mmol) were added and the mixture was stirred for 10 min. Subsequently diethyl azodicarboxylate (0.9 mL, 4.57 mmol) was slowly added *via* a syringe. The mixture was allowed to warm to room temperature over a period of 2 h and stirred at room temperature for an additional 24 h after which the reaction

mixture was added to H_2O (200 mL) and extracted with CH_2Cl_2 (3 x 150 mL). The combined organic extracts were dried over anhydrous $MgSO_4$. Evaporation of the solvent under reduced pressure gave the crude product. The pure product was obtained by column chromatography (SiO_2, eluent CH_2Cl_2) as a yellow oil (1.3 g, 62 % yield). ^{1}H NMR ($CDCl_3$): δ= 8.11 + 8.07 (d, 2H), 6.89 + 6.88 (d, 2H), 6.68 + 6.64 (d, 2H), 4.61+4.60 (2s, 4H), 4.25 (t, 2H), 3.95 (t, 2H), 3.83 (s, 3H), 3.64 (t, 2H), 3.48 (q, 2H), 2.32 (t, 2H), 1.78 (m, 2H), 1.66 (m, 2H), 1.49 (m, 2H), 1.21 (t, 3H); FT-IR (NaCl, cm^{-1}): 2937, 2869, 1735 (ν_{c-o}), 1596 (ν_{NO2}), 1511, 1411, 1316 (ν_{NO2}), 1275, 1219, 1113, 1032, 827, 753.

6-(2,5-Bis-chloromethyl-4-methoxy-phenoxy)-hexanoic acid 2-(ethyl-(4-(2-(4-nitro-phenyl)-vinyl)-phenyl)-amino)-ethyl ester 5. This Gilch monomer was prepared following the same procedure as described for **4** using 4-(N-(2-hydroxyethyl)-N-ethyl)-amino-4'-nitrostilbene 2 (0.6 g, 2.1 mmol) as the alcohol-functionalized molecule in the reaction. Pure **5** was obtained by column chromatography (SiO_2, eluent CH_2Cl_2) as a red oil (0.76 g, 58 % yield). ^{1}H NMR ($CDCl_3$): δ= 8.17 + 8.13 (d, 2H), 7.56+ 7.52 (d, 2H), 7.43 + 7.40 (d, 2H), 7.24 + 7.21 (d, 2H), 6.90 + 6.89 (d, 2H), 6.68 + 6.64 (d, 2H), 4.60+4.59 (2s, 4H), 4.23 (t, 2H), 3.94 (t, 2H), 3.82 (s, 3H), 3.64 (t, 2H), 3.47 (q, 2H), 2.29 (t, 2H), 1.80 (m, 2H), 1.68 (m, 2H), 1.49 (m, 2H), 1.20 (t, 3H); FT-IR (NaCl, cm^{-1}): 2934, 2863, 1729 (ν_{c-o}), 1668, 1586 (ν_{NO2}), 1521, 1461, 1410, 1336 (ν_{NO2}), 1265, 1208, 1107, 1033, 862.

6-(2,5-Bis-chloromethyl-4-methoxy-phenoxy)-hexanoic acid 2-(ethyl-(4-(4-nitro-phenylazo)-phenyl)-amino)-ethyl ester 6. An attempt to prepare this Gilch monomer was done following the same procedure as described for **4** using Disperse Red 1 (0.4 g, 1.34 mmol) as the alcohol-functionalized molecule in the reaction. However, degradation of **6** was observed during column chromatography (SiO_2, eluent CH_2Cl_2/ hexane 8/2).

Gilch polymerization of 4. In a three-necked round-bottom flask fitted with a reflux condenser and a septum, monomer **4** (0.12 g, 0.23 mmol) was dissolved in dry dioxane (15 mL) and flushed with N_2 for 15 min. Afterwards, a balloon filled with Ar was placed on top of the condenser. After heating to 98 °C, a solution of K*t*BuO (0.066 g, 0.60 mmol) in 1 mL dry dioxane was added. During this addition, the solution turned from bright yellow to black under the

formation of dark fumes. The same phenomena were observed when the reaction was performed at room temperature, just as for the polymerization of monomer **5**.

6-(2,5-Bis-(N,N-diethyl dithiocarbamate)-4-methoxy-phenoxy)-hexanoic acid 2-(ethyl-(4-nitro-phenyl)-amino)-ethyl ester 7. To a solution of **4** (1.0 g, 1.93 mmol) in EtOH (15 mL) was added sodium diethyldithiocarbamate trihydrate (1.0 g, 4.46 mmol) as a solid after which the mixture was stirred at ambient temperature for two hours. Then, water was added and the desired monomer was extracted with diethyl ether (3 x 100 mL). The combined organic layers were dried over $MgSO_4$ and the solvent was evaporated. After purification by column chromatography (SiO_2, eluent CH_2Cl_2) **7** was obtained as a yellow solid (1.04 g, 72 % yield). ^{1}H NMR ($CDCl_3$): δ= 8.06 + 8.03 (d, 2H), 6.96 (s, 2H), 6.65 + 6.62 (d, 2H), 4.50+4.48 (2s, 4H), 4.21 (t, 2H), 3.96 (q, 4H), 3.88 (t, 2H), 3.74 (s, 3H), 3.64 (m, 6H), 3.47 (q, 2H), 2.28 (t, 2H), 1.71 (m, 2H), 1.61 (m, 2H), 1.46 (m, 2H), 1.20 (t, 15H); ^{13}C NMR ($CDCl_3$): 195.7 (2C), 173.2 (1C), 152.1 (1C), 151.2 (1C), 150.5 (1C), 136.8 (1C), 126.1 (2C), 124.7 (2C), 124.5 (2C), 114.6 (1C), 113.6 (1C), 110.3 (2C), 68.3 (1C), 66.9 (2C), 60.6 (1C), 56.0 (1C), 53.4 (1C), 49.2 (1C), 48.7 (1C), 46.5 (1C), 45.6 (1C), 36.6 (1C), 36.5 (1C), 33.9 (1C), 28.8 (1C), 25.5 (1C), 24.3 (1C), 12.3 (2C), 11.8 (2C), 11.4 (1C).

Polymerization of dithiocarbamate monomer 7. A solution of monomer **7** (500 mg, 0.66 mmol) in dry THF (6.25 mL, 0.2 M) was degassed for 1 hour by passing through a continuous nitrogen flow. An equimolar LDA solution (332 μL of a 2 M solution in THF/n-hexane) was added in one go to the stirred monomer solution. The mixture was stirred for 90 minutes at room temperature while nitrogen flow was continued. Subsequently, the solution was precipitated in ice water (100 mL) and extracted with chloroform (3 x 60 mL). The solvent of the combined organic layers was evaporated under reduced pressure. Unreacted pure 7 was recovered. The reaction was repeated using dioxane as the solvent and 98 °C as reaction temperature. No polymerization was observed and monomer **7** was recovered.

Butyl-[2-(4-methoxy-phenoxy)-ethyl]-(4-nitro-phenyl)-amine 8. In a three-necked flask, a mixture of *p*-(N-butyl-N-2-hydroxyethyl)-nitrobenzene

(3.6 g, 0.015 mol), *p*-hydroxyanisol (2.8 g, 0.023 mol) and triphenyl phosphine (4.7 g, 0.018 mol) in diethyl ether (120 mL) is stirred for 1 h under Ar atmosphere. The temperature is decreased to 0 °C and diethyl azodicarboxylate (3.2 mL, 0.018 mol) is added drop wise. The mixture is stirred for 24 h at room temperature after which water is added (150 mL) and an extraction is performed (3 x 150 mL) with CH_2Cl_2. The organic layers are combined and dried over $MgSO_4$. The solvent is evaporated under vacuum to yield crude **8**. After purification by column chromatography column (SiO_2, eluent CH_2Cl_2), **8** is obtained as a yellow solid in a yield of 95%. ^{1}H NMR ($CDCl_3$): δ = 8.06 (d, 2H), 6.79 (s, 4H), 6.62 (d, 2H), 4.08 (t, 2H), 3.78 (t, 2H), 3.73 (s, 3H), 3.46 (t, 2H), 1.62 (m, 2H), 1.39 (m, 2H), 0.96 (t, 3H)□□

2-[(2,5-Bis-chloromethyl-4-nitro-phenyl)-butyl-amino]-ethanol 9. To a stirred mixture of **8** (5.0 g, 14.4 mmol) and *p*-formaldehyde (1.19 g, 39.7 mmol), concentrated HCl (7.2 mL) was added drop wise under N_2 atmosphere. Subsequently, acetic anhydride (15.0 mL) was added at such a rate that the temperature did not exceed 70 °C. After the addition was complete, the resulting solution was stirred at 70 °C for 12 h after which it was cooled down to room temperature and poured into water (100 mL). The pH is adjusted to 7 with an aqueous solution of Na*t*BuO. The product was extracted with CH_2Cl_2 (3 x 75 mL). The organic extracts were combined, dried over $MgSO_4$ and the solvent was evaporated to give the crude product, which was purified by column chromatography (SiO_2, eluent CH_2Cl_2). **9** was obtained as a yellow solid in 30 % yield (3.2 g). ^{1}H NMR ($CDCl_3$): δ = 8.12 (d, 2H), 6.90 (s, 2H), 6.71 (d, 2H), 4.56 (d, 4H), 4.18 (t, 2H), 3.89 (t, 2H), 3.78 (s, 3H), 3.49 (t, 2H), 1.63 (m, 2H), 1.41 (m, 2H), 1.01 (3H).

2-(Butyl-(2-chloromethyl-4-nitro-5-octylsulfanylmethyl-phenyl)-amino)-ethanol and its regio-isomer 10. A solution of NaOH (0.9 g, 0.022 mol) in H_2O (24 mL) is added to a solution of **9** (3.7 g, 8.34 mmol) in toluene (24 mL). Subsequently, a catalytic amount of aliquat 336, a phase-transfer reagent, is added. The reaction mixture is stirred at RT during 5 min., after which a solution of octane thiol (1.2 g, 8.34 mmol) in toluene (12 mL) is added drop wise. The resulting reaction mixture is allowed to stir for 24 h at RT. The reaction is quenched by addition of water. The product was extracted with

CH_2Cl_2 (3 x 50 mL). The organic extracts were combined, dried with $MgSO_4$ and the solvent was evaporated to give a crude thioether **10**, which is used without further purification. ^{1}H NMR ($CDCl_3$): δ = 8.10 (d, 2H), 6.82 (d, 2H), 6.69 (s, 2H), 4.58 + 4.18 (2s, 2H), 4.17 (t, 2H), 3.84 (m, 4H), 3.67+ 3.60 (2s, 3H), 3.49 (t, 2H), 2.40 (t, 2H), 1.63-1.23 (m, 16H), 0.97 (t, 3H), 0.83 (t, 3H); ^{13}C NMR ($CDCl_3$): δ = 152.6+ 152.4 (1C), 151.5+ 151.4 (1C), 150.0+ 149.8 (1C), 136.7+ 136.6 (1C), 126.4 (1C), 126.1 (2C), 120.0+ 119.8 (1C), 115.7+ 114.5+ 113.9+ 112.9 (2C), 110.2 (2C), 66.2+ 65.9 (1C), 56.0+ 55.8 (1C), 52.9 (1C), 51.6 (1C), 51.1 (1C), 49.8 (1C), 41.3+ 41.0 (1C), 31.5 (1C), 29.0 (2C), 28.8 (1C), 28.7 (1C), 22.4 (2C), 20.0 (1C), 13.9 (1C), 13.7 (1C); MS (EI, m/z): 550 [M^+].

2-(Butyl-(2-chloromethyl-4-nitro-5-(octane-1-sulfinylmethyl)-phenyl)-amino)-ethanol and its regio-isomer 11. An aqueous (35 wt%) solution of H_2O_2 (0.5 g, 5.2 mmol) was added drop wise to a mixture of **10** (1.4 g, 2.6 mmol), concentrated HCl (0.05 mL) and TeO_2 (0.05 g, 0.31 mmol) in dioxane (10 mL). As soon as **10** was consumed (TLC in hexane/EtOAc ratio 8/2), 100 mL of brine was added to quench the reaction. The reaction mixture was extracted with $CHCl_3$ (3 x 50 mL) after which the combined organic extracts were dried over anhydrous $MgSO_4$. Evaporation of the solvent under reduced pressure gave the crude product. The pure product **11** was obtained by column chromatography (SiO_2, eluent hexane/EtOAc 4/6) as a yellow solid (1/1 mixture of regio-isomers; 28% yield in relation to the dichloride). ^{1}H NMR ($CDCl_3$): δ = 8.05+ 8.01 (d, 2H), 6.89+ 6.85+ 6.80+ 6.76 (dd, 2H), 6.66+ 6.63 (d, 2H), 4.54+ 4.14 (2s, 2H), 4.13 (t, 2H), 4.02 (q, 2H), 3.92-3.79 (m, 5H), 3.42 (t, 2H), 2.50 (t, 2H), 1.67-1.28 (m, 16H), 0.92 (t, 3H), 0.81 (t,3H); MS (EI, *m/z*): 566 (M^+), 405 (M^+-S(O)C_8H_{17}), 369 (M^+- S(O)C_8H_{17}- Cl). MS (EI, m/z): 566 [M^+], 405 [M^+]-S(O)C_8H_{17}, 369 [M^+]-S(O)C_8H_{17}Cl.

Precursor polymer 12. To a solution of monomer **11** (107.6 mg, 0.19 mmol) in 2-BuOH (1.3 mL), a solution of Na*t*BuO (23.7 mg, 0.24 mmol) in 2-BuOH (0.6 mL) was added in one portion using a thermostatic flask and funnel (30 °C) after both solutions were purged with N_2. The polymerization was allowed to proceed for 1 h at 30 °C after which it was quenched by pouring the reaction mixture into a well-stirred amount of ice water (40 mL). After

extraction with CH_2Cl_2 (3 x 20 mL), the combined organic layers were evaporated under reduced pressure giving the crude product, which was used without further purification.

Conjugated polymer 13. A stirred solution of **12** (100 mg) in toluene (10 mL) was purged with N_2 for 1 h, after which the elimination reaction was allowed to proceed at 110°C and stirred for 3 h. During this time, a red precipitate was formed. The resulting orange red solution which contained particles was precipitated drop wise in cold hexane (100 mL). The resulting polymer was filtered off and washed with hexane. A soluble fraction was obtained by refluxing the polymer in THF. The insoluble fraction was removed by filtration and washed with THF. A soluble polymeric fraction was obtained by evaporation of the solvent. SEC (THF): $M_w = 3 \times 10^4$ g/mol (PD = M_w/M_n = 2.1). However, this fraction appeared impure. Attempts to purify the polymer failed.

Post-polymerization functionalization towards complex ester-functionalized PPV derivatives

Poly(1,4-(2-(5-carboxypentyloxy)-5-methoxyphenylene)vinylene (CPM-PPV). This polymer was prepared and characterized as described in Chapter 5.

(MDMO-CPM)-PPV (n/m=1,9). These copolymers were prepared and characterized as described in Chapter 5.

- ***Via* the Mitsunobu reaction conditions**

5-(methyl)furfural ester of CPM-PPV (A). A solution of polymer CPM-PPV (100 mg, 0.38 mmol repeating units) in dry THF (10 mL) was cooled to 0°C under N_2 atmosphere. To this solution an alcohol-functionalized molecule, *i.e.* 5-(hydroxy methyl)furfural (0.048 g, 0.38 mmol) and triphenylphosphine (120 mg, 0.46 mmol) were added and the mixture was stirred for 10 min. Subsequently diethyl azodicarboxylate (0.2 mL, 0.46 mmol) was slowly added *via* a syringe. The mixture was allowed to warm to room temperature over a period of 2 h and stirred at room temperature for an additional 24 h after which the reaction mixture was added drop wise to a non-solvent, *i.e. n*-hexane (100

mL) whereupon the polymer precipitated. After filtration and drying under vacuum polymer **A** was obtained as a red solid (42 mg, 30% yield). FT-IR (NaCl, cm^{-1}): 2983, 2871, 1724(ν_{c-o}), 1680, 1522, 1484, 1438, 1410, 1380, 1342, 1207, 1120, 1064, 723; SEC (DMF) $M_w = 1.29x10^4$ g/mol (PD = M_w/M_n = 2.6); UV-Vis λ_{max}= 469 nm (THF), λ_{max}= 438 nm ($CHCl_3$); Photoluminescence emission maximum 530 nm (λ_{ex}= 438 nm, $CHCl_3$).

2-nitrobenzyl ester of CPM-PPV (B). Polymer **B** was prepared following the Mitsunobu procedure described for polymer **A** using 2-nitrobenzylalcohol (0.058 g, 0.38 mmol) as the alcohol-functionalized molecule in the reaction and methanol (100 mL) as the non-solvent in the precipitation. After filtration and drying under vacuum polymer **B** was obtained as a red solid (67 mg, 43% yield). FT-IR (NaCl, cm^{-1}): 2932, 2867, 1739(ν_{c-o}), 1613, 1528 (ν_{NO2}), 1504, 1464, 1411, 1343(ν_{NO2}), 1208, 1035, 790, 727; SEC (DMF) $M_w = 5.09x10^4$ g/mol (PD = M_w/M_n = 2.7); UV-Vis λ_{max}= 488 nm (THF), λ_{max}= 437 nm ($CHCl_3$); Photoluminescence emission maximum 536 nm (λ_{ex}= 437 nm, $CHCl_3$).

4-nitrobenzyl ester of CPM-PPV (C). Polymer **C** was prepared following the procedure described for polymer **A** using 4-nitrobenzylalcohol (0.058 g, 0.38 mmol) as the alcohol-functionalized molecule in the reaction and methanol (100 mL) as the non-solvent in the precipitation. After filtration and drying under vacuum polymer **C** was obtained as a red solid (86 mg, 55% yield). FT-IR (NaCl, cm^{-1}): 2939, 2867, 1737 (ν_{c-o}), 1606, 1520 (ν_{NO2}), 1504, 1438, 1410, 1341 (ν_{NO2}), 1206, 1157, 1119, 1030, 859, 722; SEC (DMF) $M_w = 1.82x10^4$ g/mol (PD = M_w/M_n = 2.4); UV-Vis λ_{max}= 486 nm (THF), λ_{max}= 431 nm ($CHCl_3$); Photoluminescence emission maximum 533 nm (λ_{ex}= 431 nm, $CHCl_3$).

3-N,N-dimethylamino-1-propane ester of CPM-PPV (D). Polymer **D** was prepared following the procedure described for polymer **A** using 3-N,N-dimethylamino-1-propanol (0.039 g, 0.38 mmol) as the alcohol-functionalized molecule in the reaction and *n*-hexane (100 mL) as the non-solvent in the precipitation. After filtration and drying under vacuum polymer D was obtained as a red solid (54 mg, 38% yield). Polymer **D** is insoluble in common

organic solvents. FT-IR (NaCl, cm^{-1}): 2937, 2864, 1730(ν_{c-o}), 1501, 1462, 1406, 1389, 1206, 1033.

Hydrolysis of Polymer A. A solution of polymer **A** (28 mg, 0.077 mmol repeating units) in dioxane (8 mL) was heated to reflux temperature after which a solution of K*t*BuO (0.02 g, 0.77 mmol) in water (0.5 mL) was added. After 4 h stirring at reflux temperature the reaction mixture was added drop wise to a well stirred amount of ice water (100 mL), neutralized with aqueous HCl (1 M) and the resulting precipitate was filtered off and washed with water (3 x 25 mL). The polymer was dried at room temperature under reduced pressure as a red fibrous polymer. FT-IR (NaCl, cm^{-1}): 3426, 3016, 2927, 2861, 1706 (ν_{C-O}), 1608, 1493, 1451, 1404, 1208, 1094, 1050, 874, 824; SEC (DMF) M_w = 9.63 x 10^4 g/mol (PD = M_w/M_n = 2.6); UV-Vis λ_{max}= 485 nm (DMSO).

Grafting of push-pull substituents on CPM-PPV. Post-polymerization functionalization of CPM-PPV with push-pull molecules was accomplished according to the same Mitsunobu procedure as described for polymer **A** using 4-(N-(2-hydroxyethyl)-N-ethyl)-amino-4'-nitrostilbene (118.6 mg, 0.38 mmol) as the alcohol-functionalized molecule in the reaction and cold diethyl ether (100 mL) as the non-solvent in the precipitation. After filtration and drying under vacuum the grafted polymer was obtained as a red solid (114 mg, 54% yield). FT-IR (NaCl, cm^{-1}): 2934, 2876, 1799(ν_{c-o}), 1168, 1582, 1520 (ν_{NO2}), 1464, 1410, 1338 (ν_{NO2}), 1261, 1209, 1107; DSC T_g = 110 °C; SEC (DMF) M_w = 3.0 x 10^4 g/mol (PD = M_w/M_n= 1.9); UV-Vis λ_{max}= 461 nm (film).

- ***Via* the DCC/DMAP-esterification method**

5-(methyl)furfural ester of CPM-PPV (A'). CPM-PPV (45 mg, 0.17 mmol repeating units) was dissolved in dry CH_2Cl_2 (10 mL) and cooled down to 0°C. The alcohol-functionalized reagent, *i.e.* 5-(hydroxy methyl)furfural (0.026 g, 0.21 mmol, 1.2 eq.) and N,N'-dicyclohexylcarbodiimide (DCC) (0.042g, 0.21 mmol, 1.2 eq.) were added. Subsequently 4-(N,N'-dimethylamino)pyridine (DMAP) (0.025 g, 0.21 mmol, 1.2 eq.) in CH_2Cl_2 (2 mL) is added drop wise over a period of 15 minutes under Ar atmosphere. The reaction was allowed to proceed for 1 h at 0 °C and for an additional 24 h at room temperature after which the solution was precipitated drop wise to a non-

solvent, *i.e.* MeOH. The resulting red polymer was filtered off, washed and dried under reduced pressure. (19 mg, 30% yield). FT-IR (NaCl,cm^{-1}): 2989, 2869, 1725(ν_{c-o}), 1682, 1522, 1486, 1436, 1414, 1376, 1338, 1208, 1121, 1064, 725; SEC (DMF) M_w = 1.59 x10^4 g/mol (PD = M_w/M_n = 2.5); UV-Vis λ_{max}= 478 nm (THF); ^{1}H NMR (300 MHz, DMSO): δ= 9.6 (1H), 7.5-6.5 (6H), 5.1 (2H), 4.2-3.7 (5H), 2.2 (2H), 1.9-1.2 (6H).

2-nitrobenzyl ester of CPM-PPV (B'). Polymer B' was prepared following the DCC/DMAP-procedure described for polymer **A'** using 2-nitrobenzylalcohol (0.029 g) as the alcohol-functionalized molecule in the reaction and methanol as the non-solvent in the precipitation. After filtration and drying under vacuum polymer **B'** was obtained as a red solid (28 mg, 43% yield). ^{1}H NMR (300 MHz, DMSO): δ= 8.1 (2H), 7.8-7.3 (4H), 7.2 (2H), 5.4 (2H), 4.1-3.9 (5H), 2.3 (2H), 1.9-1.2 (6H). UV-Vis λ_{max}= 484 nm (THF).

4-nitrobenzyl ester of CPM-PPV (C'). Polymer **C'** was prepared following the DCC/DMAP-procedure described for polymer **A'** using 4-nitrobenzylalcohol (0.027 g) as the alcohol-functionalized molecule in the reaction and methanol as the non-solvent in the precipitation. After filtration and drying under vacuum polymer **C'** was obtained as a red solid (39 mg, 67% yield). ^{1}H NMR (300 MHz, DMSO): δ= 8.1 (2H), 7.6-7.3 (4H), 7.2-7.1 (2H), 5.2 (2H), 4.2-3.8 (5H), 2.4 (2H), 1.9-1.2 (6H); UV-Vis λ_{max}= 489 nm (THF).

Phthalocyanine-grafted copolymer. The phthalocyanine-functionalized copolymer was prepared following the DCC/DMAP-procedure described for polymer **A'** using (MDMO-CPM)-PPV (n/m=1) as the carboxylic acid-substituted polymer (49 mg, 0.09 mmol carboxylic acid functionalities) and hydroxy methyl phthalocyanine (83 mg, 0.11 mmol) as the alcohol-functionalized molecule. The reaction was performed in dry THF (45 mL). After addition of DCC and DMAP, the reaction was allowed to proceed for 6 h at 0 ºC and for an additional 72 h at room temperature, after which the reaction mixture was poured into MeOH (200 mL). The resulting polymer was filtered over a glass frit and washed in a Soxhlet extraction using methanol as the extraction solvent (3 x 60 mL). Subsequently, THF is used as the extraction solvent in a Soxhlet extraction for 14 h, so that 15 mg of a dark-green soluble polymeric fraction was obtained after redistillation of the solution in the flask.

Post-polymerization functionalization towards amide-bearing PPV derivatives

Di-n-butylamide of (MDMO-CPM)-PPV. (MDMO-CPM)-PPV (50 mg, 0.09 mmol carboxylic acid functionalities) is dissolved in THF (100 mL) by refluxing the copolymer in THF for one hour. After cooling to room temperature, di-n-butylamine (118 mg, 0.91 mmol) and coupling reagent X (0.91mmol) were added. The resulting reaction mixture was stirred at room temperature for 72 hours. Additional amine (0.91 mmol) and coupling reagent X (0.91 mmol) were then added and the reaction was stirred for an additional 72 hours. The total volume was reduced to 50 mL by evaporation, and the polymer was precipitated in cold MeOH/ water (9/1, 100 mL), filtered and finally washed thoroughly with water and MeOH. After drying under vacuum, the amide-functionalized PPV derivative was obtained as a red solid (54 mg, 90 % yield). ^{1}H NMR ($CDCl_3$): δ= 7.5 (4H), 7.2 (4H), 4.1 (4H), 3.9 (6H), 3.2 (4H, NC*H*$_2$), 2.4 (2H, C*H*$_2$CO), 2.1-0.8 (36H); Anal. Calcd. For $C_{42}H_{63}O_5N$: C 76.21, H 9.59, N 2.12, O 12.08; Found C 76.43, H 10.19, N 1.98, O 11.39; FT-IR (NaCl, cm^{-1}): 2956, 2929, 2871, 1645 (ν_{CO-N}), 1505, 1464, 1415, 1353, 1205, 1036, 970; SEC (DMF) M_w = 3.87 x 10^5 g/mol (PD = M_w/M_n = 8.2); UV-Vis λ_{max}= 500 nm ($CHCl_3$).

7.7 References

[1] a) Liang, Z.; Cabarcos, O. M.; Allara, D.L.; Wang, Q. *Adv. Mater.* **2004**, *16*, 823-827. b) Chan, E. W. L.; Lee, D. C.; Ng, M. K.; Wu, G. H.; Lee, K. Y. C.; Yu, L. P. *J. Am. Chem. Soc.* **2002**, *124*, 12238-12243.

[2] a) Mitsunobu, O.; Yamada, M. *Bull. Chem. Soc. Jpn.* **1967**, *40*, 2380-2392. b) Hughes, D. L. *Org. Reactions* **1992**, *42*, 335. c) Hughes, D. L. *Organic Preparations and Procedures Int.* **1996**, *28 (2)*, 127-164. d) Hughes, D. L.; Reamer, R. A.; Bergan, J. J.; Grabowski, E. J. J. *J. Am. Chem. Soc.* **1988**, *110*, 6487-6491.

[3] Sentein, C.; Fiorini, C.; Lorin, A.; Nunzi, J. M. *Adv. Mater.* **1997**, *9 (10)*, 809-811.

[4] Bosshard, C.; Sutter, K.; Prêtre, P.; Hulliger, J.; Flörsheimer, M.; Kaatz, P.; Günter, P. *Organic Nonlinear Optical Materials 1*, Gordon and Breach, London, **1995**.

[5] a) Sentein, C.; Fiorini, C.; Lorin, A.; Nunzi, J. M.*;* Raimond, P.; Sicot, L. *Synthetic Metals* **1999**, *102*, 989-990. b) Singer, K. D.; Kuzyk, M. G.; Sohn, J. E. *J. Opt. Soc. Am. B* **1987**, *4*, 968. c) Sicot L.; Fiorini C.; Lorin A.; Raimond P.; Sentein C.; Nunzi J.-M. *Solar Energy Materials & Solar Cells* **2000**, *63*, 49-60.

[6] Wöhrle, D.; Meissner, D. *Adv. Mater.* **1991**, *3*, 129.

[7] Liptay, W. *Angew. Chem. Internat. Edit.* **1969**, *8 (3)*, 177-188.

[8] Spreitzer, H.; Becker, H.; Kluge, E.; Kreuder, W.; Schenk, H.; Demandt, R.; Schoo, H. *Adv. Mater.* **1998**, *10*, 1340.

[9] Henckens, A.; Lutsen, L.; Vanderzande, D.; Knipper, M.; Manca, J.; Aernouts, T.; Poortmans, J. *Proc. Spie – Int. Soc. Opt. Eng.* **2004**, *5464*, 52-59. Henckens, A.; Duyssens, I.; Lutsen, L.; Vanderzande, D.; Cleij, T. J. *Polymer* **2006**, *47*, 123-131.

[10] a) Wöhrle, D. *Macromol. Rapid Commun.* **2001**, *22*, 68-97. b) Leznoff, C. C.; Lever, A. B. P. *Phthalocyanines*: *Properties and Applications*; Eds. VCH, Weinheim, **1996,** Vols. 1–4.

[11] Coakley, K. M.; McGehee, M. D. *Chem. Mater.* **2004**, *16*, 4533-4542.

[12] a) Fernández-Lázaro, F.; Sastre, A.; Torres, T. *J. Chem. Soc., Chem. Commun.* **1994**, 1525. b) Cabezón, B.; Rodríguez-Morgade, S.; Torres, T. *J. Org. Chem.* **1995**, *60*, 1872. c) Armand, F.; Martínez-Díaz, M. V.; Cabezón, B.; Albouy, P. A.; Ruaudel-Texier, A.; Torres, T. *J. Chem. Soc., Chem. Commun.* **1995**, 1673.

[13] a) Halls, J. J. M.; Walsh, C. A.; Greenham, N. C.; Marseglia, E. A.; Friend, R. H.; Moratti, S. C.; Holmes, A. B. *Nature* **1995**, *376*, 498. b) Yu, G.; Gao, Y.; Hummelen, J. C.; Wudl, F.; Heeger, A. *Science* **1995**, *270*, 1789. c) Dhanabalan, A.; van Duren, J. K. J.; van Hal, P. A.; van Dongen, J. L. J.; Janssen, R. A. J. *Adv. Funct. Mater.* **2001**, *11 (4)*, 255. d) Shaheen, S. E.; Brabec, J. C.; Padinger, F.; Fromherz, T.; Hummelen, J. C.; Sariciftci, N. S. *Appl. Phys. Lett.* **2001**, *78*, 841. e) Reyes-Reyes, M.; Kim, K.; Carroll, D. L. *Appl. Phys. Lett.* **2005**, *87*, 083506.

[14] Cravino, A.; Sariciftci, N. S. *J. Mater. Chem.* **2002**, *12*, 1931-1943.

[15] Martínez-Díaz, M. V.; Esperanza, A.; de la Escosura, A.; Catellani, M.; Yunus, S.; Luzzati, S.; Torres, T. *Tetrahedron Letters* **2003**, *44*, 8475-8478.

[16] Mitsunobu, O. *Synthesis* **1981**, 1-28.

[17] Hassner, A.; Alexanian, V. *Tetrahedron Letters*, **1978**, *46*, 4475-4478.

[18] a) Steglich, W.; Höfle, G. *Angew. Chem. internat. Edit.* **1969**, *8 (12)*, 981. b) Neises, B.; Steglich, W. *Angew. Chem. internat. Edit.* **1978**, *17 (7)*, 522.

[19] Detert, H.; Sugiono, E. *Synthetic Metals* **2002**, *127*, 233-235.

[20] Zhang, R.; Rhang, G.; Shen, J. *Chem. Commun.* **2000**, 823-24.

Chapter 8

Application of Functionalized PPV-type Polymers as Transducer in Impedimetric Biosensors

This chapter is realized in co-operation with the Materials Physics research group at the Institute for Materials Research and focuses on bio-functionalizing conjugated PPV-type (co)polymers which were prepared earlier in this work, with antibodies. In a prototype impedimetric biosensor, antibody-antigen binding on these polymer films can readily be observed. It is shown that functionalized PPV derivatives prepared via the sulfinyl precursor route are promising candidates for application as transducer layers in an immunosensor and that the sensor characteristics are dependent on the functional groups of the polymers. By alternating the side chains, we can tune the properties of the polymer film and influence the blocking or binding behaviour of the transducer layer.

8.1 Introduction to biosensors

Biosensors are defined as analytical devices consisting of biological sensing elements either integrated within or in close vicinity of transducer elements, which transform selective information of the presence of the analyte of interest into a quantifiable signal. Biosensors are a hot topic in life sciences. The main drive for this interdisciplinary research is to explore new ways of measuring biological entities that may lead to innovative analytical techniques in biomedical research, or even commercial user applications beneficial to personal healthcare. Faster, more cost-effective and electronic sensor devices to detect medically relevant biomolecules in human body fluids are being developed all over the world.

Figure 8-1 shows a schematic representation of a biosensor. A biosensor always contains two key parts: the bioreceptor layer, which recognizes the analyte and reacts or binds to it and a transducer layer, which is the detector monitoring the chemical or biochemical reaction initiated by the sample.

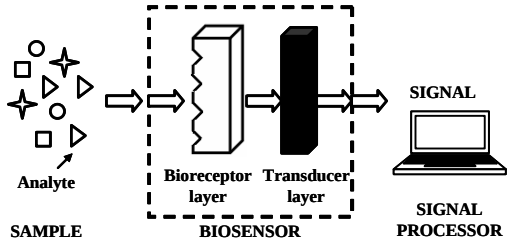

Figure 8-1 Schematic representation of a biosensor

Biomolecules such as enzymes, antibodies, receptors and nucleic acids, as well as whole cells, organelles and tissues can be used as the sensory element. The biosensor described in this chapter uses antibodies as the bioreceptors. Antibodies are immunoglobulins (Ig's) which are produced by the body in response to antigens. An antigen is any molecular species that is recognized by the body as foreign and triggers an immune response. Biosensors that use antibodies as the recognition element are termed immunosensors. The antibodies used throughout this chapter are monoclonal mouse antibodies (IgG's) against the fluorescent dye fluorescein isothiocyanate (FITC), in the following referred to as 'anti-FITC'. FITC is a light, fluorescent molecule with a mass smaller than 1 kDa. Therefore, it is conjugated to a 250 base pair double-stranded DNA fragment to obtain a molecule of 154 kDa. This has the advantage that the antigens can easily be detected by atomic force microscopy (AFM). Moreover, heavy molecules correspond better to the macromolecular antigens relevant in human pathology.

8.2 Application of conjugated polymers as transducer in a biosensor

In recent years, an increasing number of papers is published dealing with biosensors utilizing electrically conducting polymers as transducer layer.[1] Conjugated polymers are promising transducer materials for biosensors for various reasons. The unusual surface chemistry of these semi-conductors, being organic in nature as opposed to metallic, appears to facilitate interactions with biological macromolecules, while the read-out can occur *via* electronic and/or fluorescence techniques. Moreover, the fabrication of polymer based sensors is relatively cheap, which make them suitable for large-scale production and single-use applications. Finally, conjugated polymers are known to possess numerous features, which allows for tuning the properties of the polymer film in order to optimize the immobilization of biomolecules and the electron transfer for the fabrication of efficient transducer layers for biosensors. In the biosensor that we have in mind, the function of the conjugated polymer is twofold: first of all the polymer serves as an immobilization platform for biological receptors and secondly its semi-conductive properties provide us with the possibility of electric read-out.

As already mentioned, the transducer (shown as the 'black box' in Figure 8-1) relates the information of the biomolecular events occurring on the biolayer back to the electronic interface to produce analytical signals. The information related back may be due to direct oxidation/ reduction of the analyte or a product from an enzymatic reaction involving the analyte. This simple and most sensitive mechanism of detection is based on a 'shuttle' mechanism, whereby reactions at the active site, following the binding of the substrate, create diffusing electron carrier species that migrate *via* the conjugated polymer to the electrode where they are detected. Traditional enzyme-electrode systems, such as the well-known example of the glucose biosensor are based on this detection method.[2] In cases where no electro-active species are present, such as for the antibody-antigen affinity binding, no direct amperometric signal can be detected. However, changes occurring in the

impedance of the bioactive film can be measured.[3] Antigens present in the sample associate to polymer surface-immobilized antibodies, forming a complex. The formation of antigen-antibody complexes on the semi-conductive support yields a chemically modified film that perturbs the charged double-layer existing at the electrode/electrolyte interface resulting in the capacitance change and electron transfer resistance change at the interface. Impedance spectroscopy is a very powerful tool for the analysis of interfacial properties changes of modified electrodes upon biorecognition events occurring at the modified surfaces and allows for visualisation of the changes in the charge transfer process on the polymer after the affinity reaction.

The differential impedance spectroscopy measurements were recently utilized to evaluate the conjugated polymer polypyrrole.[4] We choose to work with functionalized PPV derivatives. PPV derivatives are stable in aqueous media, have sufficiently high conductivities and the chemical modifications possible on this class of polymers are virtually unlimited. Throughout the previous chapters it became clear that the sulfinyl precursor route results in PPV-type polymers with increased purity and low defect levels compared to other precursor routes, which make this route extremely suitable for the preparation of polymers for application in sensor applications. In addition, this route offers the possibility to attach a variety of side chains, which allows for tuning of the electronic and hydrophilic/hydrophobic properties of the PPV-type polymers.

8.3 Application of MDMO-PPV as transducer in a biosensor

Since MDMO-PPV acts as a kind of benchmark in the field of conjugated polymers, this polymer was the first choice to test as a transducer layer in a biosensor. During the past year, major progress was made in the Materials Physics research group (IMO) with impedimetric immunosensors based on thin films of MDMO-PPV.[5] Antibodies were immobilized on the spin coated polymer by physical adsorption from buffer solutions. Results from contact

angle measurements, atomic force microscopy (AFM) and fluorescence spectroscopy confirmed that antibodies can be adsorbed to a MDMO-PPV film and that a stable, presumably monomolecular layer is formed. Furthermore, the antibodies retain their biological activity. The binding of fluorescent antigens to antibodies was demonstrated *via* fluorescence microscopy. Using the enhancement of the polymer fluorescence by excitation of FITC bound to its antibody, the increase in fluorescence intensity could be related to the concentration of the antigen FITC in solution over a wide range. Furthermore, the biofilms were tested in an impedimetric biosensor. A prototype biosensor consists of four regions, which can be activated with different antibodies (Figure 8-2). The impedance of each sensor site is recorded when an oscillating voltage is applied. A syringe-based flow trough system is integrated to introduce the antigens in the sensor. The electronic biosensing measurements are based on the electrochemical impedance principle. The measurements are performed time-resolved and in a differential way to characterize the sensitivity and selectivity of this biosensor using different analytes and antigen concentrations.

a) b)

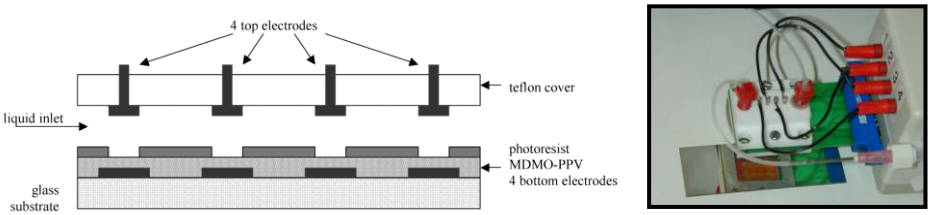

Figure 8-2 a) Schematic representation of the prototype impedimetric immunosensor used for measuring the conjugated polymer based transducer layers. MDMO-PPV is packed into a flow cell with 4 sensing sites consisting of a bottom electrode coated with polymer and a top electrode in the liquid. b) Picture of a prototype biosensor

From the first impedance measurements based on MDMO-PPV, Cooreman *et al.* concluded that conjugated PPV-type polymers are promising materials for biosensor application since antibodies can be successfully adsorbed onto a MDMO-PPV film while keeping their biological activity.[5] The conjugated

polymer layer demonstrated a good sensitivity while converting the recognition event in a distinctive impedance difference. Antigen concentrations as low as 10 pmol per mL were detected within minutes.

Nevertheless, there are some drawbacks associated with immunosensors based on thin films of the conjugated polymer MDMO-PPV. First of all, non-specific interactions on the MDMO-PPV polymer film may result in fouling of the sensor surface. Figure 8-3 shows the outcome of Enzyme-Linked ImmunoSorbent Assay (ELISA) measurements. This technique utilizes a second antibody coupled to an enzyme to causes a chromogenic or fluorogenic substrate to produce a signal. The light absorption is a measure for how many FITC-labelled DNA strands are captured by the polymer film. The polymer coated with the blocking protein bovine serum albumin (BSA) is the reference sample that indicates the zero level. Signal from the antibody-functionalized polymer sample is due to antibody-antigen reaction (third column in Figure 8-3). The first column in Figure 8-3 reveals non-specific adsorption of antigens onto the bare MDMO-polymer film. Obviously, the performance of the immunosensors will suffer adverse consequences of this non-specific adsorption.

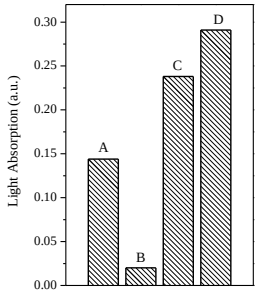

Figure 8-3 Comparative evaluation of ELISA measurements A) plain MDMO-PPV B) MDMO-PPV coated with BSA C) MDMO-PPV with physically adsorbed antibodies D) MDMO-PPV with physically adsorbed antibodies and subsequently exposed to BSA

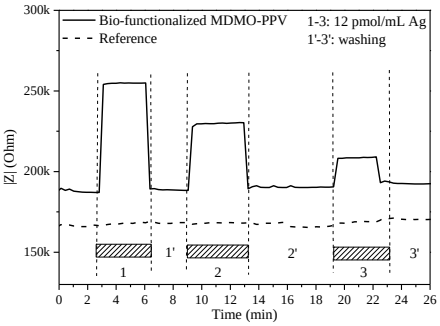

Figure 8-4 Impedance amplitude (Z) graph for the bio-active MDMO-PPV sample and a reference sample, taken at 300 Hz.

Moreover, as is demonstrated by Figure 8-4, the stability of the bio-functionalized MDMO-PPV film leaves rooms for improvement. Figure 8-4 shows the outcome of a measurement in which the impedance amplitude is recorded in time while applying an oscillating voltage. At different intervals of time 12 pmol per mL FITC-DNA antigens are added, followed by washing with a buffer solution. The lowest curve is the response of the reference electrode, *i.e.* MDMO-PPV coated with the blocking protein BSA. This reference electrode shows no measurable change in impedance amplitude within the noise level. The upper curve is the response of the biofilm containing MDMO-PPV with immobilized antibodies against FITC. One can see that the anti-FITC sample responds *via* a change in impedance amplitude when the antigens are added and returns to the original value after washing. However, it is clear that the impedance signal becomes weaker for repeated additions of antigens; although for every addition the same concentrations of FITC-labelled DNA are used. This is an indication that the biofilm is instable. Probably during washing between the different additions, antibodies are washed away. Since the IgG's are immobilized on the spin coated polymer layers by physical adsorption, the bond between the polymer and the antibodies is based on hydrophobic interactions instead of covalent bonds. This may negatively impact the biosensors stability and lifetime. Additionally, hydrophobic interactions have a tendency to denature antibodies as a result of the fact that their hydrophobic part is usually turned inwards. Finally, the direction in which the antibodies are immobilized on the surface is random, leading to lower sensitivities.

8.4 Application of carboxylic acid-functionalized PPV derivatives as transducer in a biosensor

It is clear from Figure 8-3 and Figure 8-4 that further improvements with regard to selectivity and stability of the bio-functionalized polymer film are necessary. One may expect that higher stabilities of the biofilm can be reached if the IgG's are bound to the polymer film *via* strong covalent bonds. Moreover, covalent chemistry does not suffer the adverse consequences of

denaturation of the antibodies in contrast to the hydrophobic interactions. Finally, the use of specific covalent chemistry may offer more control of the direction in which the antibodies are immobilized onto the polymer surface, preferably with the two binding sites for antigens upwards. Since proteins posses amine groups, we could use the carboxylic acid-functionalized PPV derivative prepared in Chapter 6 (CPM-PPV in Figure 8-5) to form strong amide bonds *via* the well described and widely used protocols of peptide synthesis.

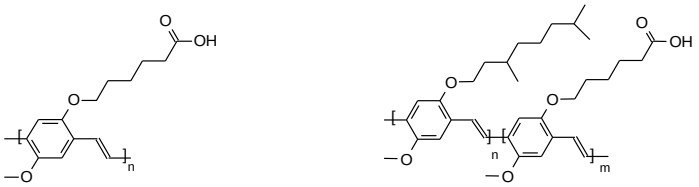

CPM-PPV **(MDMO-CPM)-PPV**

Figure 8-5 Carboxylic acid-functionalized PPV (co)polymers prepared in Chapter 6

One common protocol to obtain synthetic peptides is the EDC protocol.[6] 1-Ethyl-3-(3-dimethylaminopropyl)-carbodiimide (EDC) is a water-soluble derivative of carbodiimide used for the formation of amide bonds between carboxylic acids and amines by activating carboxylic acids to form an O-urea derivatives that react readily with nucleophiles. N-hydroxysuccinimide (NHS) is used to assist the carbodiimide coupling in the presence of EDC. NHS produces a more stable reactive intermediate which has been shown to give a greater reaction yield. Since antibodies contain both carboxylic acid and amine functionalities, the risk of cross linking exists. Therefore, one opts for a two-step variation of the EDC protocol which allows the covalent coupling of antibodies onto the polymer film without exposing the carboxylic acid groups on the antibodies to EDC. This allows these functionalities to remain unaltered (Figure 8-6).[7] In a first step, EDC binds a molecule NHS to the carboxylic groups on the polymer. The amine-reactive NHS ester intermediate has sufficient stability to permit the two-step cross-coupling procedure.

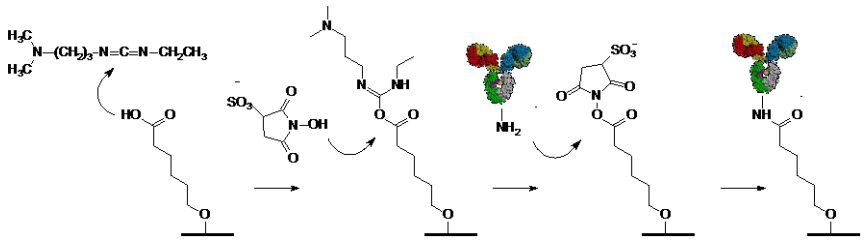

Figure 8-6 Schematic overview of covalent bonding of antibodies onto a PPV polymer film using a two-step variation of the EDC protocol

Since the density of carboxylic acid functionalities in CPM-PPV is likely too high to allow quantitative functional group substitution with IgG's, a copolymer of CPM-PPV and MDMO-PPV is used (Figure 8-5). The spin coating parameters of (MDMO-CPM)-PPV are similar to these of the well established MDMO-PPV.

Unfortunately, contact angle measurements of distilled water with a film of the copolymer (MDMO-CPM)-PPV immobilized with different antibody concentrations, reveal that the antibodies also physically adsorb on the copolymer. Figure 8-7 shows the outcome of contact angle studies between the polymer surface of MDMO-PPV and (MDMO-CPM)-PPV with distilled water at different antibody concentrations. The (co)polymers are spin coated from chlorobenzene onto a glass substrate. Then antibodies from a buffer solution are adsorbed onto the polymer film for 1 hour at 37 °C. The polymer MDMO-PPV is hydrophobic, with a contact angle of approximately 95° with water. The bare copolymer shows a lower contact angle due to the polar acid side groups. The contact angle of the (co)polymer surface with distilled water decreases with increasing antibody concentration, indicating that antibodies physically adsorb to (MDMO-CPM)-PPV similar to the homopolymer MDMO-PPV. From the curves, one can see that high concentrations lead to a saturation value.

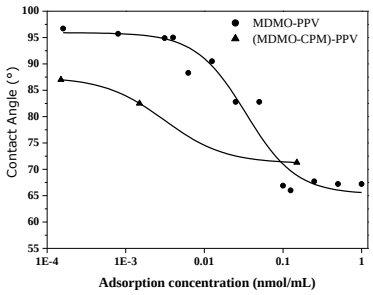

Figure 8-7 Contact angle measurements of distilled water with MDMO-PPV and (MDMO-CPM)-PPV on which different concentrations of IgG's are absorbed

This physical adsorption has implications for the use of the two-step EDC protocol (Figure 8-6). The last step in this protocol, *i.e.* the replacement of the NHS groups on the polymer by antibodies takes at least an hour. During this time, simultaneous with the specific covalent bonding, antibodies can adsorb *via* non-specific hydrophobic interactions onto the MDMO-PPV parts of the copolymer. Hence, immunosensors based on thin films of the copolymer (MDMO-CPM)-PPV do not bring in a significant advantage compared to immunosensors based on MDMO-PPV. However, it should be noted that it is likely that the EDC protocol commonly used in literature for peptide synthesis is not optimal for the covalent bonding of antibodies onto a PPV polymer film. Probably longer reaction times are necessary for the covalent bonding to occur. Therefore, it might also be useful to test other, more effective routes.

In order to overcome the drawbacks associated with the physical adsorption of antibodies onto the conjugated polymer film, we need a copolymer which has a 'blocking component' to dilute the 'covalent component', *i.e.* CPM-PPV. On this blocking component no proteins may adsorb, the so called 'non-fouling' behaviour. The most common material displaying non-fouling characteristics known in literature is poly(ethylene glycol) (PEG, Figure 8-8).[8] PEG chains tethered on a surface exhibit the ability to exclude other macromolecules and particles. This is particularly useful for preventing the adsorption of proteins. A conjugated equivalent of PEG is a PPV derivative bearing a oligo(ethylene oxide) side chain. Such a

functionalized PPV derivative was prepared in Chapter 2, namely poly(2-methoxy-5-(triethoxymethoxy)-1,4-phenylene vinylene) (MTEM-PPV, Figure 8-8).

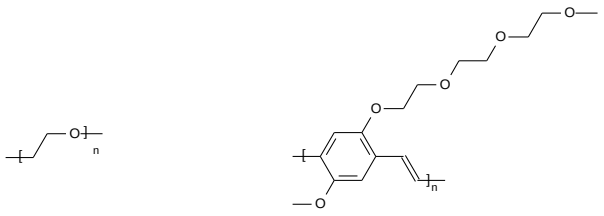

Figure 8-8 Poly(ethylene glycol) (PEG) and a conjugated equivalent of PEG, *i.e.* MTEM-PPV

8.5 Application of MTEM-PPV as transducer in a biosensor

Prior to the characterization measurements of a copolymer with a blocking component (MTEM-PPV) and a covalent binding component (CPM-PPV), we are interested in the non-fouling behaviour of MTEM-PPV. The contact angle of distilled water with a thin film of MTEM-PPV is much lower compared to the contact angle of MDMO-PPV, due to the hydrophilic oligo(ethylene oxide) side chains (Figure 8-9). More importantly, antibody treatment of the surface of MTEM-PPV does not influence the contact angle, indicating that MTEM-PPV is biologically 'inert'. The polar side chains prevent biomolecules from adsorbing to the surface, so a MTEM-PPV film results indeed in a non-fouling surface. This is further confirmed by the comparative evaluation of the ELISA measurements. All the MTEM-PPV samples have intensities around the zero level, indicating that only a limited number of antibodies are adsorbed onto the hydrophilic polymer film. In order to investigate the topology of these samples into more microscopic detail, non-contact mode atomic force images are made. As shown by the second picture of Figure 8-10, BSA seems to have interacted with the MTEM-PPV polymer film. However, after washing (third picture in Figure 8-10), the molecules are rinsed away.

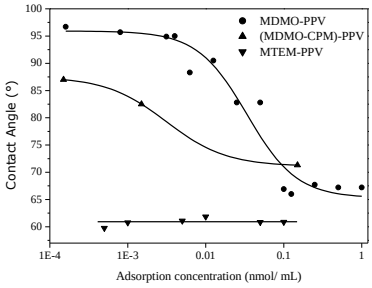

Figure 8-9 Contact angle measurements of distilled water with MTEM-PPV on which different concentrations of IgG's are absorbed (the curves of MDMO-PPV and (MDMO-CPM)-PPV are there for comparison)

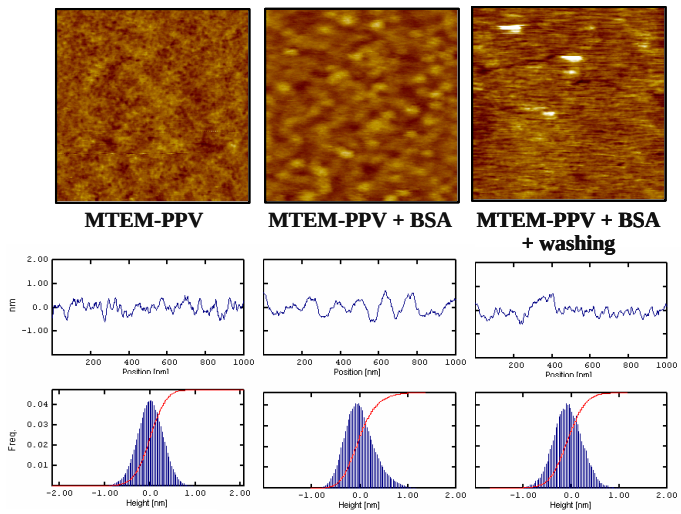

Figure 8-10 AFM images showing the surface topology of bare MTEM-PPV, MTEM-PPV after addition of BSA proteins and MTEM-PPV after addition of BSA proteins and subsequent washing. The images are 1 square μm

All characterization measurements seem to indicate that MTEM-PPV films form a non-fouling surface. Therefore, we can state that we have found a suitable system to dilute the carboxylic acid-substituted PPV.

8.6 Application of (MTEM-CPM)-PPV as transducer in a biosensor

The carboxylic acid functionalities of CPM-PPV provide the possibility of strong covalent bonding with the amine-functionalities of antibodies. MTEM-PPV on the other hand, is characterized by non-fouling properties. Therefore, the combination of the two polymers into the copolymer (MTEM-CPM)-PPV (Figure 8-11) yields a promising material in which the covalent binding components are diluted by a blocking component.

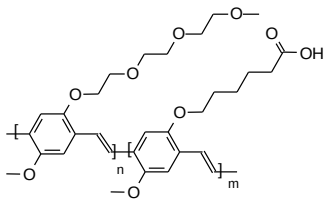

Figure 8-11 (MTEM-CPM)-PPV, a copolymer with a non-fouling and a covalent binding component

Currently extensive characterization measurements of (MTEM-CPM)-PPV are ongoing as well as studies on the effectiveness of the two-step EDC protocol on the copolymer film. First results of this coupling protocol are ambiguous and clearly substantial optimization has to be achieved in order to obtain quantitative conversion of the carboxylic acids side groups of (MTEM-CPM)-PPV into amide functionalities by means of the two-step EDC protocol. Much more promising are the preliminary results of the coupling method described in Chapter 7. As mentioned in this chapter, the carboxylic acid-substituted PPV copolymer can be converted into amide-bearing PPV derivatives by reaction with an amine and a coupling agent under mild conditions.

8.7 Conclusions

This chapter focused on the interaction of biomolecules with a selection of functionalized PPV-type (co)polymers prepared earlier in this work *via* the sulfinyl precursor route. It is demonstrated that high purity functionalized PPV-type polymers can detect and transduce biochemical information and that we are able to influence the blocking or binding behaviour of the transducer layer by alternating the side chains on the PPV backbone. By incorporation of appropriate side chains, smart materials are formed that can provide new platforms for the electronic transduction of binding interactions. The carboxylic acid-substituted PPV derivative CPM-PPV was chosen for its potential ability to covalently tether antibodies onto the polymer film. In order to dilute the amount of functionalities, a copolymer has been prepared. However, the copolymer (MDMO-CPM)-PPV did not yet result in the desired advantages, as besides the covalent bonding, non-specific interactions still occurred. To further improve the selectivity of the biofilm, the hydrophilic MTEM-PPV derivative was investigated and showed the desired non-fouling properties. Therefore, the copolymer (MTEM-CPM)-PPV, which is made up of non-fouling components as well as of components allowing covalent bonding of IgG's, arouses high hopes. More measurements have to be done to determine the possible impact of this copolymer in its use as transducer material in a biosensor.

8.8 Experimental Section

Materials

All (co)polymers described in this chapter were prepared as described in previous chapters. Antibodies and antigens were obtained from the Biomedical Research Institute of the Hasselt University. The immunoglobulins (IgG's) were specific antibodies against the fluorescent dye FITC, linked to a 250 base pair DNA chain from the human phenylketonurea (PKU) gene and

amplified *via* the polymerase chain reaction to make them comparable with real serum antigens. All solutions were prepared in phosphate buffered saline (PBS).

Characterization

For the contact angle measurements, the polymers were spin coated from a chlorobenzene solution onto glass substrates (10 mm × 10 mm) to form films of 100 nm thickness. To minimize the transversal electrical resistance in actual biosensor measurements, a low thickness is desirable. However, the polymer also has to form a dense and smooth film on the sensor electrode. The films were easily reproduced and had a roughness of about 4 Å (rms) on a scale of 20 sq. μm (compared to 21 Å for the glass substrate). Antibodies from a neutral 10 mM phosphate buffered saline solution were adsorbed onto the polymer films for 1 h at 37 °C in an incubation oven. Concentrations of anti-FITC ranging between 0.01 pmol/ mL and 1 nmol/ mL were used. The static contact angle was measured with distilled water using a Dataphysics OCA 15 Plus. The atomic force microscope used, was a Park Scientific Instruments Autoprobe CP with SPIP image-processing package. The reactivity of adsorbed antibodies on the polymer was verified with a customized ELISA-procedure. First, a digoxigenin (DIG)-labelled FITC-DNA was incubated for 2 hours at 37° on the polymer films, followed by a washing and drying step. Then a peroxidase antibody, anti-DIG-POD, incubated for 1 hour at room temperature, was allowed to bind to the DIG. Afterwards, a droplet of hydrogen peroxide and tetramethylbenzidine (TMD) results in the oxidation of TMB and this gives a blue colour of the droplet. This reaction is quenched after 2 minutes with a 0.1 M sulphuric acid solution. Finally the droplets were transferred onto a Nunc 96-well microplate and the light absorption was measured in a Bio-rad benchmark microplate reader using a 450 nm wavelength. The electrodes of the biosensor experiments were prepared using the same spin coat and antibody adsorption conditions as for the characterization measurements, only a gold contact layer was evaporated onto the glass substrate prior to spin coating. The polymer electrode with adsorbed antibodies was then placed into a liquid cell,

together with an inactive polymer film coated with the blocking protein BSA to allow differential measurements. The biosensor prototype consists of flow cell in which four electrodes can be placed. Each electrode can be activated with different antibodies and has a counter electrode on top. Using a switch system, the impedance between one of the polymer electrodes and the corresponding counter electrodes can be measured separately. A syringe based flow trough system is integrated to introduce the antigens in the sensor (FITC-DNA of 0.1 nmol/ mL or less). The impedance of this cell was measured with an HP4194A Impedance Analyzer with a spectral range of 100Hz to 1MHz. Frequency-dependent measurements ranged from 20 Hz to 1 MHz, and time-dependent measurements were carried out at a fixed frequency of 300 Hz.

8.9 References

[1] a) Gerard M.; Chaubey, A.; Malhotra, B. D. *Biosensors and Bioelectronics* **2002**, *17*, 345-359 b) Wallace, G. G.; Smyth, M.; Zhao, H. *Trends in Analytical Chemistry* **1999**, *18 (4)*, 245-251.

[2] a) Kros, A.; van Hövell, S. W. F. M.; Sommerdijk, N. A. J. M.; Nolte, R. J. M. *Adv. Mater.* **2001**, *13 (20)*, 1555-1557. b) Hiller, M.; Kranz, C.; Huber, J.; Bauerle, P. Schuhmann, W. *Adv. Mater.* **1996**, *8*, 219-222.

[3] a) Bender, S.; Sadik, O. A. *Environ. Sci. Technol.* **1998**, *32*, 788-797. b) Farace, G.; Lillie, G.; Hianik, T.; Payne, P.; Vadgama, P. *Bioelectrochemistry* **2002**, *55*, 1–3. c) Katz, E.; Willner, I. *Electroanalysis* **2003**, *15 (11)*, 913–947. d) Lillie, G.; Payne, P.; Vadgama, P.; *Sens. Actuators B-Chem.* **2001**, *78*, 249–256.

[4] a) Sadik, O. A.; Xu, H.; Gheorghiu, E.; Andreescu, D.; Balut, C.; Gheorghiu, M.; Bratu, D. *Anal. Chem.* **2002**, *74 (13)*, 3142–3150. b) Fernandez-Sanchez, C.; Gallardo-Soto, A. M.; Rawson, K.; Nilsson, O.; McNeil, C. J. *Electrochem. Commun.* **2004**, *6*, 138–143.

[5] Cooreman, P.; Thoelen, R.; Manca, J.; vandeVen, M.; Vermeeren, V.; Michiels, L.; Ameloot, M.; Wagner, P. *Biosensors and Bioelectronics* **2005**, *20*, 2151-2156.

[6] a) Staros, J.V.; Wright, R.W.; Swingle, D.M. *Anal. Biochem.* **1986**, *156*, 220-222. b) Fung, Y. S.; Wong, Y. Y. *Anal. Chem.* **2001**, *73*, 5302-5309.

[7] Grabarek, Z.; Gergely, J. *Anal. Biochem.* **1990**, *185*, 131-135.

[8] a) Österberg, E.; Bergström, K.; Holmberg, K.; Schuman, T. P.; Riggs, J. A.; Burns, N. L.; Van Alstine, J. M.; Harris J. M., *J. Biomed. Mater. Res.* **1995**, *29*, 741-747. b) Emoto, K.; Nagasaki, Y.; Iijima, M.; Kato, M.; Kataoka, K. *Colloids and Surfaces B: Biointerfaces* **2000,** *18 (3-4)*, 337-346. c) Herren, B. J.; Shafer, S. G.; Van Alstine, J. M.; Harris, J. M.; Snyder, R. S. *J. Colloid Interface Sci.* **1987**, *115 (1)*, 46-55. d) Emoto, K.; Harris, J. M.; Van Alstine, J. M. *Anal. Chem.* **1996**, *68*, 3751.

Summary

In **Chapter one**, a concise description of conjugated polymers is given. Conjugated materials combine the electronic and optical properties of semi-conductors with the processability and mechanical characteristics of polymers and with the readily-tailored properties of functional organic molecules. In particular the potential use of these materials in light-emitting diodes, photovoltaic cells and other opto-electronic devices has motivated the development of synthesis and processing methods of conjugated polymer materials with unique properties. Within the wide range of different classes of conjugated polymers, poly(*para*-phenylene vinylene) (PPV) and its derivatives are known as promising materials. Hence, we chose this existing backbone structure for the design of novel materials by applying strategies towards tailored functionalization. Specifically, we designed, synthesized and characterized non-ionic polar functionalized PPV-type polymers in order to adapt the chemical and physical properties of this conjugated material to specification.

Functionalities were built in as side chains onto the phenyl groups of the PPV backbone with a variety of objectives in mind. A first objective for the polar functionalization of the PPV backbone was to find PPV-type polymers which are compatible with processing from environmentally friendly solvent systems. A second objective was to improve the performance of PPV-type materials in opto-electronic devices. Polar functionalized PPV derivatives are interesting materials for application in plastic photovoltaic cells since it is anticipated that an increased polarity leads to higher dielectric constants and therefore to an enhanced charge dissociation efficiency. In addition, tailored functionalization might lead to a better morphology and thus to an enhanced photovoltaic performance. Efforts were made to develop PPV-type material systems fitted with complex and specific functionalities for application in solar cells. Finally, also the application of functionalized PPV-type polymers as transducer layer in biosensors was within the objectives of our work.

Two major approaches are described in this work to introduce functionality into a PPV-type material. In the first approach (Chapters 2 to 6) the desired functionalized side chain is incorporated into the reactive monomer, which is subsequently polymerized *via* a precursor route. In the second approach (Chapter 7), the reactions are performed on the polymer itself, rather than going *via* a sometimes cumbersome monomer synthesis approach.

Chapter two focuses on a series of functionalized conjugated polymers with a 2,5-substituted PPV base structure. By employing the sulfinyl precursor route, these materials were prepared in a defined way and with a low defect level. The impact of the variation of the polarity of the side chains *i.e.* various combinations of oligo(oxyethylene) and alkyl substituents, on the optical, electronic and solubility characteristics was investigated with spectroscopic and electrical measurements. It was shown that the variation of the polarity of the side chains does not significantly alter the thin film optical properties of these polymers and that also the FET-mobility remains unchanged. However, the solubility as well as the solution properties are significantly affected by the polarity of the substituents. This results in a considerably expanded accessible solvent range. In addition, solvatochromism and aggregation phenomena were observed. The effect of side chain polarity was also observed in the electrical properties as a significant increase in relative permittivity, charge dissociation efficiency and conductivity.

In **Chapter three**, two strategies were developed to further increase the polarity of PPV and to fine-tune the solubility properties in order to find environmentally friendly processing solvents for this type of polymers. In the first strategy, two branched oligo(ethylene glycol) side chains were introduced at every repeating unit of the PPV backbone. The resulting conjugated material is soluble in a variety of media at the most polar side of the polarity scale, including alcohols and water. In a second approach, a tetra-substituted PPV derivative bearing four triethylene glycol derived side chains was prepared. In order to demonstrate the accessibility of tetra-substituted PPV derivatives, a tetra-alkoxy PPV derivative was prepared first. This polymer is highly soluble

in solvents at the most apolar side of the polarity scale such as cyclohexane. In addition, this tetra-alkoxy PPV appears to be strongly fluorescent and shows interesting thermotropic liquid crystalline behaviour. This behaviour is characteristic for highly ordered structures, which makes these PPV derivatives promising materials for tests in advanced polymer based devices. Replacement of the tetra-hexyloxy side chains by polar tri(ethylene glycol) side chains gave a material which is again soluble in a variety of media at the most polar side of the polarity scale, including alcohols and water.

Chapter four describes the optimization of the synthesis of two neutral crown ethers containing *para*-phenylene units. The ability of these *para*-substituted polyethers to form host–guest complexes with Na^+, K^+ and Rb^+ ions was investigated by ^1H NMR spectroscopic titrations. Low complexation constants were found. Subsequently, these crown ether compounds were further functionalized towards Gilch monomers and polymerized to form the first *para*-crown ether-functionalized PPV derivatives known in literature. The resulting PPV-type polymers show only moderate reduction of emission upon addition of metal cations.

Chapter five demonstrates the synthesis of an alcohol-functionalized PPV derivative *via* the sulfinyl precursor route. Due to aggregation, the conjugated homopolymer is insoluble. A successful approach to improve the solubility properties of the alcohol-substituted polymer was the synthesis of a copolymer. The copolymer composition was characterized using ^{13}C NMR spectroscopy. In order to explain the composition of the copolymer, a UV-Vis study on the actual monomers – the *p*-quinodimethane derivatives- was performed.

In **Chapter six**, the synthesis and characterization of a carboxylic acid-functionalized PPV derivative is discussed. This polar polymer was obtained by quantitative hydrolysis of the corresponding ester-substituted PPV derivative, which was prepared *via* the sulfinyl precursor route. The carboxy-substituted polymer is soluble in common organic solvents and in basic water. In addition, significantly improved optical properties were obtained, as

compared to previously reported similar polymers. Furthermore, carboxy-substituted copolymers were prepared.

Thus, Chapters 2 to 6 successfully demonstrated the synthesis of a number of polar functionalized conjugated PPV-type materials *via* the direct polymerization of functionalized monomers. In **Chapter seven** however, it is shown that this direct approach can give rise to difficulties for functionalized monomers with highly tailored or complex side groups. Therefore, a second possible approach towards tailored structures and tunable properties was developed. In this approach, functionalities are attached to a preformed polymer scaffold. Different post-polymerization functionalization methods were put to the test, all starting from the carboxylic acid-containing PPV (co)polymers prepared in Chapter 6. Using the Mitsunobu reaction conditions, various substituents were covalently attached to the PPV backbone in a quantitative way *via* an ester linkage. Further improvements were achieved using the DCC activation method. This method even showed promising results for the covalent tethering of phthalocyanine molecules onto the PPV backbone. In addition, it was shown that the carboxylic acid-substituted PPV-type polymer can be converted into amide-bearing PPV-type polymers.

Finally, in **Chapter eight**, some of the functionalized PPV-type polymers, described throughout this work, were tested for application as transducer layer in an impedimetric biosensor.

In general, this work shows that the introduction of functionalities to the existing PPV backbone provides access to a wide variety of material properties that stem from the functional groups used. The evaluation of some of the functionalized PPV-type materials prepared throughout this work, in advanced polymer based devices is still in process. Nevertheless, we can already state that the conjugated polymer properties can be adjusted by a careful choice of the substituents so that the chemical and physical properties of this conjugated material can be adapted to specification; In this way, new opportunities are created for PPV-type polymers in ‘plastic electronic’ device operation.

Samenvatting

In **hoofdstuk één** wordt een beknopte beschrijving gegeven van geconjugeerde polymeren. Geconjugeerde materialen combineren de elektronische en optische eigenschappen van halfgeleiders met de mechanische eigenschappen en de goede verwerkbaarheid van polymeren. Bovendien bestaat er een grote verscheidenheid aan synthesewegen die het mogelijk maakt om de eigenschappen van deze organische materialen aan te passen. De mogelijke toepassing van geconjugeerde polymeren in lichtemitterende diodes, zonnecellen en andere opto-elektronische toepassingen heeft wereldwijd geleid tot de ontwikkeling van nieuwe geconjugeerde polymeren met unieke eigenschappen.

In de onderzoekswereld van geconjugeerde polymeren staan poly(*para*-fenyleen vinyleen) (PPV)-type polymeren reeds lang bekend als veelbelovende kandidaten. Daarom werd dit type polymeer ook de basis van deze thesis. Meer specifiek werden niet-ionische, polair gefunctionaliseerde PPV-type polymeren gesynthetiseerd en gekarakteriseerd waarbij de functionaliteiten werden ingebouwd als zijgroepen op elke fenylring van de PPV-ruggengraat met als primaire doelstelling de chemische en fysische eigenschappen van het geconjugeerde materiaal aan te passen aan de vereiste toepassing. Een belangrijk doel was PPV-type materialen te ontwikkelen die oplosbaar zijn in milieuvriendelijke solventen. Een andere doelstelling die ons ertoe aanzette de PPV ruggengraat polair te functionaliseren, zijn de veelbelovende eigenschappen van deze polaire materialen als actieve laag in plastic zonnecellen. Een verhoogde polariteit van de materialen zou kunnen leiden tot een hogere diëlektrische constante en daardoor tot een betere ladingsscheiding. Ook de morfologie kan verbeterd worden door zorgvuldige keuze van de substituenten ten voordele van de toepassing van deze materialen als actieve laag in fotovoltaïsche cellen. Tot slot lag ook de toepassing van gefunctionaliseerde PPV-type polymeren in biosensoren binnen het bestek van dit proefschrift.

In het algemeen werden twee procedures toegepast om functionaliteiten in te bouwen in een PPV-type polymeer. Bij de eerste aanpak (Hoofdstuk 2 t.e.m. 6) werden de gewenste functionaliteiten ingebouwd als zijgroepen in de monomeereenheden. De gefunctionaliseerde monomeren werden vervolgens gepolymeriseerd *via* een precursorroute. Bij de tweede aanpak (Hoofdstuk 7) werd de functionalisatie uitgevoerd op het geconjugeerde polymeer zelf.

Hoofdstuk twee beschrijft de synthese van een serie polair gefunctionaliseerde PPV-type polymeren. Door gebruik te maken van de sulfinylprecursorroute slaagden we erin om goed gedefinieerde polymeren met weinig defecten te bereiden. Door verschillende combinaties te maken van oligo(ethyleenoxide) en alkylsubstituenten op de 2- en de 5-positie van het polymeer, kon de invloed van de polariteitsverandering van de zijgroepen op de optische, elektronische en oplosbaarheidseigenschappen van het materiaal onderzocht worden. Op deze manier werd aangetoond dat de polariteit van de zijgroepen weinig effect heeft op de optische eigenschappen van het conjugeerde materiaal in dunne film en dat ook de FET-mobiliteit weinig invloed ondervindt van de polariteitswijziging. De oplossingseigenschappen bleken wel beïnvloed te worden door de polariteit van de substituenten. De polaire materialen bleken oplosbaar in een breed spectrum van solventen. Tot slot werd aangetoond dat een verhoogde polariteit van de zijketens een verhoging van de relatieve permittiviteit, de ladingsscheiding en de geleidbaarheid veroorzaakt.

In **Hoofdstuk drie** worden twee strategieën beschreven die ontwikkeld werden om de polariteit van het geconjugeerde materiaal verder te verhogen zodat de oplossingseigenschappen van PPV verder aangepast worden aan polaire solvent-systemen en verwerking vanuit milieuvriendelijke solventen mogelijk wordt. In een eerste strategie werd een PPV-type materiaal bereid met op elke repeteereenheid twee vertakte oligo(ethyleenglycol)zijgroepen. Dit polymeer bleek oplosbaar te zijn in alle solventen aan de meest polaire zijde van de polariteitsschaal, inclusief in de milieuvriendelijke solventen zoals alcoholen en water. In een tweede aanpak werd een PPV-type materiaal bereid

met vier polaire triethyleenglycol-zijgroepen op elke repeteereenheid van de PPV-ruggengraat. Omdat tetra-gesubstitueerde PPV-type materialen nauwelijks beschreven zijn in de literatuur, werd deze aanpak eerst uitgetest door een tetra-alkoxy PPV-derivaat te bereiden. De synthese van dit tetrahexyloxy-gesubstitueerde polymeer bleek ongecompliceerd. Het nieuwe materiaal bleek goed oplosbaar in alle solventen aan de meest apolaire kant van de polariteitsschaal, zoals in cyclohexaan. Bovendien werden interessante fluorescentie-eigenschappen en vloeibaar kristallijn gedrag vastgesteld. Dit laatste duidt op een sterke ordening, waardoor het materiaal een veelbelovende kandidaat is voor geavanceerde polymeergebaseerde toepassingen. Door de hexylstaarten te vervangen door polaire triethyleenglycolgroepen werd een materiaal verkregen dat terug oplosbaar is in alle polaire solventen, inclusief in alcoholen en water.

Hoofdstuk vier beschrijft de synthese van twee kroonethermoleculen opgebouwd uit een *para*-fenyleeneenheid. De complexatie-eigenschappen van deze kroonethers met Na^+-, K^+- en Rb^+-ionen werd onderzocht aan de hand van ^1H NMR-titraties. Lage complexatieconstanten werden vastgesteld. Vervolgens werden deze kroonethers verder gefunctionaliseerd en gepolymeriseerd tot de eerste *para*-kroonethergefunctionaliseerde PPV-type polymeren. De emissie-eigenschappen van deze kroonetherpolymeren bleken slechts matig te wijzigen bij toevoeging van kationen.

In **Hoofdstuk vijf** wordt de synthese beschreven van een alcoholgefunctionaliseerd PPV *via* de sulfinylprecursorroute. Het homopolymeer bleek onoplosbaar te zijn in de gebruikelijke organische solventen, waarschijnlijk door aggregatie als gevolg van waterstofbrugvorming. Om de oplosbaarheidseigenschappen te verhogen werd een copolymeer bereid. De samenstelling van het copolymeer werd vastgesteld aan de hand van ^{13}C NMR-spectroscopie en verklaard aan de hand van UV-Vis-studies van de twee *p*-quinodimethaansystemen in de copolymerisatiereactie.

Hoofdstuk zes beschrijft de bereiding van een carbonzuurgefunctionaliseerd PPV-type polymeer. Dit polymeer werd bereid door kwantitatieve hydrolyse van het overeenkomstig estergesubstitueerde derivaat dat gepolymeriseerd werd volgens de sulfinylprecursorroute. Het carbonzuurgefunctionaliseerd PPV bleek oplosbaar te zijn in een aantal veel gebruikte organische solventen en in basisch water. Bovendien werden duidelijk verbeterde optische eigenschappen waargenomen t.o.v. eerder in de literatuur beschreven gelijkaardige polymeren. Verder werden in dit hoofdstuk carbonzuurgefunctionaliseerde copolymeren bereid.

In de Hoofdstukken 2 t.e.m. 6 werd dus aangetoond dat polair gefunctionaliseerde geconjugeerde PPV-type materialen bereid kunnen worden door de directe polymerisatie van gefunctionaliseerde monomeren. In **Hoofdstuk zeven** stellen we echter vast dat deze aanpak problemen oplevert bij gebruik van sterk vertakte of complex gefunctionaliseerde monomeren. Om deze problemen te omzeilen, werd er overgestapt op de aanpak van 'functionalisatie na polymerisatie'. Hierbij werd gebruik gemaakt van het carbonzuurgefunctionaliseerde polymeer dat bereid werd zoals beschreven in Hoofdstuk 6. Verschillende post-polymerisatie-functionalisatiemethoden werden uitgetest. De Mitsunobu-reactiecondities bleken geschikt om verschillende moleculen covalent te koppelen aan de PPV-ruggengraat *via* een esterbinding. Betere reproduceerbaarheid en oplosbaarheidseigenschappen werden bekomen door gebruik te maken van de DCC-activatiemethode. Deze methode bleek bovendien veelbelovend voor de covalente aanhechting van ftalocyanine-moleculen. Verder toont hoofdstuk zeven aan hoe carbonzuurgefunctionaliseerde polymeren omgezet kunnen worden naar amide-gesubstitueerde PPV-type polymeren.

In **Hoofdstuk acht** tenslotte, werden enkele gefunctionaliseerde polymeren die bereid werden zoals eerder beschreven in voorgaande hoofdstukken, getest voor toepassing in een prototype impedimetrische biosensor.

In het algemeen toont dit werk aan dat de materiaaleigenschappen van het geconjugeerde polymeer poly(*para*-phenylene vinylene) gewijzigd kunnen worden door het inbouwen van functionaliteiten. Enkele polymeren bereid in dit werk, worden momenteel nog getest in geavanceerde polymeergebaseerde toepassingen. Toch kunnen we nu al stellen dat we door een zorgvuldige keuze van de substituenten, de chemische en fysische eigenschappen van PPV-type materialen kunnen aanpassen in functie van de gewenste toepassing zodat nieuwe vooruitzichten gecreëerd worden voor PPV-type polymeren in 'plastic elektronica'.

Words of Thanks- Dankwoord

Een maandagmorgen, eind juli. Eindelijk kan ik beginnen aan het laatste onderdeeltje van dit boekje, dat ongetwijfeld door velen het eerst gelezen wordt. De dapperen onder ons, nu ja, onder jullie, die toch op deze pagina zijn geraakt door alle voorgaande te lezen, zullen begrijpen dat ik dit onmogelijk allemaal had kunnen schrijven zonder de hulp en inspiratie van anderen. Daarom wil ik mijn thesis graag afsluiten met een dankwoord. Hier mag ik de wetenschappelijke termen achterwege laten en het gevoel de bovenhand geven. Toch valt het me moeilijker dan ik had gedacht. Hoe kan ik nu in een paar zinnen iedereen bedanken die zijn steentje heeft bijgedragen tot het voltooien van dit proefschrift? Velen hebben wel eens gevraagd: 'Hoe is het nu? Vordert het een beetje?' En ook al was het niet altijd eenvoudig om uit te leggen hoe het nu werkelijk zat, de blijk van interesse door velen zorgde voor nieuwe brandstof om door te zetten.

Laat ik beginnen met die personen die meestal aan het eind vermeld worden, maar die eigenlijk op de eerste plaats komen: Mijn ouders. Zonder hun nooit-aflatende steun, bezorgdheid, liefde, raad maar vooral ook daad zou ik dit niet hebben kunnen verwezenlijken. Mama, papa, bedankt voor alles!

Zonder Prof. Dirk Vanderzande en Prof. Jan Gelan was ik misschien nooit aan dit doctoraat begonnen. Ondertussen bijna 8 (!) jaar geleden waren zij degenen die me warm maakten voor het vak 'organische scheikunde'. Vier jaar later kostte het Dirk weinig moeite om me te overtuigen om terug te keren naar Diepenbeek. Hij bezorgde me een interessant projectvoorstel en werd mijn promotor. Zijn belofte over de toffe werksfeer in de onderzoeksgroep organische en polymere scheikunde bleek helemaal te kloppen.

Prof. Thomas Cleij wil ik graag bedanken voor zijn interesse in mijn onderzoek en voor zijn nuttige suggesties, advies en tips van uiteenlopende aard. Ondanks zijn druk onderwijsschema, vond hij tijd om mijn artikels en presentaties zorgvuldig na te kijken en me met raad én daad in het labo bij te staan. Zonder zijn inbreng zou deze thesis niet dezelfde zijn geweest.

Ook een welgemeend dankjewel aan Prof. Peter Adriaensens, die altijd tijd voor me kon maken om deskundige toelichting te geven bij een spectrum, een extra meting op te zetten of om tijdrovende NMR-titraties uit te voeren.

Je voudrais aussi remercier le Dr. Laurence Lutsen pour la définition des projets dans lesquels nos polymères trouvent leur destin.

Het Fonds voor Wetenschappelijk Onderzoek Vlaanderen ben ik erkentelijk omdat ze mij het mandaat van Aspirant hebben toegekend.

De bibliothecaire, administratieve en technische krachten zorgden ervoor dat ik me niet moest bezighouden met dingen waar ik niets vanaf weet. Christel, bedankt dat je ervoor zorgde dat we nooit lang moesten wachten op onze producten. Jos, bedankt voor de keren dat je mijn gesneuveld glaswerk herstelde en voor het helpen ontwerpen van mijn hydrogeneringsopstelling. Steven, merci om AL mijn bestellingen tot een goed einde te brengen. Ook alle mensen die tijd gestoken hebben in de opnames van diverse analyses van mijn materialen ben ik dankbaar. Koen, Raoul en Kristof, bedankt voor het opnemen van talloze NMR's. Huguette en Veerle, bedankt voor de talrijke IR-, UV-Vis- en fluorescentiemetingen. Ook Sofie mocht ik altijd aanspreken als het toestel weer eens niet wou werken. Jan, bedankt voor de opname van alle massaspectra. Tom, dank je voor de elementanalyses. Iris en Veerle, bedankt voor de vele GPC-analyses. Guy, bedankt voor de TGA- en DSC- metingen. De mensen van het IMO wil ik bedanken voor de fysische metingen. Peter, bedankt voor de vlotte samenwerking.

Doctoreren zou heel wat minder leuk geweest zijn zonder afwisseling, ontspanning en afleiding. Daarom wil ik zeker een aantal mensen bedanken voor de toffe werksfeer, de vriendschap en de onvergetelijke tijd. Laat ik beginnen met de gezellige bende (Filip, Anja, Hilde en Jos) die ondertussen al een tijdje weg is, maar die ik nog lang niet vergeten ben. Een speciaal woordje van dank gaat naar Filip, omdat hij me het eerste jaar op de goede weg hielp. Zijn mopjes en zever nam ik er maar al te graag bij! Sofie, in jou vond ik niet alleen een leuke studiegenoot en een toffe collega, maar vooral (en hopelijk nog voor heel lang) een heel lieve vriendin. Lien en Kristof, het was heel leuk om vier jaar doctoreren met jullie in Atlanta te mogen afsluiten. Nog veel succes met het afronden van jullie thesis. Veerle Vrindts uit Hasselt, ik heb steeds genoten van onze babbels en hoop echt die nog heel lang te mogen voeren. En dat shoppen, dat moet er toch zeker ook nog van komen! Iris, ik wens je heel veel succes met jullie huis en hoop snel bevestiging te krijgen dat voorspellingen niet uitkomen… Liesbet, ik ben heel blij dat je bent blijven hangen op het LUC, want je was altijd aangenaam gezelschap.

Raoul, ik wens je nog veel goede resultaten en knappe studentjes toe. Wibren, het was fijn om zo'n ervaren postdoc in mijn buurt te hebben. Ik wens je echt het allerbeste toe. Jérôme, arrivée à la fin de cette thèse, je ne sais pas encore exactement ce qu'il en deviendra, mais je suis sure et certaine que tout se terminera bien pour toi. Zarina, jij was altijd bereid om te helpen. Zo zal ik nooit die keer vergeten dat je speciaal citroenen ging kopen. Fateme, mi ha fatto tanto piacere di conoscerti. In boc' al luppo con il lavoro e non lascia nessuno tocare di te! Jimmy, jij was de redder in nood voor mijn computerproblemen. Ik hoop echt dat je er snel in slaagt om die eindgroepen te bepalen. Arne, we moeten echt nog eens gaan tennissen! Misschien in je dertiende maand? Jan en Bert, ik wens jullie veel goede onderzoeksresultaten en vooral een leuke tijd toe, maar ik heb al door dat dit geen probleem zal zijn. Mijn stagiairs, Jef en Nick, wil ik hier bedanken omdat ze me, elk op hun manier, op een andere manier deden kijken naar organische synthese en de hierbij bijhorende vragen en moeilijkheden. Juanjo, un hombre muy sabio un día dijo: 'Uno no descubre nuevas tierras sin perder de vista la costa durante mucho tiempo'. Me alegro de que finalmente todo te esté saliendo bien y te deseo mucha suerte! Tot slot wil ik ook de anorganici en TOES-ers bedanken voor de babbels en de taart. Aan Marjoleine wil ik nog even zeggen: Volhouden, laat maar zien wat die 'kleintjes' in hun mars hebben!

Ook alle overige familie en vrienden, voor wie het ongetwijfeld heel wat minder duidelijk is wat ik de afgelopen jaren op het LUC heb uitgespookt, wil ik bedanken voor hun steun, interesse en gewoon omdat ze er zijn. In het bijzonder wil ik Evie bedanken om mijn grote zus te zijn, op wie ik altijd kan rekenen. Lander, mijn kleinste vriend, jouw lieve snoetje doet me altijd even al de rest vergeten, en dat is in drukke tijden, goud waard! Cati, Jean en Antje ook jullie wil ik bedanken voor de interesse en het meeleven tijdens de voorbije jaren.

Save the best for last: Michael. Jij hoort niet onderaan deze rij te staan, ook niet bovenaan, maar erboven. En daar sta je ook voor mij. De eindsprint naar het doctoraat en naar ons eigen stekje viel ongelukkigerwijs samen. Zonder jou was het nooit gelukt. Ik wil je bedanken, gewoon omdat je bent wie je bent.

Dank je wel!